

8-1-2014

# Monitoring drought intensity in Illinois with a combined index

GUANLING FENG

*Southern Illinois University Carbondale, fguanling1004@gmail.com*

Follow this and additional works at: <http://opensiuc.lib.siu.edu/theses>

---

## Recommended Citation

FENG, GUANLING, "Monitoring drought intensity in Illinois with a combined index" (2014). *Theses*. Paper 1480.

This Open Access Thesis is brought to you for free and open access by the Theses and Dissertations at OpenSIUC. It has been accepted for inclusion in Theses by an authorized administrator of OpenSIUC. For more information, please contact [opensiuc@lib.siu.edu](mailto:opensiuc@lib.siu.edu).

MONITORING DROUGHT INTENSITY IN ILLINOIS WITH A COMBINED INDEX

by

Guanling Feng

B.S., Wuhan University, 2011

A Thesis

Submitted in Partial Fulfillment of the Requirements for the  
Master of Science Degree

Department of Geography and Environmental Resources  
In the Graduate School  
Southern Illinois University Carbondale  
August 2014

THESIS APPROVAL

MONITORING DROUGHT IN ILLINOIS WITH A COMBINED INDEX

By

Guanling Feng

A Thesis Submitted in Partial

Fulfillment of the Requirements

for the Degree of

Master of Science

in the field of Geography and Environmental Resources

Approved by:

Dr. Guangxing Wang, Chair

Dr. Justin Schoof

Dr. Tonny J Oyana

Graduate School

Southern Illinois University Carbondale

May 12<sup>th</sup>, 2014

## AN ABSTRACT OF THE THESIS OF

Guanling Feng, for the Master of Science degree in Geography and Environmental Resources, presented on 12<sup>th</sup> May 2014, at Southern Illinois University Carbondale.

TITLE: MONITORING DROUGHT IN ILLINOIS WITH A COMBINED INDEX

MAJOR PROFESSOR: Dr. Guangxing Wang

Many traditional drought assessments are conducted based on climate and hydrologic data. The availability and precision of data limit the spatial and temporal resolution and accuracy of derived drought indices. In this study, Vegetation Condition Index (VCI) and Temperature Condition Index (TCI) were generated from Moderate Resolution Imaging Spectroradiometer (MODIS) products. The VCI was derived from Normalized Difference Vegetation Index (NDVI) that was calculated with near infrared and visible red band reflectance from MOD09Q1. The TCI was derived from land surface temperature (LST) product MOD11A2. The VCI and TCI were then combined with reference to the vegetation coverage information from MOD44B to generate the modified Vegetation Health Index (VHI). The modified VHI was applied to quantify the intensity of drought that took place in Illinois from 2000 to 2012. The results showed that the modified VHI identified the major droughts that occurred in Illinois from 2000 to 2012, especially the extreme one taking place in 2012. Moreover, the modified VHI led to the spatial distributions and temporal trends of drought severity, which were overall similar to those from the U.S. Drought Monitor (USDM) maps, but had more detailed spatial variability and much higher spatial resolution. The modified VHI also differentiated the drought impacts between the vegetated and non-vegetated areas, being a lack of the original VHI. Thus, the modified VHI takes advantage of spatially

continuous and timely data from satellites and can be applied to conduct the monitoring and detection of drought intensity at local, regional, and national scales. The modified VHI can effectively synthesize the drought information of LST and NDVI to differentiate the effects of land use and land cover (LULC) types and provide the detailed spatial variability of drought intensity and thus enhance the understanding of relationship between drought condition and LULC types.

## ACKNOWLEDGMENTS

I would like to thank my advisor, Dr. Guangxing Wang for all his assistance during the project. He provided lots of help and suggestions and I really appreciate for what he has done. I would also like to thank Dr. Justin Schoof and Dr Tonny J Oyana for their comments and inputs on this thesis. Lastly I would like to thank other faculty and staff at the Department of Geography and Environmental Resources and my friends who supported me in completing the project.

## TABLE OF CONTENTS

| <u>CHAPTER</u>                          | <u>PAGE</u> |
|---|-------------|
| ABSTRACT .....                          | ii          |
| ACKNOWLEDGMENTS .....                   | iii         |
| LIST OF TABLES .....                    | vi          |
| LIST OF FIGURES .....                   | vii         |
| CHAPTER 1. INTRODUCTION .....           | 1           |
| 1.1 Background .....                    | 1           |
| 1.2 Problem Statement .....             | 4           |
| 1.3 Research Objectives .....           | 6           |
| CHAPTER 2. LITERATURE REVIEW .....      | 9           |
| 2.1 Definition of Drought .....         | 9           |
| 2.2 Traditional Drought Indices .....   | 9           |
| 2.3 Remote Sensing-Based Indices .....  | 12          |
| CHAPTER 3. MATERIALS AND METHODS .....  | 16          |
| 3.1 Study Area .....                    | 16          |
| 3.2 Data Sets .....                     | 19          |
| 3.3 Computation of Indices .....        | 21          |
| 3.3.1 Data pre-process .....            | 22          |
| 3.3.2 TCI, VCI and NDVI .....           | 24          |
| 3.3.3 Vegetation Coverage and VHI ..... | 26          |
| 3.3.4 Comparison with USDM map .....    | 29          |
| CHAPTER 4. RESULTS AND ANALYSIS .....   | 31          |

|  |     |
|--|-----|
| 4.1 Temperature Condition Index .....                                | 31  |
| 4.2 Vegetation Condition Index.....                                  | 35  |
| 4.3 NDVI Anomaly .....   | 39  |
| 4.4 Vegetation Health Index .....                                    | 42  |
| 4.5 Comparison with USDM maps.....                                   | 54  |
| CHAPTER 5. CONCLUSION .....  | 61  |
| REFERENCES .....   | 65  |
| APPENDICES   |     |
| <b>Appendix A:</b> Temperature Condition Index Maps of Illinois..... | 73  |
| <b>Appendix B:</b> Vegetation Condition Index Maps of Illinois ..... | 86  |
| <b>Appendix C:</b> Vegetation Health Index Maps of Illinois.....     | 99  |
| <b>Appendix D:</b> NDVI Anomaly Maps of Illinois .....               | 112 |
| VITA .....   | 125 |



LIST OF TABLES

TABLE

PAGE

Table 1 ..... 20

## LIST OF FIGURES

| <u>FIGURE</u>   | <u>PAGE</u> |
|-----------------|-------------|
| Figure 1 .....  | 4           |
| Figure 2 .....  | 18          |
| Figure 3 .....  | 22          |
| Figure 4 .....  | 23          |
| Figure 5 .....  | 24          |
| Figure 6 .....  | 32          |
| Figure 7 .....  | 33          |
| Figure 8 .....  | 36          |
| Figure 9 .....  | 37          |
| Figure 10 ..... | 40          |
| Figure 11 ..... | 41          |
| Figure 12 ..... | 44          |
| Figure 13 ..... | 45          |
| Figure 14 ..... | 46          |
| Figure 15 ..... | 47          |
| Figure 16 ..... | 48          |
| Figure 17 ..... | 49          |
| Figure 18 ..... | 50          |
| Figure 19 ..... | 51          |
| Figure 20 ..... | 52          |
| Figure 21 ..... | 53          |
| Figure 22 ..... | 54          |

|                 |    |
|-----------------|----|
| Figure 23 ..... | 57 |
| Figure 24 ..... | 59 |

## CHAPTER 1

### INTRODUCTION

#### 1.1 BACKGROUND

Drought has been quite a hot topic in recent years. Based on the data available from U.S. Drought Monitor, the 2012 North American Drought hit nearly 80% of the contiguous United States. It has inflicted a catastrophe to several states. A total of 1,692 counties across 36 states in the US have been legally declared primary natural disaster areas as of August 17 (National Weather Service Information, 2012). Back into history, the most recent comparable drought took place in 1988. It is one of the costliest natural disasters in American history since its impact on the US economy has been estimated at \$40 billion, which is 2 - 3 times the estimated loss caused the 1989 San Francisco earthquake (Riebsame et al., 1990). And compared to other severe droughts, which happened before 1980s, the impacts and frequency of droughts in the last two decades has increased rapidly, which brings much attention of experts in different fields to this disaster.

Drought can be described as a chronic, potential natural disaster characterized by a prolonged, abnormal water shortage (Ghulam et al., 2007). However, the differences in hydrometeorological variables and socioeconomic factors as well as the complex nature of water demands in different regions over the world make it very difficult to give a common definition of drought. Therefore how to objectively characterize it for planning and management is still quite challenging. Precipitation deficit, evapotranspiration and stream flow are often used as indicators to provide a

comprehensive description. These indicators along with other variables are combined in various models to derive different drought indices. And the intensity, duration, severity and spatial extent of droughts can be defined from the drought index.

There is a category of the existent drought indices by their use of disciplinary data: meteorological drought indices, agricultural drought indices, hydrological drought indices, remote sensing-based drought indices, and combined drought indices (Niemeyer, 2008). As for meteorological drought indices, the most popular one is Standardized Precipitation Index (SPI) proposed by McKee et al. in 1993. Other examples are the Rainfall Anomaly Index (Van Rooy, 1965), the Bhalme and Mooley Drought Index (Bhalme and Mooley, 1980), the Drought Severity Index (Bryant et al., 1992). The specialization on soil moisture and evapotranspiration resulted in the development of agricultural drought indices, such as the Crop Moisture Index (Palmer, 1968), the Soil Moisture Drought Index (Hollinger et al., 1993), the Crop Specific Drought Index (Meyer et al., 1993), and the Soil Moisture Deficit Index (Narasimhan and Srinivasan, 2005). The hydrological drought indices focus more on analyzing stream flow data, for instance, the Surface Water Supply Index (SWSI) of Shafer and Dezman (1982), the Reclamation Drought Index of Weghorst (1996), and the Regional Stream flow Deficiency Index of Stahl (2001). Remote sensing-based drought indices are newly developed compared to above indices since they rely on the advancement of Earth observation satellites and sensors from the 1980s. There are numerous indices proposed every year, which is following the development of new sensors and approaches. Among these indices are some prominent ones: the Normalized Difference Vegetation Index (Tucker, 1979), the Vegetation Condition Index (Kogan, 1990, 1995), the Temperature Vegetation Dryness Index (Sandholt et al., 2002), the Vegetation

Temperature Condition Index (Wan et al., 2004), and the Perpendicular Drought Index (Ghulam et al., 2007). The most promising direction in development of drought indices is the combination of various indices to exploit a maximum of available and useful information. Take the Vegetation Drought Response Index (Brown et al., 2008) as an example. NDVI datasets, climate data from the stations and static biophysical information such as elevation are included in this comprehensive index. On the other hand, the US Drought Monitor (NDMC, 2008) has realized the combination of meteorological data and remote sensing images on a manual basis (see Figure 1). A limitation of drought monitor products lies in their attempt to show droughts at several temporal scales (from short term to long-term drought) on one map product (Heim, 2002).

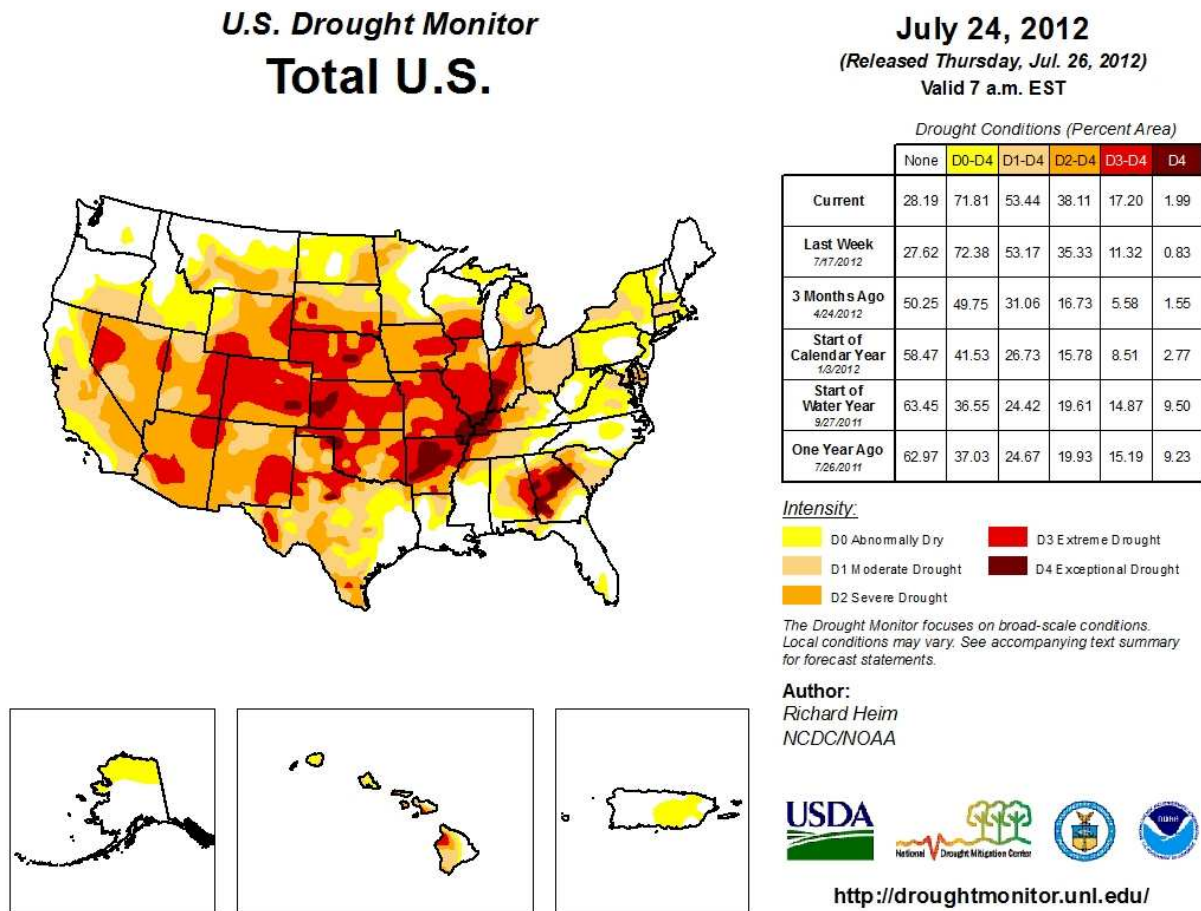


Figure 1: The USDM map for the whole United States, which is updated on July 24, 2012.

## 1.2 PROBLEM STATEMENT

For traditional climate-based indices, the spatial resolution and precision is restricted to a certain level. Because the climate data such as precipitation, air temperature and soil moisture are collected by separate weather stations, these data are only available at the points. Statistical methods are thus needed to construct a continuous coverage over the landscape. Therefore, the accuracy, detail, and resolution provided by these indices are dependent on the spatial distribution of the weather stations and the methods to be used to create the spatial distributions. With higher

density of weather stations, there will be more detailed assessment of related climate data. But for places with sparse weather stations, the resolution of the data will be much coarser and the accuracy may be poor.

The satellite observations of earth surface can provide spatially continuous and timely data for monitoring drought. On one hand, the images acquired by remote sensors can detect the apparent declines in vegetation health, which may be caused by lack of water. Nevertheless the remote sensing data alone cannot identify the specific reasons behind the vegetation condition anomalies. There is possibility that it is caused by other natural disasters such as flood or some serious communicable diseases destroy the vegetation. Thus, it is necessary to incorporate other climate data to help eliminate other possible reasons. On the other hand, the land surface temperature can be derived from remote sensing data. It is one of the common used characteristics while describing drought and can provide good assessment of drought for areas with little or no vegetation cover.

This study plans to make a combination of vegetation condition and temperature information. For areas where it is hard to monitor the drought with vegetation condition, like bared areas, land surface temperature is applied to provide information of drought stress. A comprehensive model will be built to process all the data and generate the maps, which indicate the intensity and patterns of drought over large-scale landscape.

This study assesses the comprehensive index proposed here. A visual verification is applied to compare the USDM maps and the final maps of the proposed index. Because the USDM (Svoboda et al., 2002) is a state-of-the-art drought-monitoring tool used in United States, the USDM map is updated every week and its spatial resolution is adequate for national- and state-level policy makers (Svoboda et al.,



2002). The comparison can evaluate the capability of the proposed index in monitoring drought condition at a large scale and a local scale.

### 1.3 RESEARCH OBJECTIVES

The purpose of this study is to search for a useful and relatively simple combination of various types of drought indices. Researchers try to incorporate different drought indicators and exploit a maximum of information, which is available and effective. Much work has been done in this area. For example, Vegetation Drought Response Index (VegDRI) has been combined with NDVI, SPI, and PDSI which provides near-real-time maps of drought severity and spatial extent (Brown et al. 2008). Karamouz et al. (2009) proposed the Hybrid Drought Index (HDI), which combined the SPI, SWSI, and PDSI. Among these indices, the USDM is currently widely used in the organization level by media. The USDM integrates meteorological indices and indicators such as vegetation and hydrologic conditions into a composite drought index. However, the coarse resolution of USDM maps fails to provide detailed information at the local level. The counties of every state needs more specific data to make polices and design strategies towards drought disasters (Brown et al, 2008). This study attempts to provide such kind of information to complement the USDM maps.

The severity of drought is regionally different from place to place and therefore it is essential to define a threshold value for different hydroclimatic regions (Mishra and Singh, 2009). This study tries to derive a useful drought index and categorizes drought severity. The comparison of normal years with the years of drought is necessary to distinguish the differences. For the remote sensing data, there are two aspects of the significance in exploring the historic data. On one hand, the drought impact on

vegetation condition in the past can provide reference for identifying the intensity of the future droughts. On the other hand, the long-term images over the same area can assist in tracing the change of the landscape and land using conditions, which are also very important analyzing the drought stress.

The study made an effort to build a quantitative drought monitoring which applies well to regions with varied degree of vegetation coverage. There are indices derived from satellite observations that are sensitive to vegetation condition, such as NDVI. Some indices describe more about temperature and soil moisture, such as LST. If only one index is used to make assessment of drought intensity, for example, NDVI, the assessment over bared areas or areas with few plants will be much less accurate than the areas with dense vegetation. In order to solve such kind of problems, a model is established to divide the study area into two parts: bared soil and land with vegetation coverage. For each unit of the area, the soil and vegetation fraction images can be calculated and they provide a basis for the combination of different indices. In this way, the effective information from these indices can make a reasonable integration. The fraction is considered in Modified Perpendicular Drought Index (Ghulam et al., 2007c), but not much work has been done in this direction.

The specific objective of this study is to develop a comprehensive drought index by combining the information from remotely sensed data in both vegetation condition and temperature and to monitor drought intensity in Illinois. This study aimed at answering following research questions:

1. Is the combined drought index able to provide more detailed information of drought intensity than the existing USDM?

2. Is the combined drought index able to capture the drought events that took place during the last decade, especially the one in 2012?
3. Is the combined drought index able to reveal the differences of the drought impacts between urbanized and vegetated areas?
4. Is the combined drought index better than the existing indices to quantify drought intensity?

## CHAPTER 2

### LITERATURE REVIEW

#### 2.1 DEFINITION OF DROUGHT

Drought is quite a stochastic natural phenomenon. It can be defined as the precipitation deficit over a specific area for a specific period of time (Beran and Rodier 1985; Correia et al., 1994). Tsakiris and Vangelis (2004) have included the impacts of drought on environment and society as an expansion. Wilhite (2004) underscored the human demand placed on water supply under drought condition. Much research work has been done to explore the various impacts and characteristics of drought as a natural disaster. But no common definition has been reached because of its complex nature.

It is very essential to distinguish conceptual and operational definitions of drought (Wilhite and Glantz, 1987). Conceptual definitions are formulated in general terms for overall understanding. Operational definitions are used for a specific application to analyze drought frequency, severity and duration. Based on the operational definitions, there are three main physical drought types: meteorological, agricultural, and hydrological droughts.

#### 2.2 TRADITIONAL DROUGHT INDICES

Although there are several methodologies proposed for characterizing drought, drought indices are the most popular way (Tsakiris et al, 2007). Over 150 drought indices have been proposed (Niemeyer 2008) and lately more indices appeared (Cai et al. 2011; Karamouz et al. 2009; Vasiliades et al. 2011). A drought index, generally speaking, is a prime variable for assessing the effect of a drought. It defines the

intensity, duration, severity and spatial extent of specific drought. Different indicators of drought are selected as the base data for calculating the index, such as precipitation deficit, soil moisture, water flow and so on. Usually, drought indices are categorized by these indicators or variables or the disciplinary data they use (Niemeyer 2008). There are three popular categories: meteorological, agricultural and hydrological drought indices. Niemeyer (2008) added the following categories: comprehensive, combined and remote-sensing based drought indices.

For meteorological drought indices, they use the climate data collected from synoptic meteorological stations. Therefore the development of meteorological drought indices is closely related to the availability of the climate data. Early meteorological drought indices only take precipitation into consideration, such as the Rainfall Anomaly Index (Van-Rooy 1965), the Bhalme and Mooley Drought index (Bhalme and Mooley, 1980), the Drought Severity Index (Bryant et al., 1992), NRI (Gommes and Petrassi, 1994), EDI (Byun and Wilhite 1999), and DFI (Gonzalez and Valdes, 2006). Among these indices, Standardized Precipitation Index (SPI) (McKee et al., 1993) is most frequently used. It is calculated based on the long-term precipitation record that is fitted to probability distribution. SPI has several advantages: it is simple and adaptable for the analysis of drought at variable times scales. It can be used for both agricultural and hydrological droughts (Zargar et al, 2011). But, SPI fails to take potential evapotranspiration into accounts, which is also a helpful indicator (Hu and Willson, 2000; Vicente-Serrano et al., 2010). The Reconnaissance Drought Index proposed by Tsakiris et al. (2007) solved this problem and get better correlation with impacts from agricultural and hydrological droughts. Other meteorological variables, such as

temperature, are included in newly developed index to gain a comprehensive understanding of the drought condition.

Agricultural drought indices mainly concentrate on soil moisture, evapotranspiration and soil water balance. Take Crop Moisture Index (CMI) as an example. CMI was developed by Palmer (1968) and is used to evaluate short-term moisture conditions across major crop-producing areas with a water balance model. CMI is most effective for measuring agricultural drought during warm seasons (Heim, 2002). But, it is not suitable for monitoring long-term drought since it may provide misleading information (Mishra et al., 2010). An example of other indices is Crop Specific Drought Index (CSDI) proposed by Meyer et al (1993) and estimates soil water availability for different regions and soil layers. Narasimhan and Srinivasan (2005) developed the Soil Moisture Deficit Index (SMDI) and Evapotranspiration Deficit Index (EDI). These two indices use a high-resolution comprehensive hydrologic model, which integrates a crop growth model. They improve the older indices such as SPI, PDSI and CMI, by considering the spatial variability of hydrological parameters of soil type and land cover as well as meteorological parameters. Recently Marletto et al. (2005) proposed another new agricultural drought index called DTx for regional application. It is based on the daily transpiration deficit as computed by a water balance model and describes the integrated deficit of transpiration of a crop for a period of x days.

Hydrology-oriented drought indices characterize the delayed hydrologic impacts of drought and study the water balance in a catchment area for water management purpose (Zagar et al, 2011). Palmer Hydrological Drought Index (PHDI) proposed by Palmer (1965) analyzes precipitation and temperature in water balance model and compares meteorological and hydrological drought across space and time (Heim,

2002). While PHDI does not account for snow accumulation, the Surface Water Supply Index (SWSI) of Shafer and Dezman (1982) that is probably most popular hydrological drought index takes it into consideration. Weghorst (1996) proposed the Reclamation Drought Index (RDI) which further improved the SWSI. The RDI incorporates air temperature for the demand side, and precipitation, reservoir storage, stream flow, and snowpack for the supply side, as well as the duration of a drought event. Stahl (2001) developed a Regional Streamflow Deficiency Index (RSDI) to detect drought event in each homogeneous region. The RSDI uses flow duration curves and the 90% exceeding threshold (Q90) derived from the curves. Cluster analysis is applied to calculate the value of the index. Ground Water Resource Index (GWRI) (Mendicino et al., 2008) considers geo-lithological conditions that affect the summer hydrologic response to winter precipitation. Another new hydrological drought index is Water Balance Derived Drought Index (WBDDI) (Vasiliades et al., 2011) which uses water balance model (Loukas et al., 2007) to simulate runoff.

### 2.3 REMOTE SENSING-BASED DROUGHT INDICES

Remote sensing-based drought indices are developed on the foundation of the launch of earth observation satellites with sensors mainly in the optical domain. The new technologies make it possible to generate higher resolution of drought analysis products, which is a shortcoming of previous drought indices (Niemeyer, 2008). There is a variety of satellites observation-based drought indices. Some of them are derived from information of the optical domain. The most outstanding example is the Normalized Difference Vegetation Index (NDVI) (Tucker, 1979). NDVI uses information of red and near-infrared channels from the advanced very high-resolution radiometer and it applies

simple algorithms to identify the health condition of vegetation. The basic idea is that healthy vegetation generally has higher reflectance of radiance in near infrared channel. However, moisture condition is not the only reason that will impact vegetation. Regional rainfall patterns and soil type, as well events such as insect infestation and wildfire are also possible causes for declined vegetation health condition. Therefore, many modifications have been made on the base of NDVI, for example, the Vegetation Condition Index (Kogan, 1990, 1995), the anomaly of NDVI called NDVIA (Anyamba et al., 2001), and the Standardized Vegetation Index (Peters et al., 2002). The Land Surface Temperature (LST) is different from NDVI because it exploits the information from the thermal channel. The Temperature Condition Index proposed by Kogan (1995) is another example of this kind of drought index.

More and more research has focused on the correlation between vegetation indices based on visible or near infrared information and the land surface temperature information. The Vegetation Index / Temperature Trapeziod (Carlson et al., 1994) is built on the slope of the LST versus NDVI relationship. There are two drought indices, which are constructed on the NDVI/LST reflectance space: the Vegetation Temperature Condition Index (e.g. Wan et al., 2004) and the Temperature Vegetation Dryness Index (Sandholt et al., 2002). The Perpendicular Drought Index proposed by Ghulam et al. (2007b) also explores the near-infrared and red spectral reflectance space. Moreover, Modified Perpendicular Drought Index (Ghulam et al., 2007) improved the former by incorporating the fraction of a pixel that accounted for soil moisture and vegetation growth. Some newly developed indices attempt to take advantage of information from the multi-band of sensors. One example is the Normalized Multi-Band Drought Index (Wang and Qu, 2007) using the data from MODIS.



The comprehensive and combined drought indices (Niemeyer, 2008) make use of various type of information to characterized drought condition. Compared to non-hybrid indices, they provide a comprehensive description of drought events (Kallis, 2008). Because of their composite nature, the hybrid indices usually are closely related to the actual drought influences. Vegetation Drought Response Index (Brown et al., 2008) is a prominent example, which is a combination of NDVI, SPI, and PDSI. The high resolution makes it useful for local planning and mitigation towards drought. Karamouz et al (2009) proposed the Hybrid Drought Index that includes SPI, SWISI, and PDSI. USDM integrates meteorological data with remote sensing images as well, but it provides no single reproducible quantitative index that comprises all information (NDMC, 2008).

Kogan (1995, 1997) proposed a Vegetation Health Index (VHI) by combining a temperature condition index (TCI) and vegetation condition index (VCI). TCI was derived from land surface temperature image and VCI was obtained using NDVI image calculated from red and near infrared bands of satellite images. This composite index is simple and effective to quantify drought intensity and has been successfully applied in many different environmental conditions (Kogan et al., 2005; Rojas et al., 2011; Seiler et al., 2007; Unganai & Kogan, 1998; Wu et al., 2013). To combine TCI and VCI, equal weights of 0.5 are used for them, which implies the equal contributions of temperature and vegetation on drought impacts regardless of different land use and land cover (LULC). In practice, the impacts of the same temperature on drought intensity may differ due to different LULC. For example, vegetated lands may have higher tolerance to high temperature than the lands in which no or little vegetation exists.

Combining meteorological, agricultural, hydrology-oriented, and remote sensing based drought indices into more comprehensive and integrative drought index is a

promising direction in this field. The combined information covers multiple aspects and applications of droughts. Especially, the combination of remote sensing based indices and meteorological or hydrological indicators are likely to paint a whole picture of a drought situation (Niemeyer, 2008). There is a strong need for development of more comprehensive drought indices.

## CHAPTER 3

### MATERIALS AND METHODS

#### 3.1 STUDY AREA

The proposed method is applied to the whole state of Illinois, which locates in the Midwest Region of the United States and is one of the nine states that are in the bi-national Great Lake region of North America. Illinois' eastern borders with Indiana consists of a north-south line at 87°31'30" west longitude, from Lake Michigan to the Wabash River above Post Vincennes. Its southern border with Kentucky runs along the northern shoreline of the Ohio River. Mississippi River is the western border of Illinois with Missouri and Iowa. And the northern border with Wisconsin is fixed at 42°30' north latitude.

The total area of Illinois is 149,998 km<sup>2</sup> and most parts of it are plains with northwestern parts of higher and rugged topography. The highest point of Illinois is located in Charles Mound with a height of 376.4 meters above sea level. On the contrary, the lowest point locates in the Confluence of Mississippi River and Ohio River, the height of which is 85.3 meters above sea level (Figure 2)

Midwestern United States experienced most of the severe droughts in history as mentioned in the introduction part. With over \$200 billion in farm gate value, agriculture is a major component of the Midwestern economy (NASS, 2012). There are over 400,000 farms and its corn and soybean production takes a significant portion of the global total production. This region is also a major producer of fruits, vegetables, dairy, pigs and beef cattle. Since most agriculture in this region is rain fed, it is highly vulnerable to drought. In the future it is projected that the annual temperature of the

Midwest would increase (Hayhoe et al 2007), which makes the occurrence of drought disaster more possible. Therefore it is essential to study the drought issues in the state of Illinois.

The study aims at modifying the combined drought index VHI and making it possible to effectively combine the vegetation condition information from VCI and temperature information from TCI with reference to the vegetation coverage factor. The modified VHI is applied to the growing season: June, July, August and September from 2000 to 2012 and it is expected to be applied in the future drought assessment as well.

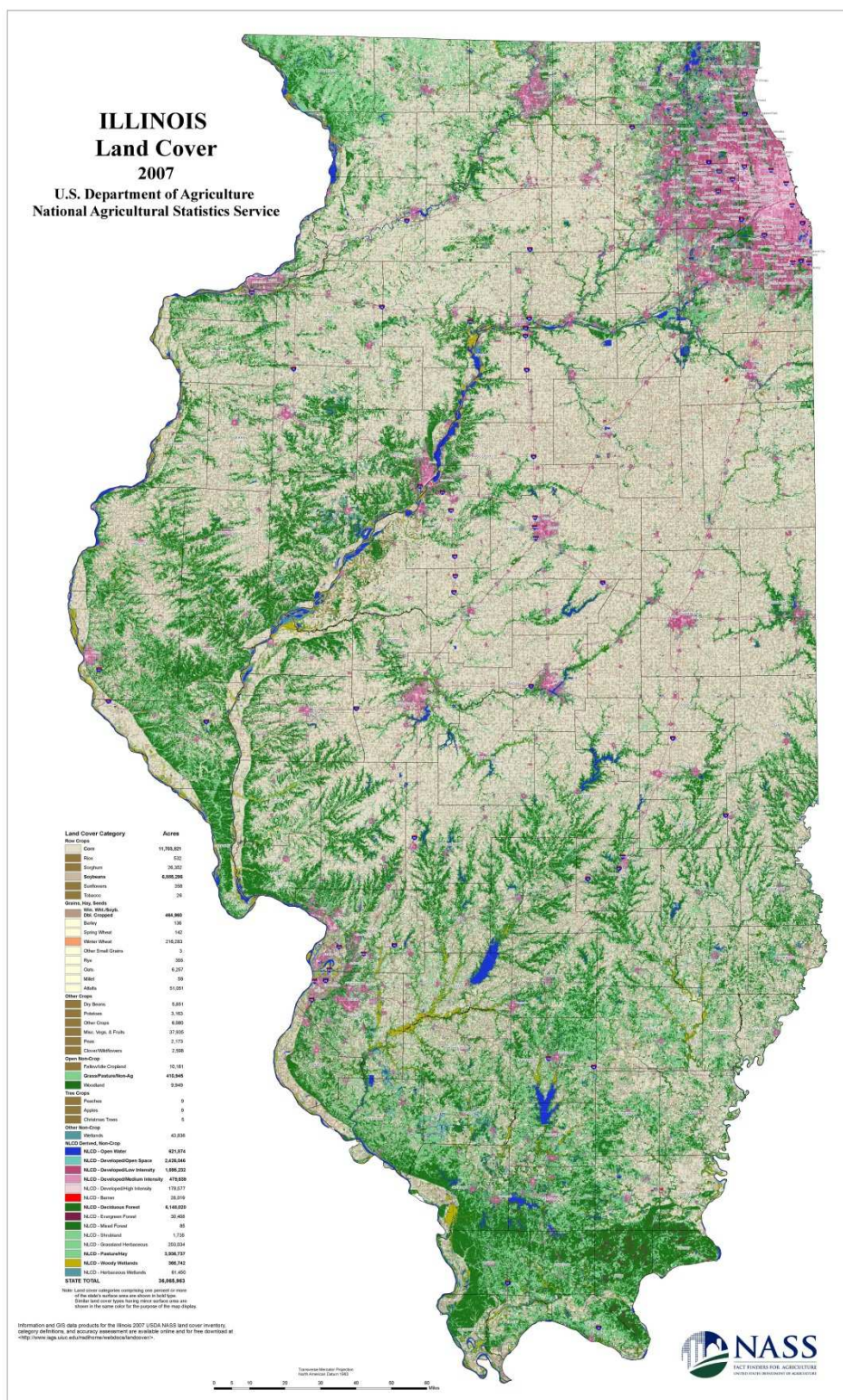


Figure 2: Land cover map of Illinois (<http://www.igs.uiuc.edu/nsdihome/webdocs/landcover/nass07.html>)

### 3.2 DATA SETS

Moderate Resolution Imaging Spectroradiometer(MODIS) products were applied in this study, including MOD09Q1, MOD11A2 and MOD44B. MODIS is a key instrument aboard the Terra (EOS AM) and Aqua (EOS PM) satellites. Terra's orbit around the Earth is timed so that it passes from north to south across the equator in the morning, while Aqua passes south to north over the equator in the afternoon. Terra MODIS and Aqua MODIS are viewing the entire Earth's surface every 1 to 2 days, acquiring data in 36 spectral bands, or groups of wavelengths (Table 1).

Table1: Spectral and spatial characteristics of MODIS (<http://modis.gsfc.nasa.gov/about/specifications.php>). The spatial resolution for bands 1-2 is 250m, for bands 3-7 is 500m and for bands 8-36 is 1000m.

| Primary Use                                 | Band | Bandwidth <sup>1</sup> | Spectral Radiance <sup>2</sup> | Required SNR <sup>3</sup> |
|---|------|------------------------|--------------------------------|---------------------------|
| Land/Cloud/Aerosols Boundaries              | 1    | 620 - 670              | 21.8                           | 128                       |
|   | 2    | 841 - 876              | 24.7                           | 201                       |
| Land/Cloud/Aerosols Properties              | 3    | 459 - 479              | 35.3                           | 243                       |
|   | 4    | 545 - 565              | 29.0                           | 228                       |
|   | 5    | 1230 - 1250            | 5.4                            | 74                        |
|   | 6    | 1628 - 1652            | 7.3                            | 275                       |
|   | 7    | 2105 - 2155            | 1.0                            | 110                       |
| Ocean Color/ Phytoplankton/ Biogeochemistry | 8    | 405 - 420              | 44.9                           | 880                       |
|   | 9    | 438 - 448              | 41.9                           | 838                       |
|   | 10   | 483 - 493              | 32.1                           | 802                       |
|   | 11   | 526 - 536              | 27.9                           | 754                       |
|   | 12   | 546 - 556              | 21.0                           | 750                       |
|   | 13   | 662 - 672              | 9.5                            | 910                       |
|   | 14   | 673 - 683              | 8.7                            | 1087                      |
|   | 15   | 743 - 753              | 10.2                           | 586                       |
|   | 16   | 862 - 877              | 6.2                            | 516                       |
| Atmospheric Water Vapor                     | 17   | 890 - 920              | 10.0                           | 167                       |
|   | 18   | 931 - 941              | 3.6                            | 57                        |
|   | 19   | 915 - 965              | 15.0                           | 250                       |

Table1: Spectral and spatial characteristics of MODIS

| Primary Use   | Band | Bandwidth <sup>1</sup> | Spectral Radiance <sup>2</sup> | Required NE[delta]T(K) <sup>4</sup> |
|---|------|------------------------|--------------------------------|-------------------------------------|
| Surface/Cloud Temperature   | 20   | 3.660 - 3.840          | 0.45(300K)                     | 0.05                                |
|   | 21   | 3.929 - 3.989          | 2.38(335K)                     | 2.00                                |
|   | 22   | 3.929 - 3.989          | 0.67(300K)                     | 0.07                                |
|   | 23   | 4.020 - 4.080          | 0.79(300K)                     | 0.07                                |
| Atmospheric Temperature   | 24   | 4.433 - 4.498          | 0.17(250K)                     | 0.25                                |
|   | 25   | 4.482 - 4.549          | 0.59(275K)                     | 0.25                                |
| Cirrus Clouds Water Vapor   | 26   | 1.360 - 1.390          | 6.00                           | 150(SNR)                            |
|   | 27   | 6.535 - 6.895          | 1.16(240K)                     | 0.25                                |
|   | 28   | 7.175 - 7.475          | 2.18(250K)                     | 0.25                                |
| Cloud Properties  | 29   | 8.400 - 8.700          | 9.58(300K)                     | 0.05                                |
| Ozone   | 30   | 9.580 - 9.880          | 3.69(250K)                     | 0.25                                |
| Surface/Cloud Temperature   | 31   | 10.780 - 11.280        | 9.55(300K)                     | 0.05                                |
|   | 32   | 11.770 - 12.270        | 8.94(300K)                     | 0.05                                |
| Cloud Top Altitude  | 33   | 13.185 - 13.485        | 4.52(260K)                     | 0.25                                |
|   | 34   | 13.485 - 13.785        | 3.76(250K)                     | 0.25                                |
|   | 35   | 13.785 - 14.085        | 3.11(240K)                     | 0.25                                |
|   | 36   | 14.085 - 14.385        | 2.08(220K)                     | 0.35                                |
| <sup>1</sup> Bands 1 to 19 are in nm; Bands 20 to 36 are in $\mu\text{m}$<br><sup>2</sup> Spectral Radiance values are ( $\text{W}/\text{m}^2 \cdot \mu\text{m}\cdot\text{sr}$ )<br><sup>3</sup> SNR = Signal-to-noise ratio<br><sup>4</sup> NE(delta)T = Noise-equivalent temperature difference<br><b>Note:</b> Performance goal is 30-40% better than required |      |                        |                                |                                     |

MOD09Q1 provides surface reflectance of band 1 (red) and band 2 (near infrared) at 250-meter resolution in the Sinusoidal projection. The products are updated every 8-day and the pixels are selected from that time period on the basis of high observation coverage, the cloud shadow, low view angle and aerosol loading. MOD11A2 provides land surface temperature and emissivity data at 1-km resolution in the Sinusoidal projection. The land surface temperature data are calculated as the

mean land surface temperatures under clear sky during an 8-day period. MOD44B is referred as the Terra MODIS vegetation continuous fields product. It contains the percent of tree cover, percent of non-tree cover and percent of bare area for each pixel. The products are produced every year at 250-meter resolution in the Sinusoidal projection.

### 3.3 COMPUTATION OF INDICES

The methodology consists of four steps (Figure 3). The first step is to collect and process the MODIS products applied in this study. The second step is to extract the information of the study area from the datasets and use the information for calculation of VCI and TCI. The third step is to incorporate the two different indices: VCI and TCI with the vegetation coverage information and generate VHI. The final step is the analysis of mean VHI, VCI, TCI and NDVI-z values during the 13 years.



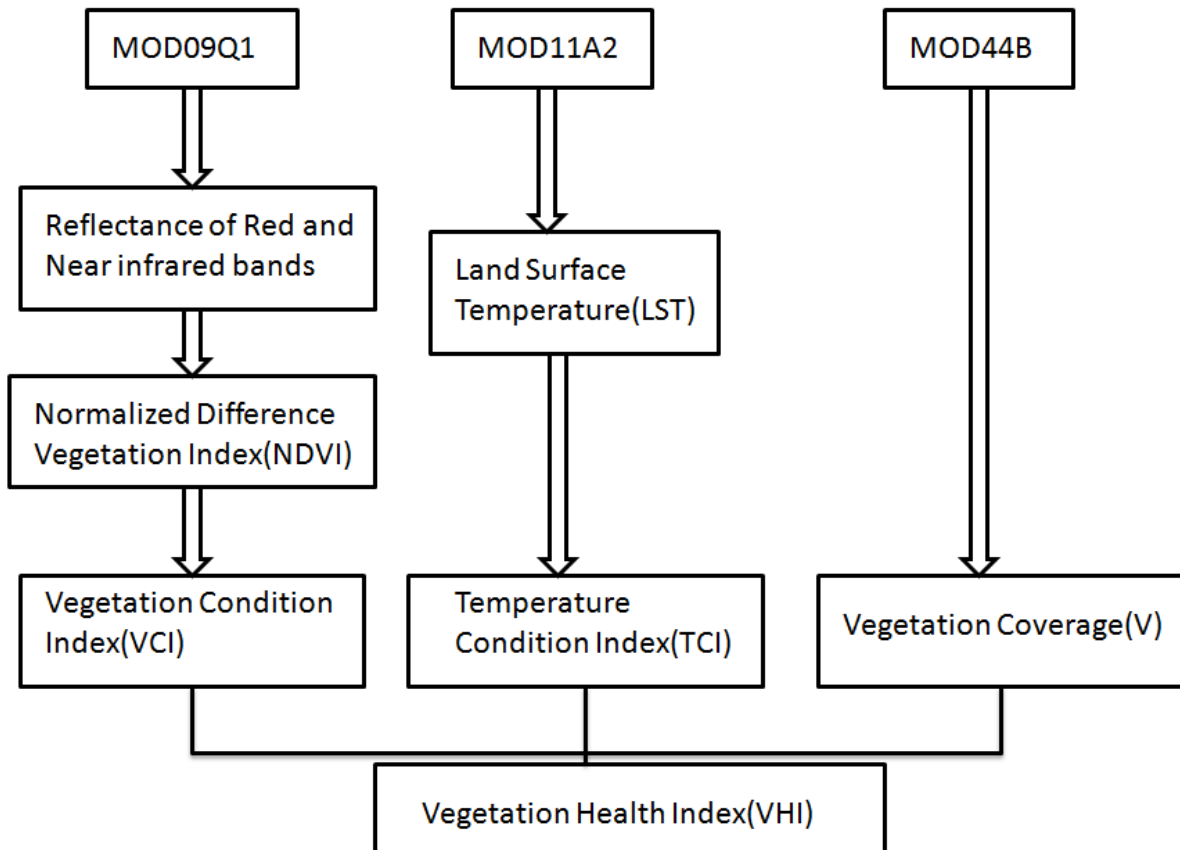


Figure 3: Methodological framework.

### 3.3.1 DATA PRE-PROCESS

MOD09Q1, MOD11A2 and MOD44B were acquired from NASA's Earth Observing System Clearing House (ECHO). The website is [http://reverb.echo.nasa.gov/reverb/#utf8=%E2%9C%93&spatial\\_map=satellite&spatial\\_type=rectangle](http://reverb.echo.nasa.gov/reverb/#utf8=%E2%9C%93&spatial_map=satellite&spatial_type=rectangle). MOD09Q1 and MOD11A2 were downloaded for four growing seasonal months: June, July, August and September from year 2000 to 2012. The study area was covered by four scenes of MODIS images and every month sixteen images were collected for each product. Because of a power outage in June 2001 and satellite problem in 2000, some of the data were missing for both products. MOD44B were

available only from 2000 to 2010 and all of them were downloaded. The study area was also covered by four scenes and finally 44 images were collected.

MODIS Reprojection Tool (MRT) was applied to process the downloaded data. The image processing began with image mosaic. Four scenes acquired at the same date, which covered the study area, were mosaicked into one file. Then the projection system of the output file was transformed from Sinusoidal projection to Universal Transverse Mercator (UTM) projected coordinate system, zone 16 north with datum WGS 1984. Finally, MRT wrote the output to tagged image file format (TIF) so that these data can be read in ArcMap and ERDAS Imagine. Since the number of images was very large, two batch files were written to conduct transformation of map projection and coordinate systems and to realize the mosaic of images for each product. The codes of the batch files for MOD09Q1 are displayed here as examples (Figure 4 and Figure 5).

```
set MRTDATADIR=C:\MRT\data
set /a DAY=2000161 rem **batch data start time**
set /a DEADLINE=2000281 rem **batch data end time**
:start
if %DAY% leq %DEADLINE% (goto ORDER) else exit
:ORDER
rem **save the file name into a notepad**
dir %%DAY%.*.hdf/a/b/s > MOSAICINPUT.TXT
rem **execute mosaic **
rem set the mrtmosaic.exe directory.
c:/mrt/bin/mrtmosaic.exe -i MOSAICINPUT.TXT -s "0 0 1" -o MOSAIC_TMP_%DAY%.hdf
rem **copy the result to a file and delete the input data**
copy MOSAIC_TMP_%DAY%.hdf Result MOSAIC_TMP_%DAY%.hdf
set /a DAY= %DAY% + 8
goto start
```

Figure 4: Batch Java code for mosaic process of MODIS images.

```

INPUT_FILENAME = R:\GEOG300\gfeng\MOD09Q1\2001\data\MOSAIC_TMP_2001161.hdf
SPECTRAL_SUBSET = ( 1 1 )
SPATIAL_SUBSET_TYPE = INPUT_LAT_LONG
SPATIAL_SUBSET_UL_CORNER = ( 49.999999996 -124.457906126 )
SPATIAL_SUBSET_LR_CORNER = ( 29.999999997 -69.282032295 )
OUTPUT_FILENAME = R:\GEOG300\gfeng\MOD09Q1\2001\data\1.tif
RESAMPLING_TYPE = NEAREST_NEIGHBOR
OUTPUT_PROJECTION_TYPE = UTM
OUTPUT_PROJECTION_PARAMETERS = (
  87.0 0.0 0.0
  0.0 0.0 0.0
  0.0 0.0 0.0
  0.0 0.0 0.0
  0.0 0.0 0.0 )
DATUM = WGS84
UTM_ZONE = 16

```

---

```

set MRTDATADIR=C:\mrt\data
for %%i in (*.hdf) do c:\mrt\bin\resample -p project.prm -i %%i -o %%iout.tif

```

Figure 5: Batch java codes for reprojection parameters.

### 3.3.2 TCI, VCI AND NDVI

The data acquired from first procedure covered a larger area and the images that only covered study area were extracted with raster calculation function of ArcMap. The temperature condition index (TCI) was produced by the land surface temperature (LST) images. The TCI was proposed to estimate the thermal impact of drought. It was computed as

$$TCI_i = \frac{T_{max} - T_i}{T_{max} - T_{min}} \quad (1)$$

Where  $T_i$  is the 8-day temperature,  $T_{\max}$  and  $T_{\min}$  are the absolute maximum and minimum temperature, respectively, calculated for each pixel and 8-day period during the time period 2000 to 2012. The values of TCI vary from 0 to 1. The low values of TCI imply serious condition of drought.

Using the reflectance values of band 1 and band 2 images, 8-day NDVI values from June to September were calculated using following expression:

$$NDVI = \frac{NIR-RED}{NIR+RED} \quad (2)$$

Since NDVI values can be seriously influenced by cloud and other factors, the NDVI data were pre-processed. Quality data was employed to identify and discard low-quality pixels. Then the mean value for the period 2000-2012 of each pixel was calculated without the bad data. In the end, the pixels of poor quality were filled with corresponding mean values and the pre-processed NDVI images served as an input for the computation of vegetation condition index (VCI). The VCI is a pixel-wise normalization of NDVI, which filters out the contribution of local geographic resources to the spatial variability of NDVI in relative assessment of NDVI signal changes (Quiring and Ganesh, 2009). The following expression was used for computing the VCI:

$$VCI_i = \frac{NDVI_i - NDVI_{\min}}{NDVI_{\max} - NDVI_{\min}} \quad (3)$$

Where  $NDVI_i$  is the pre-processed 8-day NDVI,  $NDVI_{\min}$  and  $NDVI_{\max}$  are the absolute minimum and maximum values, respectively, calculated for each pixel and 8-day period during the time period 2000-2012. The values of VCI range from 0 to 1. The low values

indicate stressed vegetation condition and the high values indicate good vegetation condition.

NDVI anomaly (z-value) was also calculated to assess the departure from long-term average value for each pixel during the time period 2000 to 2012. The Z value accounts for the anomaly of vegetated areas compared to normal condition.

$$Z_i = \frac{NDVI_i - \overline{NDVI}}{\sigma_{NDVI_i}} \quad (4)$$

Where  $NDVI_i$  is the pre-processed 8-day NDVI,  $\overline{NDVI}$  is the multiyear average value and  $\sigma_{NDVI_i}$  is the standard deviation.

### 3.3.3 VEGETATION COVERAGE AND VHI

On the base of VCI and TCI, VHI can be calculated by the following expression:

$$VHI = \alpha \times VCI + (1 - \alpha) \times TCI \quad (5)$$

Where  $\alpha$  and  $(1-\alpha)$  indicate the relative contribution of VCI and TCI to the value of VHI, respectively. In the previous studies, equal values of  $\alpha$  are used to account for the contributions of both VCI and TCI. However, the impacts of the same temperature and the same time period of drought vary depending on how an area is vegetated. On the other hand, in an urbanized area that is not vegetated the impact of drought is mainly determined by temperature. In this study,  $\alpha$  was computed with the vegetation coverage for each pixel. For pixels of dense vegetation coverage, drought assessment relies more on the information provided by vegetation condition and therefore the contribution

of VCI in VHI increases as the vegetation coverage increases. For pixels of little vegetation coverage, drought assessment relies more on the information provided by temperature condition and therefore the contribution of TCI increases as the vegetation coverage decreases.

To acquire the vegetation and soil fraction for each pixel, spectral mixture analysis (SMA) (for example, Lu et al., 2003) has been applied to MOD09Q1 products with ENVI. SMA is a technique based on modeling image spectra as the linear combination of endmembers and has been used to derive the fractional contribution of endmember materials to image spectra in a wide variety of applications (Dnnison and Roberst, 2003). In SMA models, the reflectance of a pixel  $\rho_\lambda$  is determined by the sum of the reflectance values of each material within a pixel multiplied by its fractional cover:

$$\rho_\lambda = \sum_{i=1}^N f_i \times \rho_{i\lambda} + \varepsilon_\lambda \quad (6)$$

Where  $\rho_{i\lambda}$  is the reflectance of the  $i^{\text{th}}$  endmember,  $\lambda$  is a specific band,  $f_i$  is the fraction of the  $i^{\text{th}}$  endmember,  $N$  is the number of endmembers, and  $\varepsilon_\lambda$  is the residual error. The modeled fraction of the endmembers are commonly constrained by:

$$\sum_{i=1}^N f_i = 1 \quad (7)$$

Model fit is assessed using the model residuals  $\varepsilon_\lambda$  or the root mean squared error (RMSE):

$$RMSE = \sqrt{\frac{\sum_{i=1}^N (\varepsilon_\lambda)^2}{N}} \quad (8)$$

SMA assumes single interaction between photons and surface, producing linear mixing of the surface fractions and their reflectance. Its limitation lies in the inability to

account for on-linear mixing (Adams et al., 1993). But, for large areas, the mixing is very linear and approximations of the linear unmixing techniques appear to work well (Boardman and Kruse, 1994).

The whole unmixing process was implemented with ENVI software. MODIS image was selected as input data instead of Landsat image because the Landsat image, which can cover the whole state, occupied too much space and current ENVI did not work. The unmixing process includes the following procedures: (1) determining the inherent dimensionality of the data with the Minimum Noise Fraction (MNF) transform; (2) Deriving the Pixel Purity Index (PPI) to identify endmembers; (3) Selecting pure pixels with the n-D Visualizer; (4) Building model with the pure pixels and applying to the whole image to acquire the vegetation percent of every pixel. However, the result image was not accurate while comparing to the aero photos of some counties. The possible reason was that the spatial resolution of MODIS image was coarse and the area that was presented by single pixel usually contained more than one kind of physical material, such as water and land. Therefore the pure pixel selected in this way actually was not “pure” and the errors occurred in the model. To avoid above situation, the vegetation coverage information was extracted directly from MOD44B. The products only cover 11 years from 2000 to 2010. For 2011 and 2012, the vegetation coverage data was extracted from the image of 2010 since the change in vegetation coverage is relatively small over a short period of time. And the products were produced by linear and non-linear spectral mixture analysis as described above.

For each pixel with vegetation coverage  $V$ , the contribution factor  $\alpha$  was computed as:

$$\alpha = \frac{V}{100} \quad (9)$$

$$1 - \alpha = \frac{100-V}{100} \quad (10)$$

Therefore the expression of VHI can be transformed to

$$VHI = \frac{V}{100} \times VCI + \frac{100-V}{100} \times TCI \quad (11)$$

The modification is based on the idea that the vegetation coverage is an important factor while assessing the drought condition. For areas of dense vegetation coverage, such as forest, the contribution factor  $\alpha$  is high and therefore the vegetation health index relies more on the information of vegetation. For areas of sparse vegetation coverage, such as urban area, the contribution factor  $\alpha$  is low and therefore the vegetation health index relies more on the information of temperature.

### 3.3.4 COMPARISON WITH USDM MAPS

The mean values of VHI, VCI and TCI for the whole state every month during the time period from 2000 to 2012 were computed to provide more comprehensive understanding of the changing trend and variations. The annual average values of VHI, VCI and TCI were derived to identify the differences among these three indices. Cook county and Pope County were selected as the representatives of areas with dense vegetation coverage and with little vegetation coverage. The mean values of VHI for these two counties were computed and compared. Another comparison was



implemented between the VHI maps, NDVI-z maps, USDM maps and unmodified VHI maps, which were produced for similar time period.

## CHAPTER 4

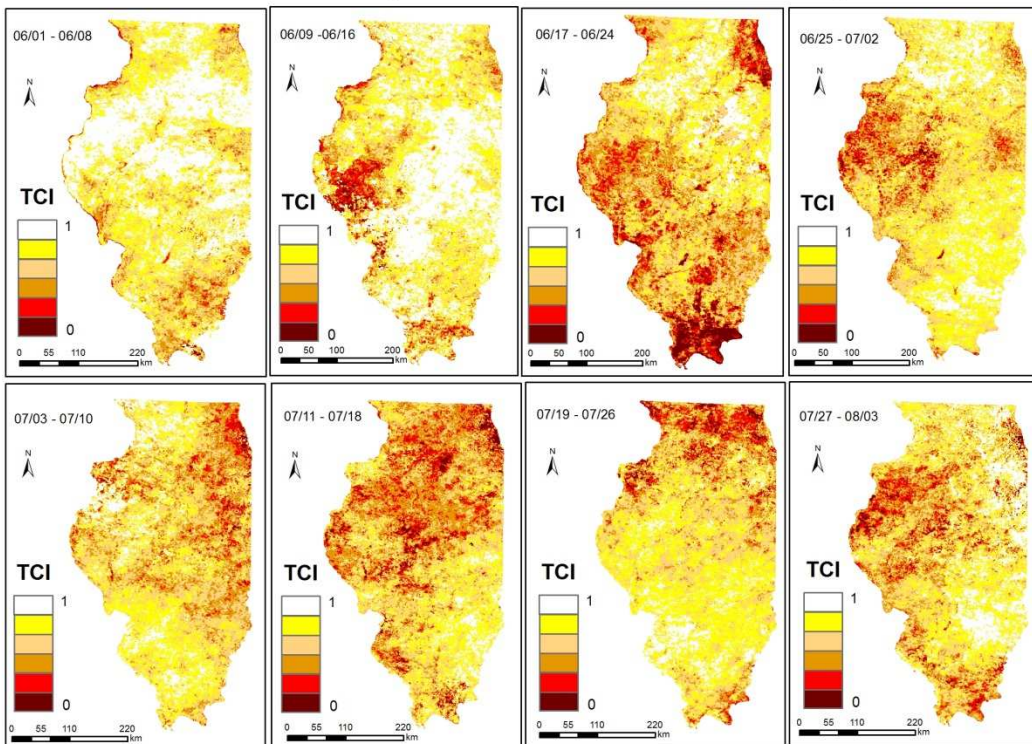
### RESULTS AND ANALYSIS

#### 4.1 TEMPERATURE CONDITION INDEX (TCI)

The 8-day TCI maps at 1 km spatial resolution were produced using MODIS land surface temperature product (MOD11A2) for the time period 2000 to 2012 (Appendix A). The value of TCI ranges from 0 to 1. The low values represent high temperature condition and the high values imply low temperature conditions. In the maps, the darker color indicates hotter conditions for the responding area. The maps are updated for every 8 days and 16 maps were derived for June, July, August and September of each year. A total of 208 TCI maps were obtained for a time period of 13 years from 2000 to 2012. The first row of maps represents the temperature condition in June. The second row shows the temperature condition of July. The third and fourth rows indicate the condition in August and September. To display the variation of TCI with time and spatial distribution, the TCI maps for 2010, and 2012 were shown in Figures 6 and 7, respectively. The reason for selection of these three years was mainly because the years of 2010 and 2012 represent the normal and dry year, respectively, based on climate data.

The maps in Figure 6 show the evolution of temperature condition from June to September in 2010. Overall, the colors of the first, second and third row maps look quite light and therefore the temperature was relatively low in June and July. The temperature started to increase in the middle of August and continued in September as the dark color of some area shows.

## 2010 Illinois Temperature Condition Index Map I



## 2010 Illinois Temperature Condition Index Map II

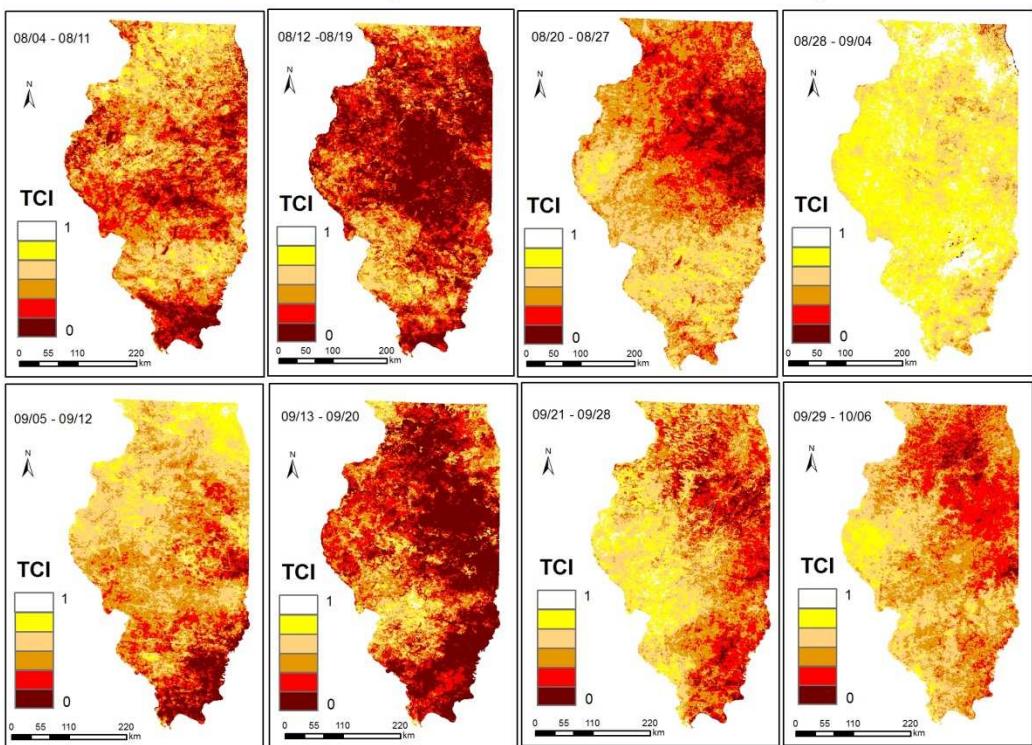
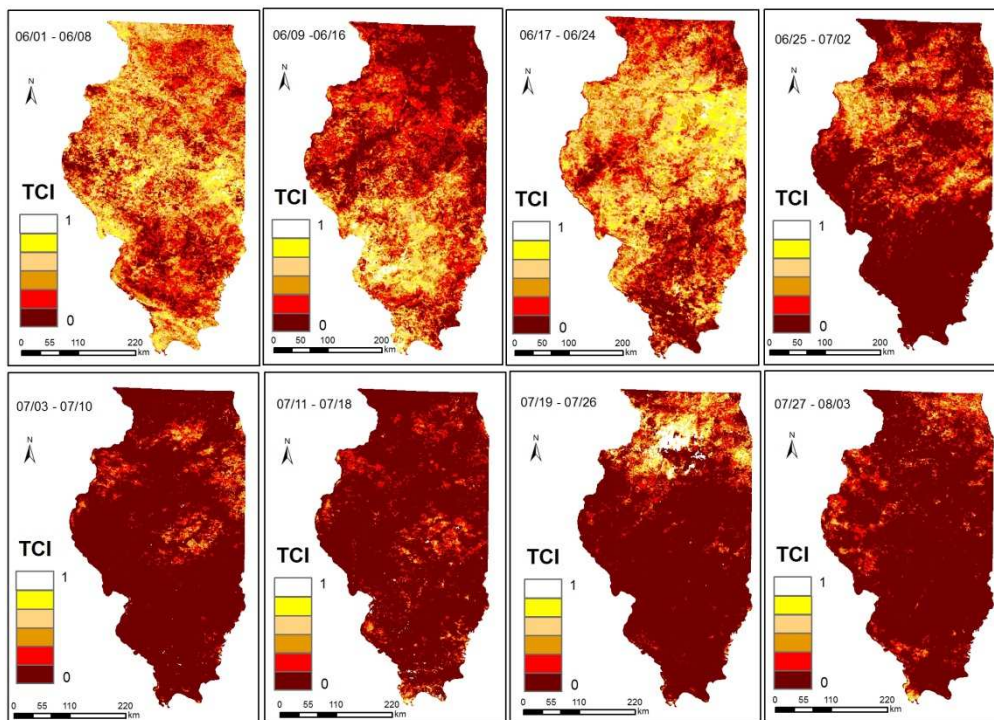


Figure 6: 2010 Illinois Temperature Condition Index Maps.

The maps in Figure 7 show the evolution of temperature condition from June to September in 2012. Compared to the maps in Figures 7 for years 2010, it is obvious that the temperature was abnormal during June, July and September. The dark colors covering most areas of Illinois indicated very low TCI values and very high temperature during that period. Especially in July, the dark umber color covered nearly the whole state and shows the extreme temperature condition. In September, the weather started to become better with lower temperature.

2012 Illinois Temperature Condition Index Map I



## 2012 Illinois Temperature Condition Index Map II

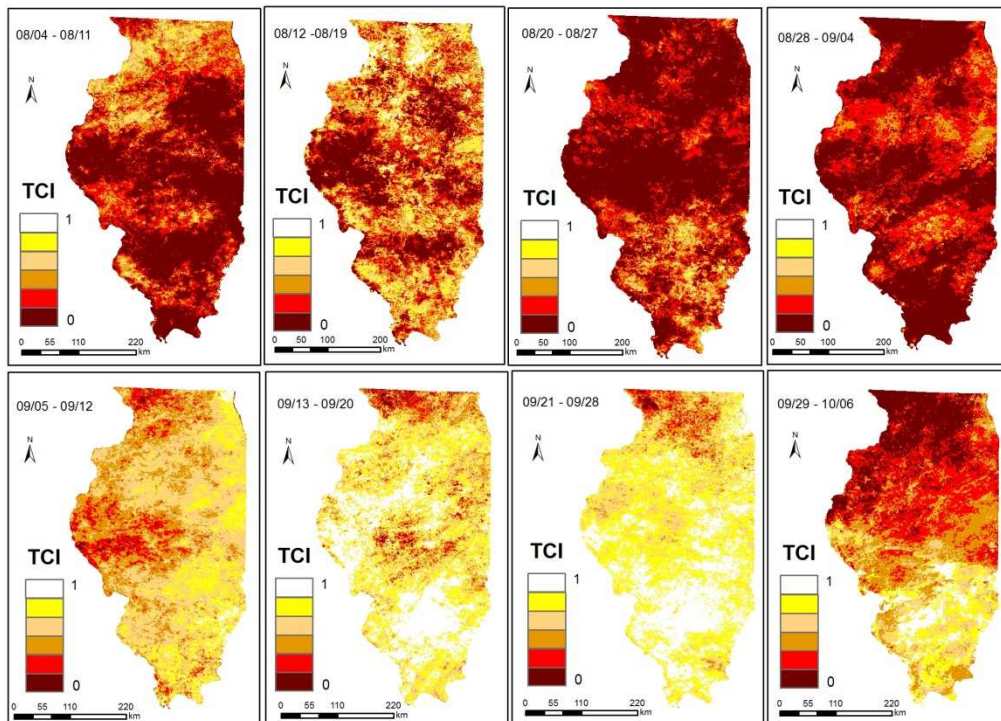


Figure 7: 2012 Illinois Temperature Condition Index Maps.

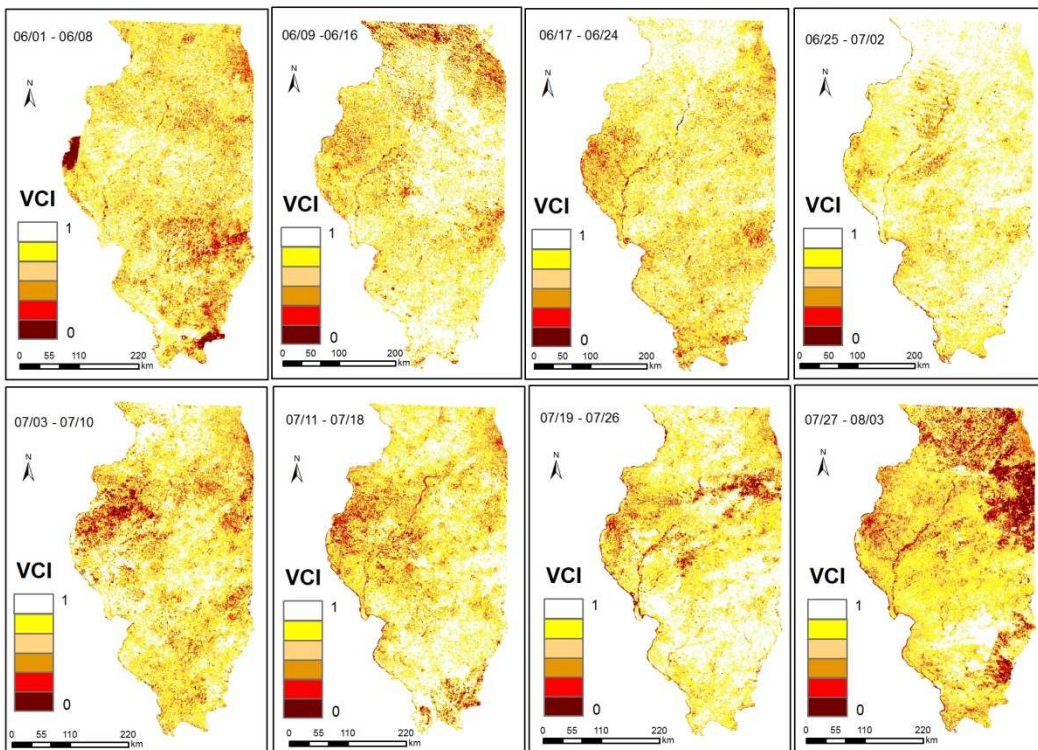
Overall, the years 2002, 2005, 2007, and 2012 had the condition of high temperature and other years the temperatures were low (Appendix A). The late June and beginning of September in 2002 had higher temperature. In 2005, high temperature took place through the whole time period of June to September, especially at the beginning of September. In 2007, high temperature mainly happened in August and September, also on June 9 to 16. Extremely high temperature condition existed in June July and August of 2012 and the temperature started to become normal until September.

## 4.2 VEGETATION CONDITION INDEX (VCI)

The 8-day VCI maps at a spatial resolution of 250 m × 250 m were produced based on NDVI obtained from MODIS MOD09Q1 products (red and near infrared bands) for the time period 2000 to 2012 (Appendix B). The value of VCI ranges from 0 to 1. The low values represent stressed vegetation condition and the high values imply favorable vegetation conditions. In the maps, dark color represents low VCI values and light color represents high VCI values. The maps are updated every 8 days for June, July, August and September of each year. They are arranged in appendix B with the same order of the above TCI maps. In Figures 8 and 9, the TCI maps for 2010 and 2012 are shown as examples to account for the variation of VCI over time and space.

In Figure 8, the maps show the spatial distribution and temporal dynamics of vegetation condition from June to September for year 2010. In June and July, the red and dark umber color only covered small areas for a short period of time and the overall vegetation condition was good. However, from the end of August, the areas of stressed vegetation condition started to expand from the central areas to the most parts of Illinois. The vegetation condition was worse in September as red color stayed in those areas for the whole month.

## 2010 Illinois Vegetation Condition Index Map I



## 2010 Illinois Vegetation Condition Index Map II

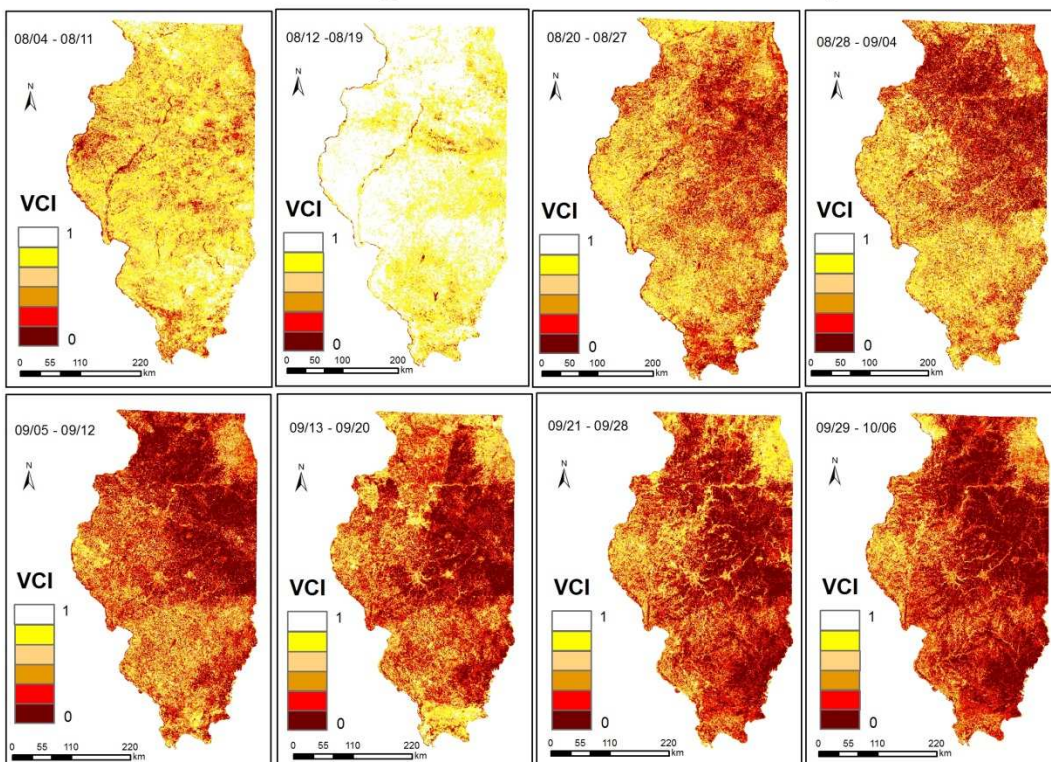
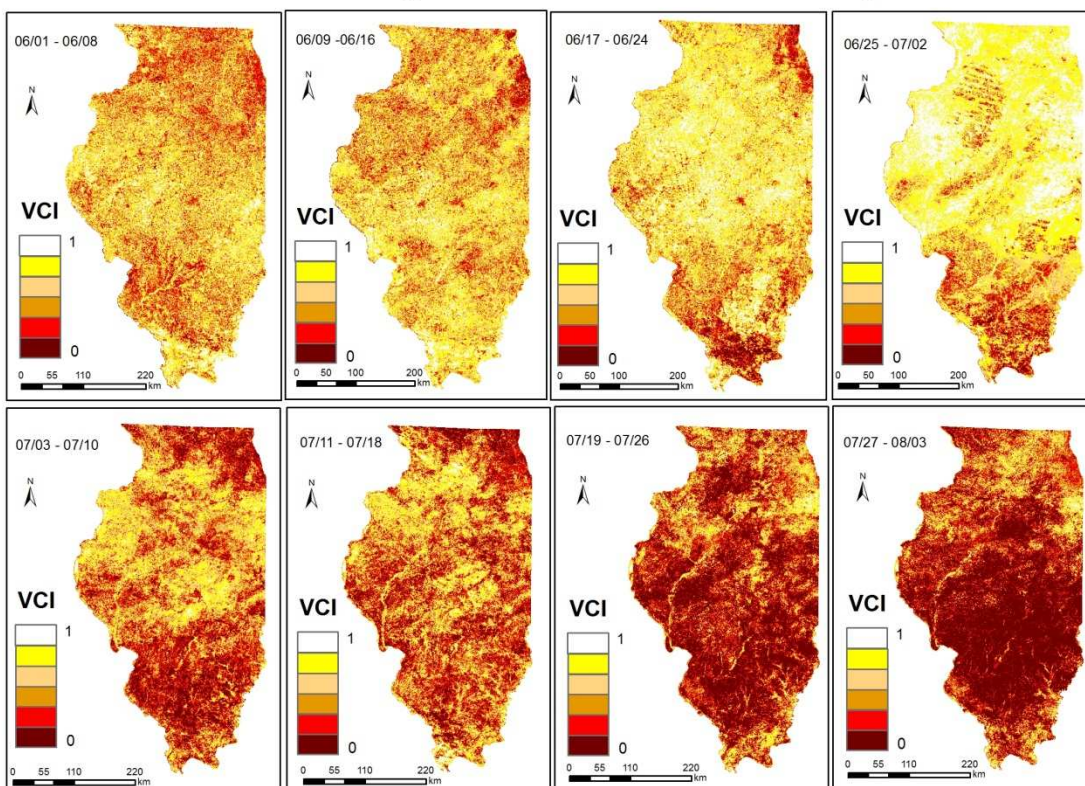


Figure 8: 2010 Illinois Vegetation Condition Index Maps.

The maps in Figure 9 show the evolution of vegetation condition from June to September in 2012. Overall, the red and dark umber colors covered most of the state from June to September in 2012, and only June 25<sup>th</sup> to July 2<sup>nd</sup> and August 12<sup>th</sup> to 19<sup>th</sup> showed relatively good vegetation condition. This implied the potential drought intensity shown by the VCI vegetation condition was much worse in 2012 than 2010 for this time period of June to September.

### 2012 Illinois Vegetation Condition Index Map I





## 2012 Illinois Vegetation Condition Index Map II

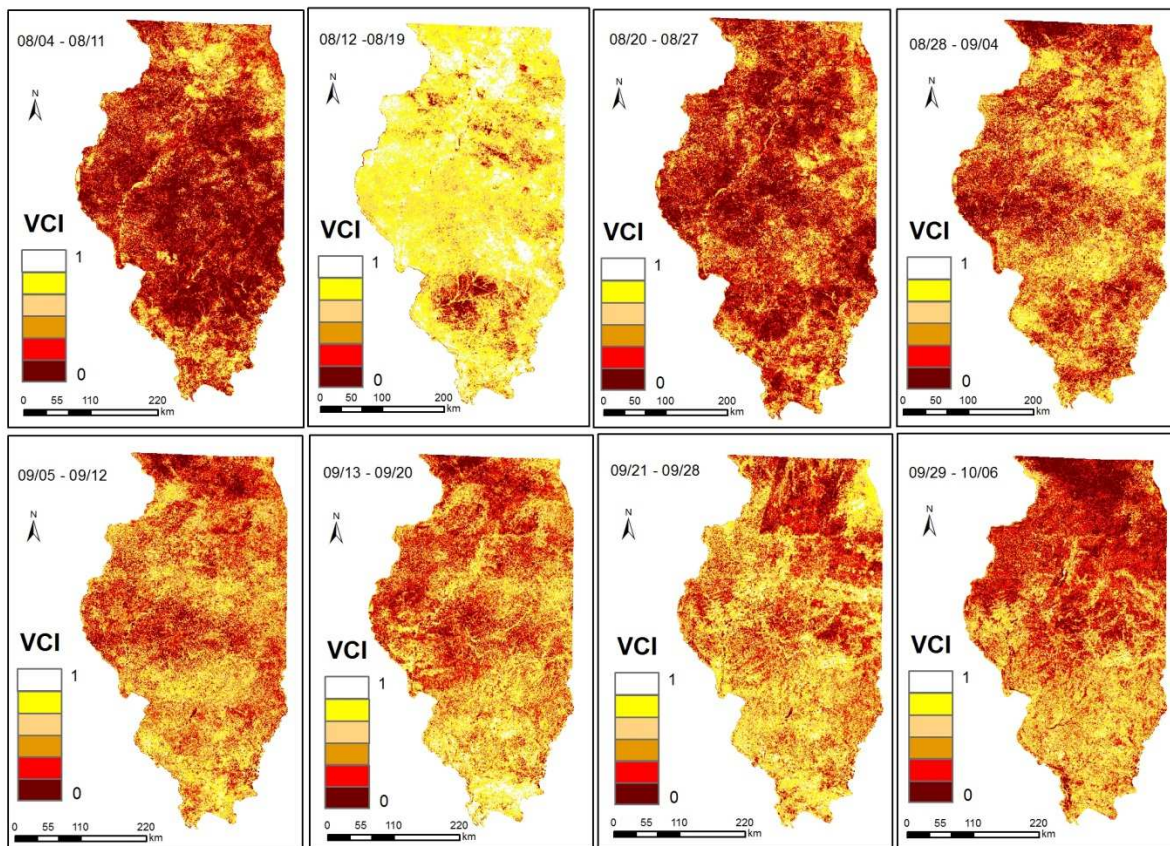


Figure 9: 2012 Illinois Vegetation Condition Index Maps.

Overall, the years 2002, 2005, 2007, 2010, and 2012 had more stressed vegetation condition than the other years (Appendix B). The worst case took place in 2012 in which there were strongly stressed vegetation conditions. Moreover, there was a trend that indicated the stressed vegetation condition often started in September for all the years except for 2003, 2008 and 2009.

### 4.3 NDVI ANOMALY

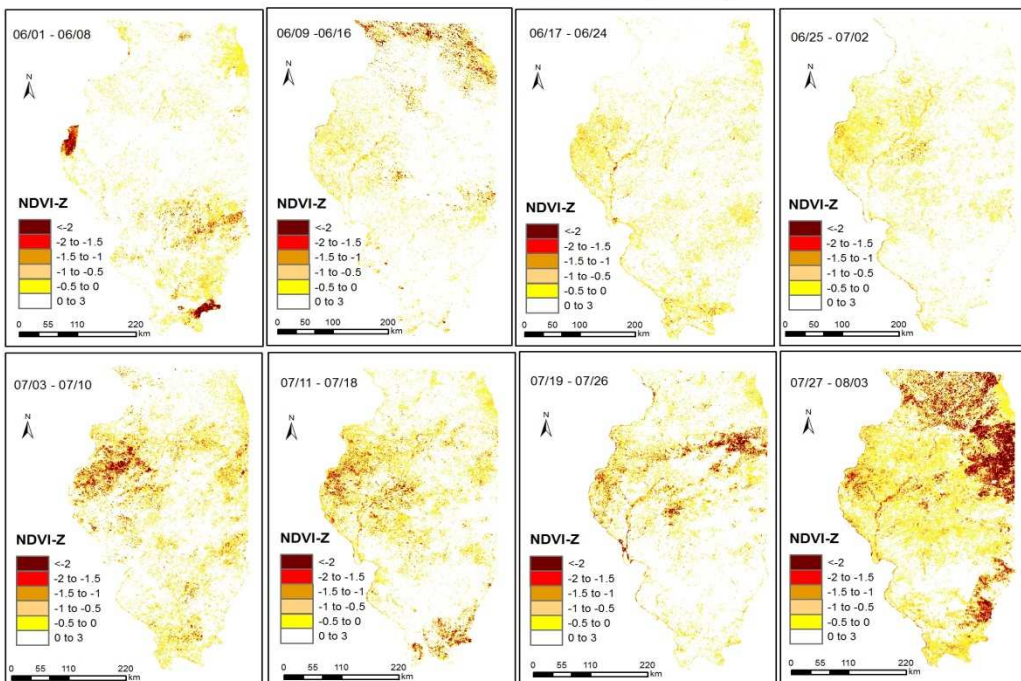
The 8-day NDVI anomaly (Z values) maps at a spatial resolution of 250 m × 250 m were produced by comparison with average NDVI in normal vegetation condition obtained from MOD09Q1 products (red and near infrared bands) for the time period of June to September for each of years 2000 to 2012 (Appendix D). The values of NDVI anomaly range from -3.5 to 3.5. The negative values represent below-normal vegetation condition and the positive values indicate good vegetation conditions. There are 16 maps obtained for each year. In Figures 10 to 11, the spatial distributions and temporal variation of NDVI anomaly were shown for 2010 and 2012, as examples.

The NDVI anomaly maps in Figure 10 show the spatial distribution and temporal dynamics evolution of NDVI anomaly for the whole state of Illinois from June to September in 2010. During June and July, the white color covered most of the state with dark color scattered in some small areas, which meant the vegetation condition was better than normal. In the late of August, the vegetation condition in some areas started to become worse and this bad vegetation condition was intensified during the whole September. The yellow and dark red colors covered the state, indicating the vegetation condition was worse than the normal. For September 6<sup>th</sup> to 12<sup>th</sup>, the serious vegetation condition dominated the northeast part.

The NDVI anomaly maps in Figure 11 show the spatial and temporal variability of NDVI anomaly for the whole state of Illinois from June to September in 2012. The vegetation condition in June was not as good as the previous years as almost the whole state was in yellow. In July and August, the vegetation condition became worse as the dark umber color covered most of the area. Then, it was gradually improved in September.

Overall, most of the years 2000 to 2012 had normal vegetation condition (Appendix D). The anomaly vegetation condition mainly took place in 2002, 2007, 2009, and 2012, especially in July and August of 2012. The NDVI anomaly maps could be used to identify and track the abnormal vegetation condition. However, without supplementary information, it is hard to confirm the real reason behind the phenomena. There are many possible causes, such as insect damage, flood and fire. Drought is definitely one of these. But more data is needed to rule out other possibilities.

2010 Illinois NDVI Anomaly Map I



## 2010 Illinois NDVI Anomaly Map II

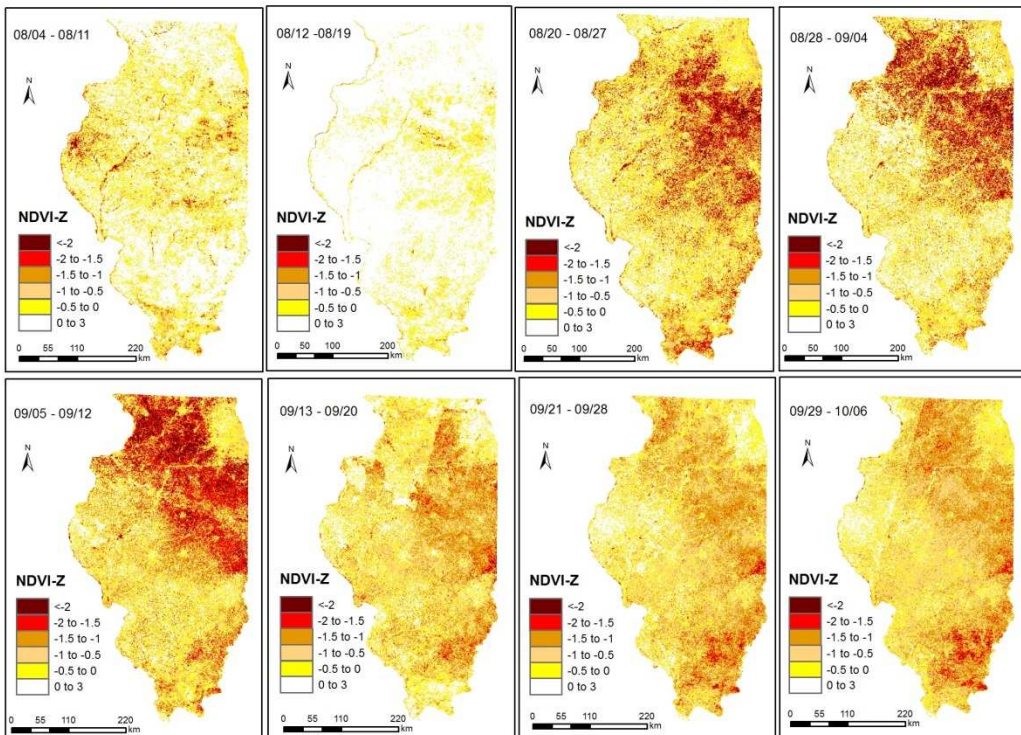
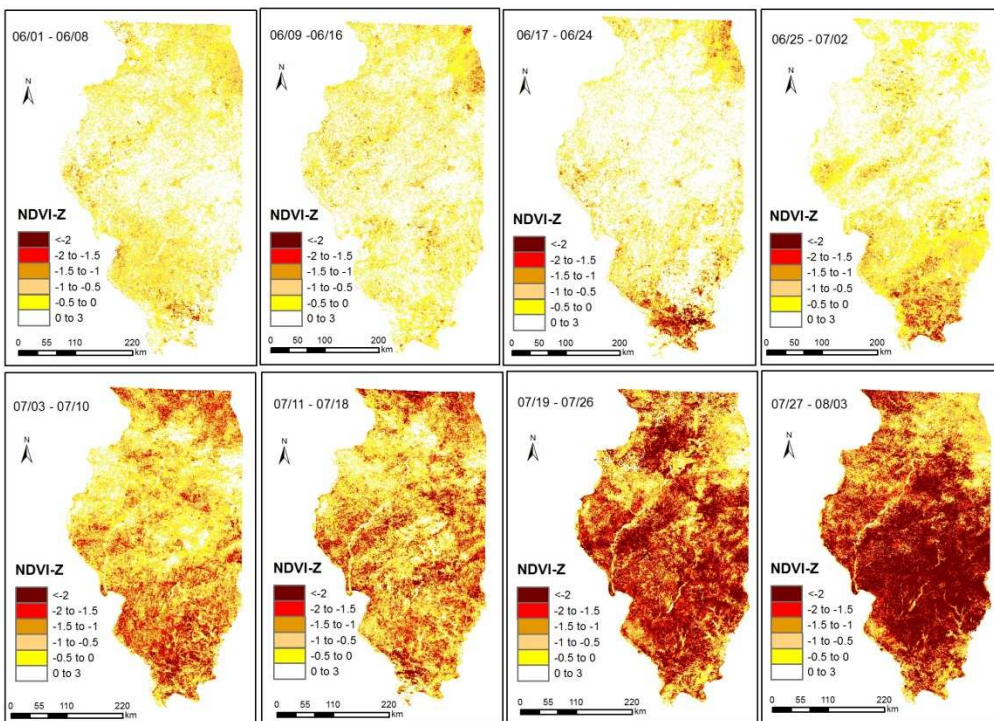


Figure 10: 2010 Illinois NDVI Anomaly Maps.

## 2012 Illinois NDVI Anomaly Map I



## 2012 Illinois NDVI Anomaly Map II

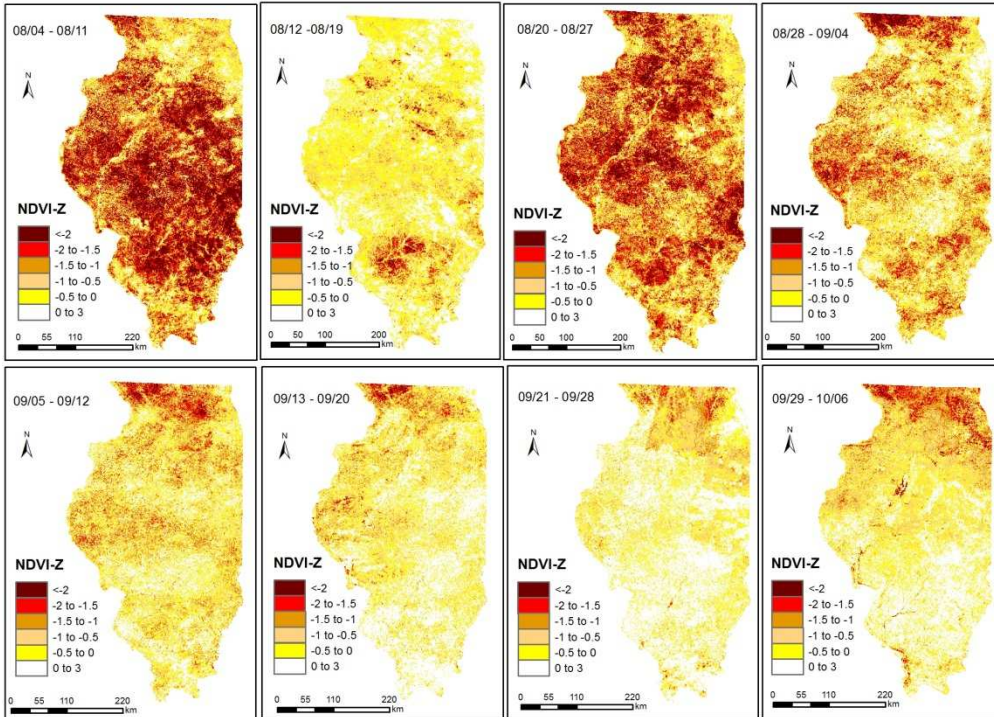


Figure 11: 2012 Illinois NDVI Anomaly Maps.

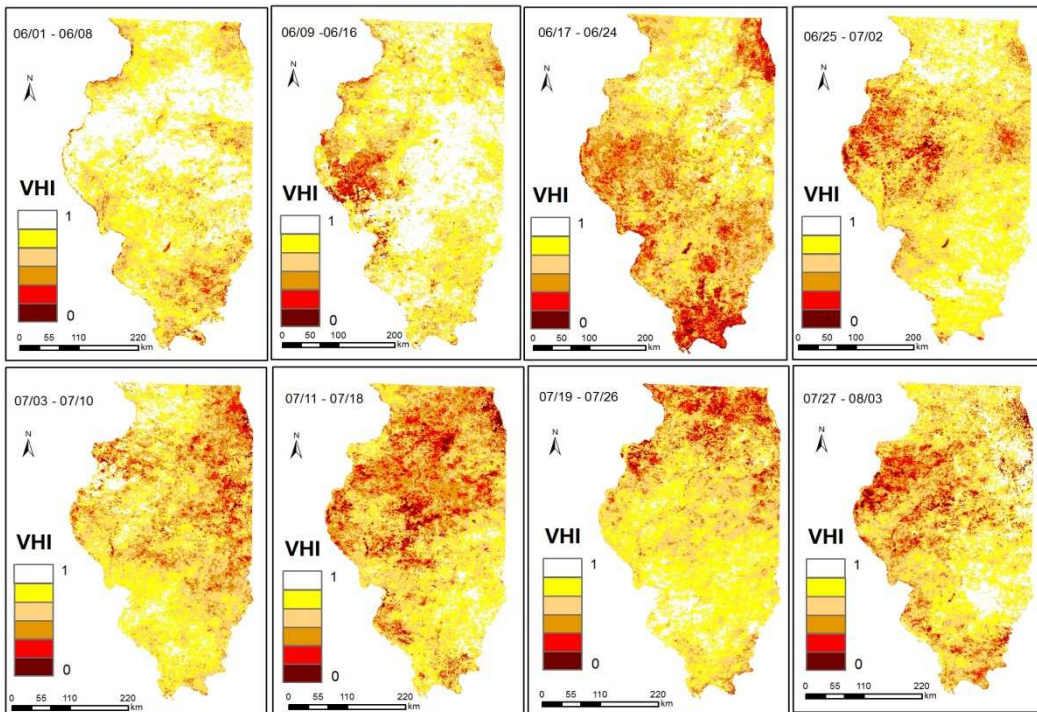
### 4.4 VEGETATION HEALTH INDEX (VHI)

The 8-days VHI maps at 1 km spatial resolution were produced using Eq. (11) based on the mentioned VCI maps and TCI maps for the time period of June to September for each of years 2000 to 2012 (Appendix C). Before that, the VCI maps were aggregated from a spatial resolution of 250 m  $\times$  250 m to 1 km  $\times$  1 km using a window average method. There were 16 maps created for each year and a total of 208 maps for the time period of years 2000 to 2012. The values of VHI vary from 0 to 1. The low values represent severe drought condition and the high values mean wet and favorable conditions. As examples, the VHI maps for 2010 and 2012 were presented in Figure 12 and 13 to show the spatial and temporal variation of VHI.

The maps in Figure 12 show the evolution of VHI for the whole state of Illinois from June to September in 2010. In June and July, most of the area had the values of VHI ranging from 0.67 to 0.83, implying good condition and the poor condition only happened in some scattered areas. In August and September, the dry condition overall became worse and the east central Illinois had severe drought condition from August 12<sup>th</sup> to 27<sup>th</sup> and September 13<sup>th</sup> to 20<sup>th</sup>. The extremely severe drought condition took place in 2012 (Figure 13). The drought condition started in June and became extremely serious in July. In August, more than half of the state still stayed in severe drought condition and the drought situation was then relieved in September as the VHI values turned to be higher than 0.5.

As mentioned in section of 4.1, the years 2010 and 2012 represented normal and dry year, respectively, based on climate data. The VHI maps in Figure 12 to 13 were able to track the changes of drought intensity among these two years. Especially for year 2012, the VHI values demonstrated the abnormal condition for most of the Illinois in July and August.

## 2010 Illinois Vegetation Health Index Map I



## 2010 Illinois Vegetation Health Index Map II

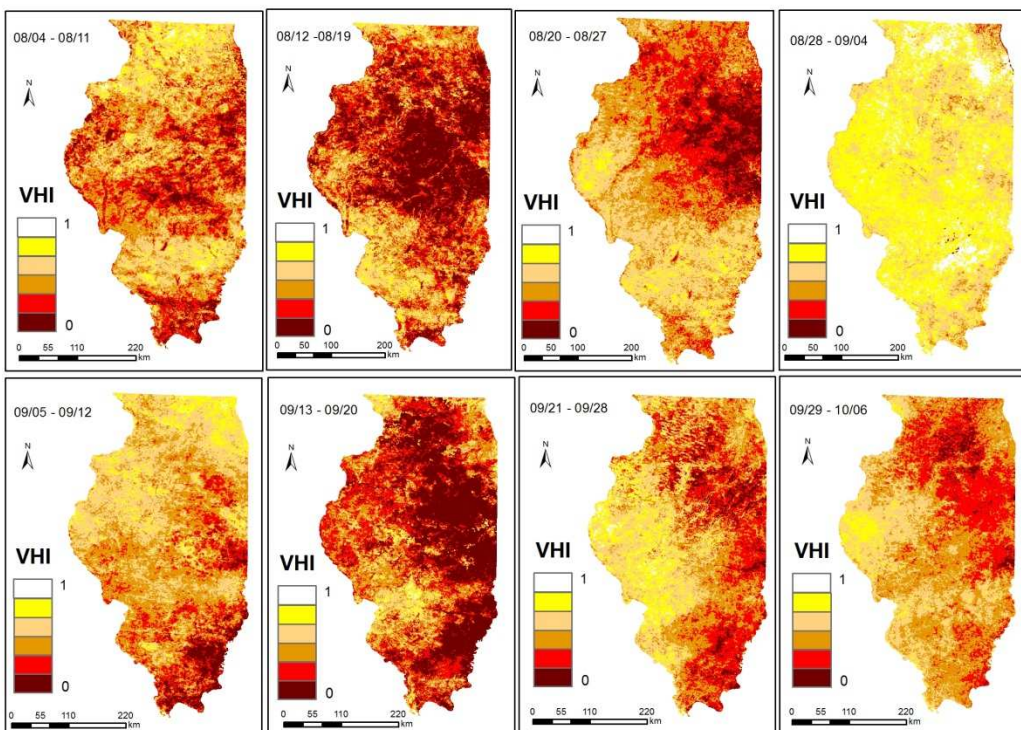
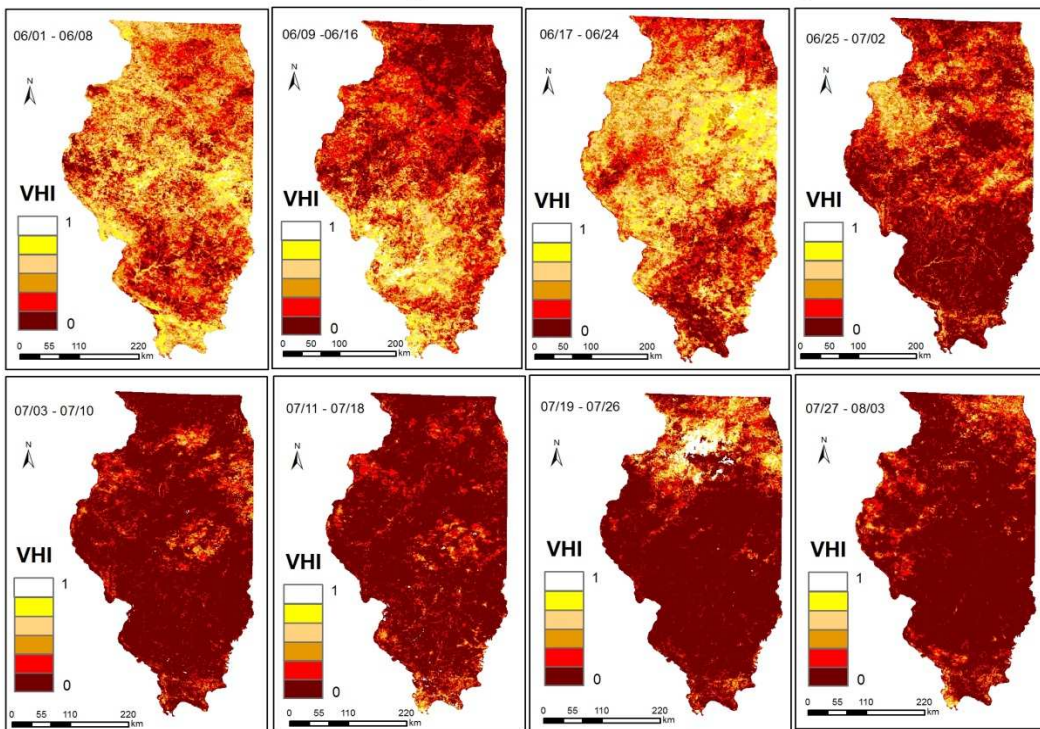


Figure 12: 2010 Illinois Vegetation Health Index Maps.

## 2012 Illinois Vegetation Health Index Map I



## 2012 Illinois Vegetation Health Index Map II

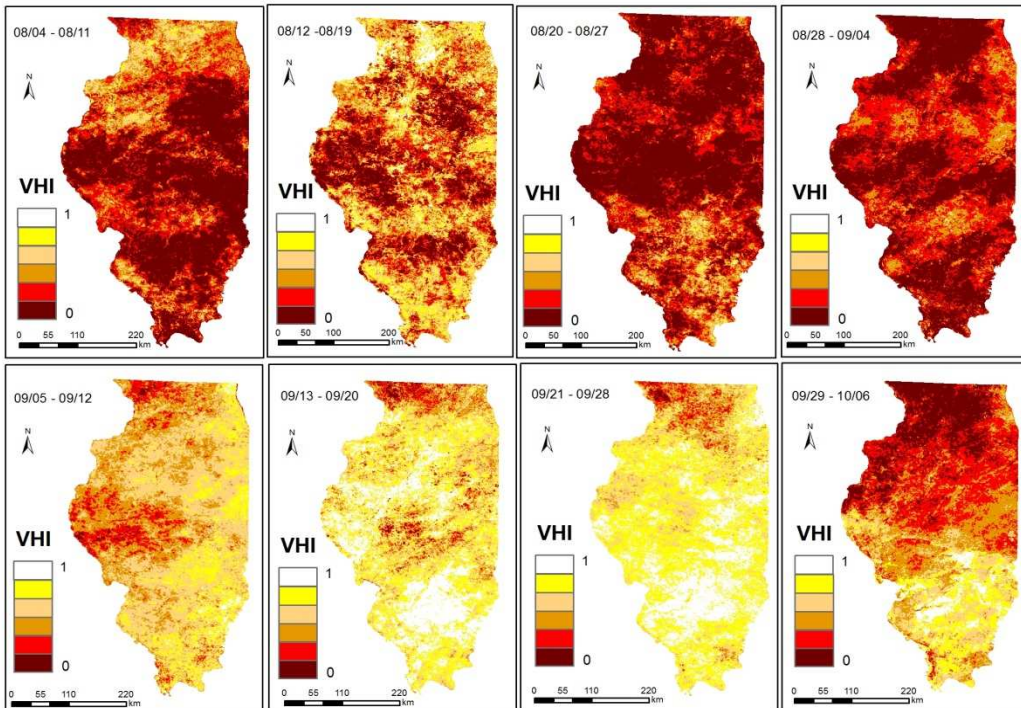


Figure 13: 2012 Illinois Vegetation Health Index Maps.



Figures 14 and 15 show the monthly average values of VHI for each of years 2000 to 2012 and overall monthly averages and standard deviations for Illinois based on the data with and without year 2012. Overall, the monthly average values of all the years except 2012 fell within the 2 standard deviations. Illinois experienced extreme drought in 2012 as showed both in Figure 14 and 15. In July, the month average VHI value of 2012 was as low as 0.083, out of the two standard deviation interval. Even in June and August, the monthly average VHI values were out of the one standard deviation interval. It is more obvious in the Figure 15 when the data of 2012 was not included in the computation of the overall mean and standard deviation. The drought intensity decreased a lot in September as the VHI value became higher than the average value. The overall monthly averages of VHI values were similar to each other for June, July, August and September, and the average for July was slightly higher than those for other months.

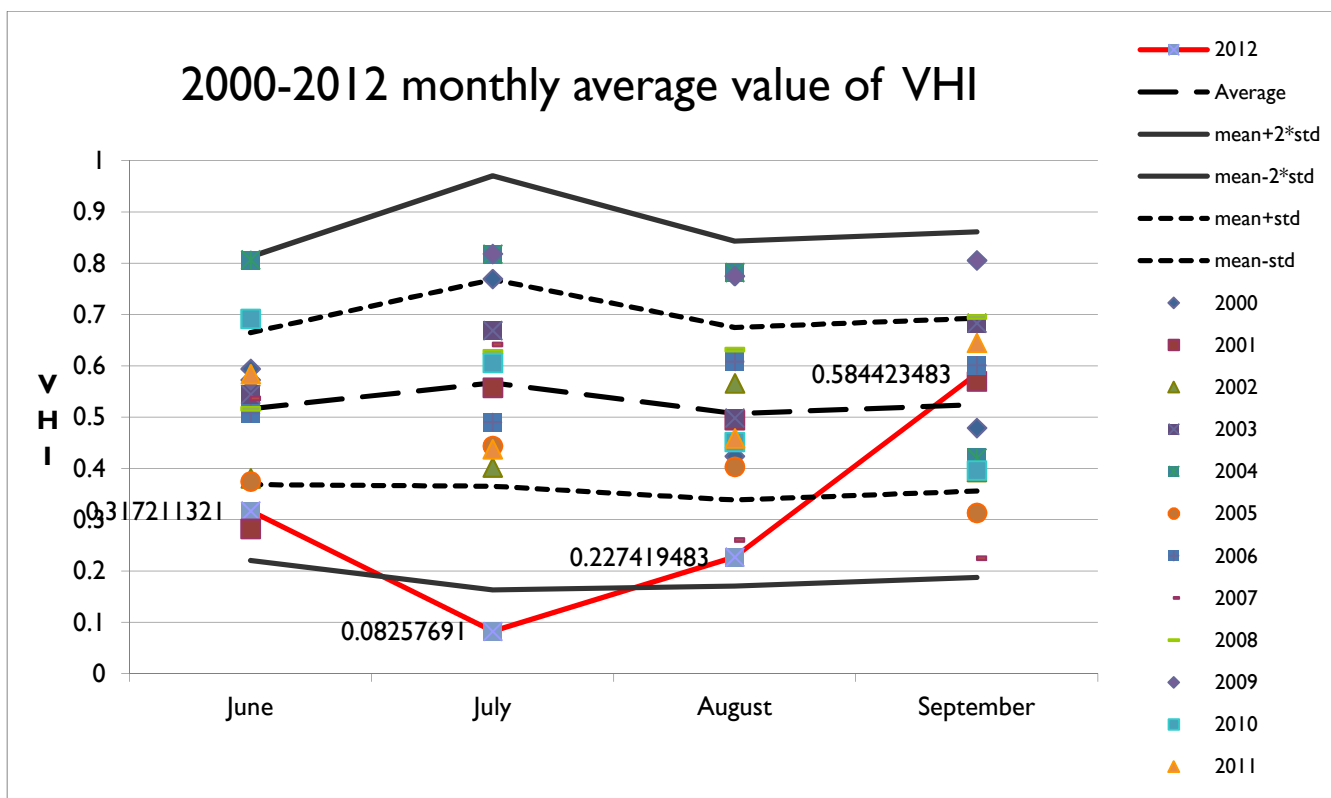


Figure 14: Monthly average values of VHI for each of the years 2000-2012 for Illinois with overall mean and standard deviation calculated based on the data with year 2012 involved.

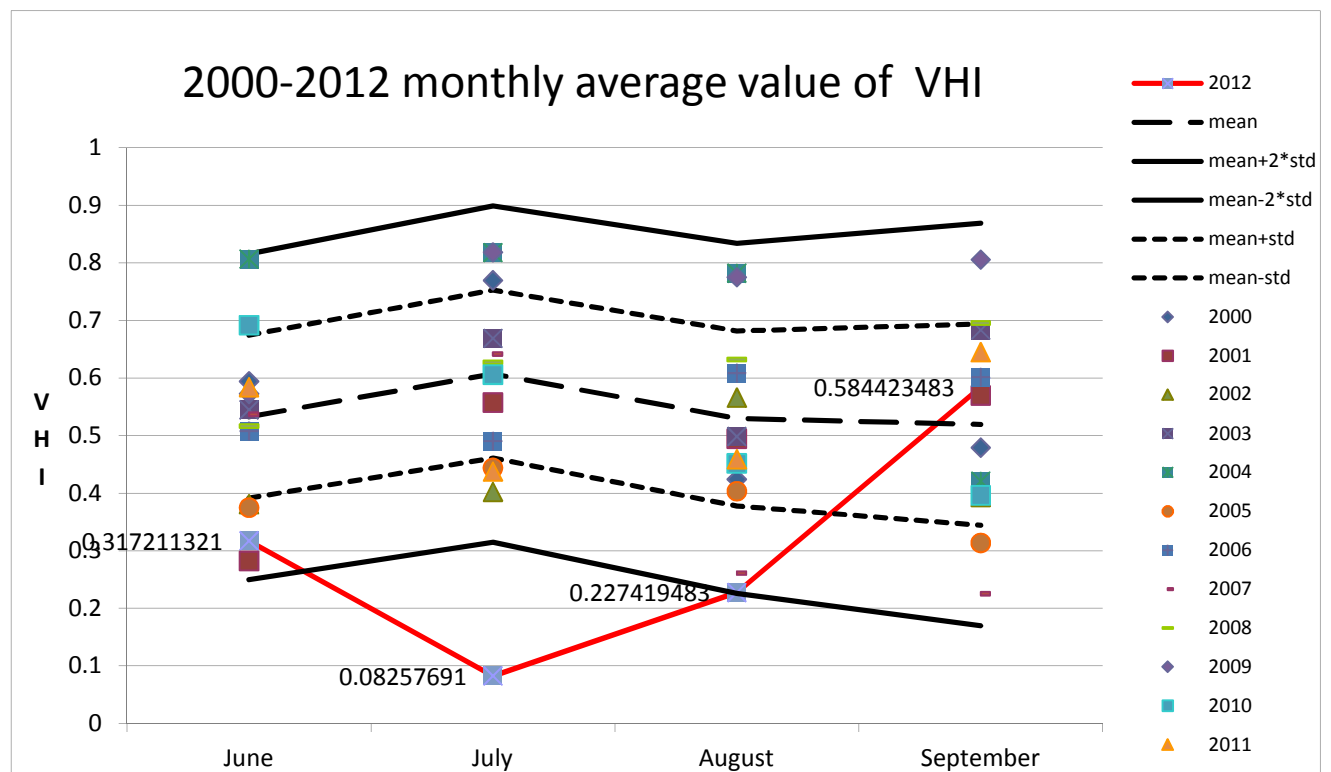


Figure 15: Monthly average values of VHI for each of the years 2000-2012 for Illinois with overall mean and standard deviation calculated based on the data with year 2012 excluded).

The monthly average values of TCI for each of the years 2000-2012 for Illinois with overall mean and standard deviation were presented in Figure 16. The TCI trends of monthly average values were similar to those of VHI. Obviously, the TCI value of 2012 July was 0.057, out of the two standard deviation interval. In June and August, the monthly TCI average values were also very low and they were out of one standard deviation interval. The temperature turned to normal level in September.

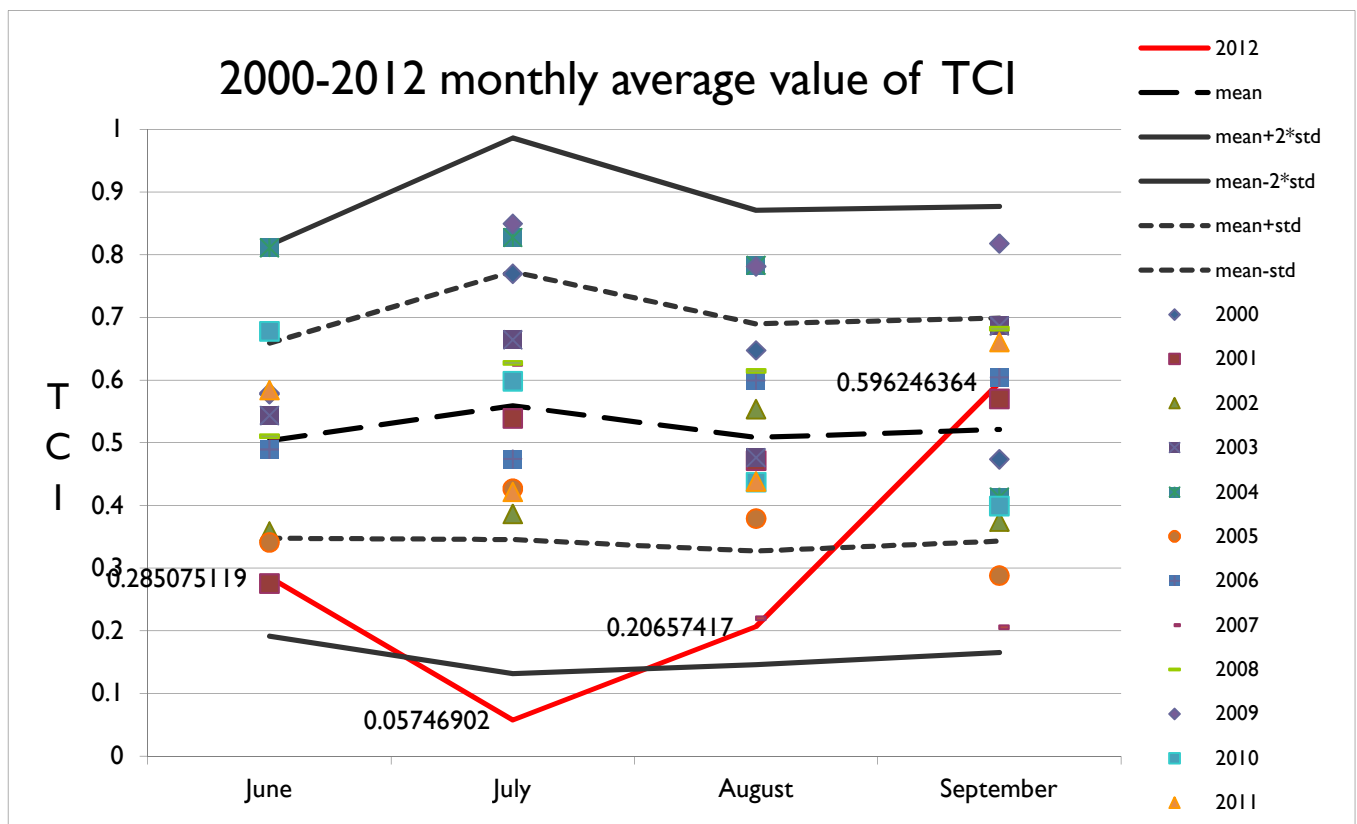


Figure 16: Monthly average values of TCI for each of the years 2000-2012 for Illinois with overall mean and standard deviation.

In Figure 17, the trends of monthly average VCI values looked different from those of TCI and VHI. For all the years except for 2012, the monthly average VCI had higher values in July and August and lower values in June and September. The higher VCI values imply better vegetation condition and vice versa. This suggested the monthly average trends looked reasonable because in Illinois vegetation generally starts growing in late April and reaches its peak in August. For the year 2012, the monthly average VCI values were slightly larger than the average value in June, then decreased to a very low value, out of the two standard deviation interval, and slightly increased. But, the VCI value was still low in August, out of the one standard deviation interval. This was mainly because in June of 2012 the temperature was high and vegetation grew very fast at the beginning, but the continuously high temperature without rain in July led to the severe drought condition that was revealed by the VCI, vegetation condition index.

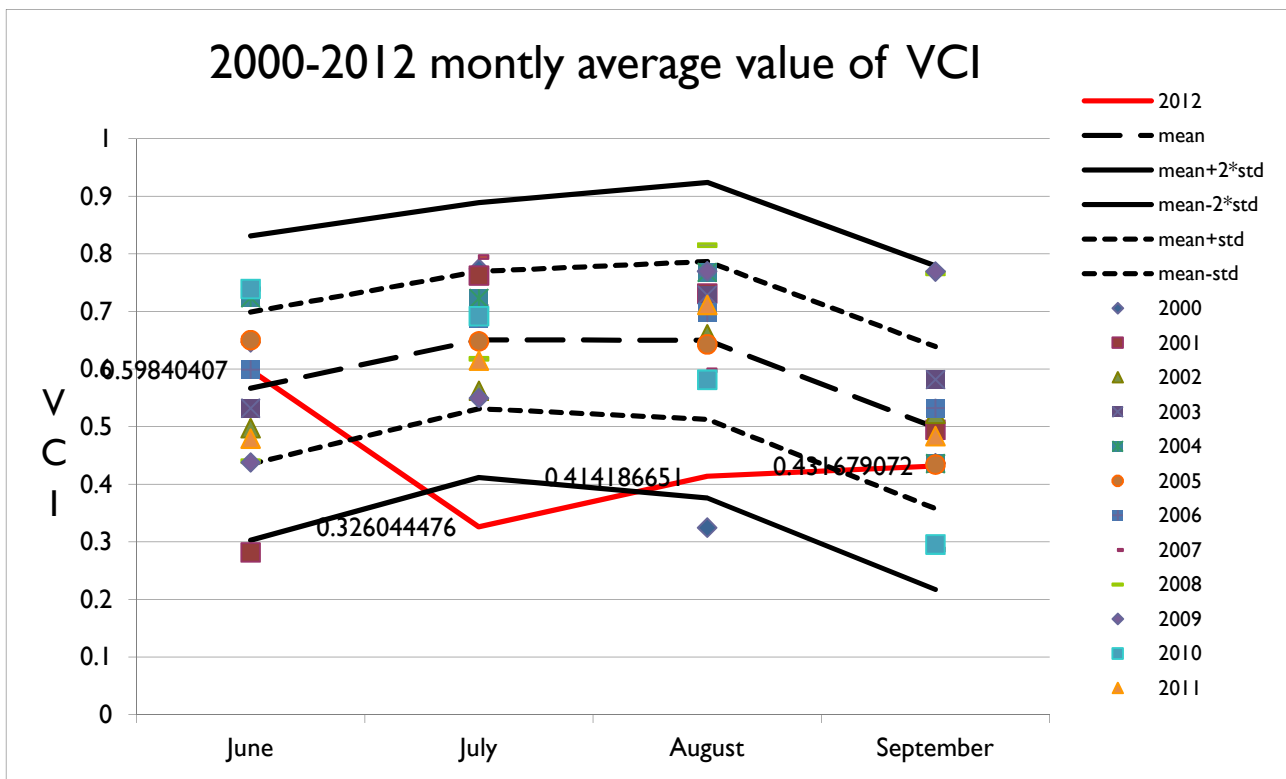


Figure 17: Monthly average values of VCI for each of the years 2000-2012 for Illinois with overall mean and standard deviation.

Figure 18 demonstrated the variation of the original or unmodified VHI from June to September during time period 2000 to 2012. The unmodified VHI was computed with fixed weights of 0.5 for both VCI and TCI. The mean values of each month are a little higher than those of the modified VHI in this study. But they still have similar trend and values climb to peak in July. For the year 2012, the unmodified VHI shows the abnormal condition with outlier values. Compared to modified VHI, the values of unmodified VHI are larger for the months: June, July and August and become closer in September.

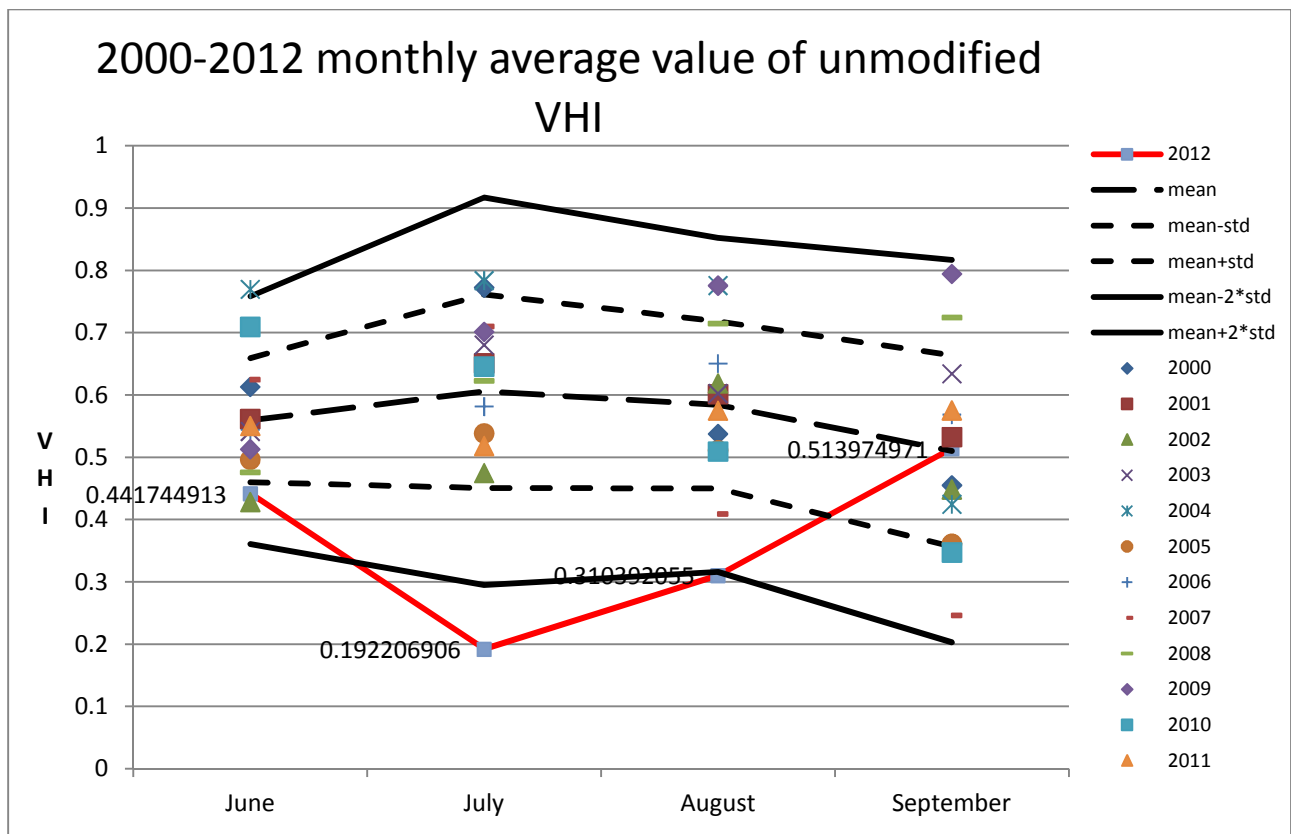


Figure 18: Monthly average values of unmodified VHI for each of the years 2000-2012 for Illinois with overall mean and standard deviation.

In Figure 19, the annual averages of VHI, TCI and VCI fluctuated from year to year. The VHI values followed the similar trend with TCI values. Compared with VHI and TCI, the annual average of VCI values had a different trend with a smaller range of variation. During the time period of 2000 to 2012, the years 2002, 2005, and 2007 had lower values of TCI and VHI, indicating that relative drought condition existed in 2002, 2005, and 2007. The year 2012 had the extremely low value of TCI, VCI and VHI, demonstrating the extremely drought took place in 2012. The results were similar to those from the maps of VHI, TCI and VCI. For years 2004 and 2009, the peak values of the VHI indicated relatively favorable condition.

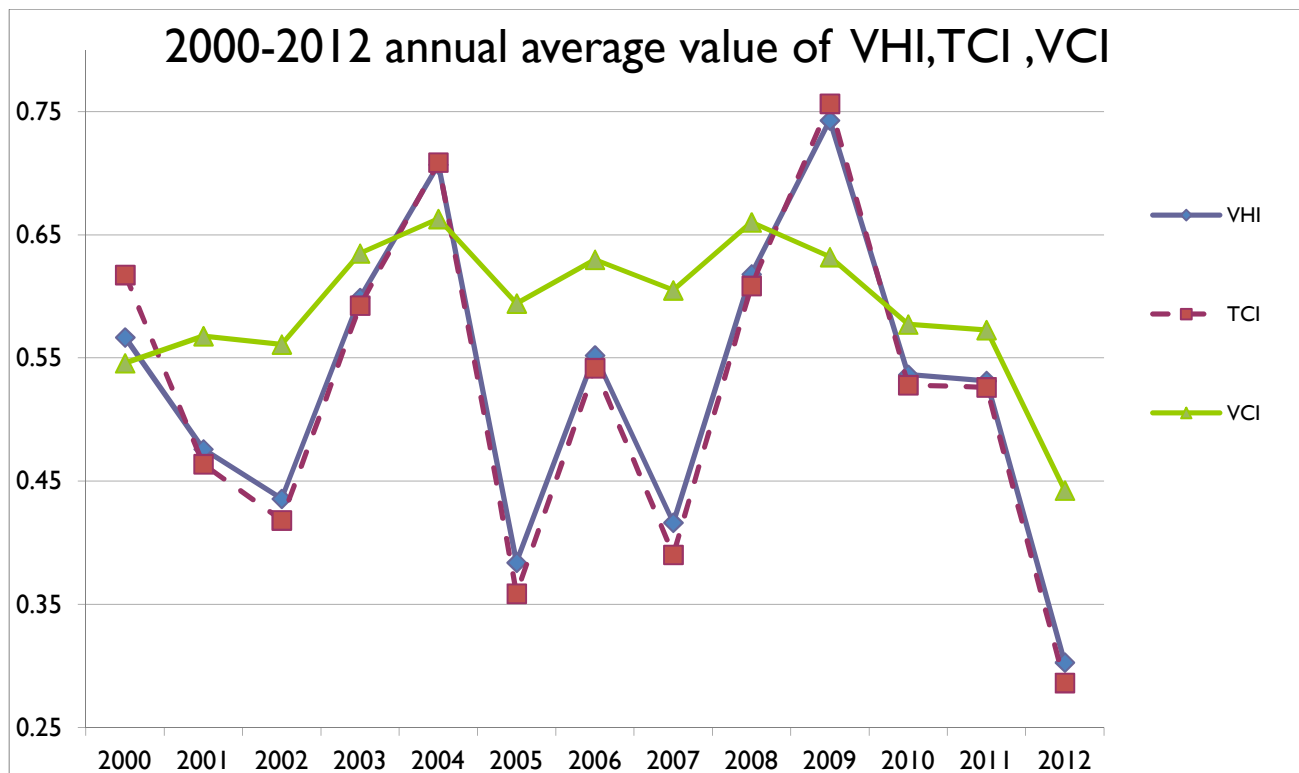


Figure 19: 2000-2012 annual average values of VHI, TCI and VCI for Illinois.

Moreover, Cook county and Pope county were used as examples to explain the combined drought index – VHI at local level in Figures 20 and 21, respectively. Cook County has the second largest population in the US after Los Angeles County, California. Most of its land is urban and dense populated. The situation in Pope County is opposite, which has very small population and where the vegetated (forested) lands dominate the whole county.

Based on monthly average values of VHI for years 2000 to 2012 with overall mean and standard deviation for Cook County in Figure 20, the severe drought in 2012 could be still identified with the VHI values of June, July and August being out of one standard deviation interval. Moreover, the severe drought in June to September of 2005 was also picked up. But the drought of 2012 was not as extreme as showed in the VHI

graph for whole state (in Figures 14 and 15) in which the VHI value of 2012 July was out of the two standard deviation interval. For Pope County, the severe drought in 2012 was quite abnormal as indicated in Figure 21. The monthly average VHI values of June and July were out of the two standard deviation interval. Especially for July, the VHI value approximated to 0.2 and was the lowest point in the graph. In August, the VHI value was still out of the one standard deviation interval. The mean values for the four months during the 13-year period were close to 0.6 and the VHI value had its lowest in July.

Compared to Cook County, the average VHI values of June, July, August and September of Pope County were larger. Even for 2012, the VHI values were lower in Cook County than in Pope County, which suggested that the drought intensity was stronger in Cook County at that time. However, within Cook County the drought intensity of 2012 was relatively not so strong compared to other years. To the contrary, within Pope County the drought of 2012 was very obvious compared to other years.

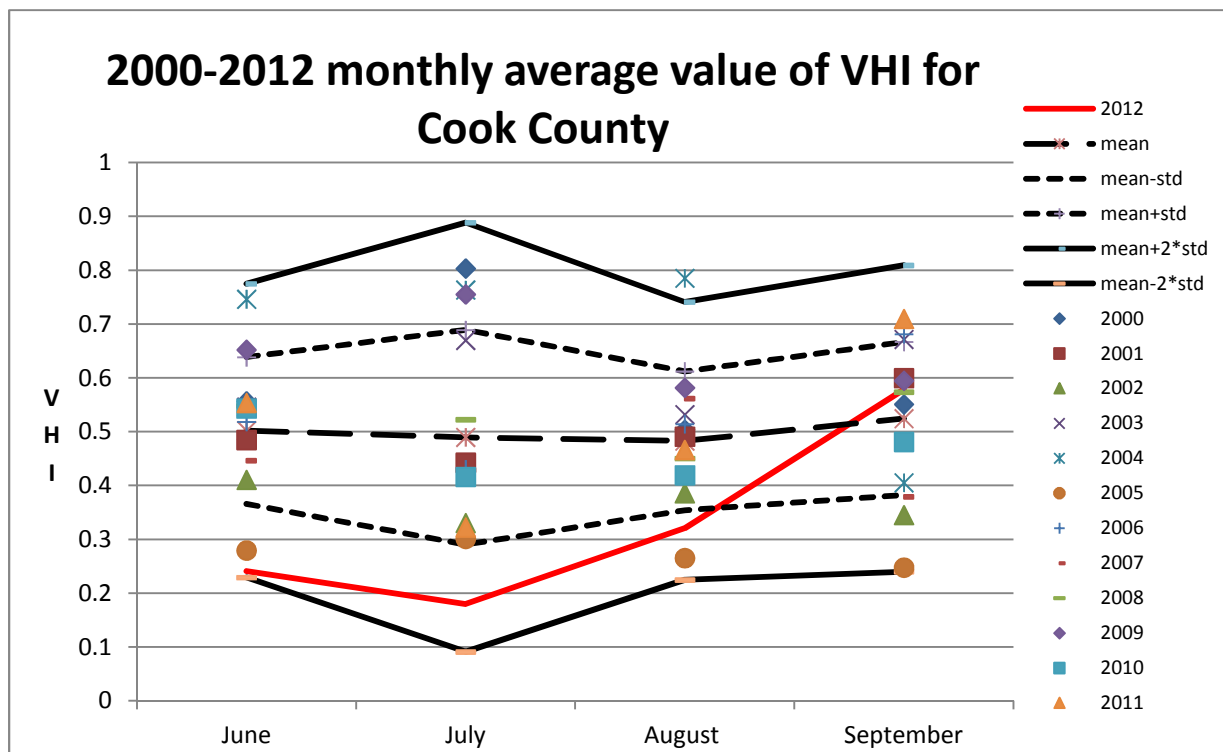




Figure 20: Monthly average values of VHI for years 2000 to 2012 with overall mean and standard deviation for Cook County.

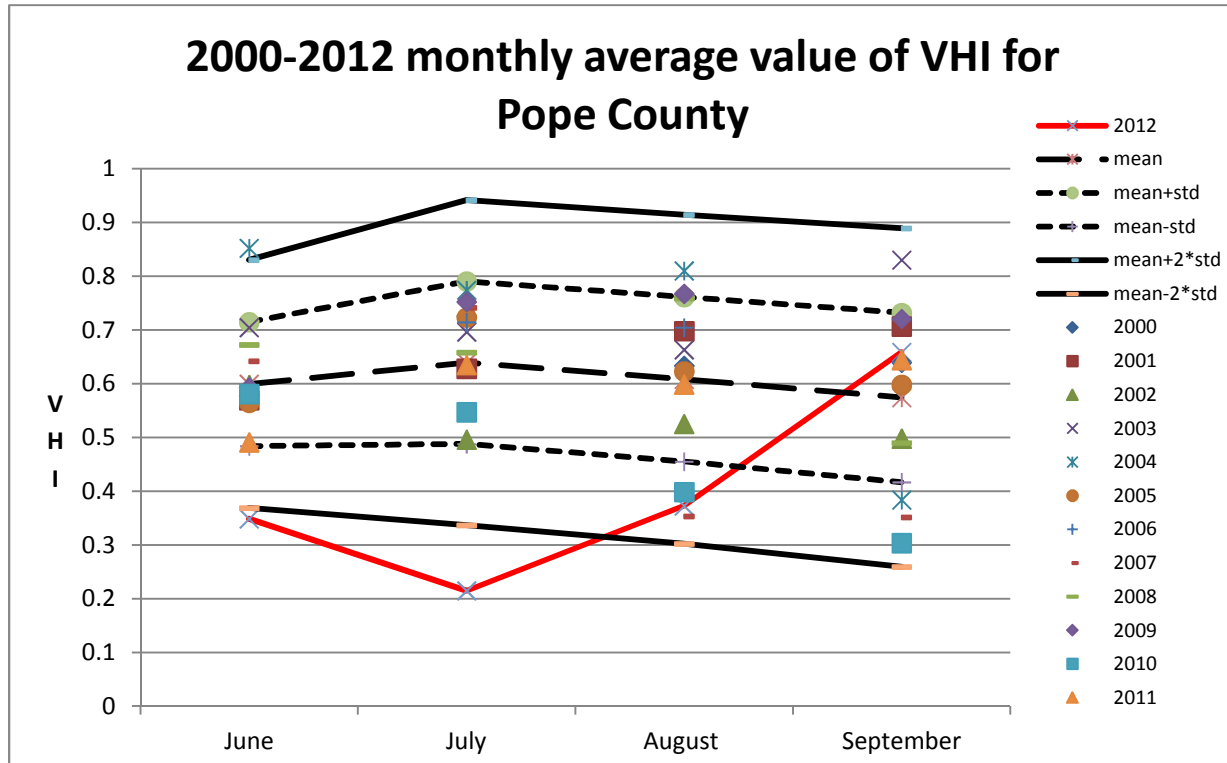


Figure 21: Monthly average values of VHI for years 2000 to 2012 with overall mean and standard deviation for Pope County.

Figure 22 shows the difference in variation of annual mean VHI from 2000 to 2012 between Cook and Pope County. Cook County was dense populated and less vegetation covered. Pope County had smaller population and higher percentage of vegetation coverage. The annual mean VHI values of Cook County had a greater range of variation than that of Pope County. The possible reason was that the environment was more stable in Pope County with more plants. The average VHI value for the 13-year period of Pope County was higher than Cook County, which indicated more

favorable condition in Pope County than Cook County. For Pope County, the drought in 2012 was extreme and the VHI value hit the bottom. Cook County experienced severe drought in 2002, 2005 and 2012, and 2005 seemed to be the worst year.

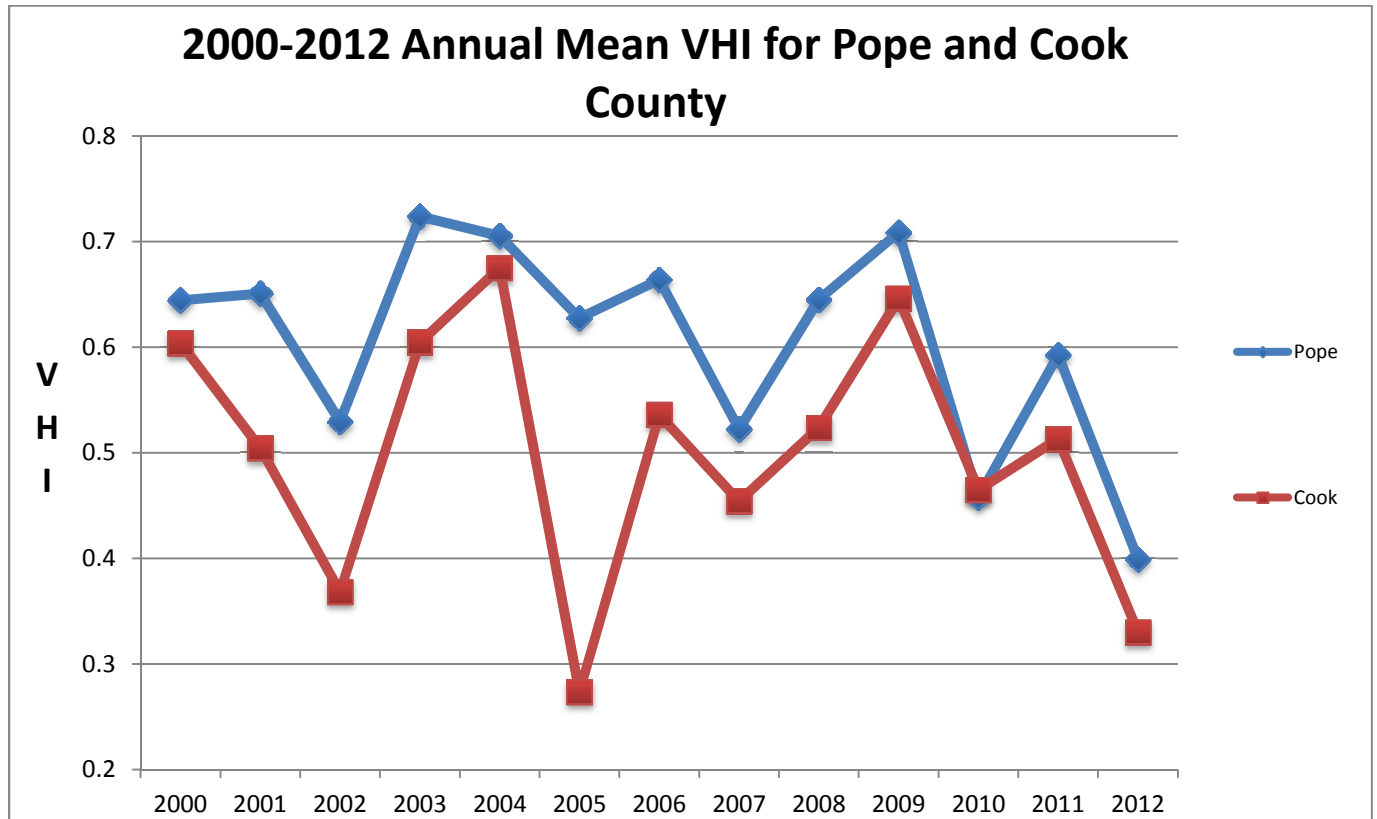


Figure 22: 2000-2012 annual mean VHI for Pope and Cook County.

#### 4.5 COMPARISON WITH USDM MAPS

U.S. Drought Monitor (USDM) provides a composite index that combines the measurements of climatic, hydrologic and soil condition. The USDM maps were jointly produced by the National Drought Mitigation Center at the University of Nebraska-Lincoln, the United States Department of Agriculture, and the National Oceanic and Atmospheric Administration. The USDM maps are not strictly quantitative and they are mainly used in discussion of drought by policymakers and media. Therefore it is difficult

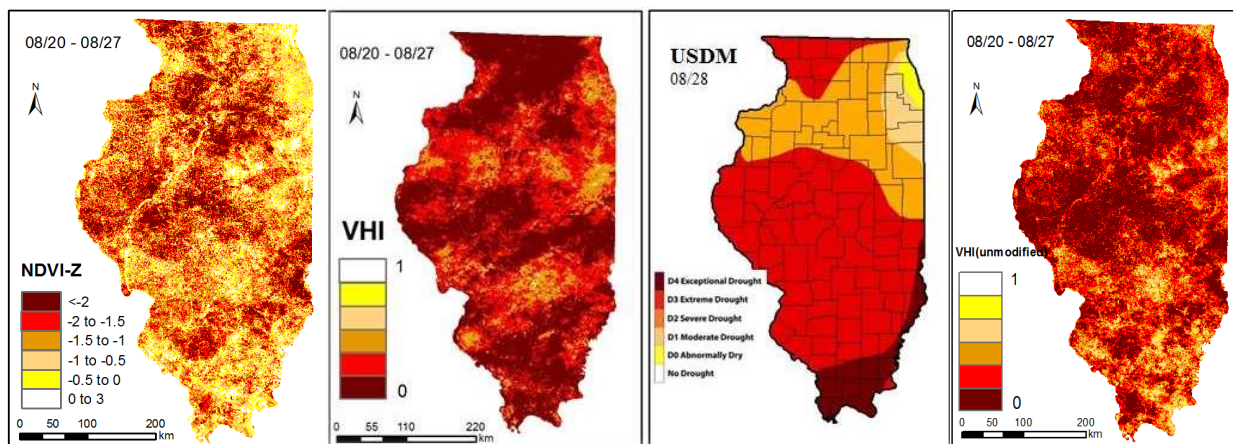
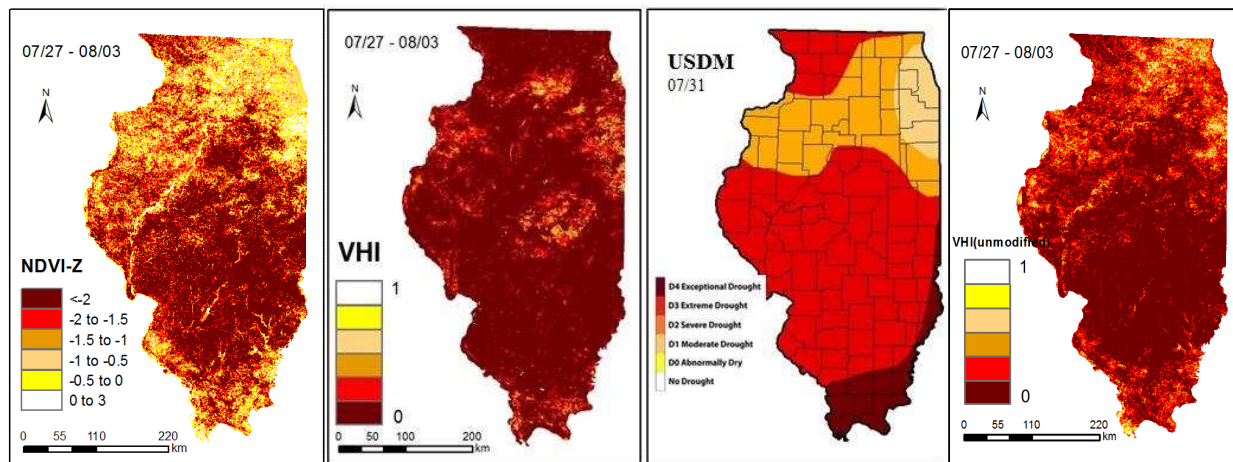
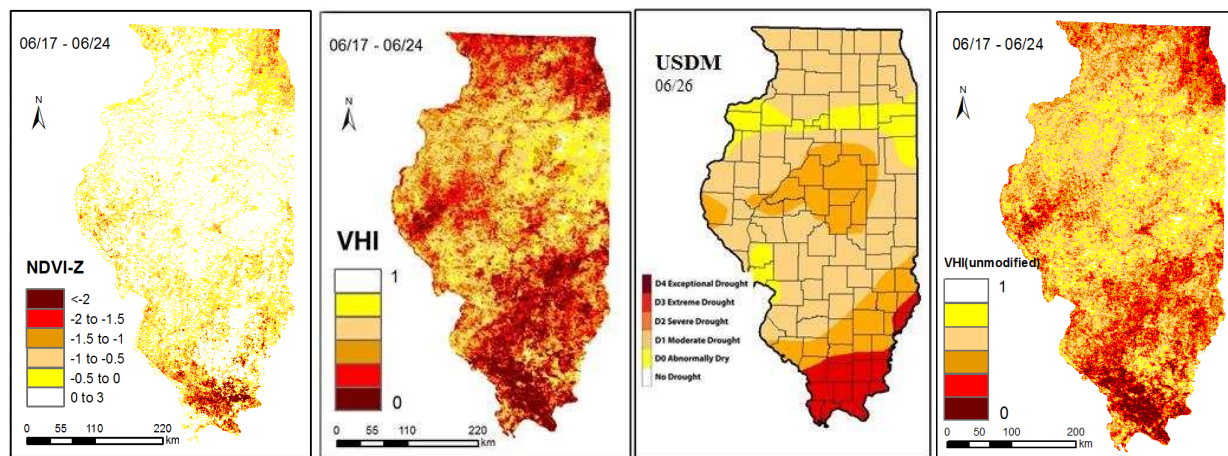
to make exact comparison between USDM maps and the VHI and NDVI anomaly maps created in this study on the basis of pixel-by-pixel, such as calculating the coefficient of determination. But the visually verification can be made with USDM maps to account for the applications of VHI and NDVI in capturing the drought pattern (Rhee, et al, 2010).

In the third column of Figure 23, the weekly USDM maps of 2012 indicate that from the beginning of June, the drought intensity started to increase from moderate to severe. In July and August, over half of the state experienced extreme drought condition. The drought condition expanded from small areas in south part to most of the Illinois area except the northeast corner. The subsequent drought condition was relieved in September. Less than 10% percent of the whole state was under extreme drought condition in September. However, the rest of the state was under moderate to severe drought condition.

As showed in the first and second column of Figure 23, the VHI and NDVI anomaly maps of 2012 corresponding to the USDM maps in time were selected for every month to make the comparison. Both VHI and NDVI anomaly indices responded to the drought condition and captured the change of drought intensity during the growing season. Especially for the extreme drought condition in July and August, the VHI and NDVI anomaly maps demonstrated similar patterns with the USDM maps. The month-to-month change in drought intensity displayed by the VHI maps agreed quite well with the USDM maps. For NDVI anomaly maps, there was a time lag as indicated in the map of June and other maps followed quite the same trend with USDM maps. The reason for the delay was that crops needed time to respond to drought conditions. However, both the VHI and NDVI anomaly maps slightly differed from the USDM maps in the spatial distribution of drought condition. For instance, the VHI and NDVI anomaly

maps of July showed that the drought condition in south corner of Illinois was better than the central part, while the USDM map indicated the most serious drought in south corner of Illinois. The discrepancy between these three maps was mainly caused by the different data that were used for generation of the USDM maps in which climatology and hydrology information was included. The NDVI anomaly maps only focused on vegetation health while the VHI took both land surface temperature and vegetation health into consideration. Therefore, the VHI maps may do better in detecting drought events than the NDVI and USDM. The VHI was able to capture the variation of both temperature and vegetation condition. Compared with USDM maps, the VHI maps also provided more localized drought information at the 1 km spatial resolution. The approach for generating VHI is repeatable and it is simpler than the method of USDM. Therefore it can be widely applied in other regions, even at global scale.

Compared to the VHI maps which are calculated with  $\alpha = 0.5$ , the maps of the modified VHI generated in this study demonstrate very similar spatial distributions of drought condition. But there are still some differences in drought intensity at local scale. From June to August, the VHI maps obtained from vegetation coverage information indicate more severe condition in central and southern parts of Illinois with darker color. As showed in USDM maps, the south part experienced extreme situation during these three months. Therefore the VHI proposed in this study provides more accurate assessment of drought event than the unmodified VHI. The drought relieved in September and the two different VHI maps both captured the change.



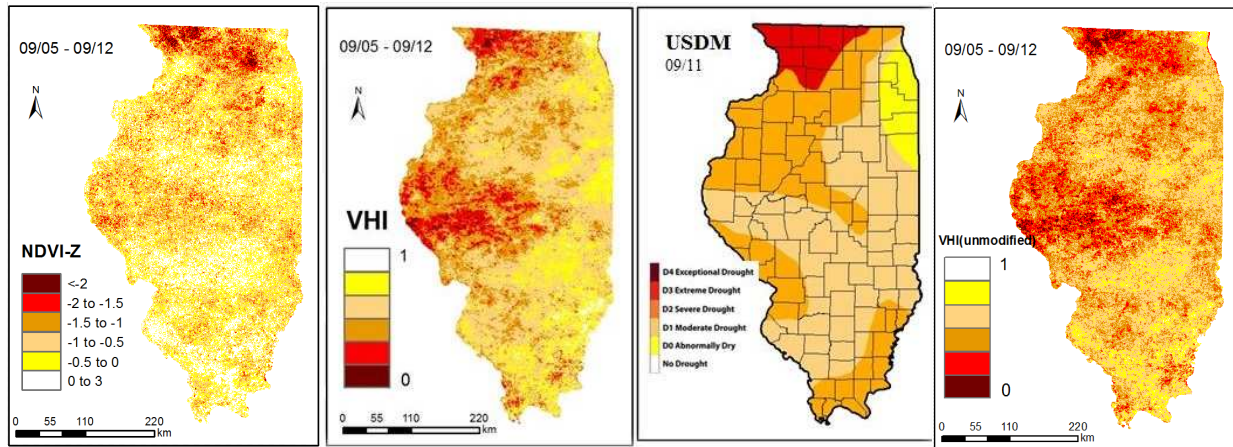


Figure 23: Comparison of NDVI Anomaly and modified VHI maps, USDM maps and unmodified VHI maps in Illinois during June, July, August and September of 2012 (The first column: NDVI anomaly maps of this study, the second column: modified VHI maps, and the third column: USDM maps, Map courtesy of NDMC-UNL, and the fourth column: unmodified VHI maps).

The correlation coefficients of spatial patterns between the modified VHI and NDVI-Z, VCI, TCI, and the unmodified VHI maps were calculated in Figure 24. It is obvious that the correlation coefficient between the modified VHI and TCI is the highest, even higher than the value between the modified VHI and the unmodified VHI. The values for June, July, August and September are all over 0.9. The spatial patterns between the modified VHI and VCI are less correlated compared to those from other indices.

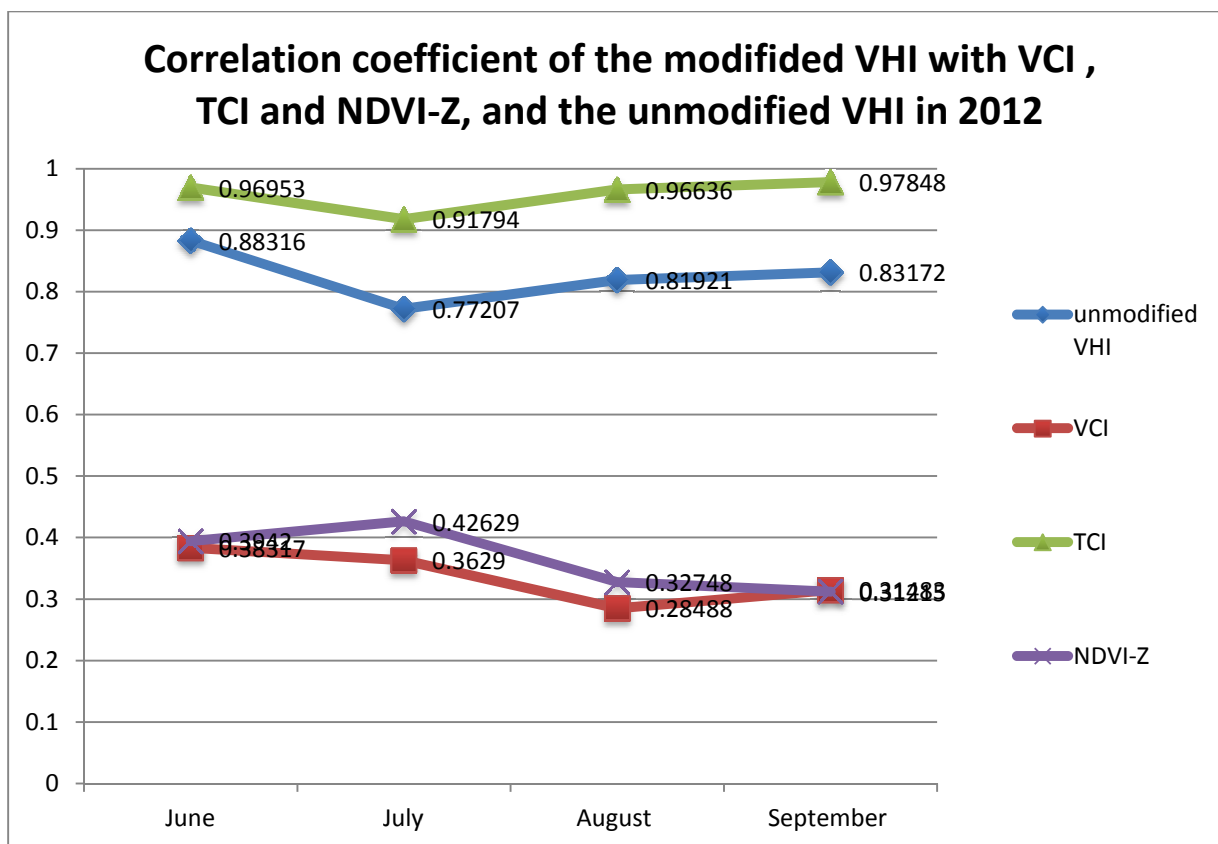


Figure 24: Correlation coefficient of the modified VHI with VCI, TIC and NDVI-Z, and unmodified VHI in 2012.

## CHAPTER 5

### CONCLUSION

According to the recent records, the global and regional land surface temperature has increased in the twentieth century (WMO 2005). Among the warmest years observed since 1850, a total of 11 occurred between 1995 and 2006 (Alley et al. 2007). There is a lot of concern about the impact of global warming on drought occurrence at regional and global scales. Particularly, for the state of Illinois, agriculture is of central importance for the economy in this region and the production of corn and soybean is well known in the United States and the whole world. There is a direct relationship between the occurrence and magnitude of drought and the variability in the regional hydrologic cycle. It is essential to monitor the drought condition in this area because of serious influence on the agriculture, especially the quality and quantity of crop production.

VHI has been proposed as a useful means for measuring the duration, intensity and impact of drought. Since the generation of VHI is based on the satellite images, VHI has many advantages over other meteorological and hydrological indices. It has continuous spatial coverage over large areas with high temporal and spatial resolution. NOAA/NESDIS system produces the VHI products from the radiance observed by the Advanced Very High Resolution Radiometer (AVHRR). The VHI images have 4 km spatial and 7-day composite temporal resolution. In this study, the modified VHI maps can be updated every eight days and the spatial resolution is as high as 1 km × 1 km. The more detailed information will help a lot in planning, mitigation and response activities and is very meaningful for government officials and related organizations. Especially for relative small areas, such as counties, the high spatial resolution of



modified VHI maps can meet the requirement of local people. The other meteorological and hydrological indices rely on station-based data and their spatial resolution depends on the spatial distribution of the climate stations. For areas of sparse measurement networks and poor infrastructure, the modified VHI should be more useful in drought monitoring and mitigation than the traditional indices.

Originally, VHI was created by combining VCI and TCI using equal weights of 0.5. The equal weights mean the neglect of differences between urbanization and vegetated areas for impacts of drought intensity. In this study, the contribution factor of vegetation condition index with vegetation coverage in the equation for calculating VHI index was modified. The modification led to variable weights of vegetation condition index and temperature condition index from pixel to pixel based on the vegetation fraction of each pixel. The modified VHI takes the influence of vegetation coverage factor on drought assessment into consideration and effectively incorporates the meteorological information from TCI and vegetation information from VCI.

As showed in this study, VCI is much more stable than TCI since the range of VCI variation is much smaller than that of TCI. When drought takes place, the highly vegetated areas, such as forests, have higher drought resistance capability than those areas with low vegetation coverage, such as bared soil and urbanized areas. Even under the same temperature, the land of forests will not dry as quickly as cities and bare soils. Vegetation condition provides more accurate indicator of drought intensity. If there are only few trees or other plants, the drought condition for this area is strongly related to the temperature information. Therefore more weight is given to VCI for areas of dense vegetation coverage and more weight is given to TCI for areas of sparse vegetation coverage in computation of modified VHI.

After visual comparison with USDM maps, both NDVI and modified VHI demonstrate their ability in assessing the temporal and spatial variation of drought events. They captured the severe drought condition of Illinois in 2012 summer. Compared to modified VHI, there is a time lag of NDVI in detecting the occurrence of drought since crops need time to respond to the water stress caused by drought. The modified VHI shows identical temporal trend of drought intensity with USDM maps: the drought intensity started to increase in June and it became really extreme in July, then it gradually improved in August and September. The difference in spatial distribution is caused by the different datasets: the modified VHI is remote sensing based index and USDM is a composite index, which integrates traditional indices, such as PDSI and SPI. However, the severity of drought often varies greatly from place to place (Mishra and Singh, 2009). Especially, counties of every state need more specific information of drought intensity to make decision for policy and strategies towards management of drought disasters (Brown et al, 2008). Compared to USDM maps, the modified VHI provides more detailed information at local level. That is, the coarse resolution of USDM maps limits its application at local level. This study offered such potential.

Overall, this study led to a modified drought index – VHI by combining the information from remotely sensed data in both vegetation condition and temperature based on the vegetation fraction images. This index is able to monitor the drought events that took place in Illinois and quantify the drought intensity. Especially, this study well answered all the research questions proposed in the first chapter, including: 1) Is the combined drought index able to provide more detailed information of drought intensity than the existing USDM? 2) Is the combined drought index able to capture the drought events that took place during the last decade, especially the one in 2012? 3) Is

the combined drought index able to reveal the differences of the drought impacts between urbanized and vegetated areas? And 4) Is the combined drought index better than existing indices in quantifying drought intensity?

The shortcoming of the modified VHI is the uncertainty behind the change of vegetation condition. As discussed earlier in this study, the variation of vegetative status may result from insect, flood, nutrition of soil and other reasons. Drought could be part of the reasons and it is also possible that the variation has nothing to do with drought. Therefore more attention is to be paid while explaining the change of vegetation condition. The future improvement will focus on identifying the drought factor behind the vegetation condition change with meteorological data from local stations. For example, precipitation data that should be incorporated into the calculation of the modified VHI and enhance its capacity to verify whether the deteriorated vegetation health is the result of drought or not. There is still a lot of work to be done in validating and improving the VHI products.

## REFERENCES

- Adam, J.B., Smith, M.O., and Gillespie, A.R. (1993). Imaging spectroscopy: Interpretation based on spectral mixture analysis. In C.M. Pieters, P.A.J. Englert (Eds), Remote geochemical analysis: Elemental and mineralogical composition (pp.145-166). Cambridge, England: Press Syndicate of Univ. of Cambridge.
- Adams, J.B., Smith, M.O., and Johnson, P.E. (1986). Spectral mixture modeling: A new analysis of rock and soil types at the Viking Lander I site. *Journal of Geophysical Research*, 91, 8098-8812.
- Alley, R.B., and Coauthors, 2007. Summary for policymakers. *Climate Change 2007: The Physical Science Basis*, S. Solomon et al., Eds., Cambridge University Press, 1-18.
- Anyamba, A.C., Tucker, C.J., and Eastman, J.R. 2011. NDVI anomaly patterns over Africa During the 1997/98 ENSO warm event. *International Journal of Remote Sensing*, 22(10):1847-1859.
- Beran, M., and Rodier, J.A. 1985. Hydrological aspects of drought. *Studies and reports in hydrology* 39. UNESCO-WMO, Paris.
- Bbalme, H.N., Mooley, D.A., 1980. Large-scale droughts/floods and monsoon Circulation. *Mon. Weather Rev.* 108, 1197-1211
- Bryant, S., Arnell, N.W., and Law, F.M. 1992. The long-term context for the current Hydrological drought. Institute of Water and Environmental Management (IWEM) Conference on the management of scarce water resources. 13-14 October 1992.
- Brown, J.F., Wardlow, B.D., Tadesse, T., Hayes, M.J, and Reed, B.C. 2008. The Vegetation Drought Response Index (VegDRI): A new integrated approach for

- monitoring drought stress in vegetation. *GIScience and Remote Sensing*, 45(1):16-46.
- Chang, T.J., 1991. Investigation of precipitation droughts by use of kriging method . *J Irrig. Drain. Engrg. ASCE* 117(9) , 935-943.
- Cai, G., Du, M., and Liu, Y. 2011. Regional drought monitoring and analyzing using MODIS data- A case study in Yunnan Province. In *Computer and Computing Technologies in Agriculture IV*. Edited by D. Li, Yande Liu, and Y, Chen. Springer, Boston. Pp.243-251.
- Carlson, T. N., Gillies, R.R., and Perry.1994. A method to make use of thermal infrared temperature and NDVI measurements to infer surface soil water content and fractional vegetation cover. *Remote Sensing. Rev. Vol 9: 161-173*
- Cook,E.R.,Kairiukstis,L.(Eds.).1990. *Method of Dendrochronology-Applications in the Environmental Sciences*.Kluwer Accademic, Boston.
- Correia, F., Santos, M.A., and Rodrigues, R. 1994. Reliability in regional drought studies. *Water Resources Engineering Risk Assessment. Porto. Karras. NATO ASI Series,29: 43-62.*
- Gao, B., 1996. NDWI-a normalized difference water index for remote sensing of vegetation liquid water from space. *Remote Sensing of Environment* 58(3),257-266.
- Ghulam, A., Li, Z.L., Qin, Q., and Tong, Q. 2007a. Exploration of the spectral space based on vegetation index and albedo for surface drought estimation. *J. Appl. Remote Sens.* 1(013529): 1-12.
- Ghulam, A., Qin, Q., and Zhan, Z., 2007b. Designing of the perpendicular drought index. *Environment Geology*, 52 (6):1045-1052
- Ghulam, A., Qin, Q., Teyip, T and Li, Z. 2007c. Modified perpendicular drought index

- (MPDI): a real-time drought monitoring method. *ISPRS Journal of Photogrammetry & Remote Sensing* 62(2007) 150-164.
- Guttman, N.B., 1997. Comparing the Palmer drought index and the standardized precipitation index. *J. Am. Water Resour. Assoc.* 34, 113-121.
- Heim, R., 2002. A review of twentieth-century drought indices used in the United States. *Bull. Am. Meteorol. Soc.* 83,1149-1165.
- Hollinger, S.E., Isard, S.A., Welford, M.R., 1993. A New Soil Moisture Drought Index For Predicting Crop Yields. In : Preprints, Eighth Conf. on Applied Climatology. Anaheim, CA, Amer. Meteor. Soc., pp. 187-190.
- Kallis, G. 2008. Droughts. *Annu. Rev. Environ. Resour.* 33(1):85-118. doi: 10.1146/Annure.enviro.33.081307.123117.
- Karamouz, M., Rasouli, K., and Nazif, S. 2009. Development of a hybrid index for drought prediction: case study. *J. Hydrol. Eng.* 14(6): 617-627.
- Kogan, F.N. 1990. Remote sensing of weather impacts on vegetation in non-homogeneous areas. *Int. J. Remote Sens.* 11(8):1405-1419.
- Kogan, F.N. 1995. Application of vegetation index and brightness temperature for drought detection. *Adv. Space Res.* 15(11):91-100.
- Kogan, F.N. 1997. Global drought watch from space. *Bulletin of the American Meteorological Society* 7(4):621–636.
- Kogan, F., Yang, B., Guo, W., Pei, Z., and Jiao, X. 2005. Modelling corn production in China using AVHRR-based vegetation health indices. *International Journal of Remote Sensing* 26(11):2325–2336.
- Lu, D., Moran, E., and Batistella, M. 2003. Linear mixture model applied to Amazonian Vegetation classification. Vol 87.456-469.

- Meyer, S.J., Hubbard, K.G., and Wilhite, D.A. 1993. A crop-specific drought index for Corn. I: Model development and validation. *Agron.J.*85(2):388-395
- McKee, T.B., Doesken, N.J., Kleist, J., 1993. The relationship of drought frequency and duration to time scales. *Proc. Ninth Conference on Applied Climatology*, American Meteorological Society, Anaheim, CA, pp. 179-184. 17-22 January.
- Mishra, A.K., Singh, V.P., Desai, V.R., 2009. Drought characterization: a probabilistic Approach. *Stoch. Environ. Res. Risk A.* 23(1), 41-55.
- Narasimhan, B., Srinivasan, R., 2005. Development and evaluation of soil moisture deficit index (SMDI) and evapotranspiration deficit index (ETDI) for agriculture drought monitoring. *Agric. For. Meteorol.* 133, 69-88.
- Niemeyer, S. 2008. New drought indices. *Options Mediterraneennes. Serie A: Seminaires Mediterraneens*, 80: 267-274
- Palmer, W.C., 1965. *Meteorologic Drought*. US Department of Commerce, Weather Bureau, Research Paper No. 45, p. 58.
- Palmer, W.C., 1968. Keeping track of crop moisture conditions, nationwide: the new crop moisture index. *Weatherwise* 21, 156-161.
- Rhee, J., Im, J., and Carbone, G.J., 2010. Monitoring agricultural drought for arid and humid regions using multi-sensor remote sensing data. *Remote Sensing of Environment*, 114(12), pp.2875-2887.
- Riebsame, W.E., Changnon, S.A., Karl, T.R., 1990. *Drought and Natural Resource Management in the United States : Impacts and Implications of the 1987-1989 Drought*. Westview Press, p. 174.

- Rojas, O., Vrieling, A., and Rembold, F. 2011. Assessing drought probability for agricultural areas in Africa with coarse resolution remote sensing imagery. *Remote Sensing of Environment* 115:343-352.
- Sandholt, I., Rasmussen, K., and Anderson, J. 2002. A simple interpretation of the Surface temperature/vegetation index space for assessment of surface moisture Status. *Remote Sens. Environ.* 79(2-3):213-224.
- Seiler, R. A., Kogan, F., Guo, W., and Vinocur, M. 2007. Seasonal and interannual responses of the vegetation and production of crops in Cordoba, Argentina assessed by AVHRR-derived vegetation indices. *Advances in Space Research* 39(1):88–94.
- Shafer, B.A., Dezman, L.E., 1982. Development of a Surface Water Supply Index (SWSI) to Assess the Severity of Drought Conditions in Snowpack Runoff Areas. In: Preprints, Western SnowConf., Reno,NV,Colorado State University, pp. 164-175.
- Stahl, K. 2001. Hydrological drought-a study across Europe. Universitätsbibliothek Freiburg.
- Svoboda, M.D., LeComte, D., and Hayes, M.J. 2002. The Drought Monitor. *Bull.Am. Meteorol. Soc.* 93(8): 1181-1190.
- Tsakiris, G., and Vangelis, H. 2004. Towards a drought watch system based on spatial SPI. *Water Resources Management*, 18(1):1-12.
- Tsakiris, G., and Vangelis, H. 2005. Establishing a drought index incorporating evapotranspiration. *European Water*, 9(10): 3-11.



- Tsakiris, G., Loukas, A., Pangalou, D., Vangelis, H., Tigkas, D., Rossi, G., and Cancelliere. 2007. Drought characterization. Chapter 7. Options Mediterraneennes, 58:85-102.
- Tucker, C. J., 1979. Red and photographic infrared linear combinations for monitoring vegetation. *Remote Sens. Environ.* 8(2): 127-150.
- Unganai, L., and Kogan, F. 1998. Drought monitoring and corn yield estimation in Southern Africa from AVHRR data. *Remote Sensing of Environment* 63:19–232.
- Van Rooy, M.P, 1965. A rainfall anomaly index independent of time and space. *Notos* 14,43.
- Vasiliades, L., Loukas, A., and Liberis, N. 2011. A water balance derived drought index For Pinios River Basin, Greece. *Water Resource Management*, 25(4):1087-1101.
- Wan, Z., Wang, P., and Li, X. 2004. Using MODIS land surface temperature and normalized difference vegetation index products for monitoring drought in the southern Great Plains, USA. *Int. J. Remote Sens.* 25(1): 61-72.
- Wang, L. and Qu, J.J. (2007). NMDI: A normalized multi-band drought index for Monitoring soil and vegetation moisture with satellite remote sensing. *Geophys. Res Lett.*, 34, L20405.
- Weghorst, K. 1996. The reclamation drought index : guidelines and practical applications. [cedb.asce.org](http://cedb.asce.org), ASCE, Denver, Colo.
- Wilhite, D.A., Glantz, M.H., 1987. Understanding the drought phenomena: the role of Definitions. In : Donald, A., Wilhite, Eastering Willam, E., Deobarah, A., (Eds), *Planning of Drought: Towards a Reduction of Societal Vulnerability*, Westview Press, Wood, Boulder, CO, pp. 11-27.
- Wilhite, D.A. 2004. Drought as a natural hazard. In *international Perspectives on Natural*

Disasters: Occurrence, Mitigation, and Consequences. Edited by J.P. Stoltman, J. Lidstone, and L.M. Dechano. Kluwer Academic Publishers, Dordrecht, The Netherlands. pp.147-162.

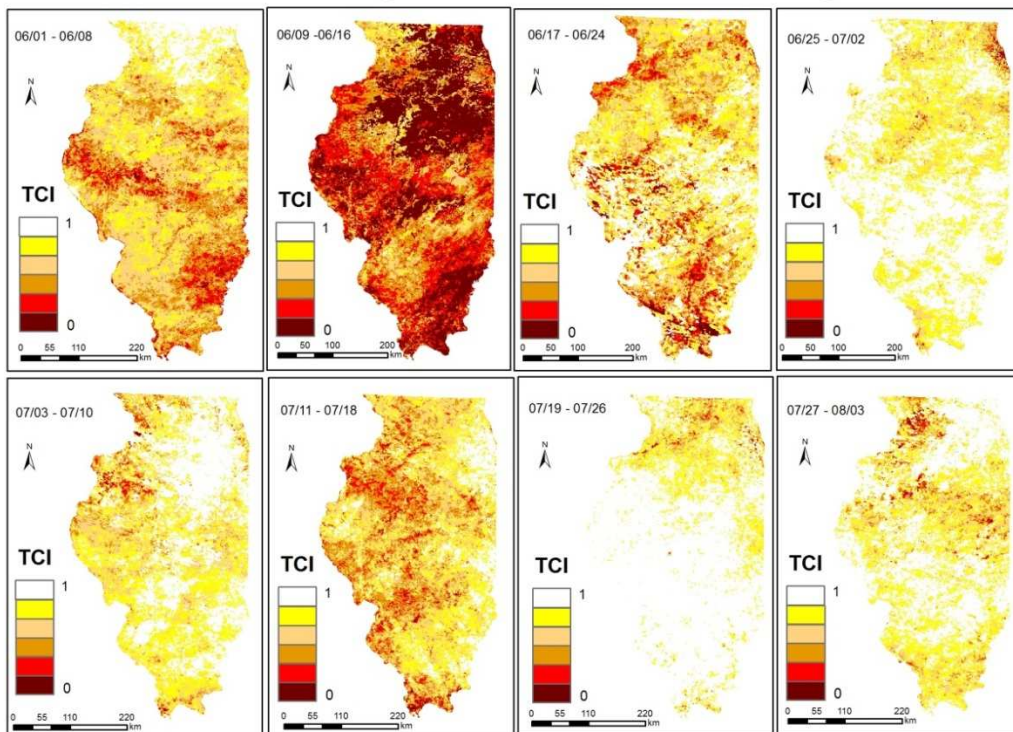
WMO,2005; Statement on the status of the global climate in 2005. WMO Rep.998,12pp.

Wu, D., Qu, J.J., Hao, X., Xiong, J. 2013. The 2012 agricultural drought assessment in Nebraska using MODIS satellite data. 2013 Second International Conference on Agro-Geoinformatics (Agro-Geoinformatics), pp, 170-175, Fairfax, VA, USA, 12-16 August, 2013.

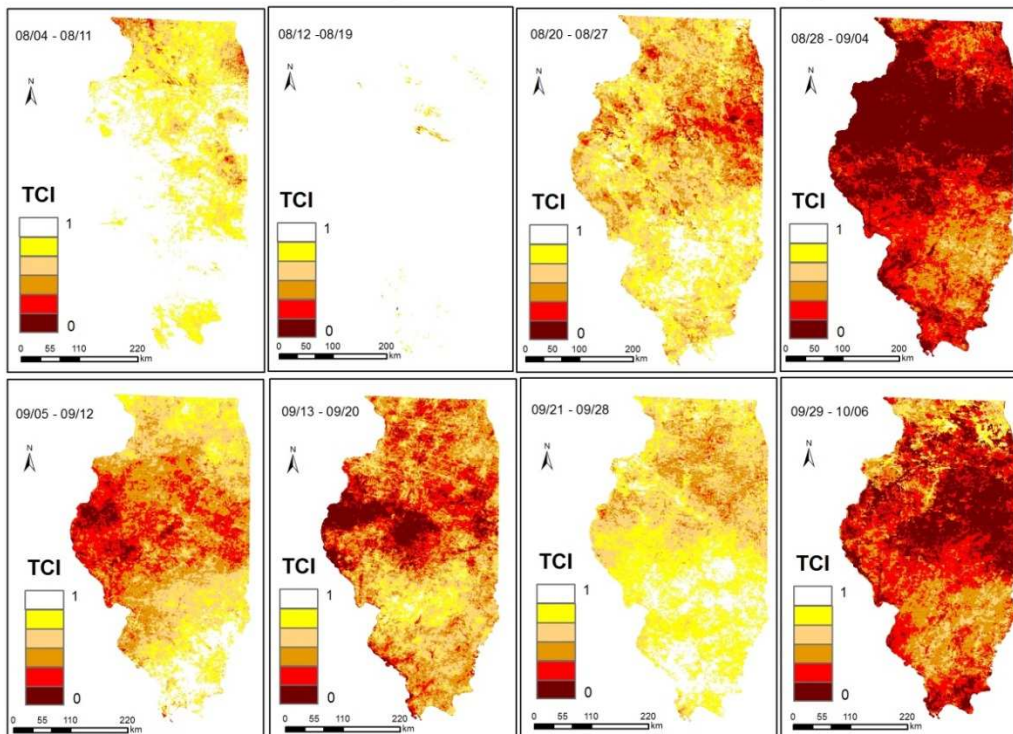
APPENDICES

Appendix A: Temperature Condition Index Maps of Illinois for years 2000-2012.

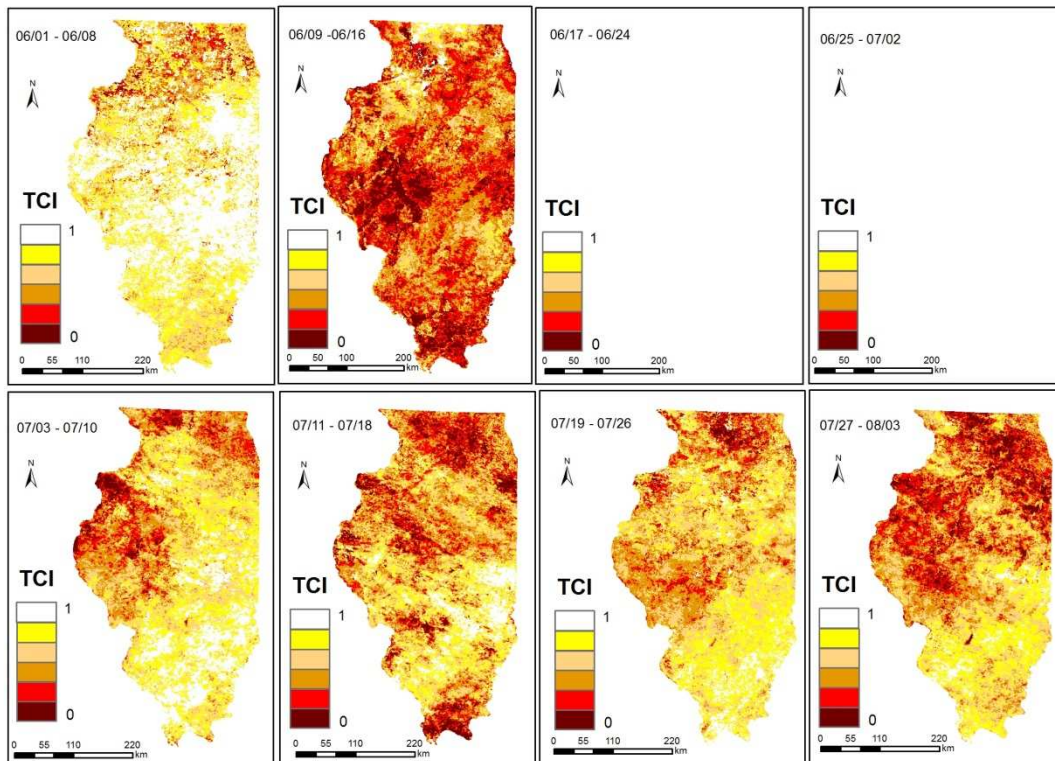
2000 Illinois Temperature Condition Index Map I



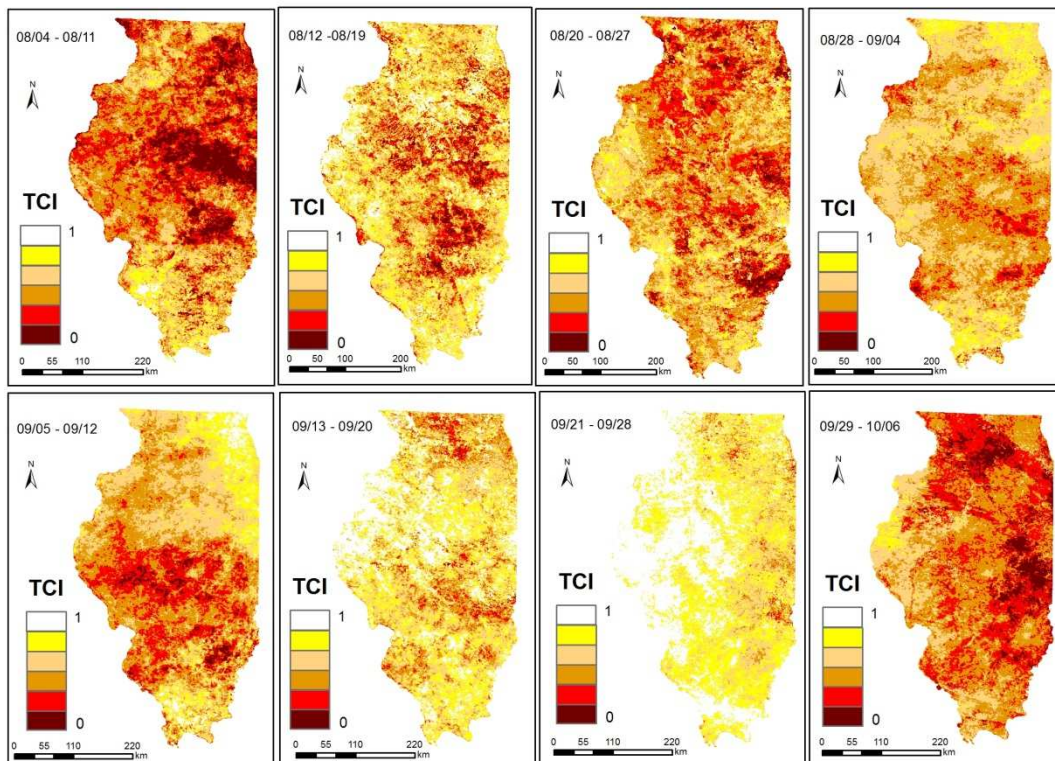
2000 Illinois Temperature Conditon Index Map II



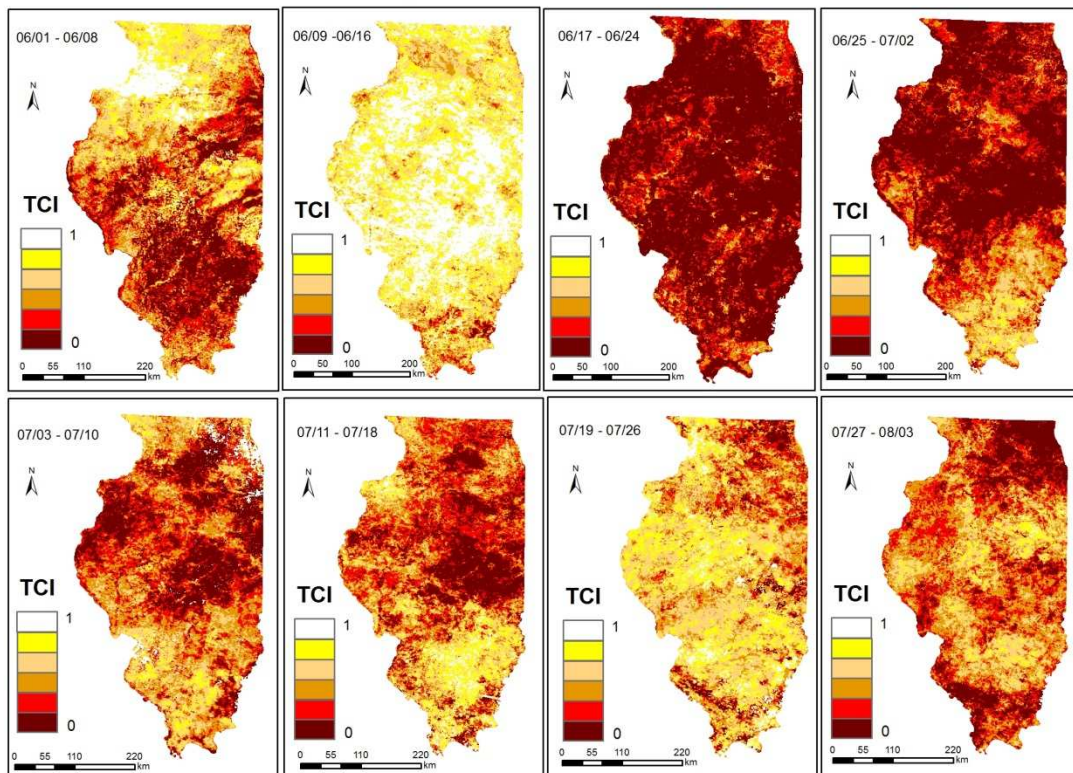
## 2001 Illinois Temperature Condition Index Map I



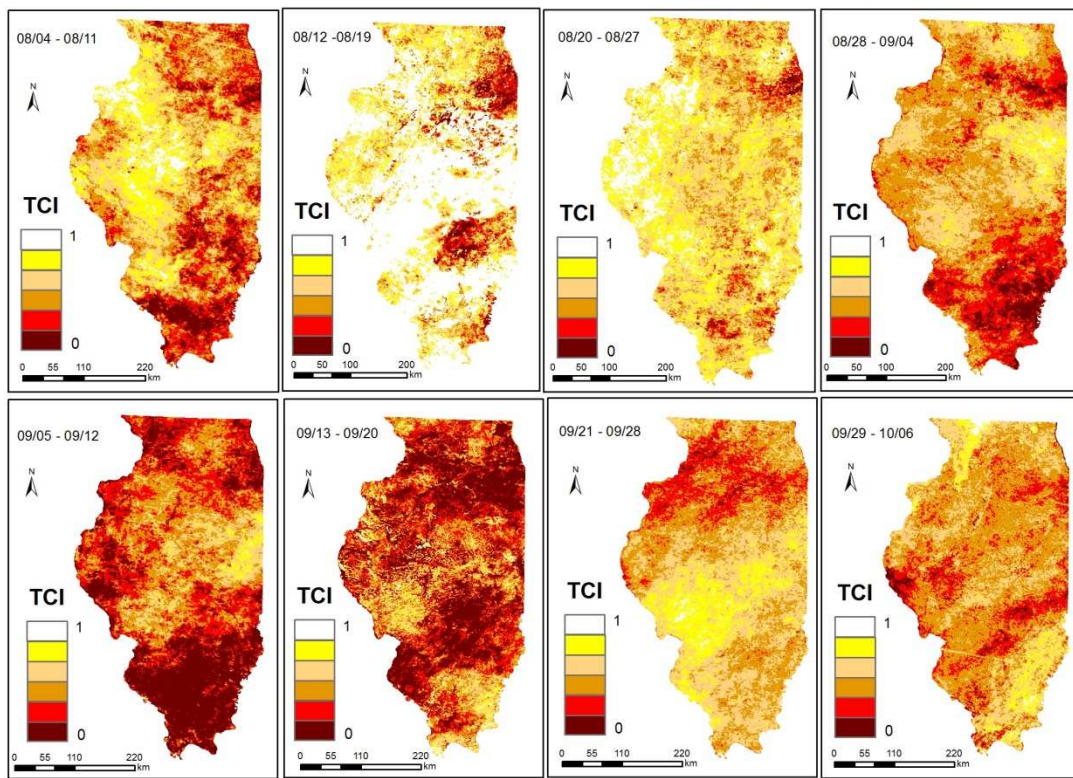
## 2001 Illinois Temperature Condition Index Map II



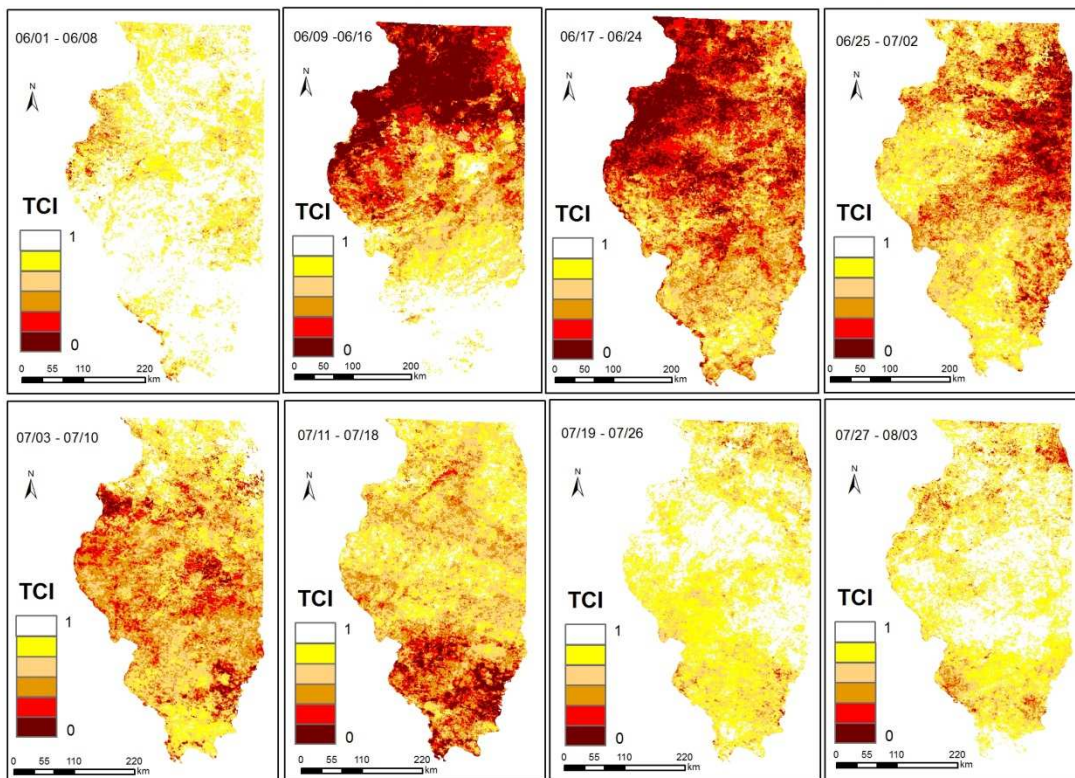
## 2002 Illinois Temperature Condition Index Map I



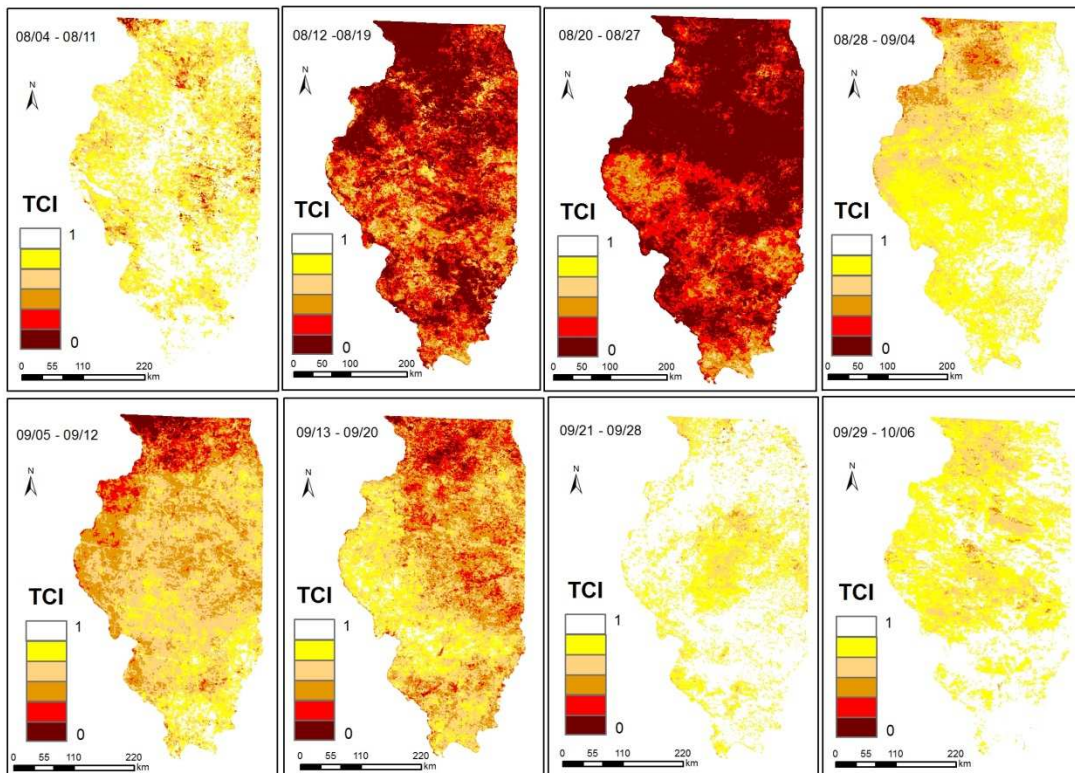
## 2002 Illinois Temperature Condition Index Map II



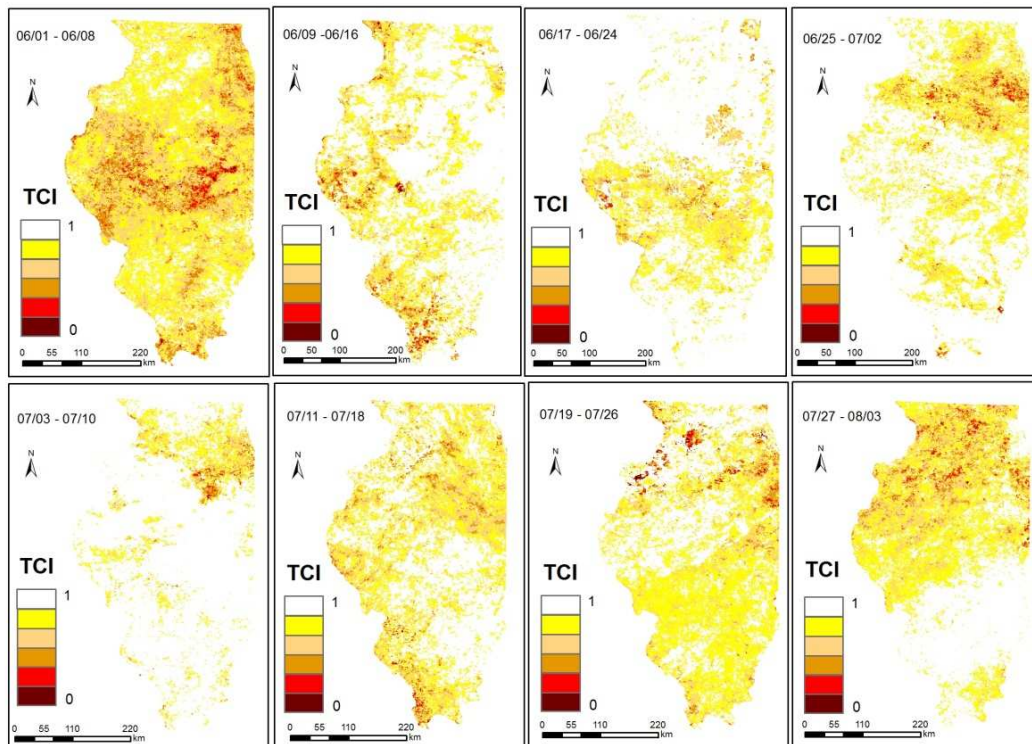
## 2003 Illinois Temperature Condition Index Map I



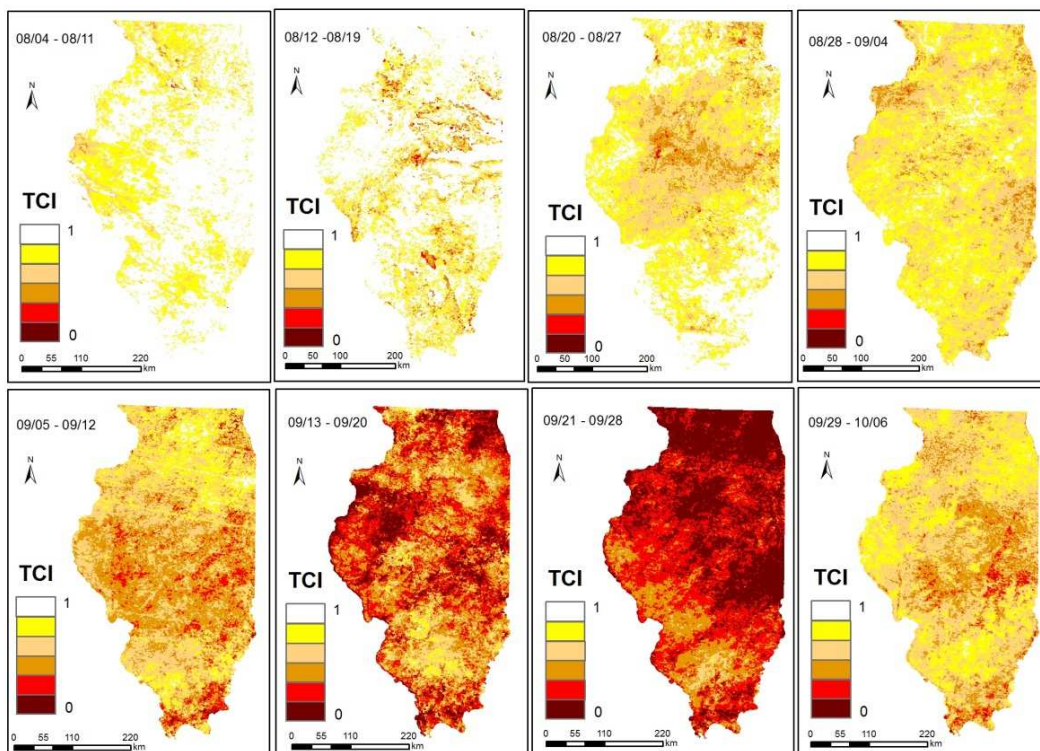
## 2003 Illinois Temperature Condition Index Map II



## 2004 Illinois Temperature Condition Index Map I

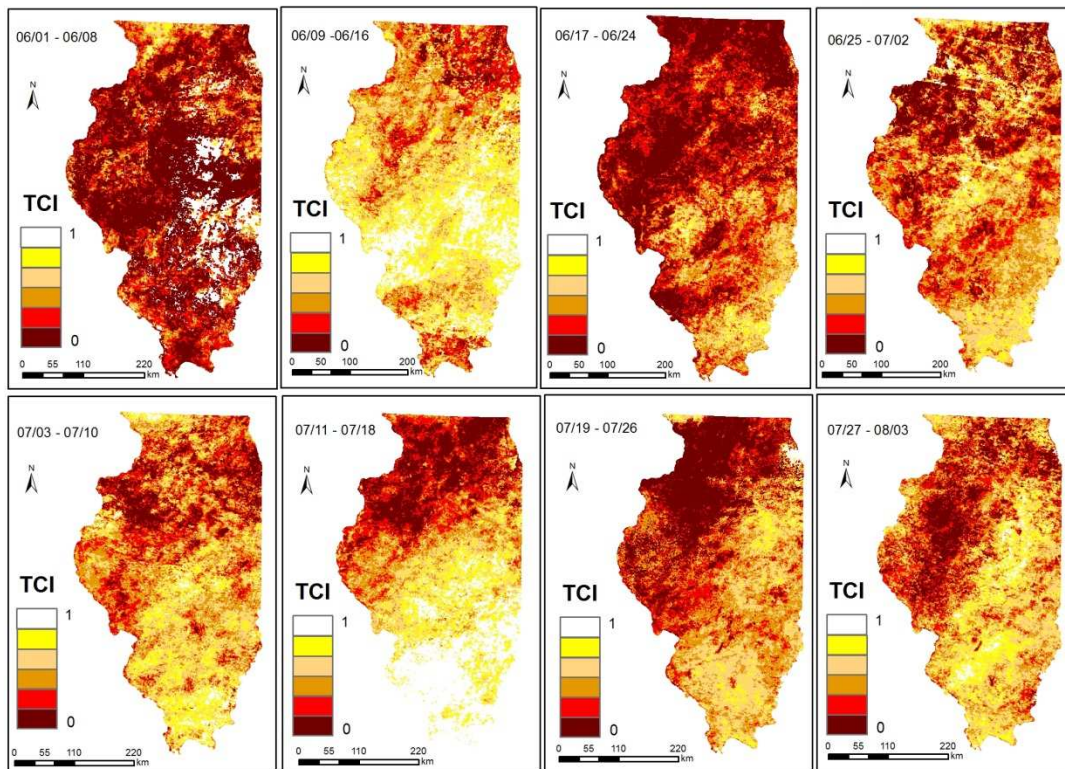


## 2004 Illinois Temperature Condition Index Map II

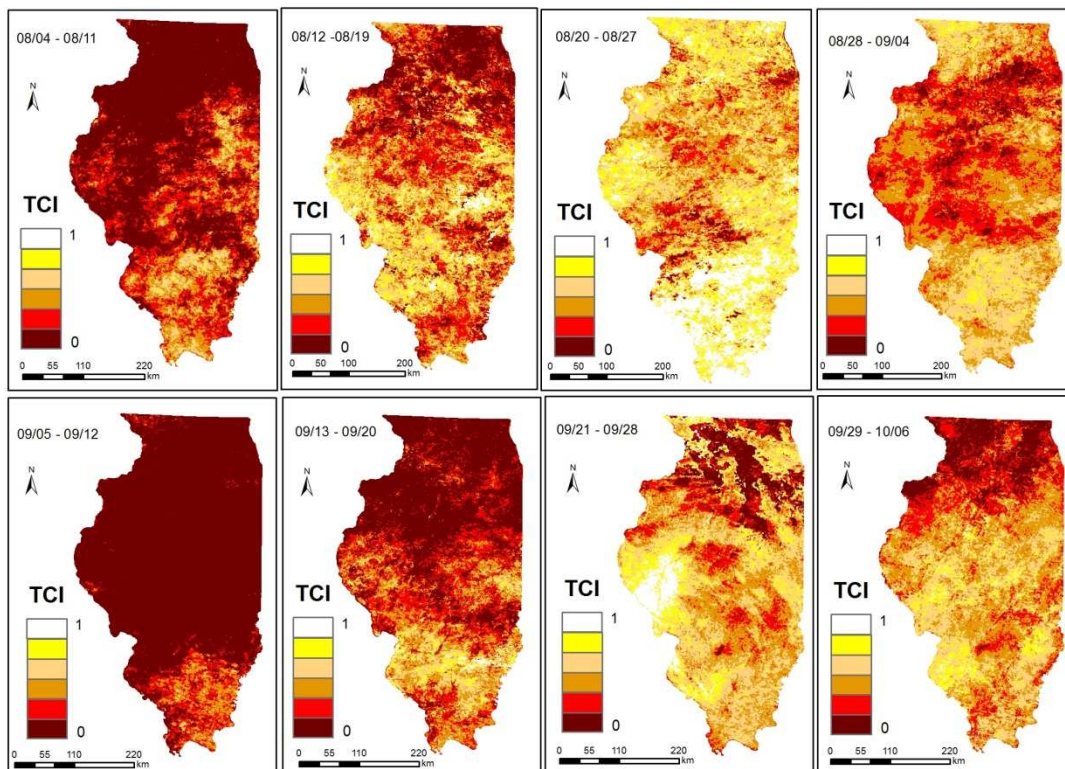




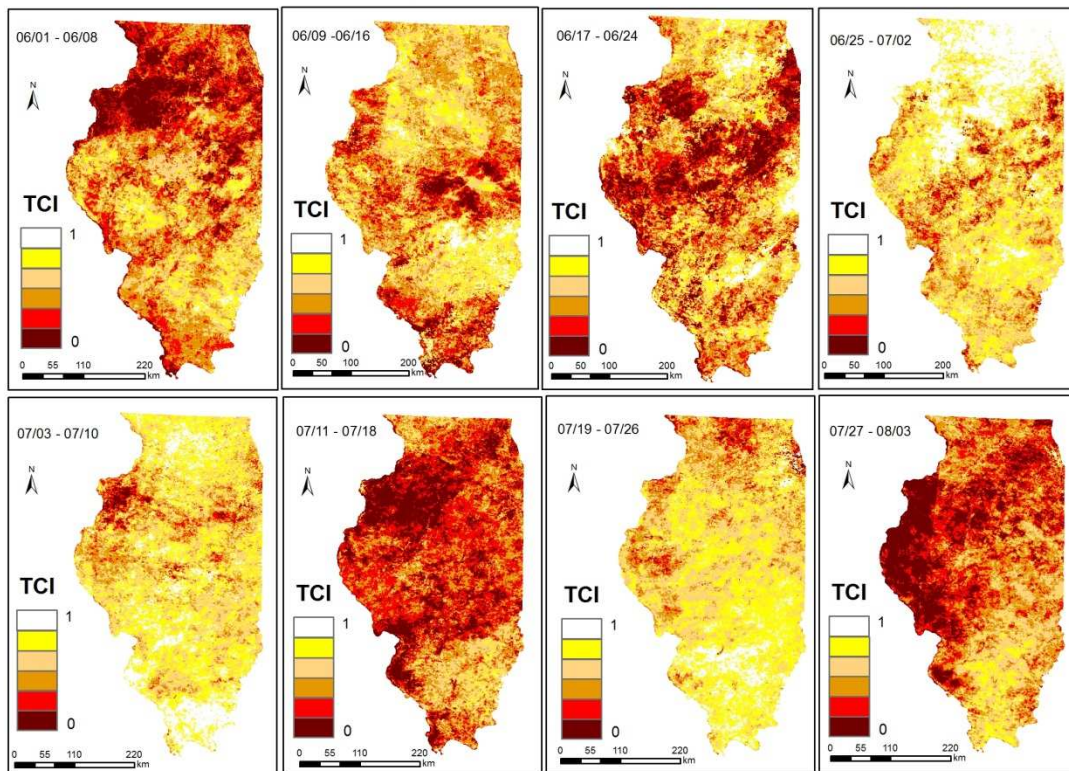
## 2005 Illinois Temperature Condition Index Map I



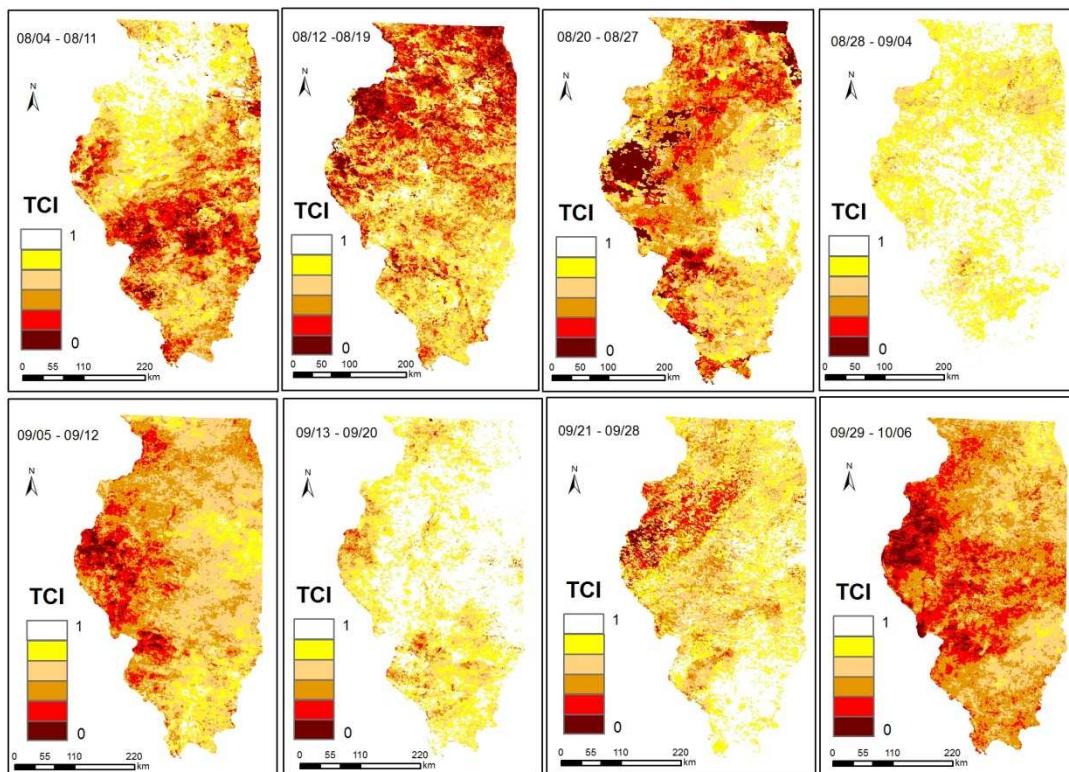
## 2005 Illinois Temperature Condition Index Map II



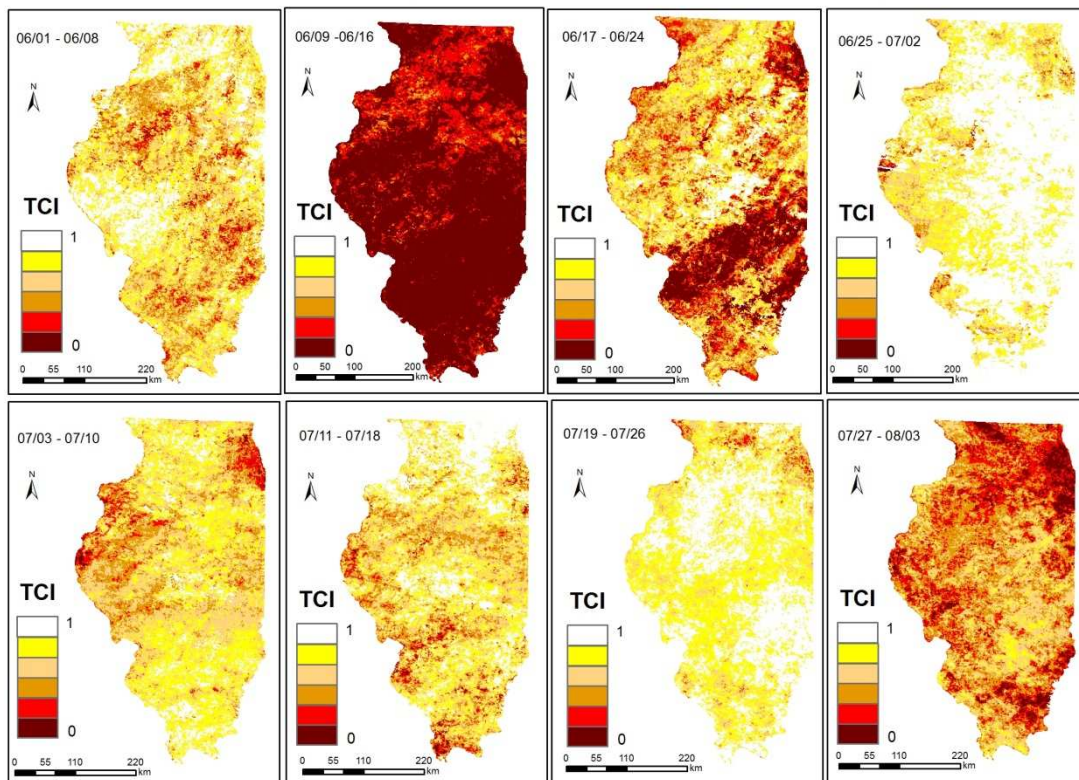
## 2006 Illinois Temperature Condition Index Map I



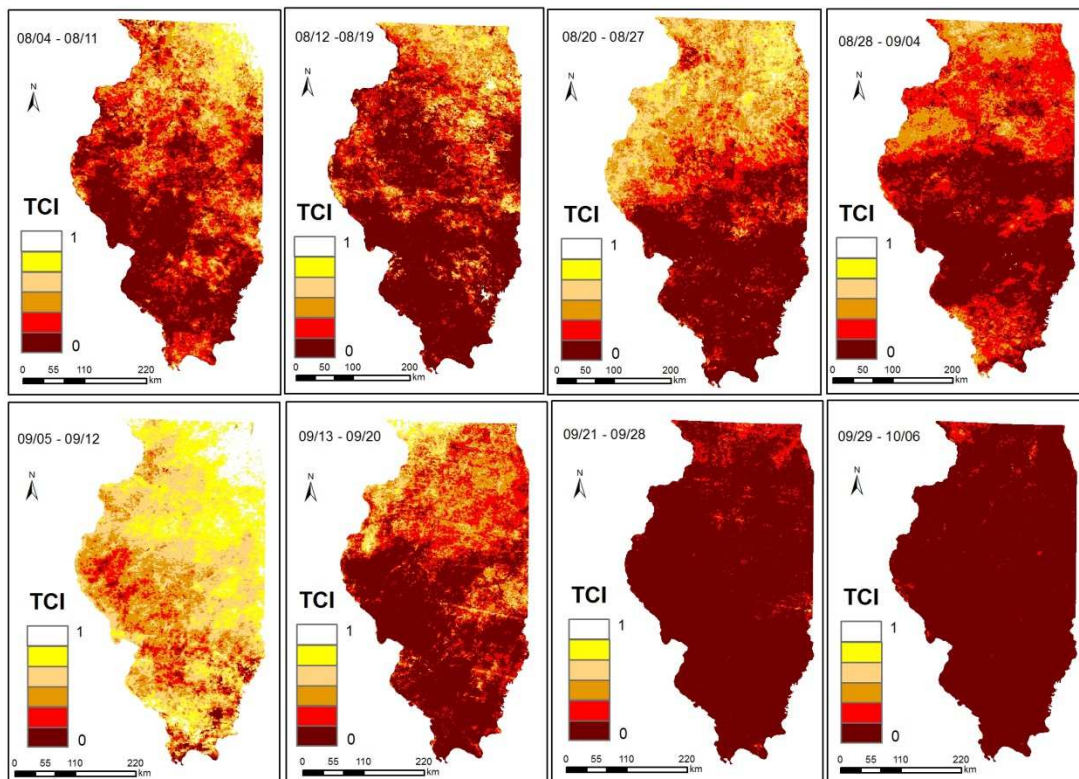
## 2006 Illinois Temperature Condition Index Map II



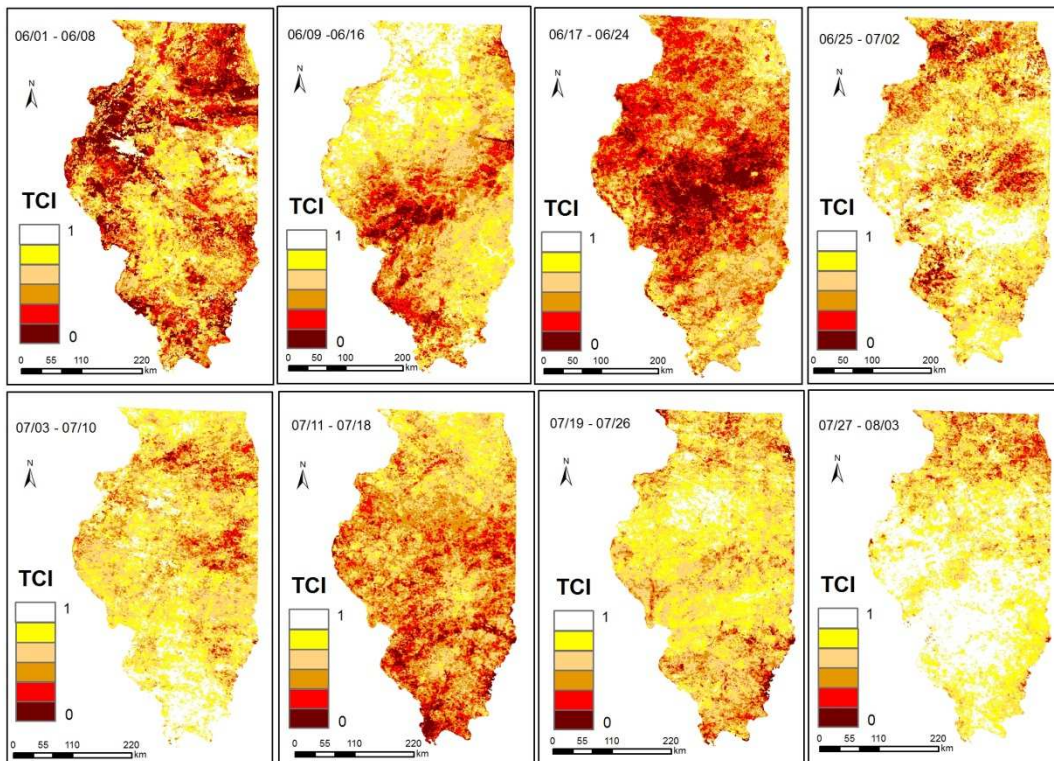
## 2007 Illinois Temperature Condition Index Map I



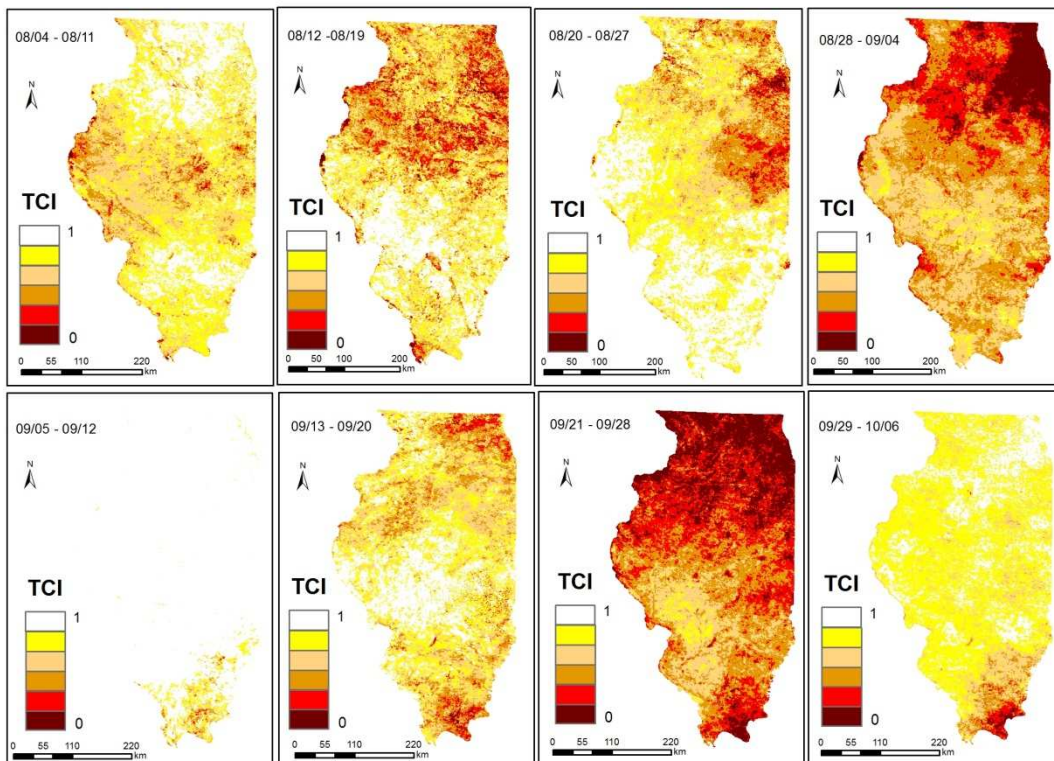
## 2007 Illinois Temperature Condition Index Map II



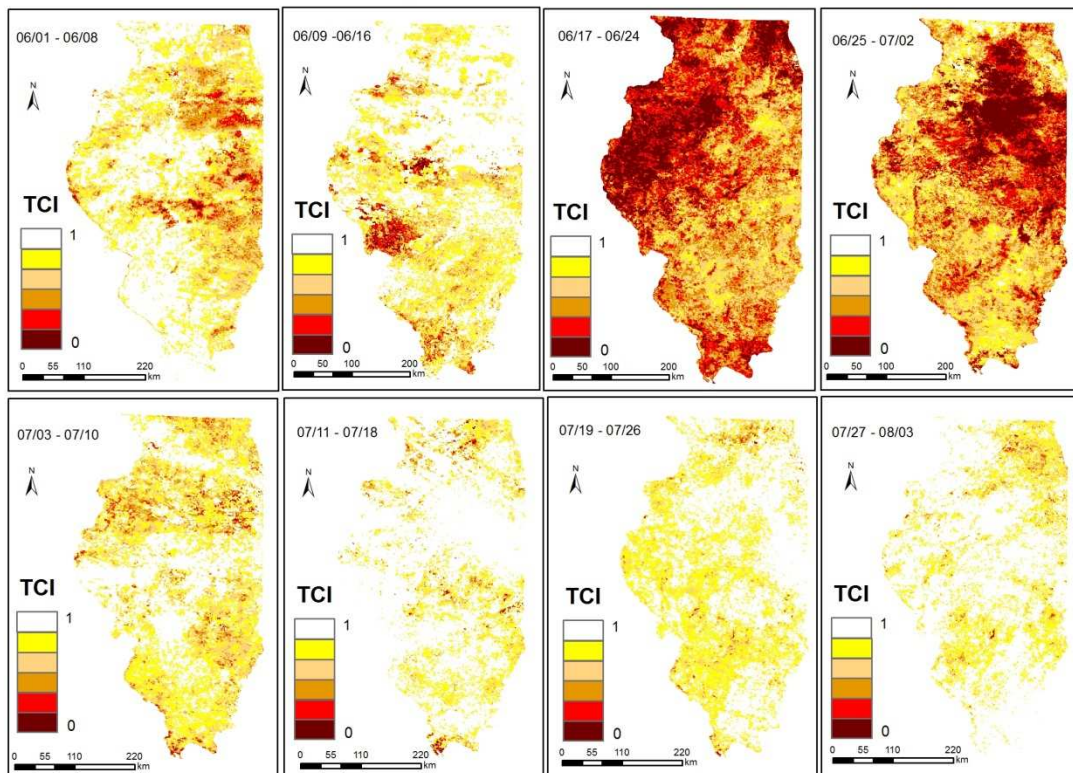
## 2008 Illinois Temperature Condition Index Map I



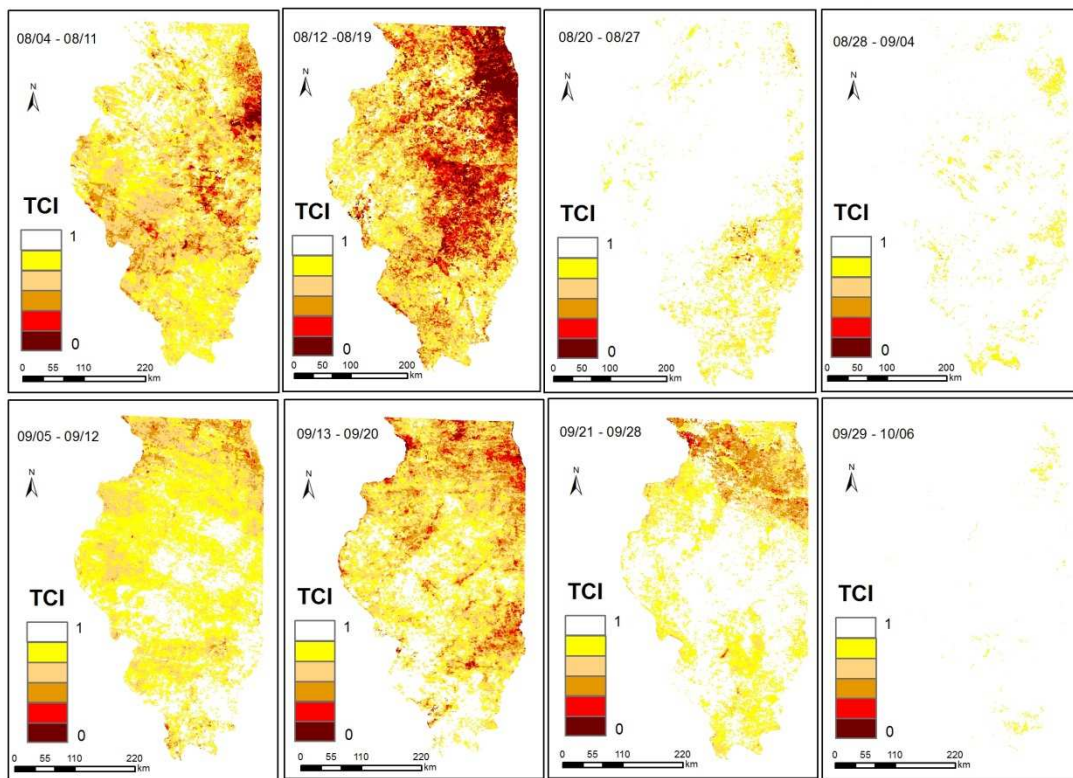
## 2008 Illinois Temperature Condition Index Map II



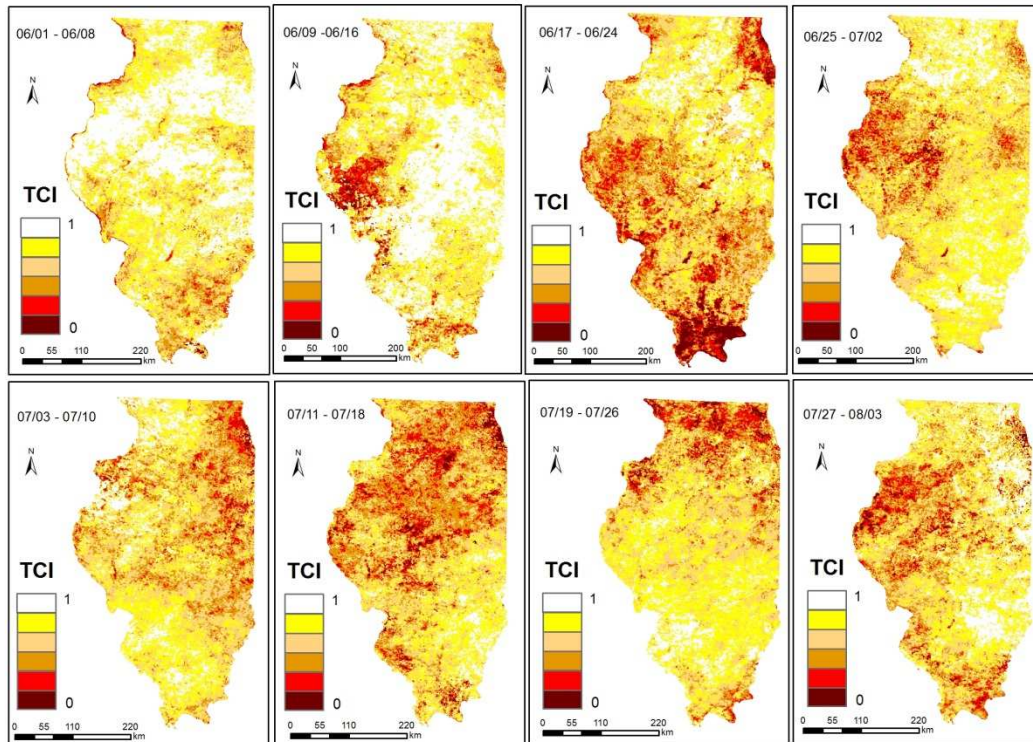
## 2009 Illinois Temperature Condition Index Map I



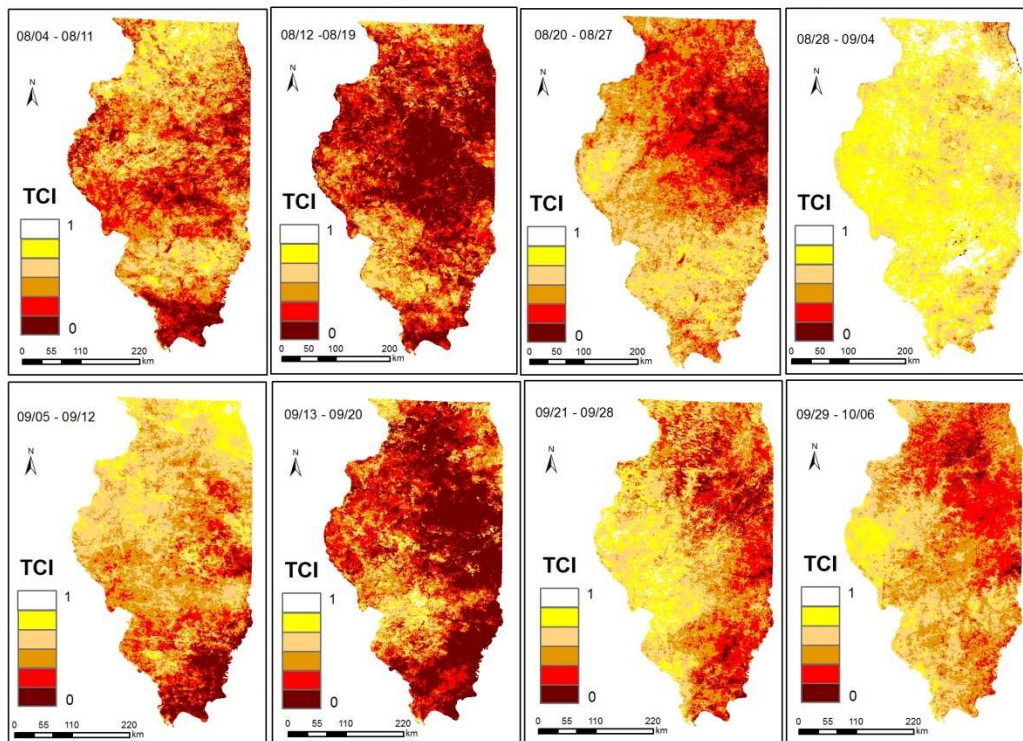
## 2009 Illinois Temperature Conditon Index Map II



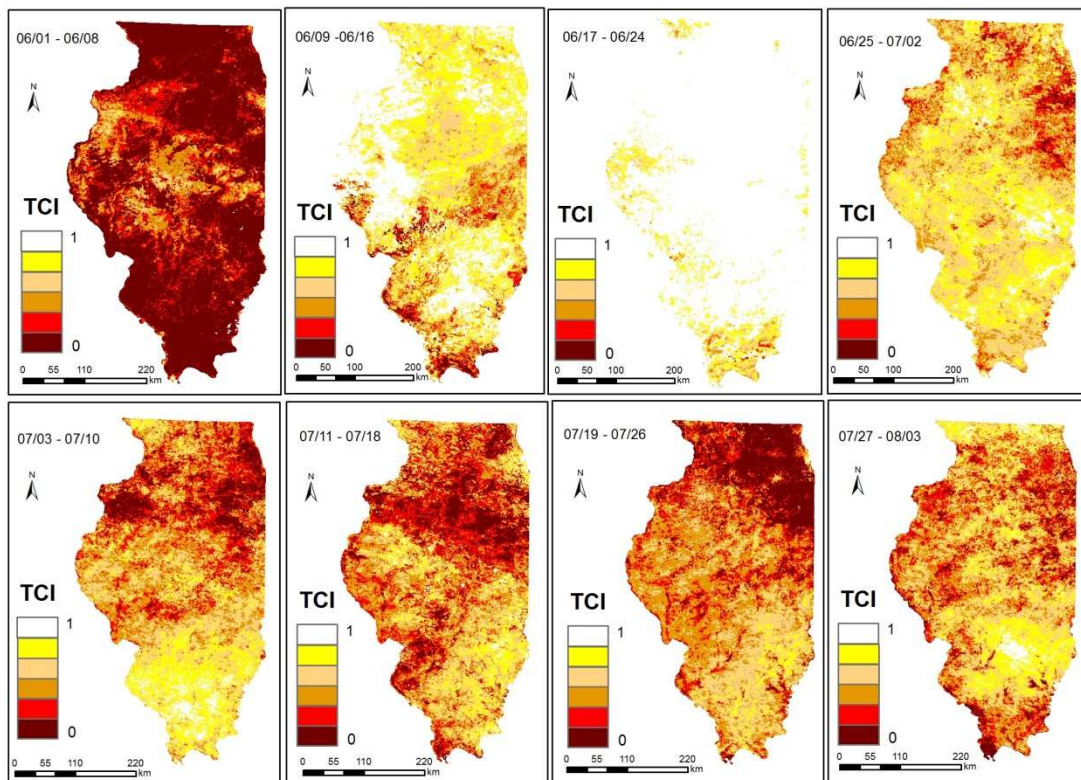
## 2010 Illinois Temperature Condition Index Map I



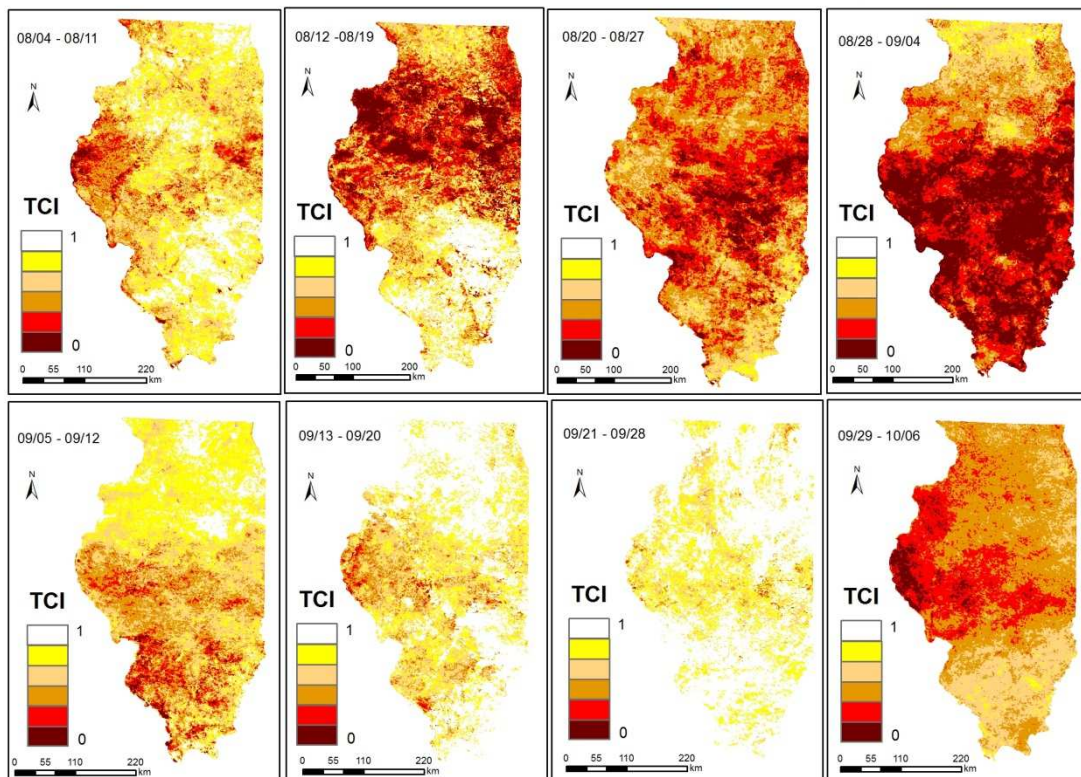
## 2010 Illinois Temperature Condition Index Map II



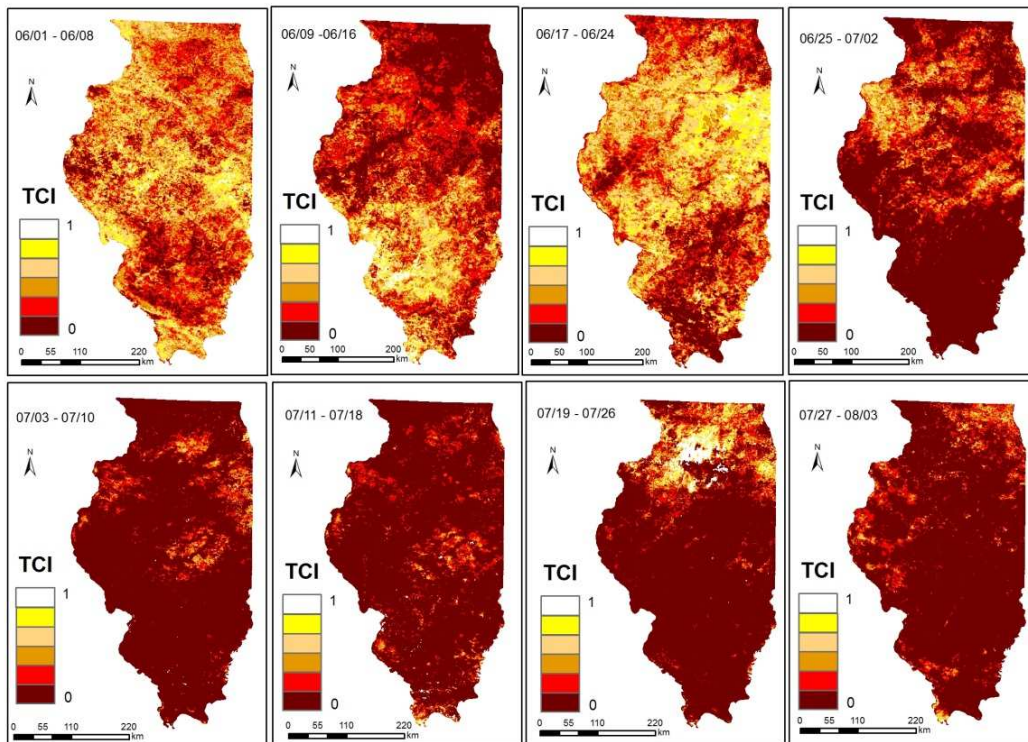
## 2011 Illinois Temperature Condition Index Map I



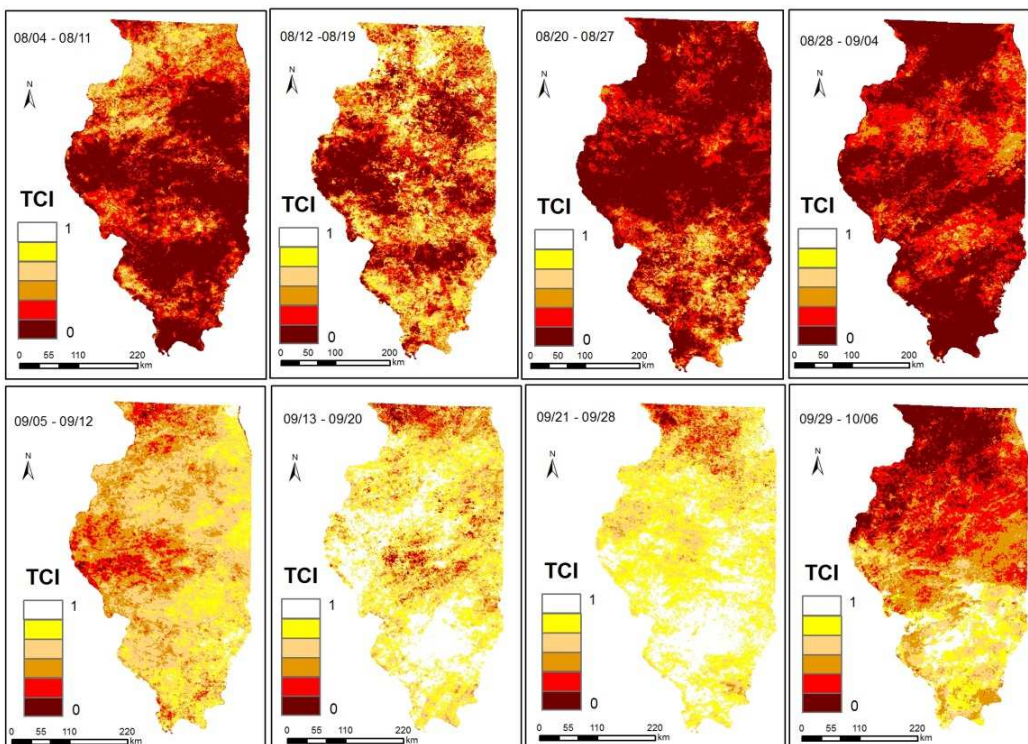
## 2011 Illinois Temperature Condition Index Map II



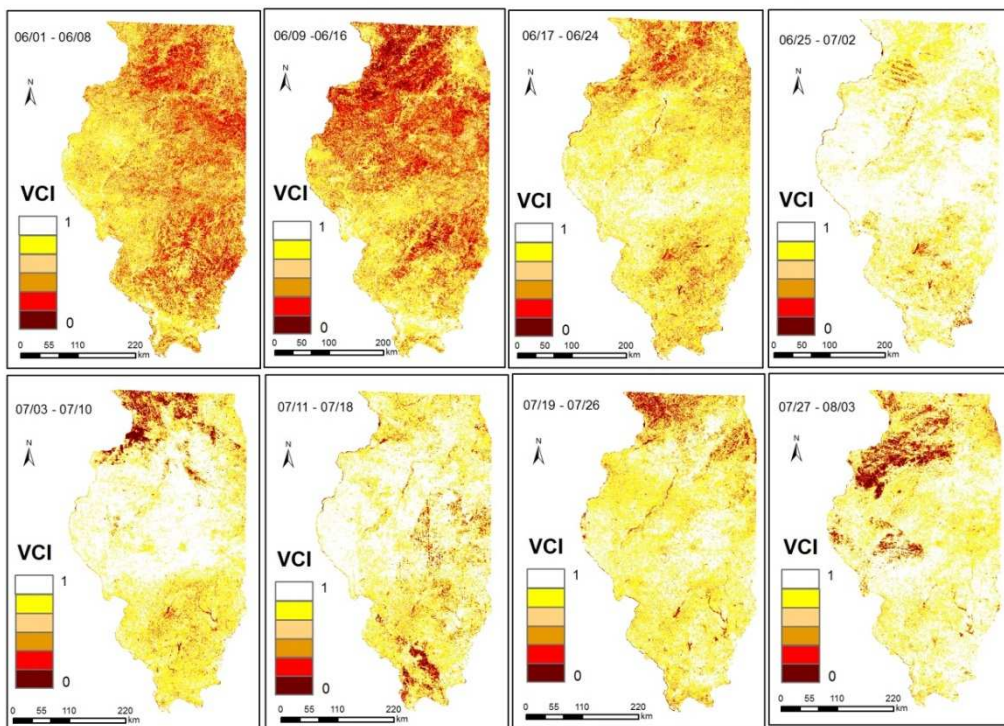
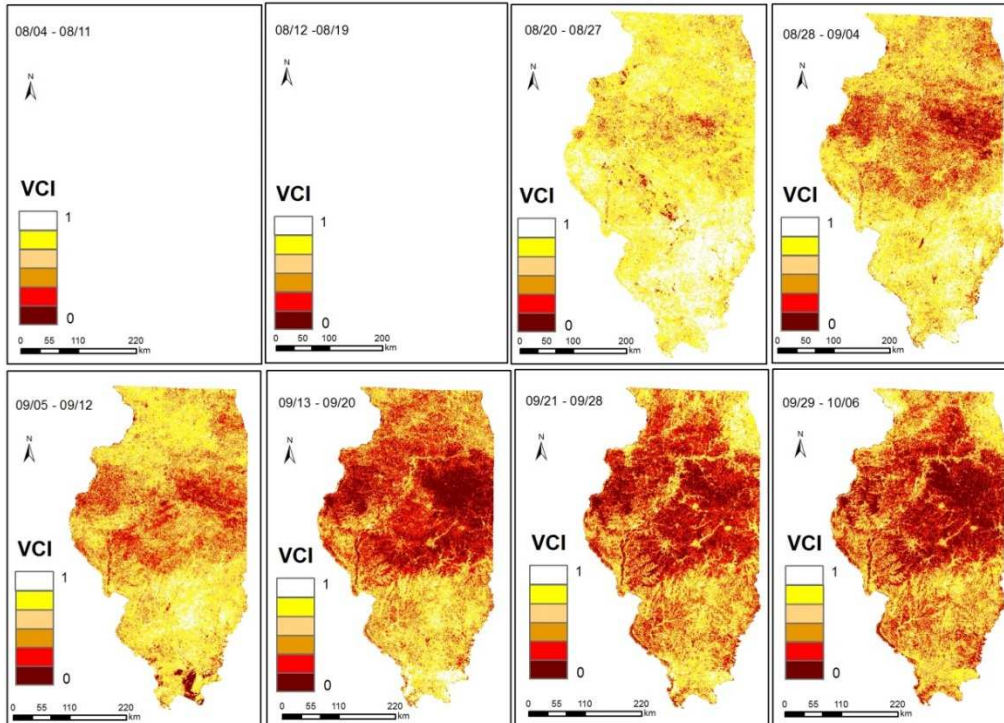
## 2012 Illinois Temperature Condition Index Map I



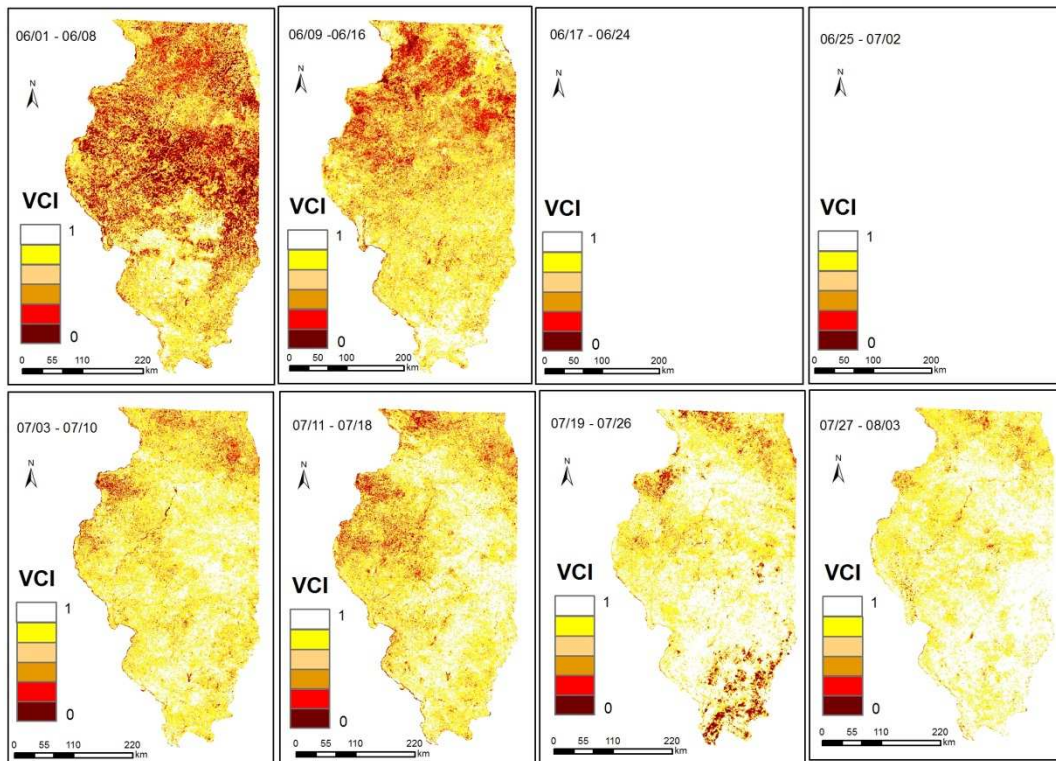
## 2012 Illinois Temperature Condition Index Map II



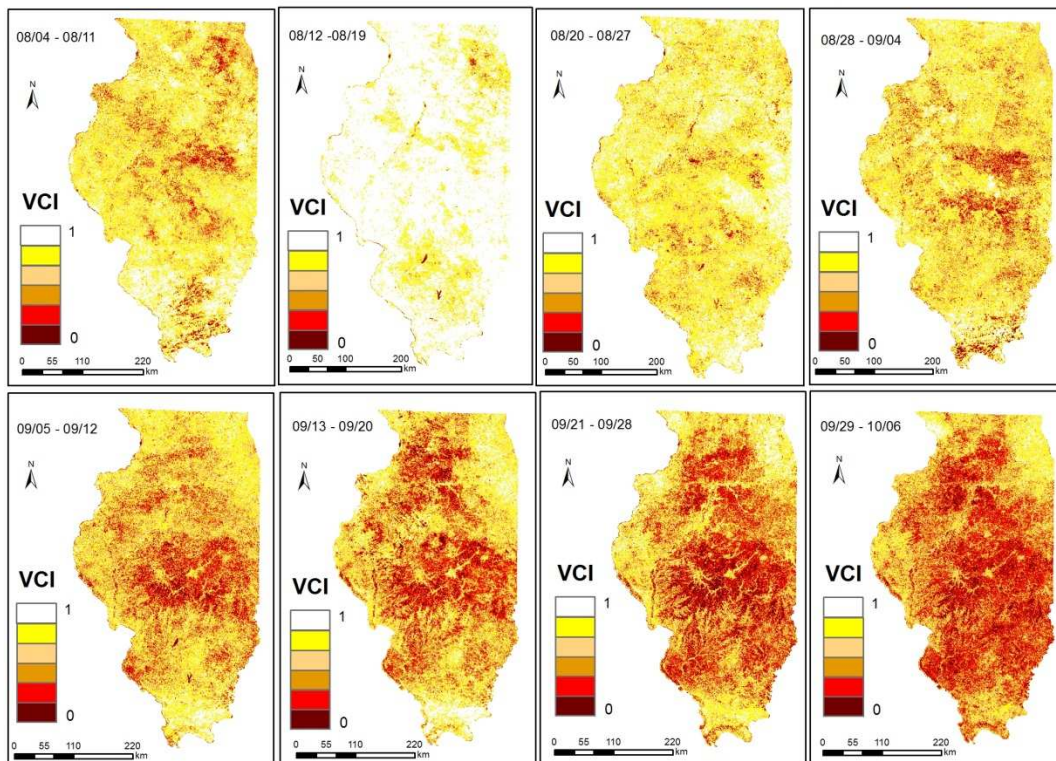


**Appendix B: Vegetation Condition Index Maps of Illinois for years 2000-2012.****2000 Illinois Vegetation Condition Index Map I****2000 Illinois Vegetation Condition Index Map II**

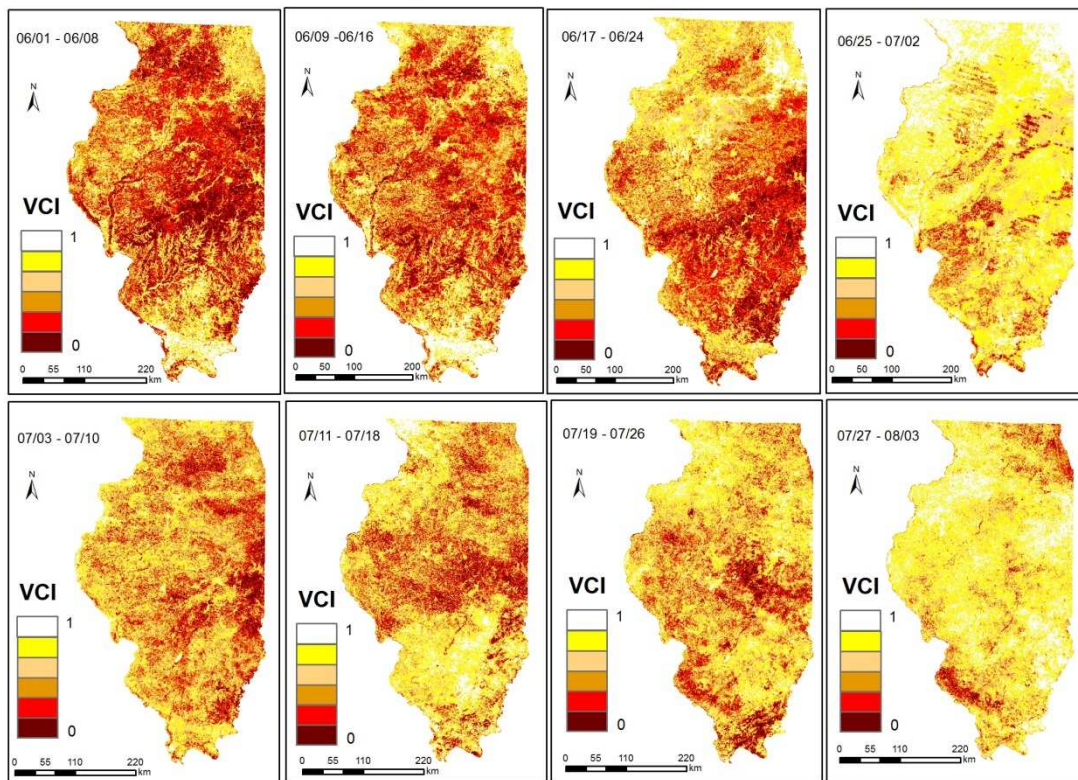
## 2001 Illinois Vegetation Condition Index Map I



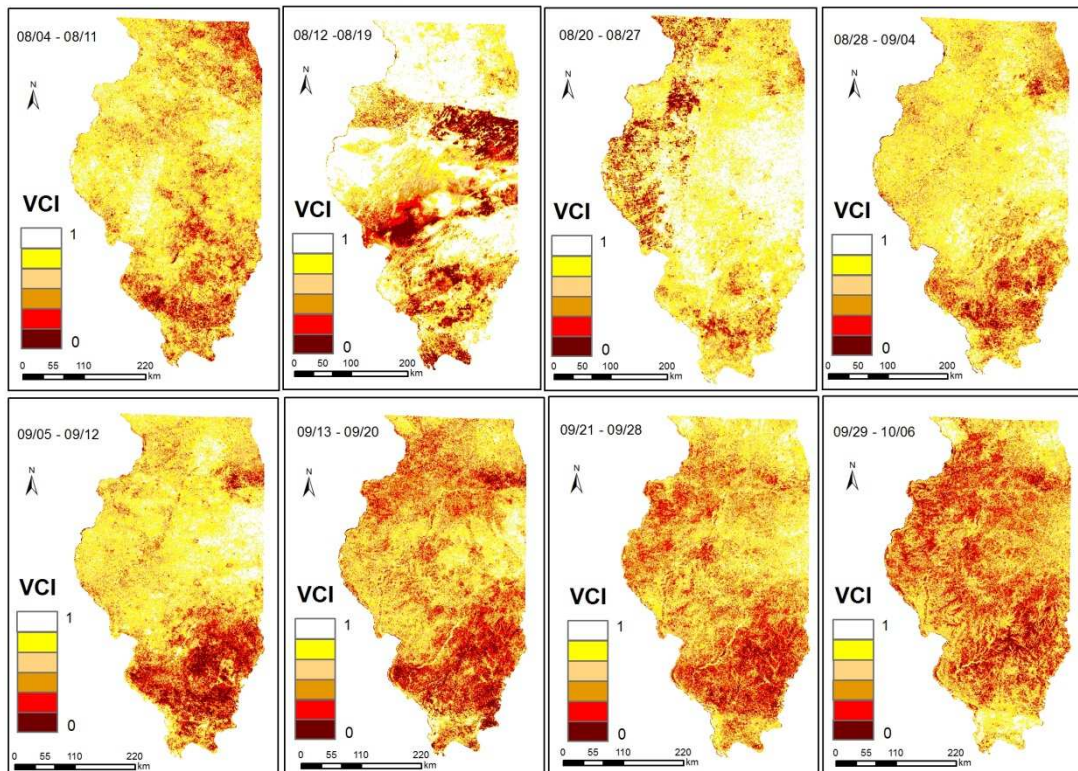
## 2001 Illinois Vegetation Condition Index Map II



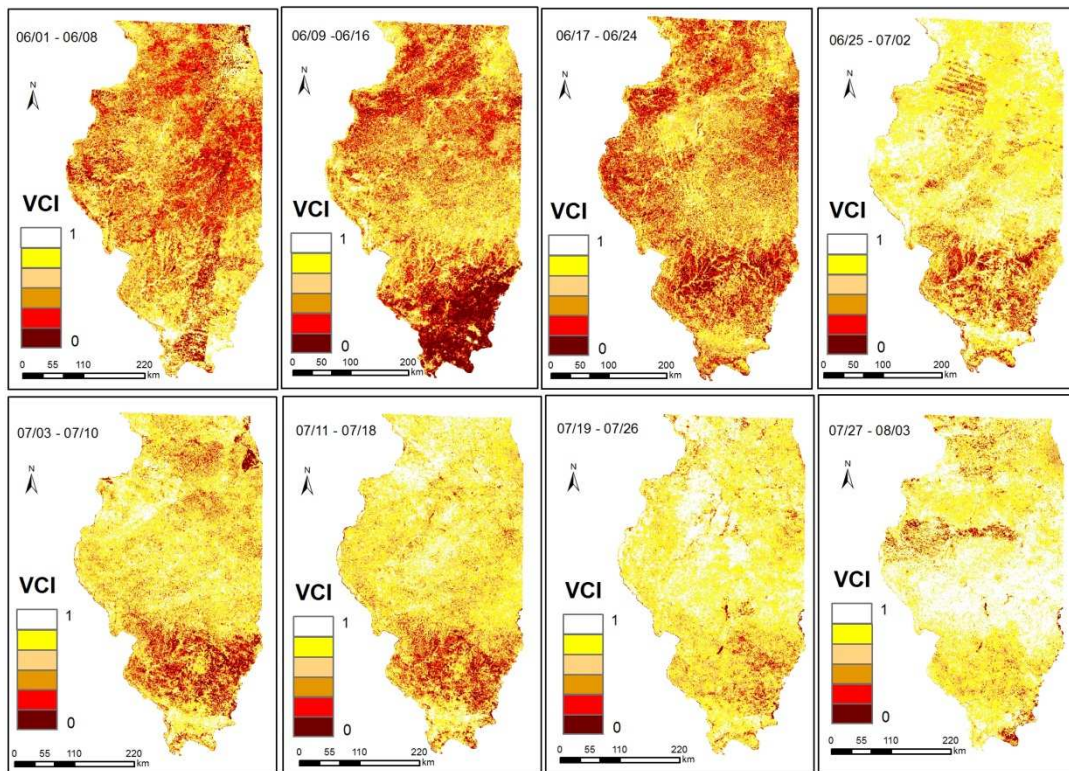
## 2002 Illinois Vegetation Condition Index Map I



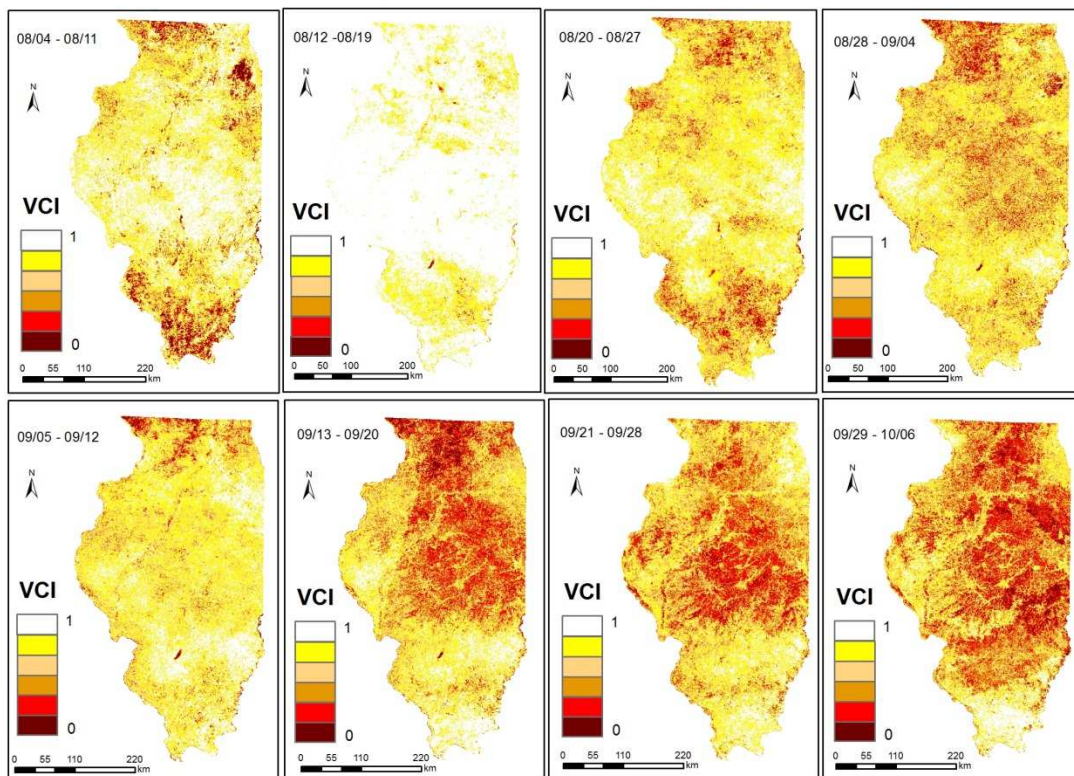
## 2002 Illinois Vegetation Condition Index Map II



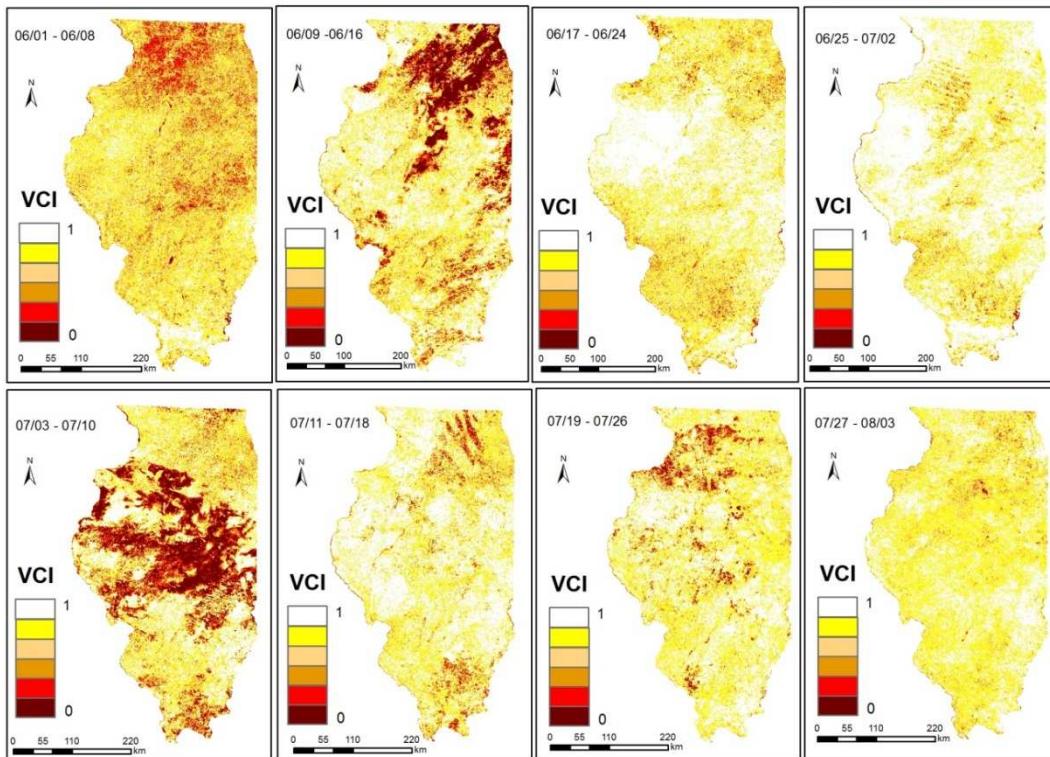
## 2003 Illinois Vegetation Condition Index Map I



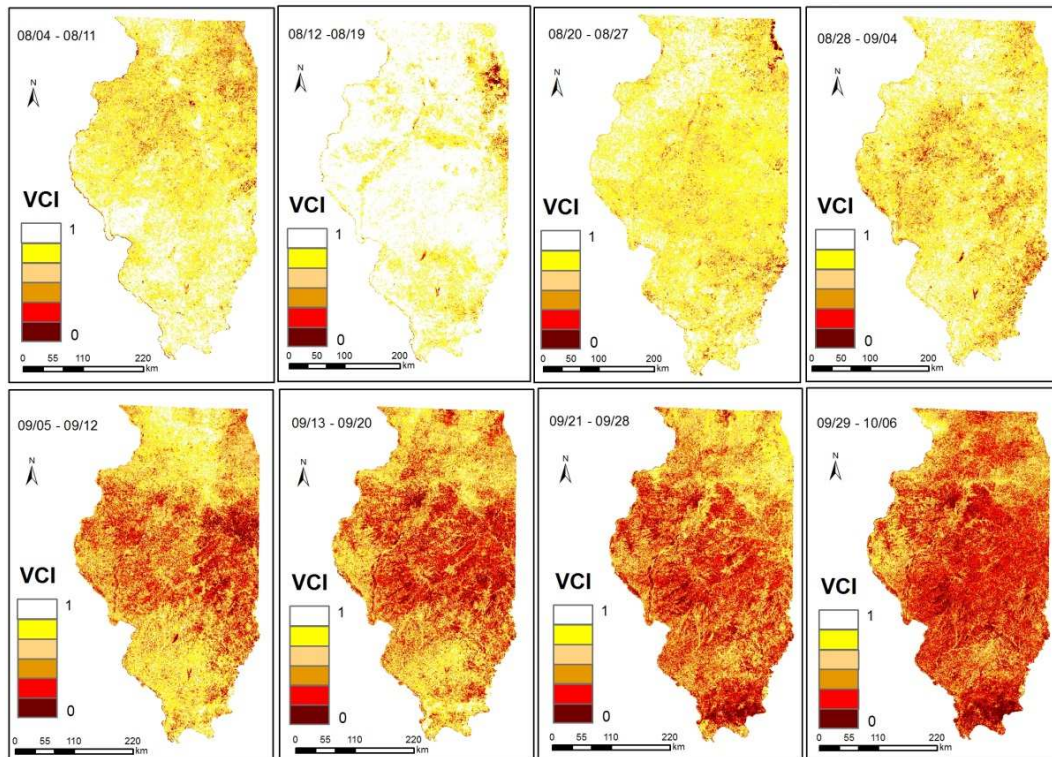
## 2003 Illinois Vegetation Condition Index Map II



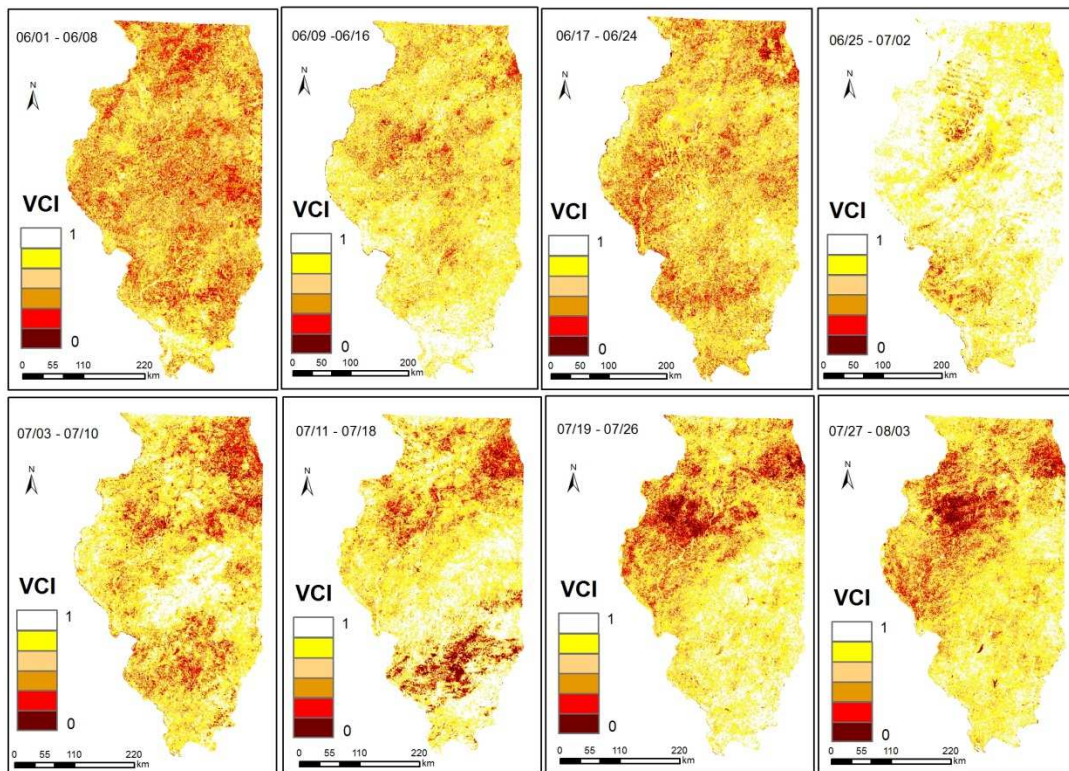
## 2004 Illinois Vegetation Condition Index Map I



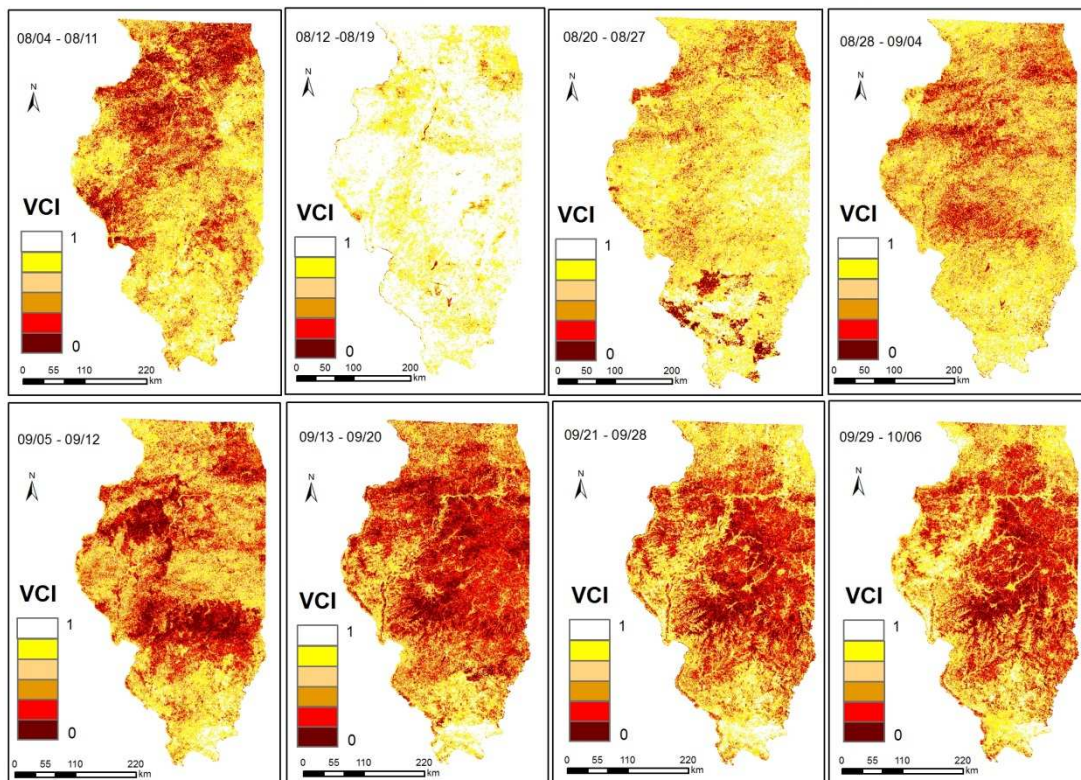
## 2004 Illinois Vegetation Condition Index Map II



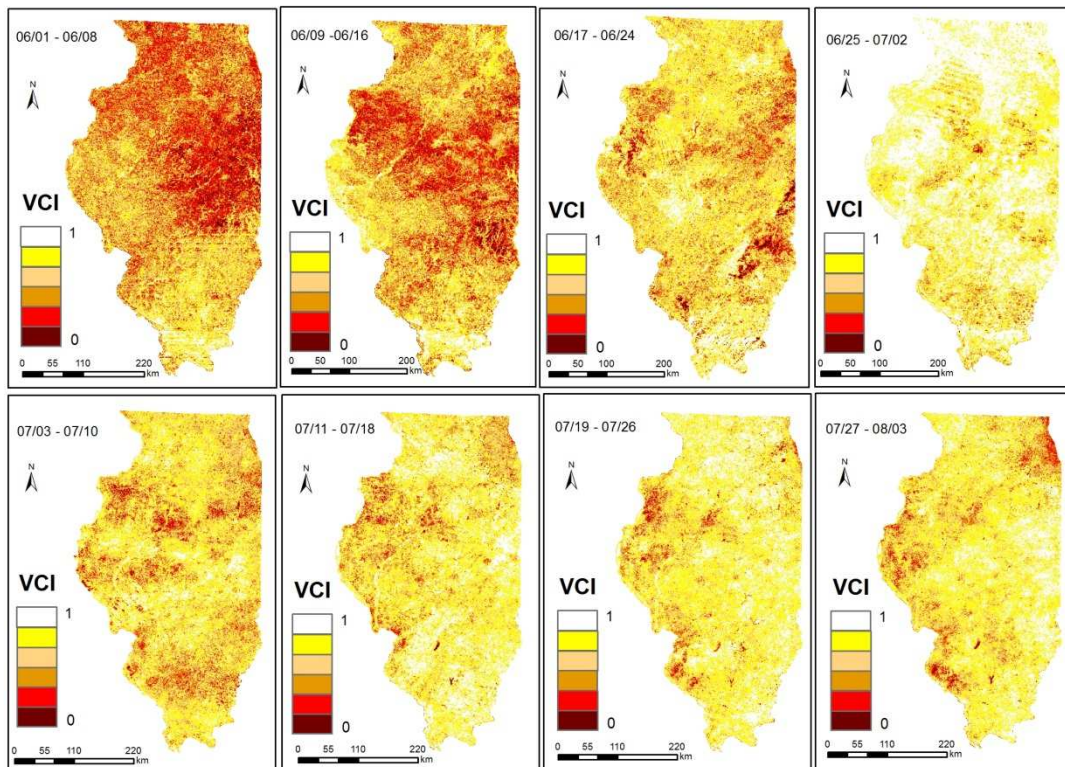
## 2005 Illinois Vegetation Condition Index Map I



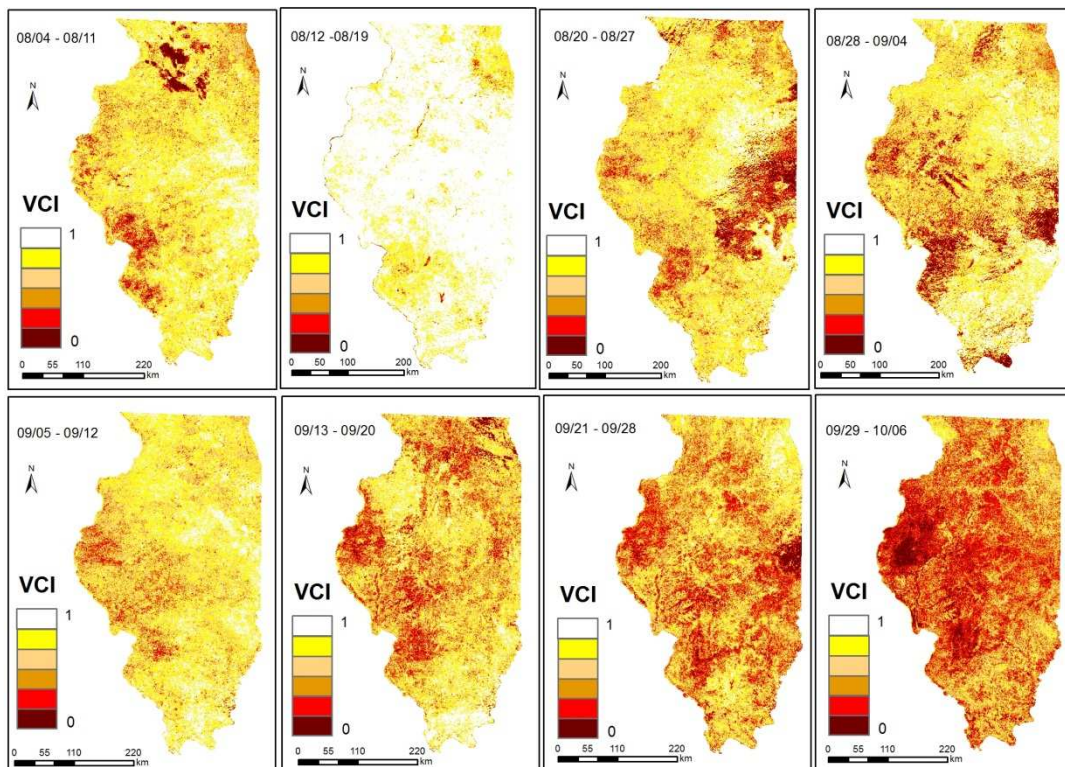
## 2005 Illinois Vegetation Condition Index Map II



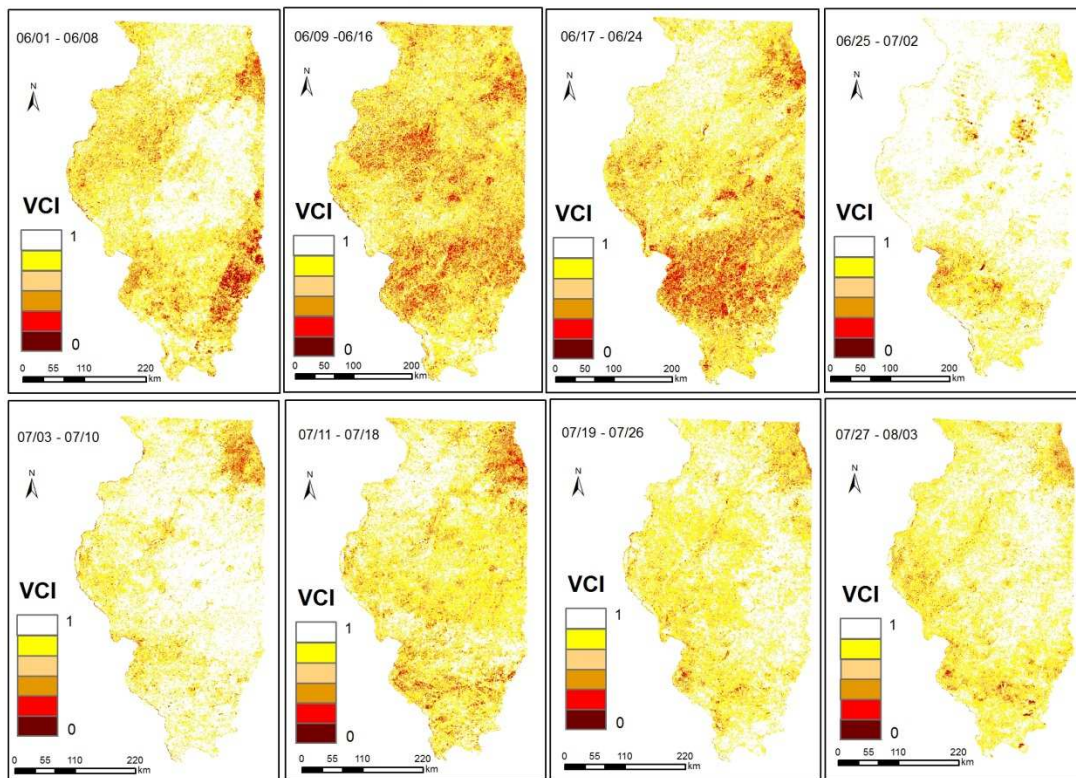
## 2006 Illinois Vegetation Condition Index Map I



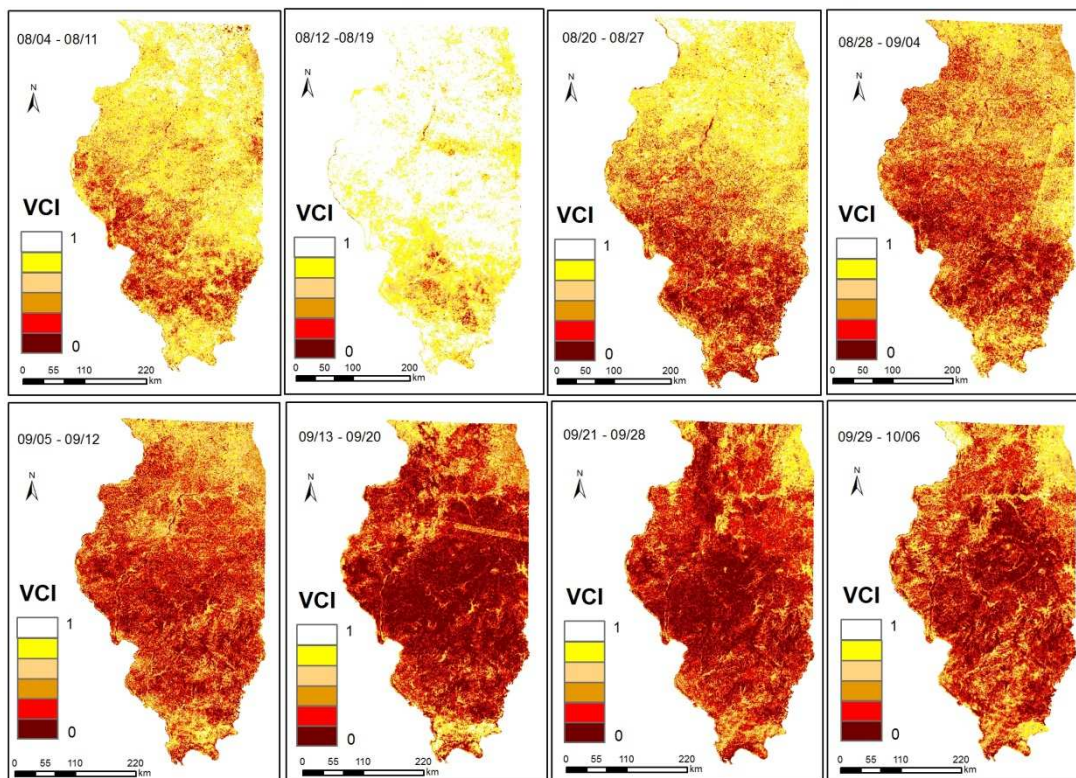
## 2006 Illinois Vegetation Condition Index Map II



## 2007 Illinois Vegetation Condition Index Map I

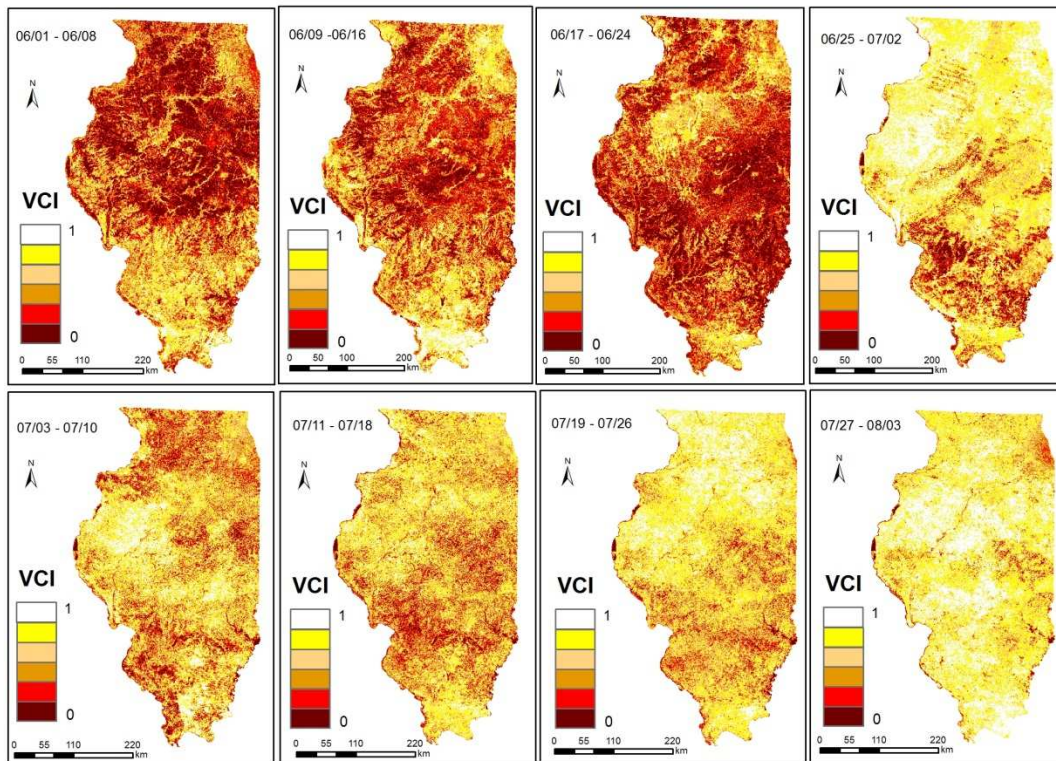


## 2007 Illinois Vegetation Condition Index Map II

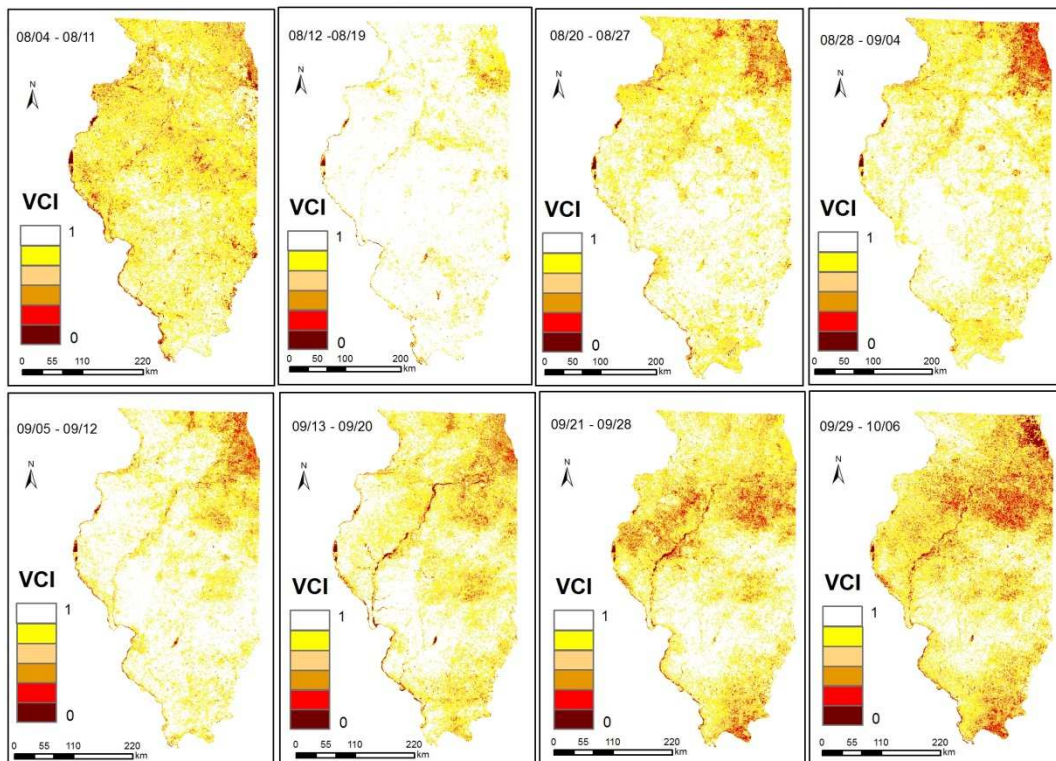




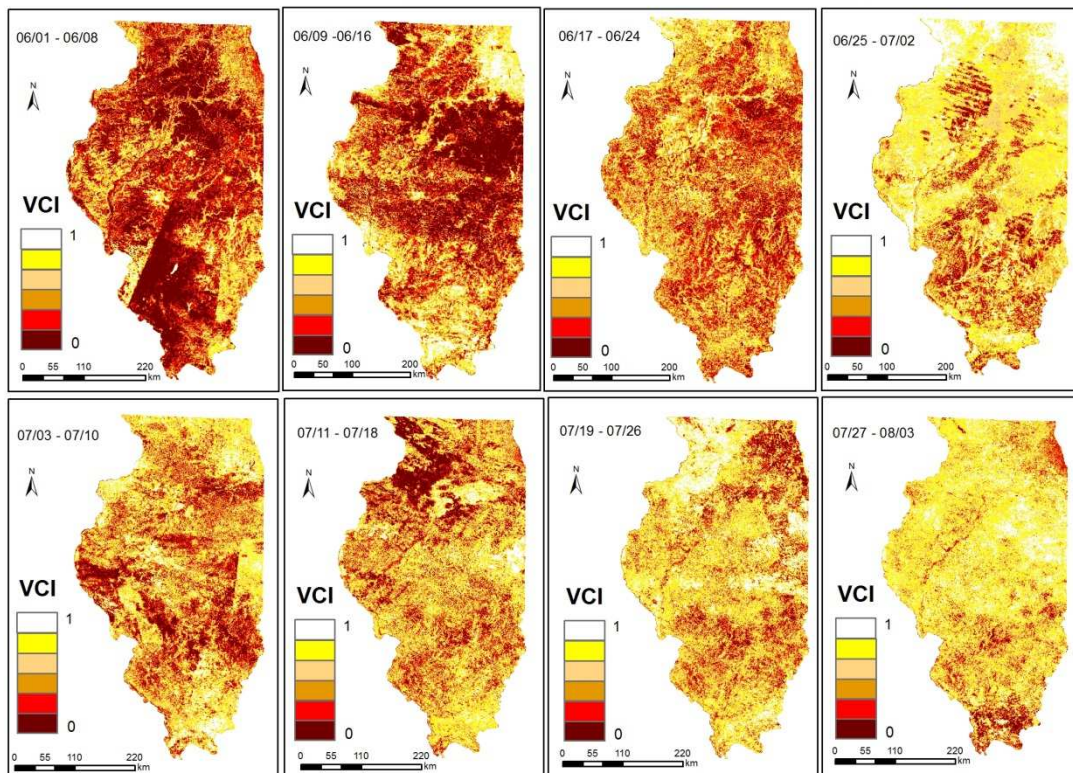
## 2008 Illinois Vegetation Condition Index Map I



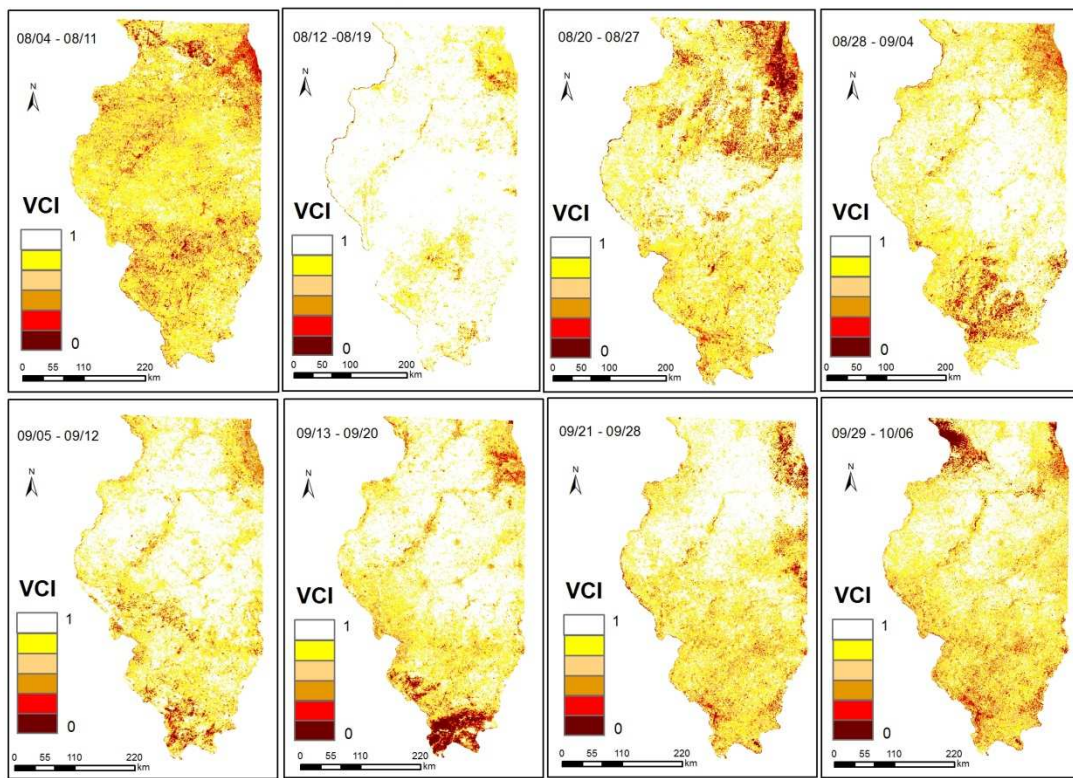
## 2008 Illinois Vegetation Condition Index Map II



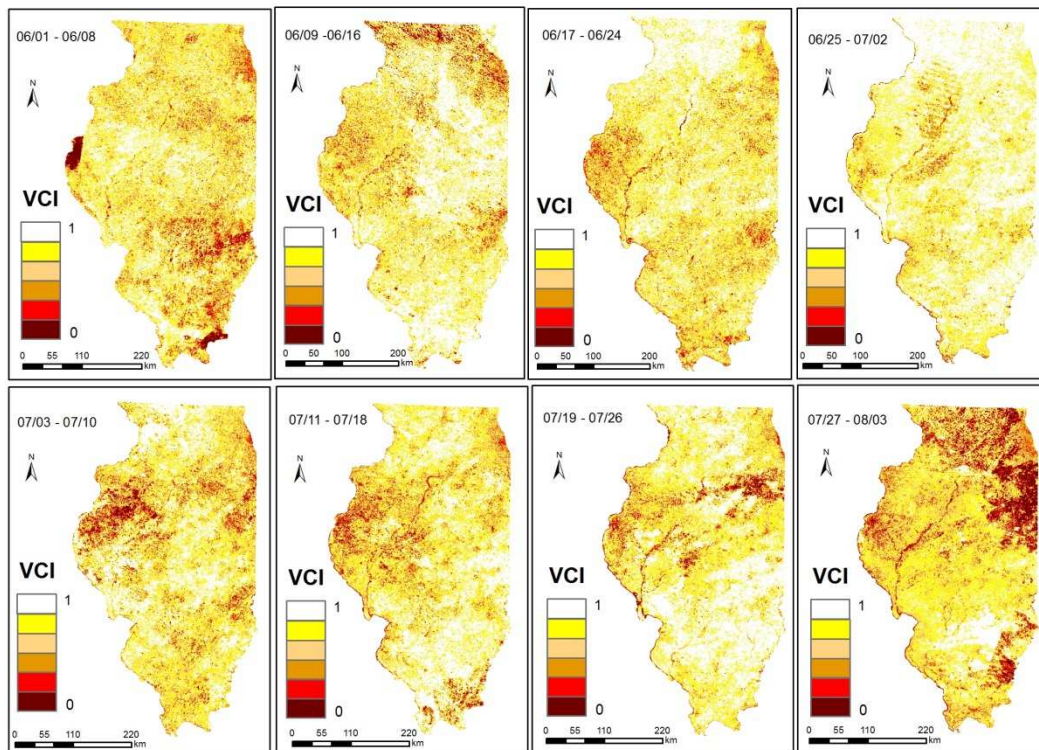
## 2009 Illinois Vegetation Condition Index Map I



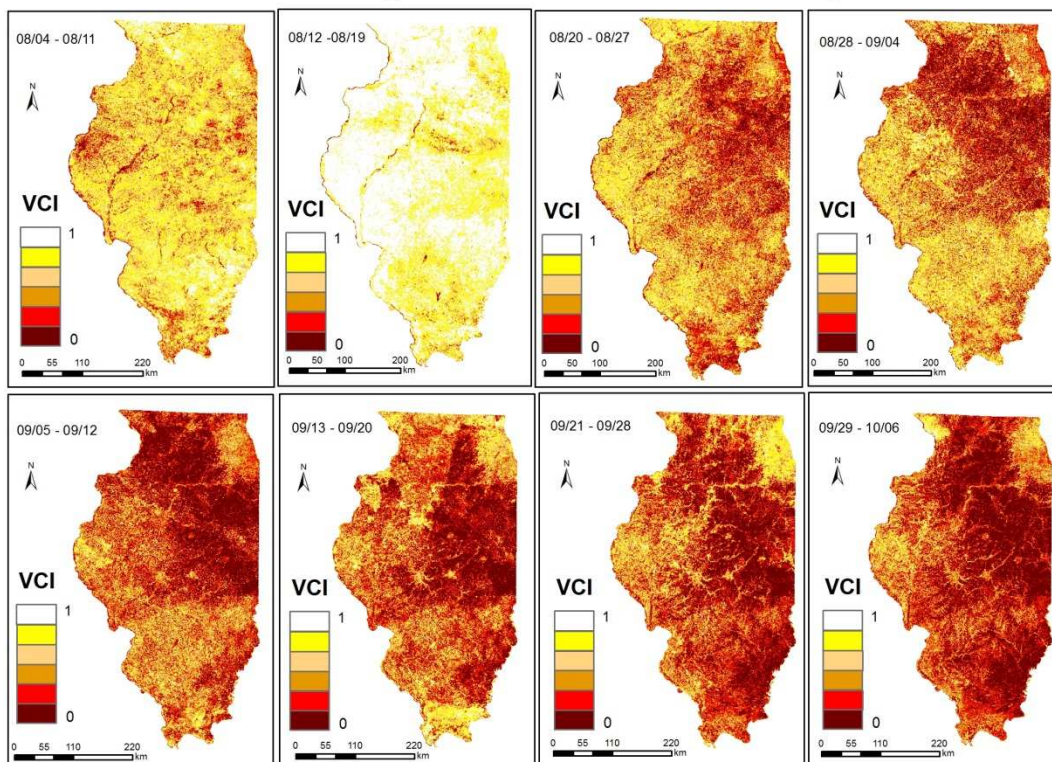
## 2009 Illinois Vegetation Condition Index Map II



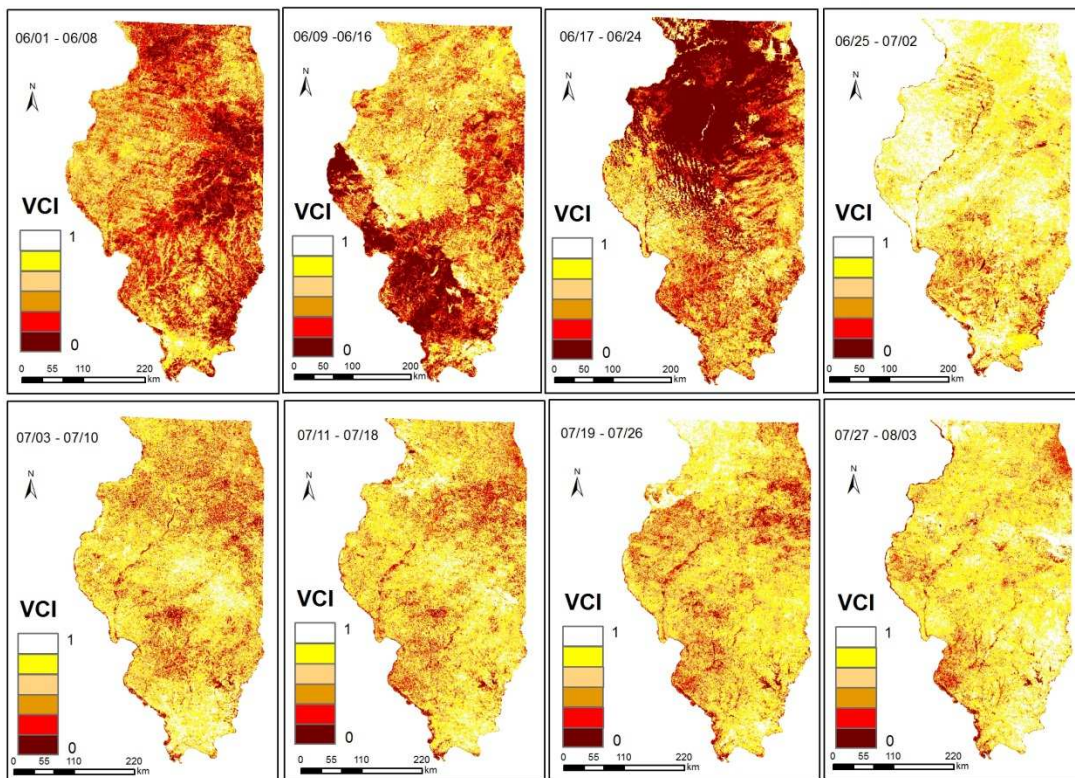
## 2010 Illinois Vegetation Condition Index Map I



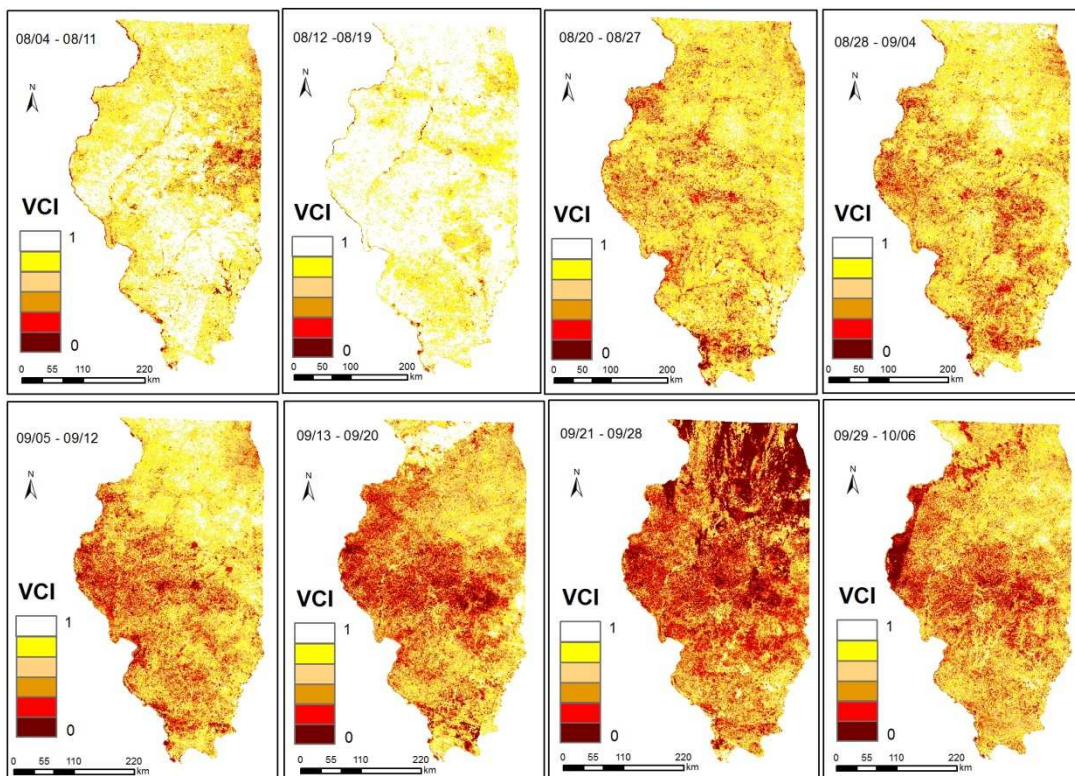
## 2010 Illinois Vegetation Condition Index Map II



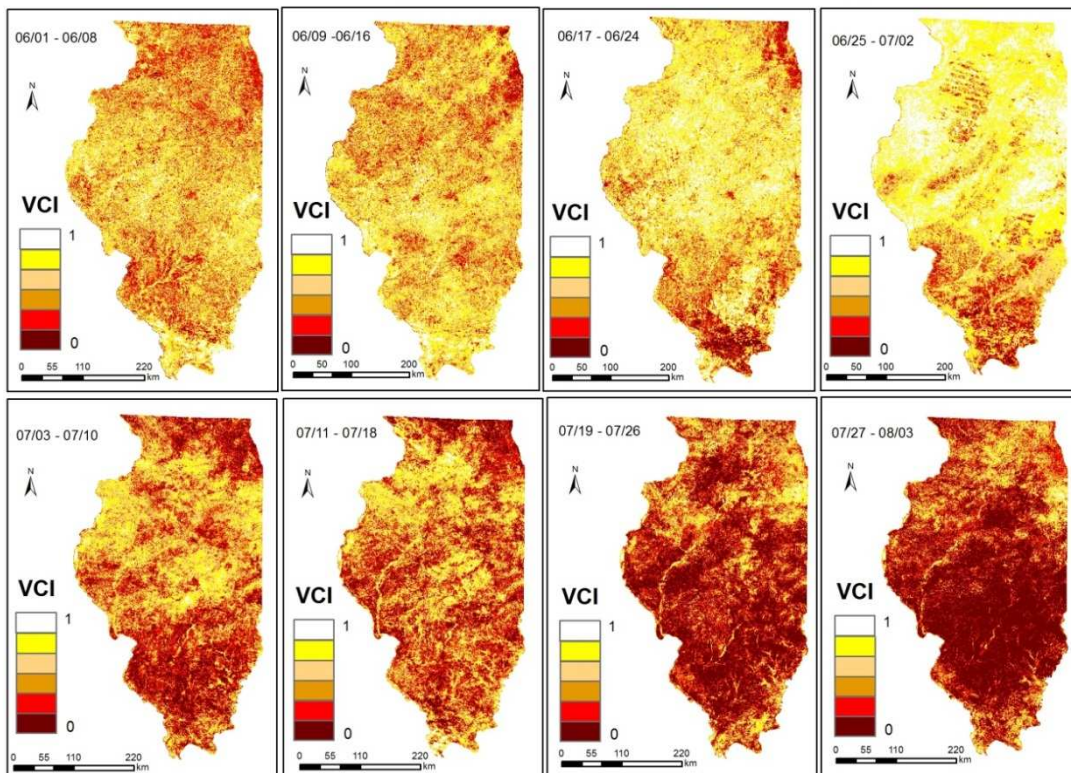
## 2011 Illinois Vegetation Condition Index Map I



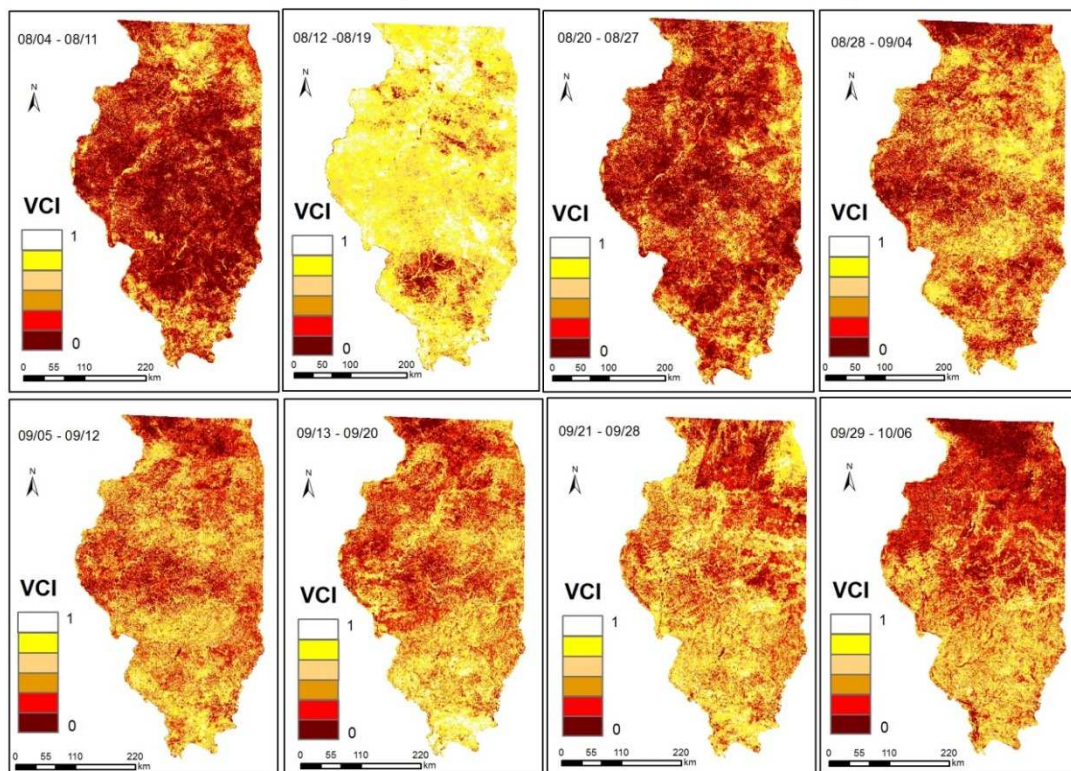
## 2011 Illinois Vegetation Condition Index Map II

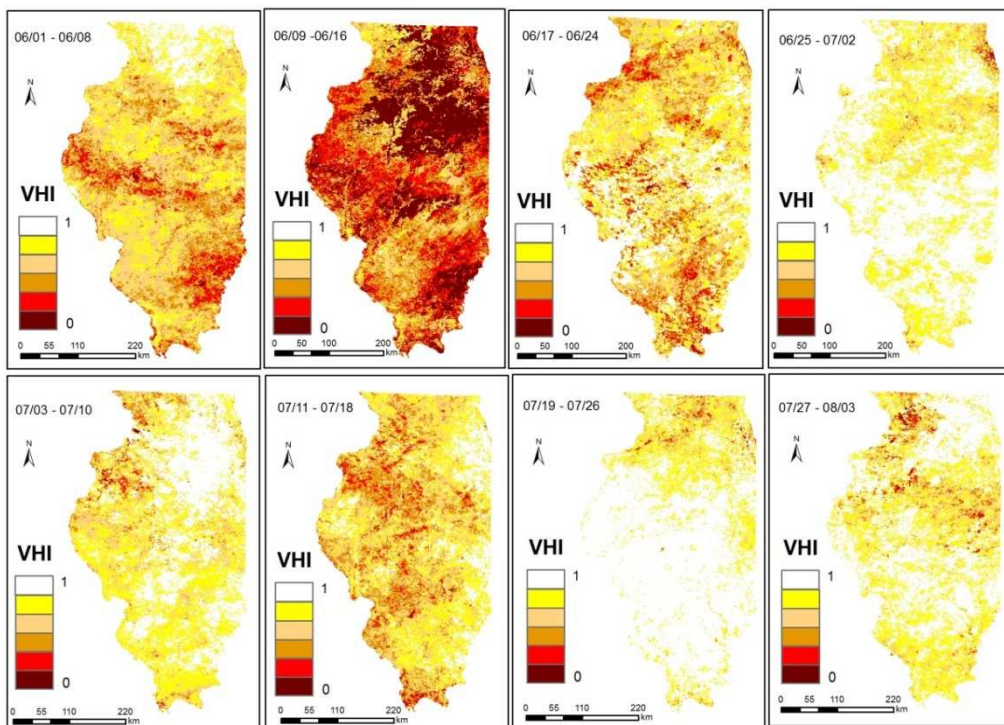
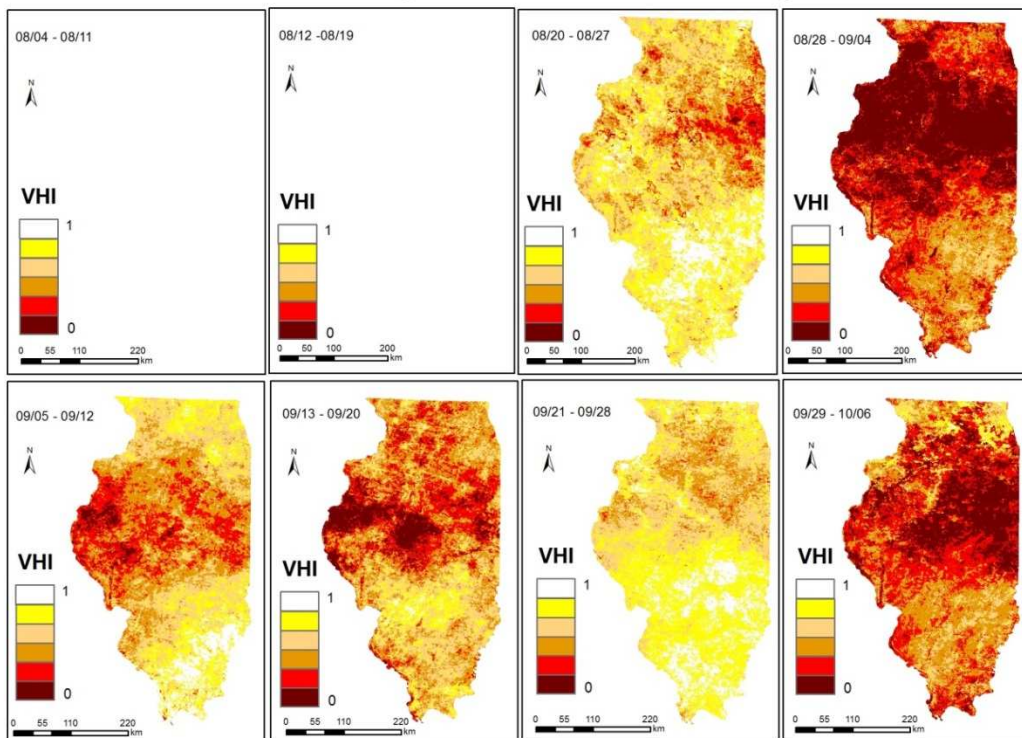


## 2012 Illinois Vegetation Condition Index Map I

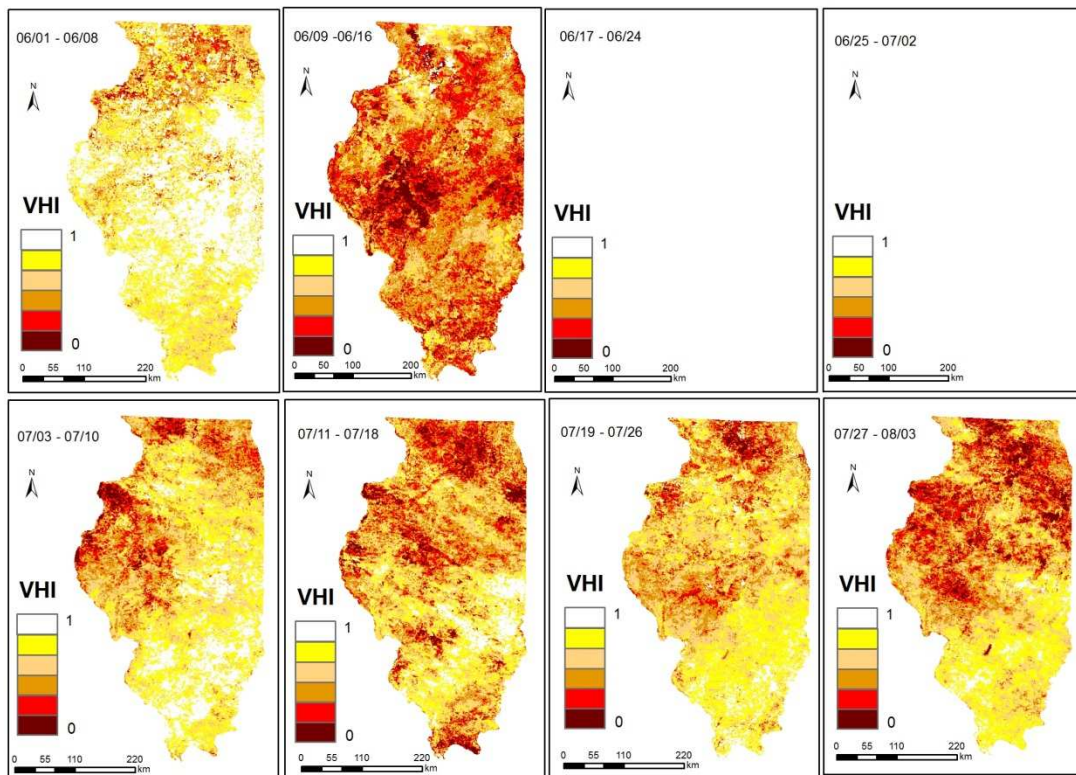


## 2012 Illinois Vegetation Condition Index Map II

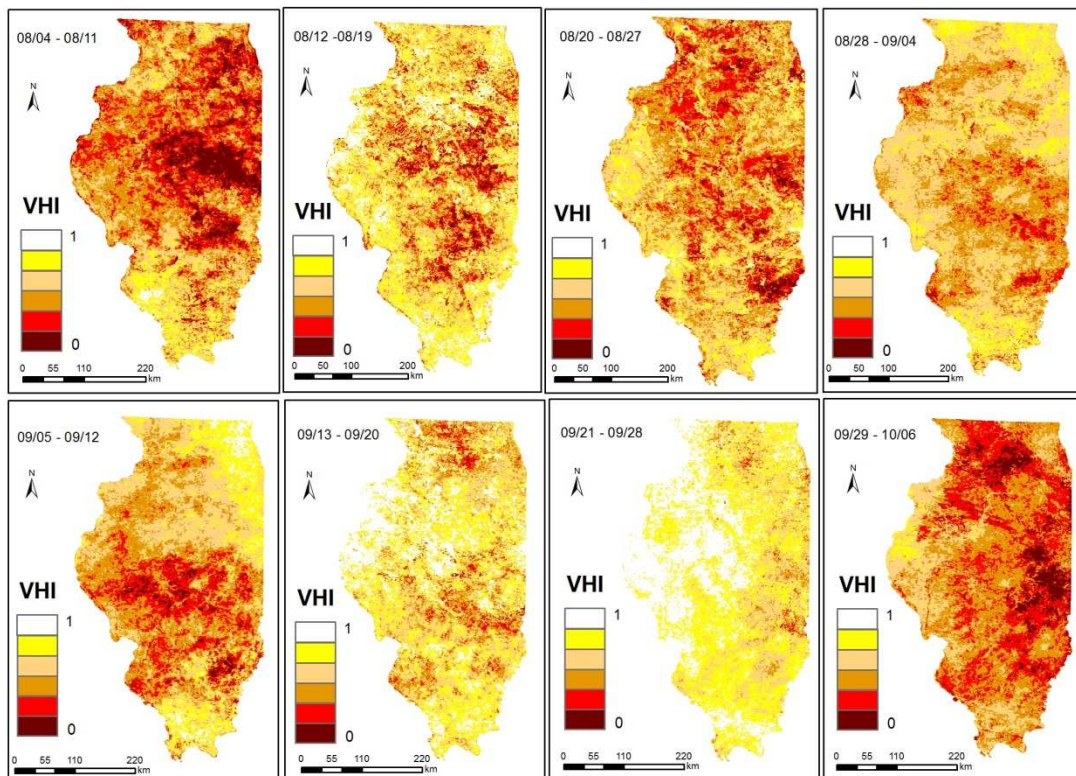


**Appendix C: Vegetation Health Index Maps of Illinois for years 2000-2012.****2000 Illinois Vegetation Health Index Map I****2000 Illinois Vegetation Health Index Map II**

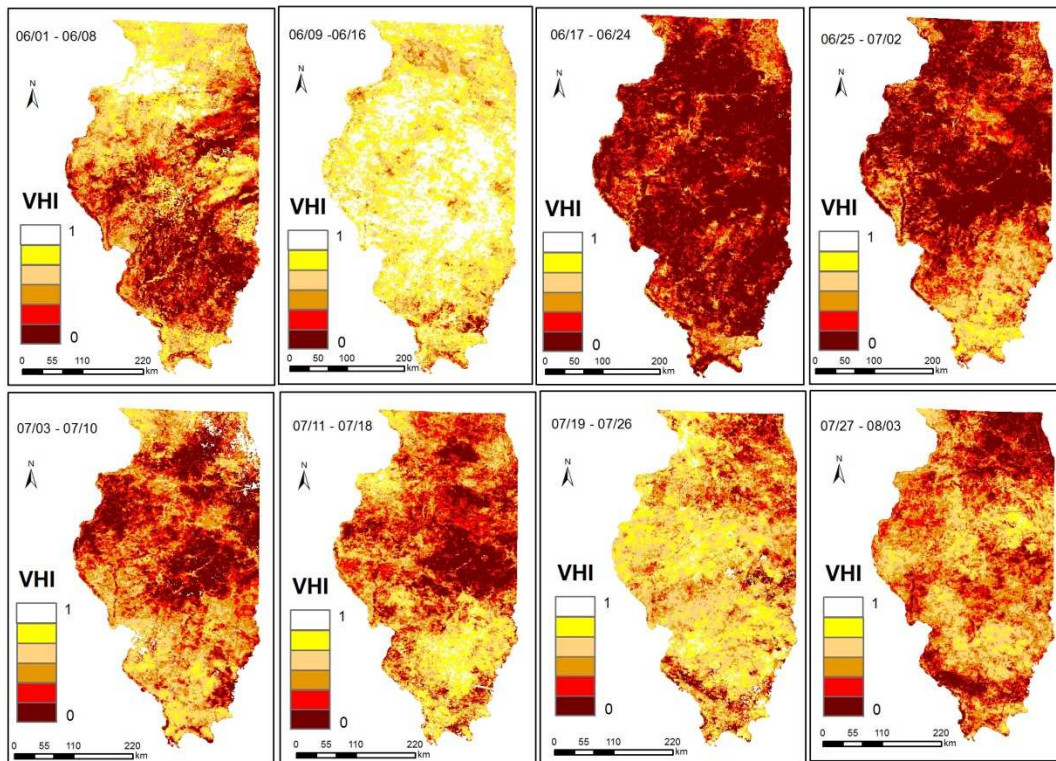
## 2001 Illinois Vegetation Health Index Map I



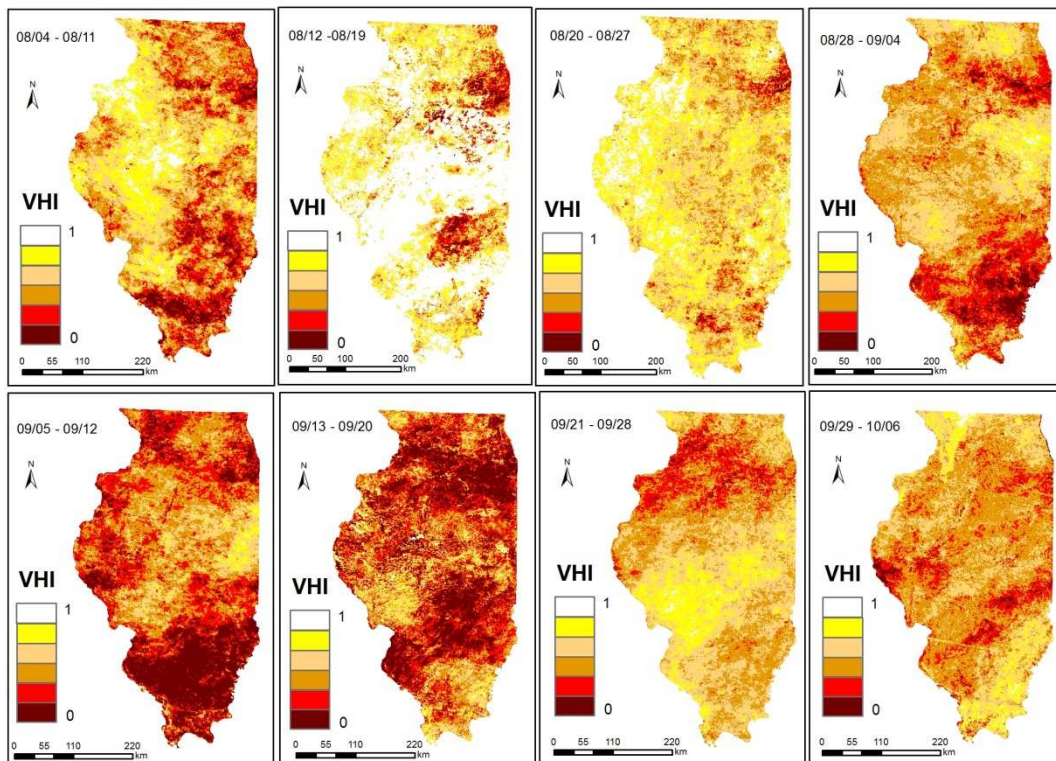
## 2001 Illinois Vegetation Health Index Map II



## 2002 Illinois Vegetation Health Index Map I

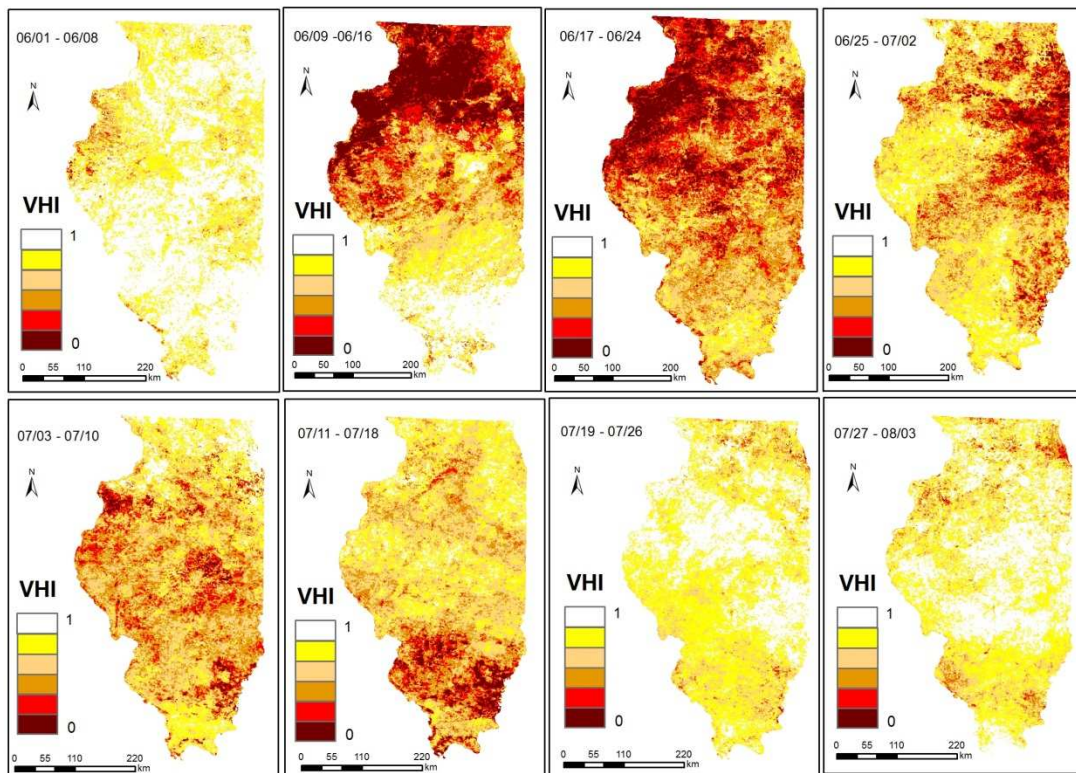


## 2002 Illinois Vegetation Health Index Map II

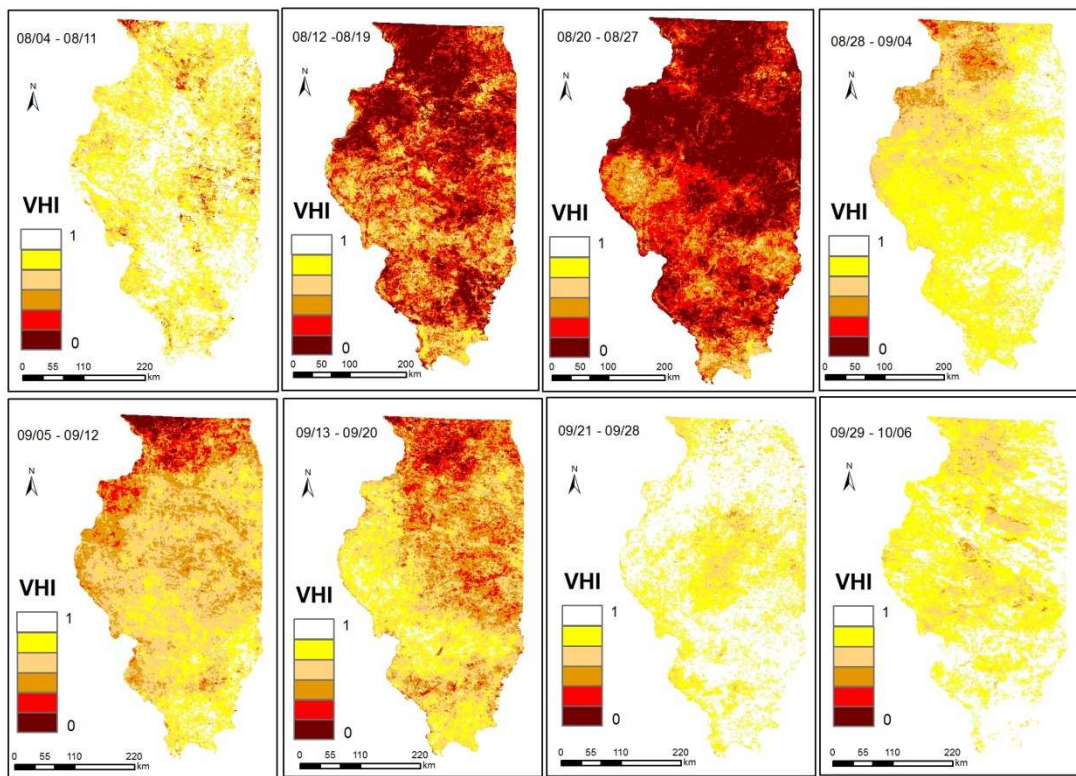




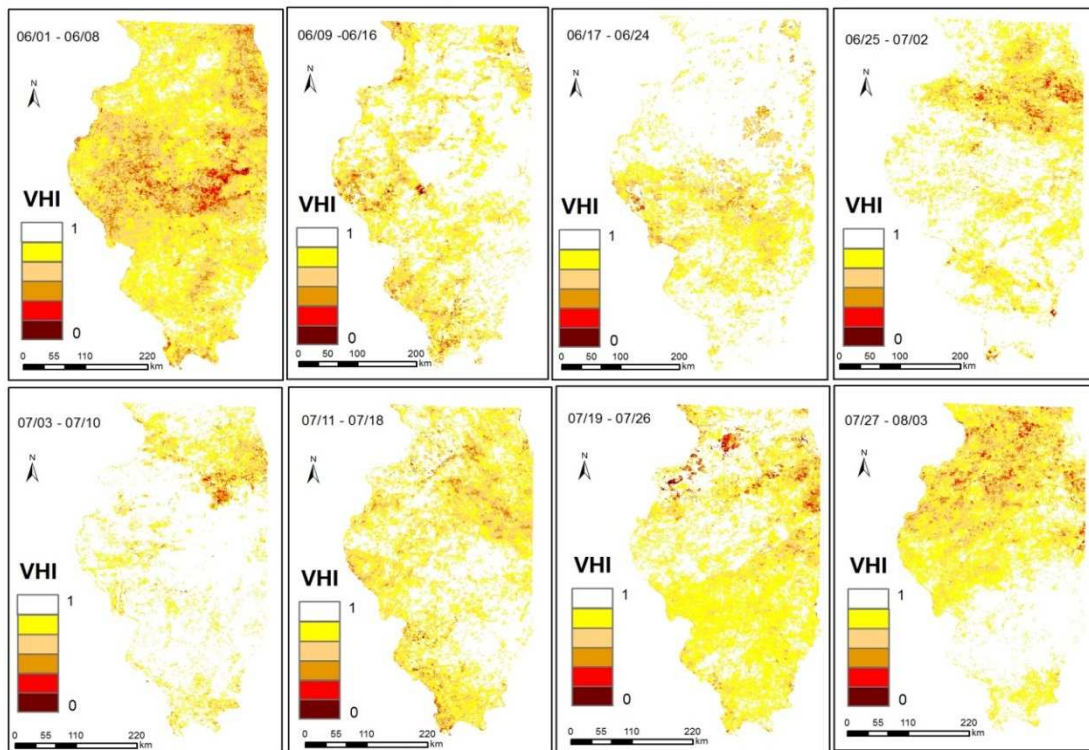
## 2003 Illinois Vegetation Health Index Map I



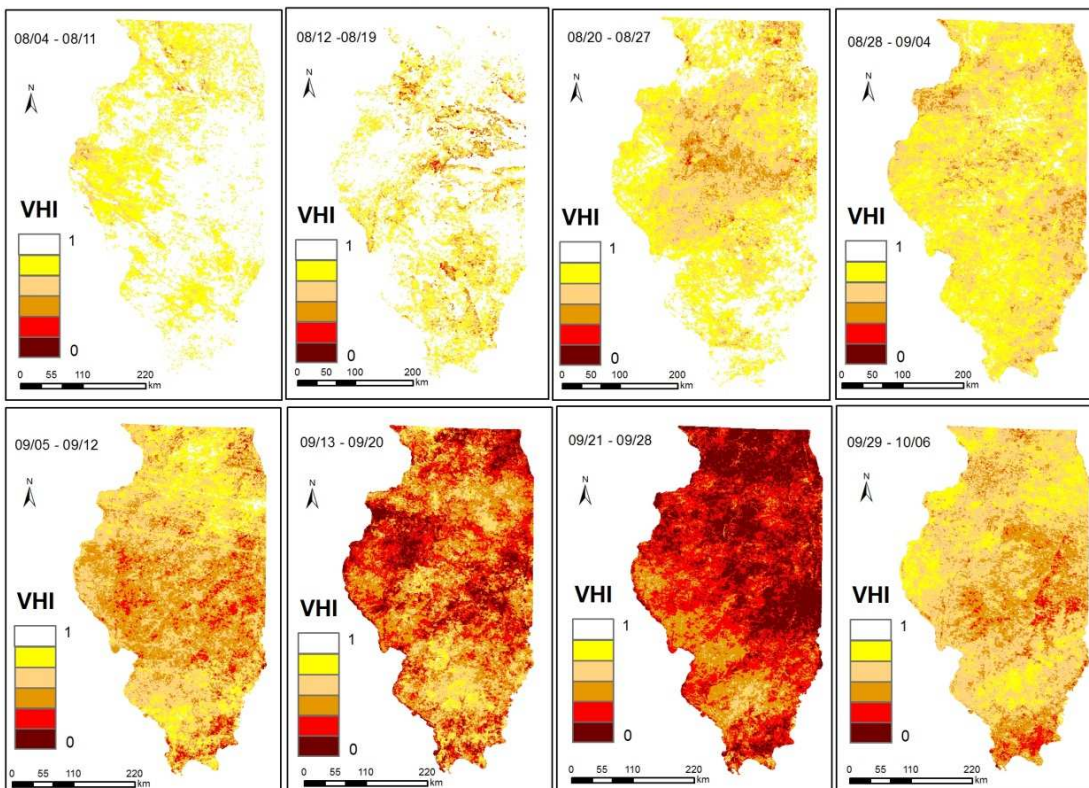
## 2003 Illinois Vegetation Health Index Map II



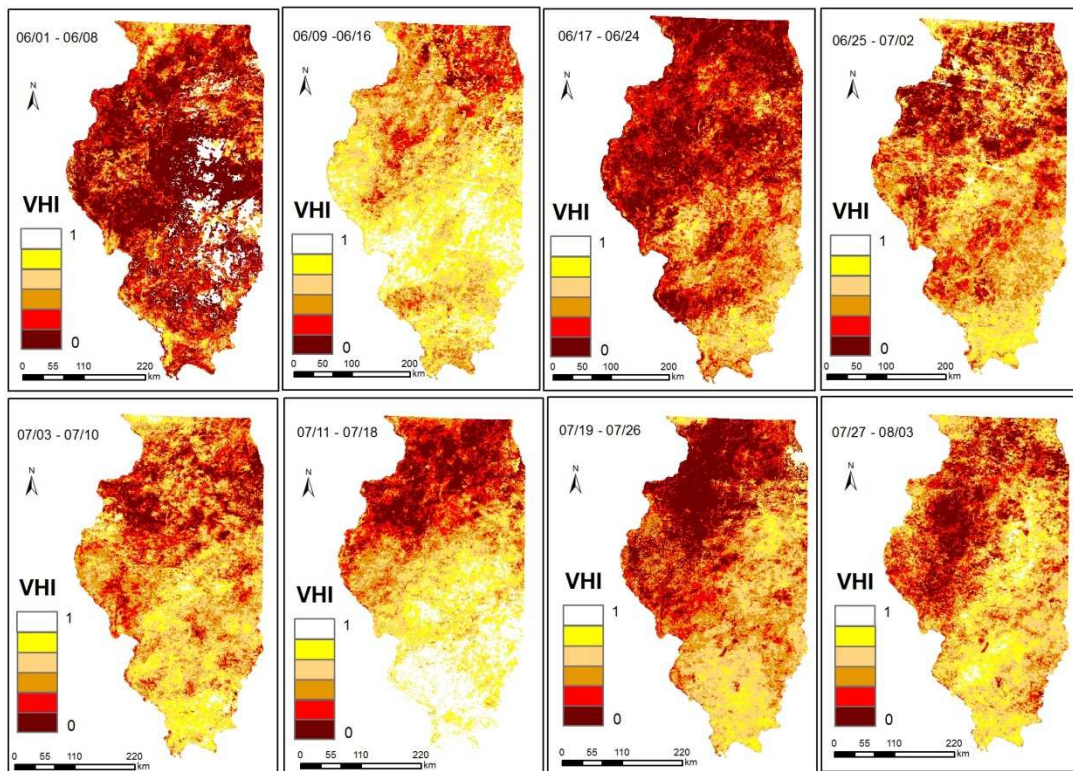
## 2004 Illinois Vegetation Health Index Map I



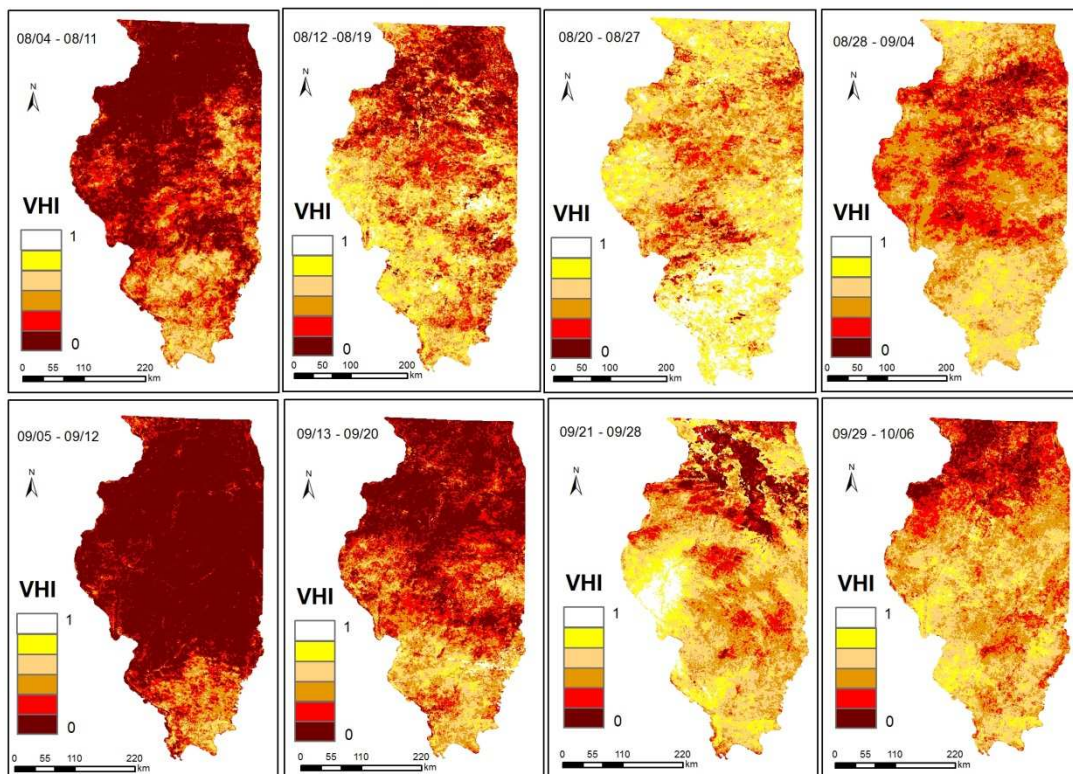
## 2004 Illinois Vegetation Health Index Map II



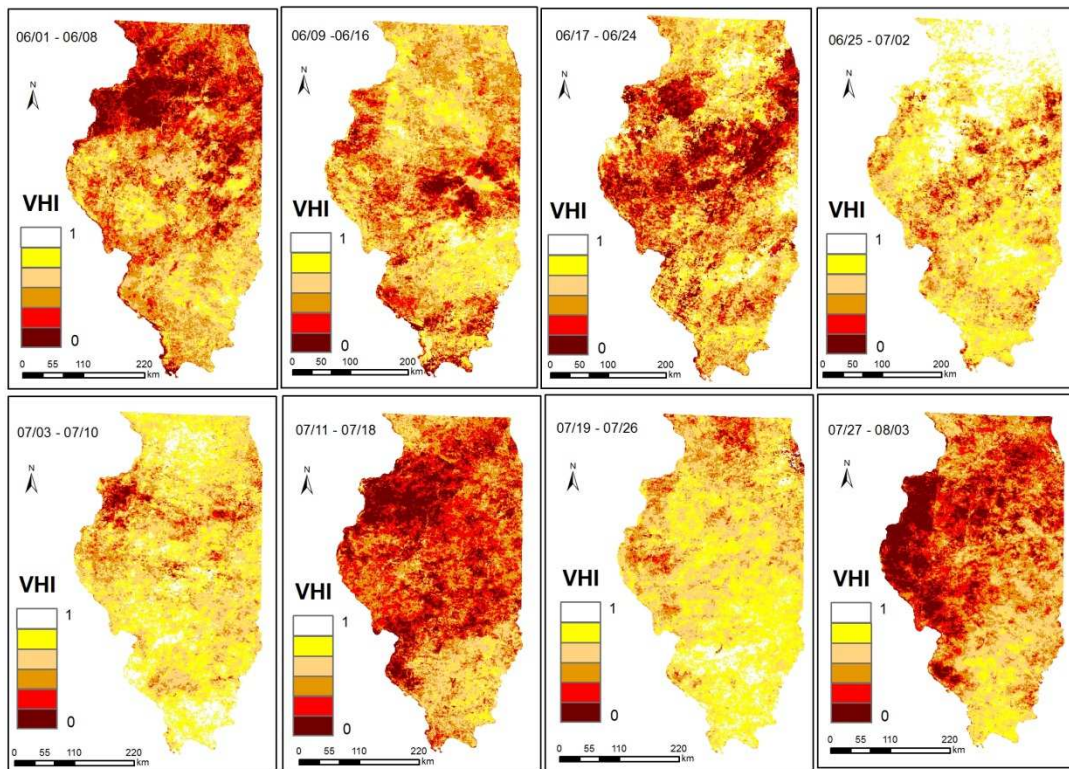
## 2005 Illinois Vegetation Health Index Map I



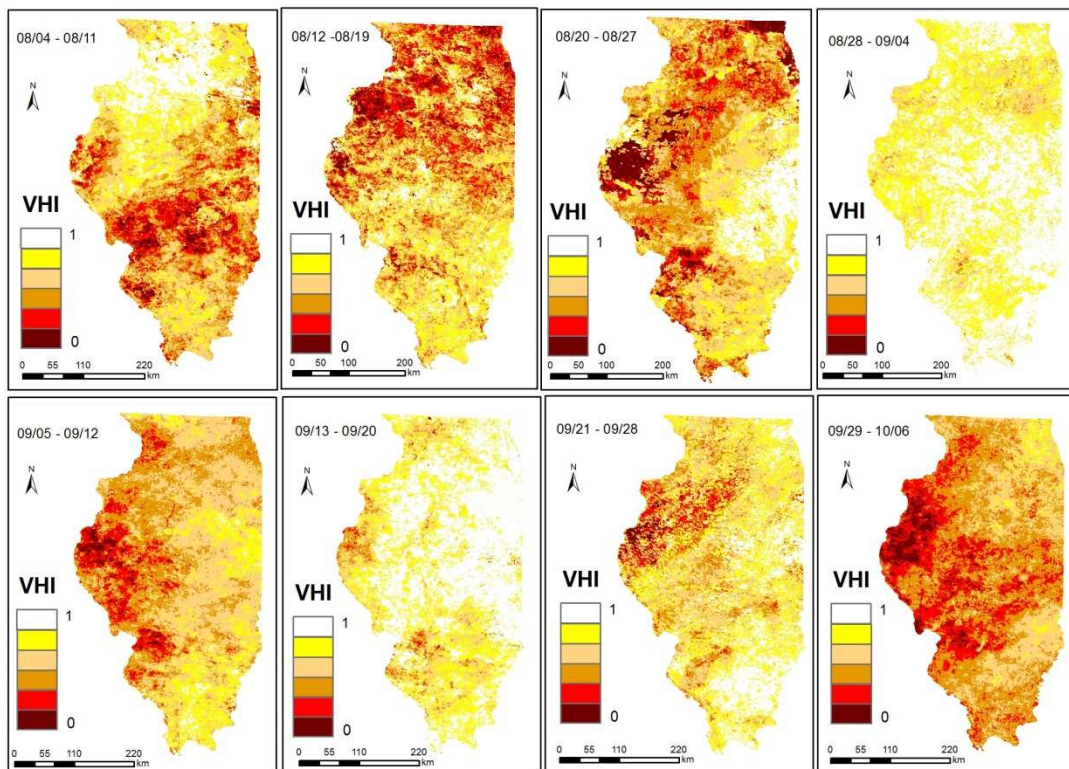
## 2005 Illinois Vegetation Health Index Map II



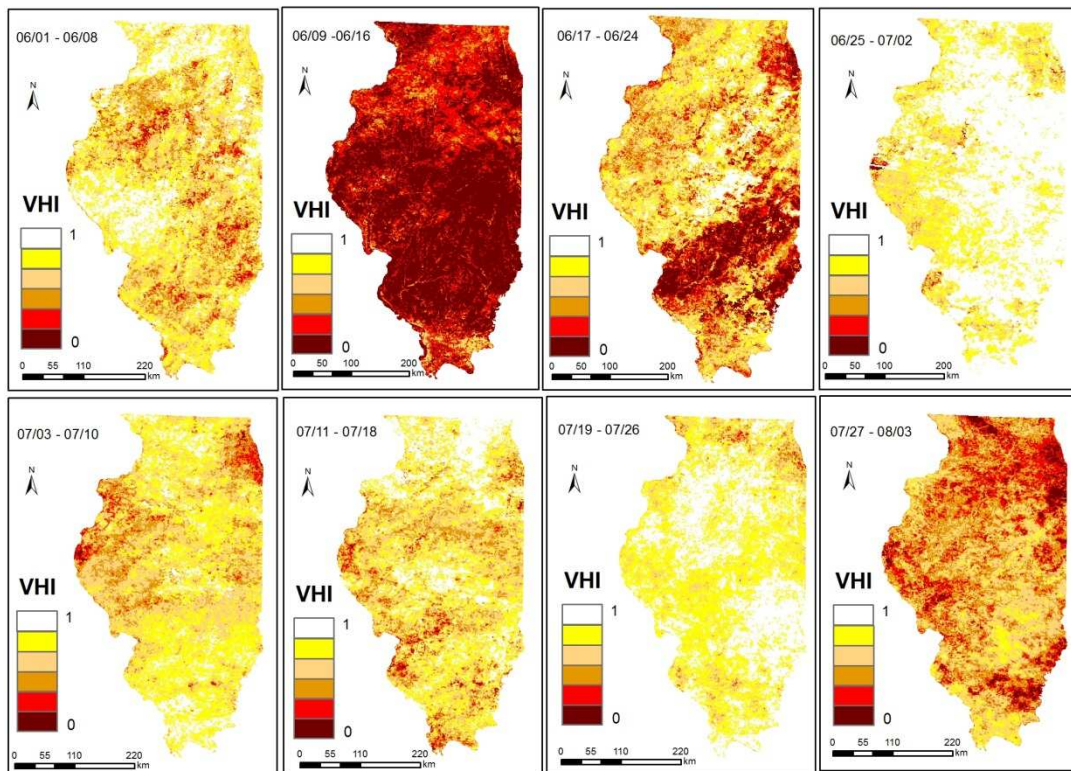
## 2006 Illinois Vegetation Health Index Map I



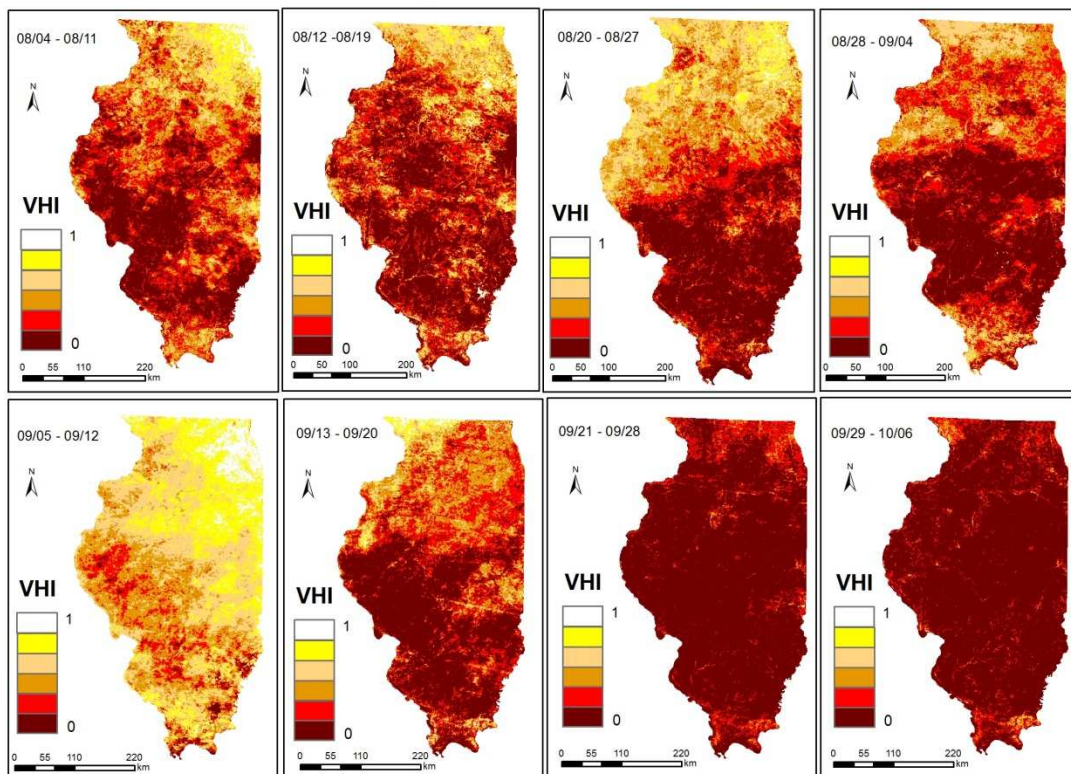
## 2006 Illinois Vegetation Health Index Map II



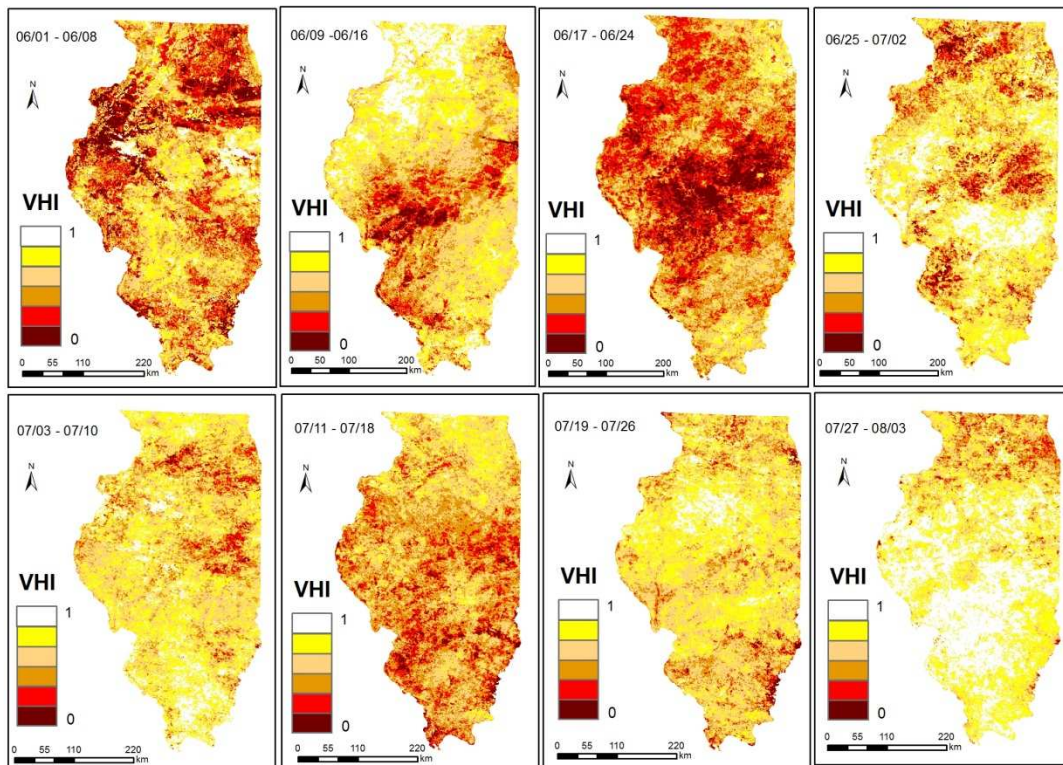
## 2007 Illinois Vegetation Health Index Map I



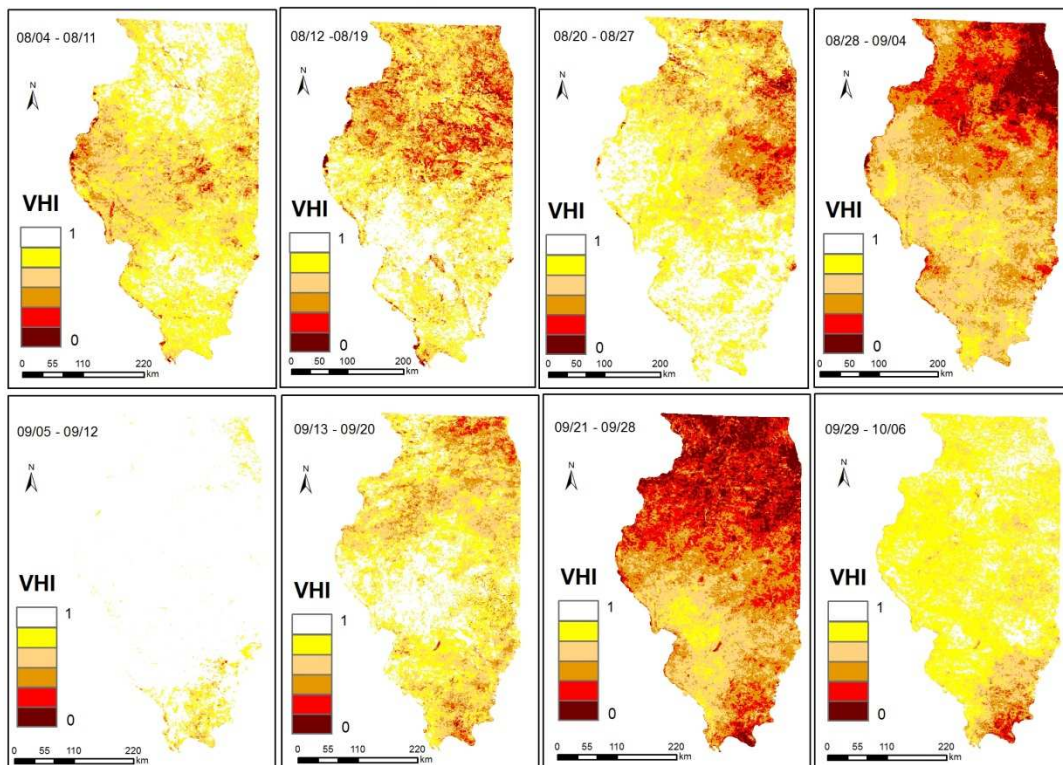
## 2007 Illinois Vegetation Health Index Map II



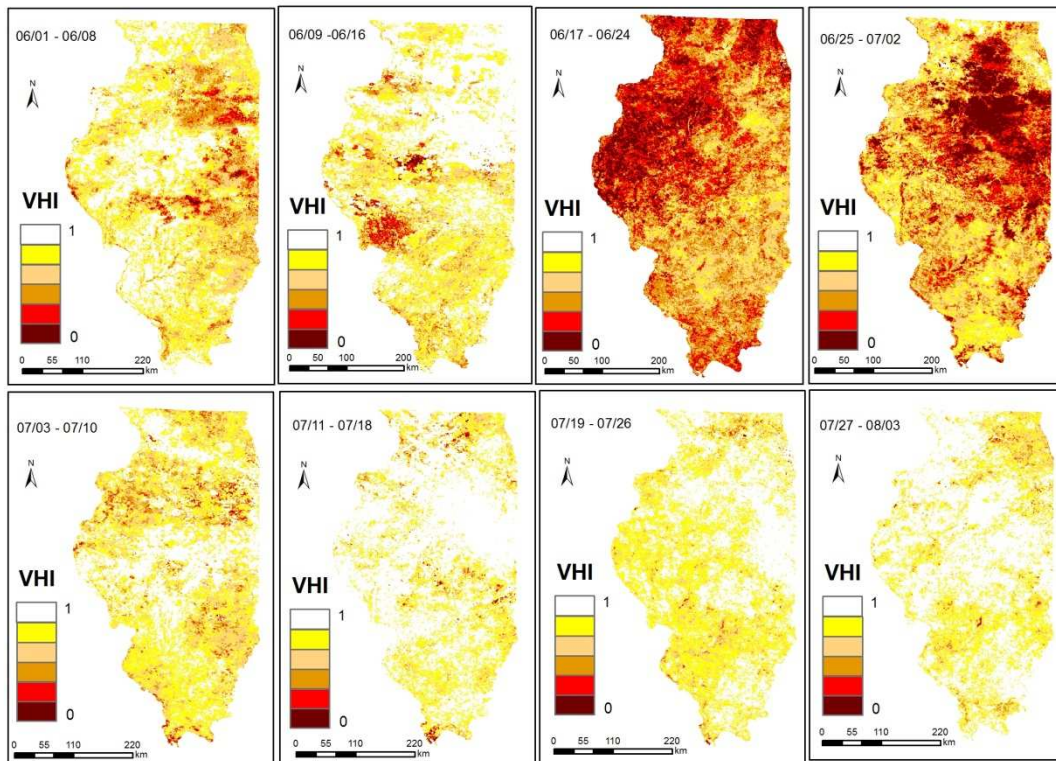
## 2008 Illinois Vegetation Health Index Map I



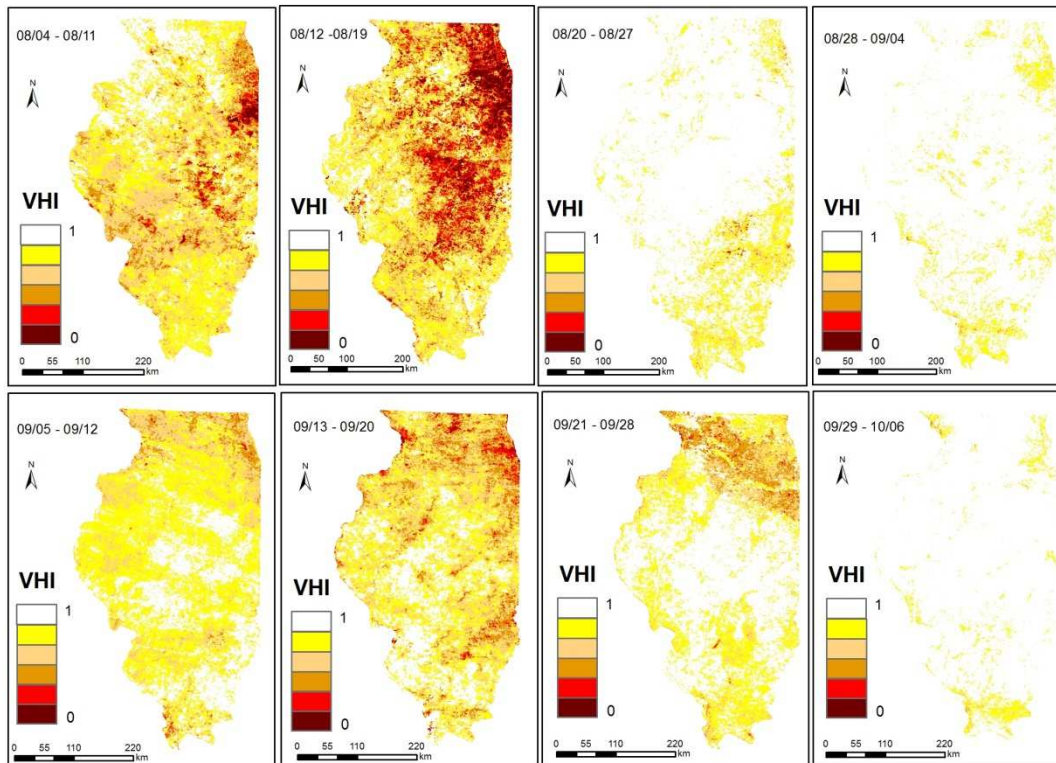
## 2008 Illinois Vegetation Health Index Map II



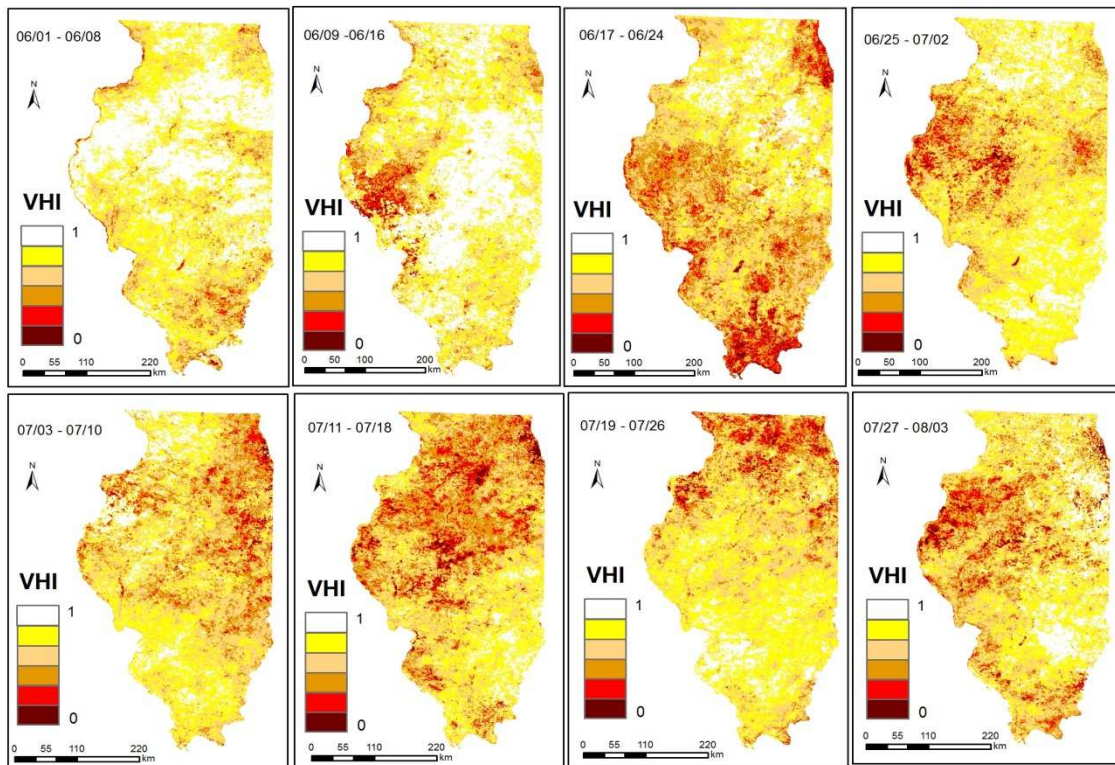
## 2009 Illinois Vegetation Health Index Map I



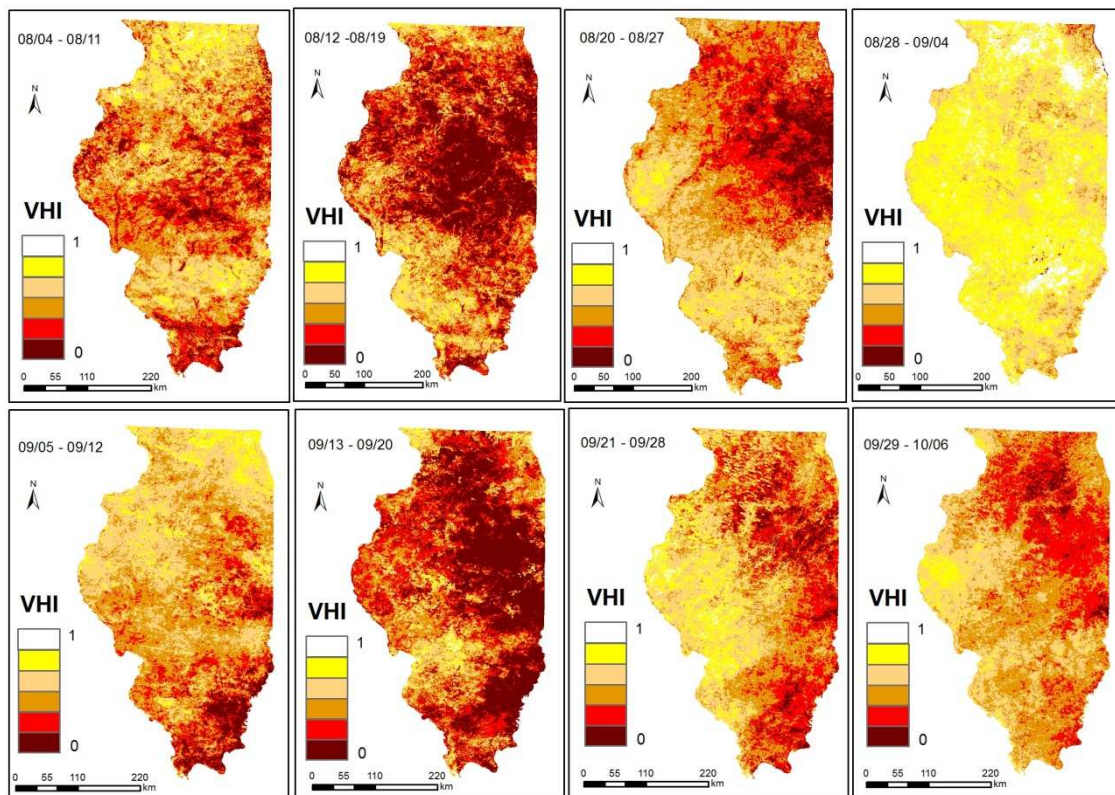
## 2009 Illinois Vegetation Health Index Map II



## 2010 Illinois Vegetation Health Index Map I

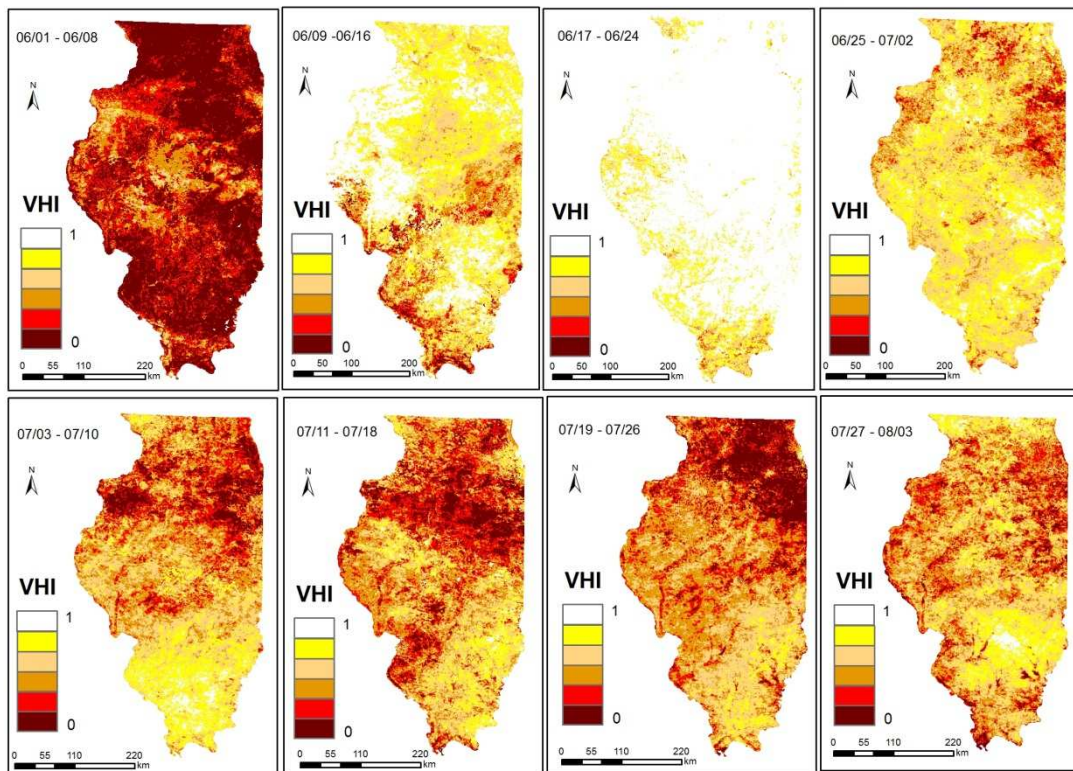


## 2010 Illinois Vegetation Health Index Map II

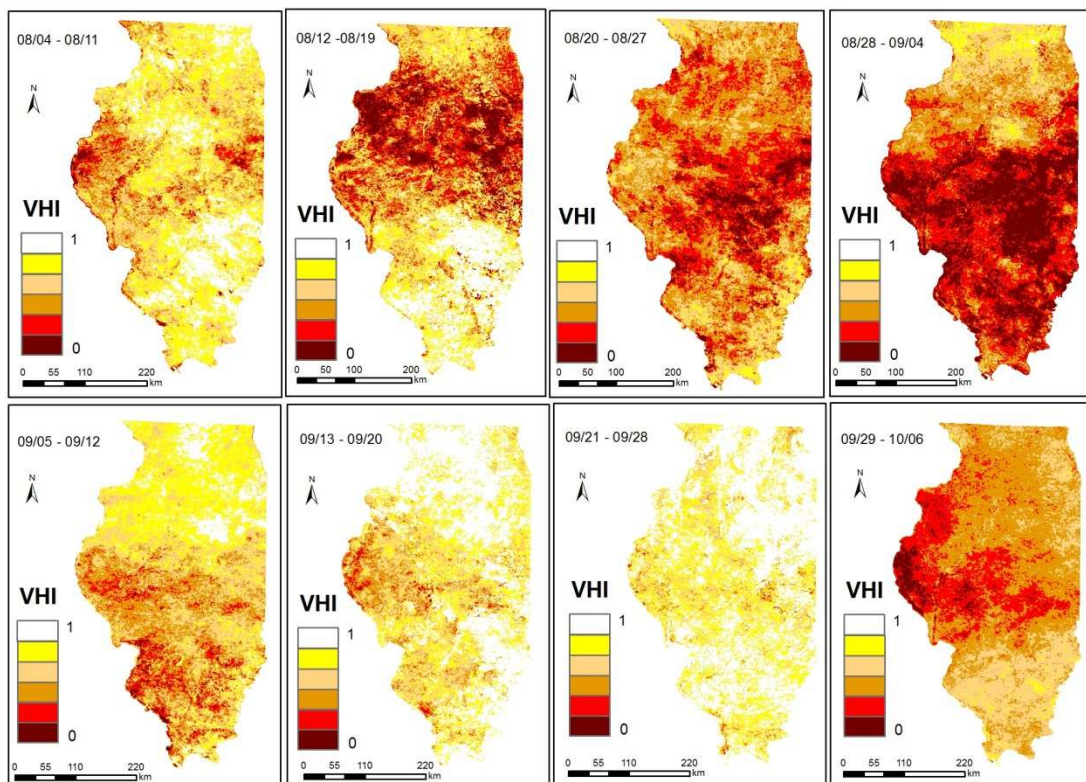




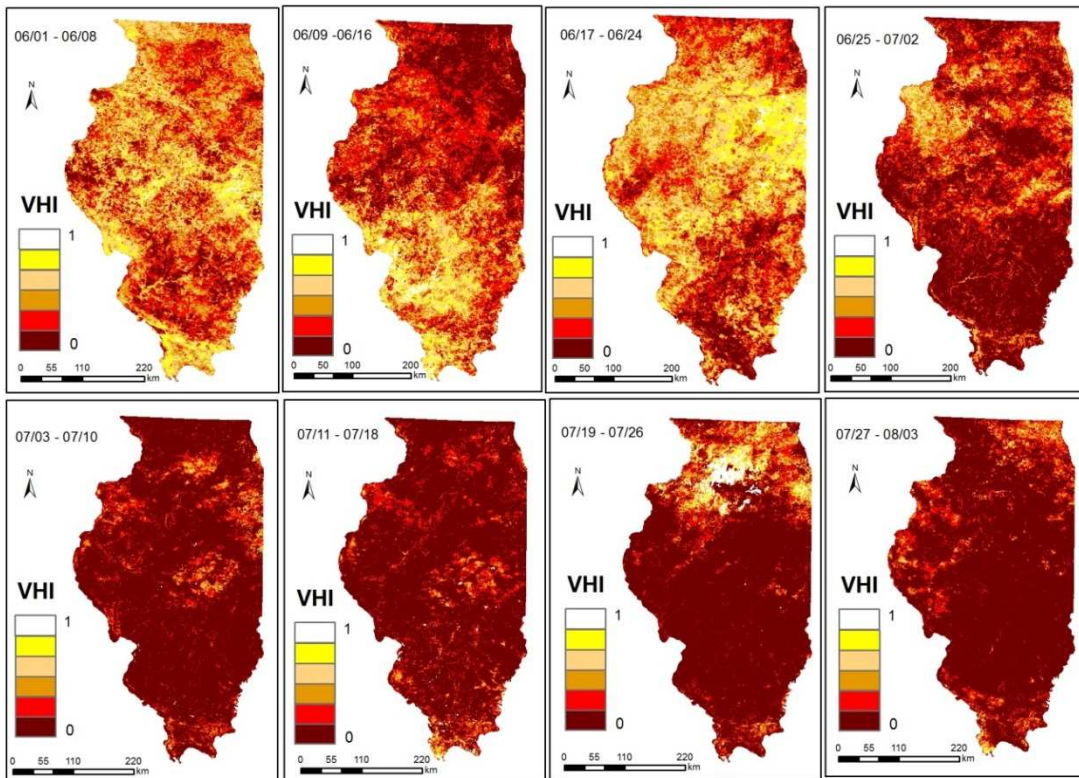
## 2011 Illinois Vegetation Health Index Map I



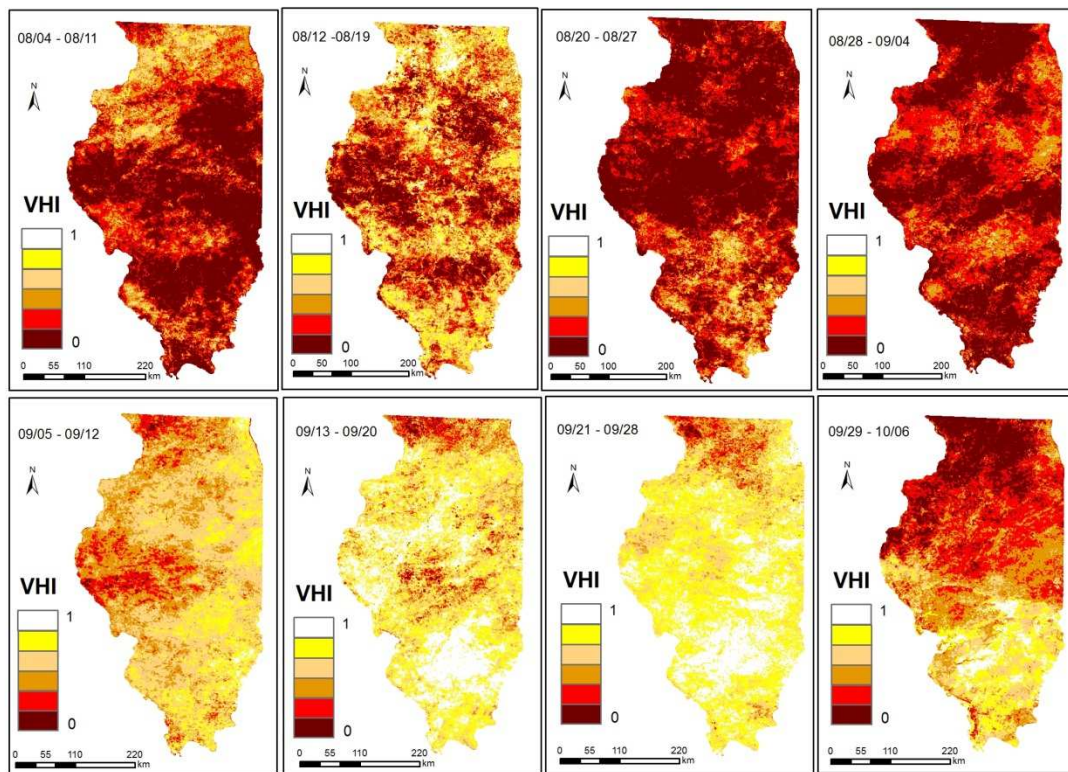
## 2011 Illinois Vegetation Health Index Map II



## 2012 Illinois Vegetation Health Index Map I

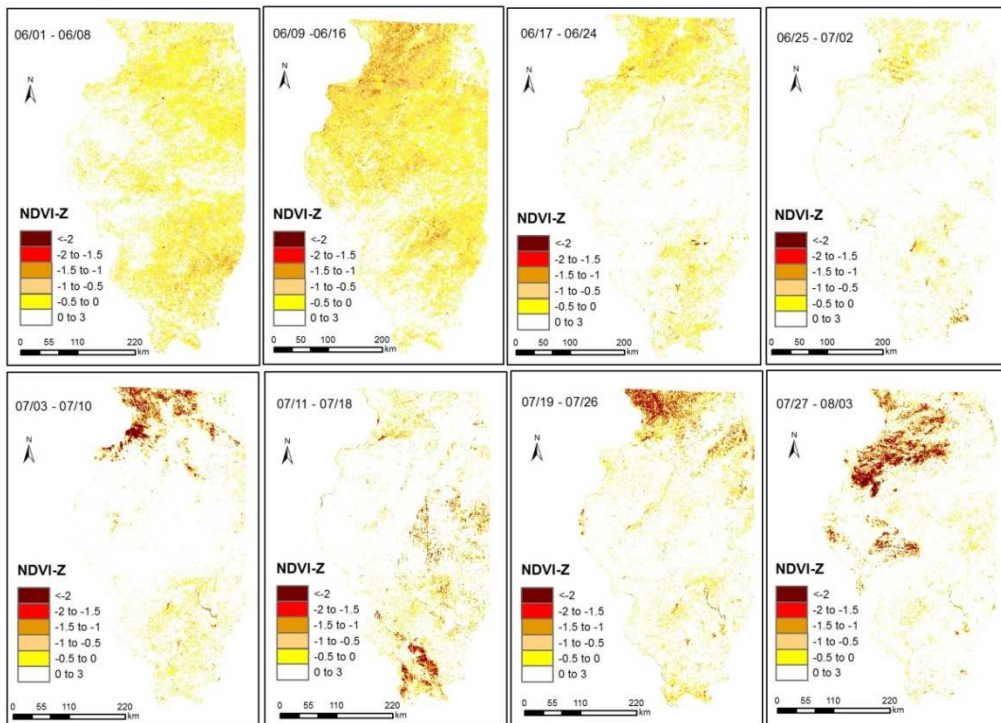


## 2012 Illinois Vegetation Health Index Map II

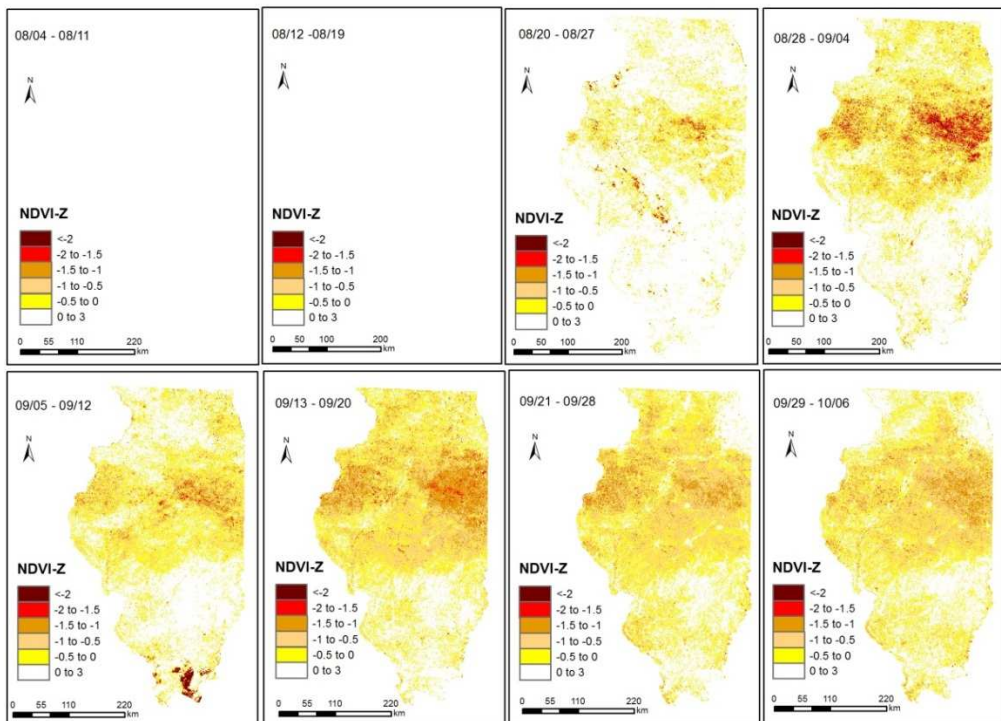


Appendix D: NDVI Anomaly Maps of Illinois for years 2000 to 2012

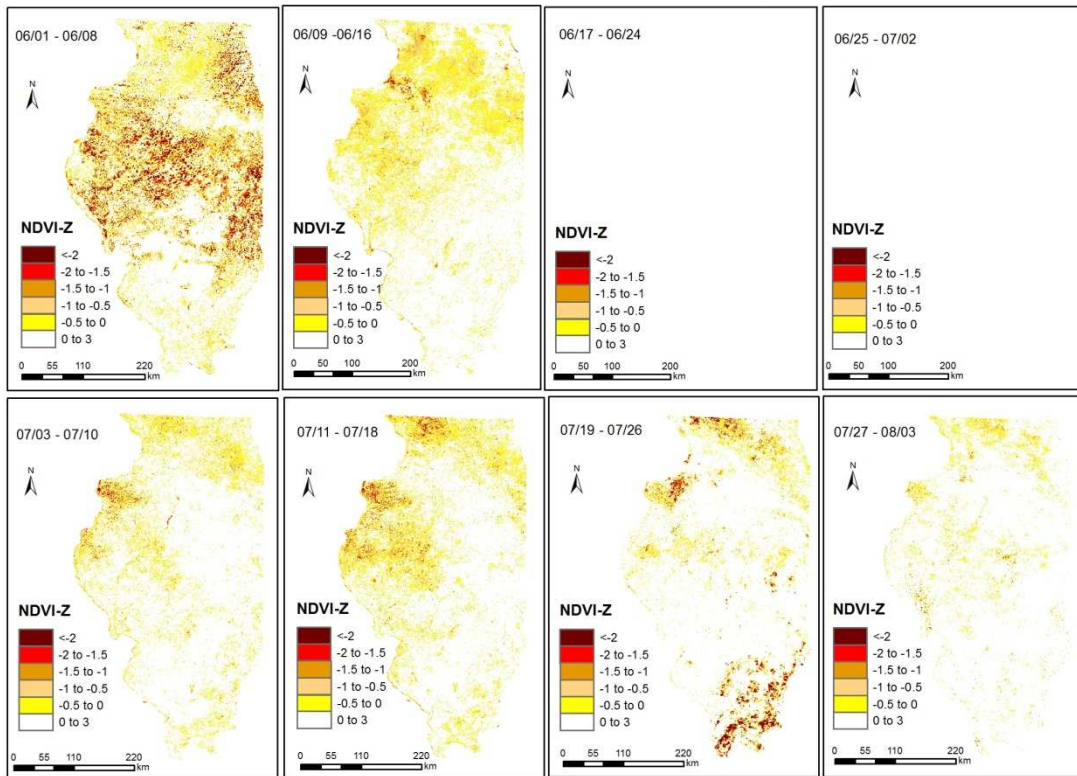
2000 Illinois NDVI Anomaly Map I



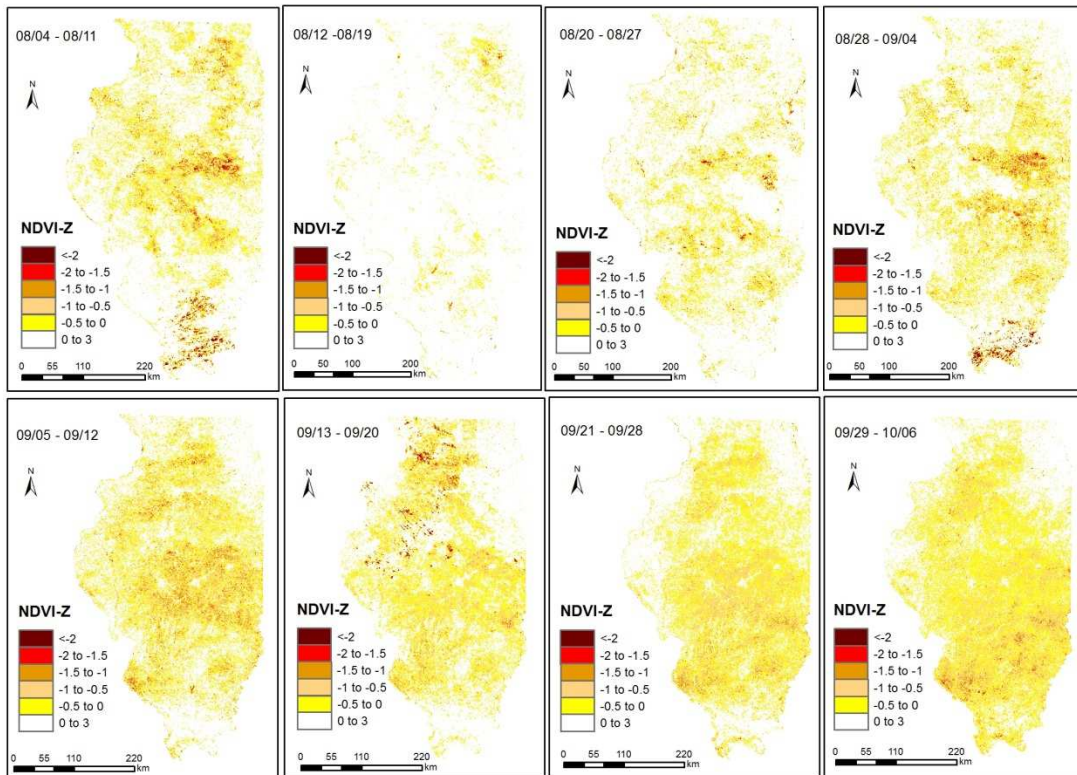
2000 Illinois NDVI Anomaly Map II



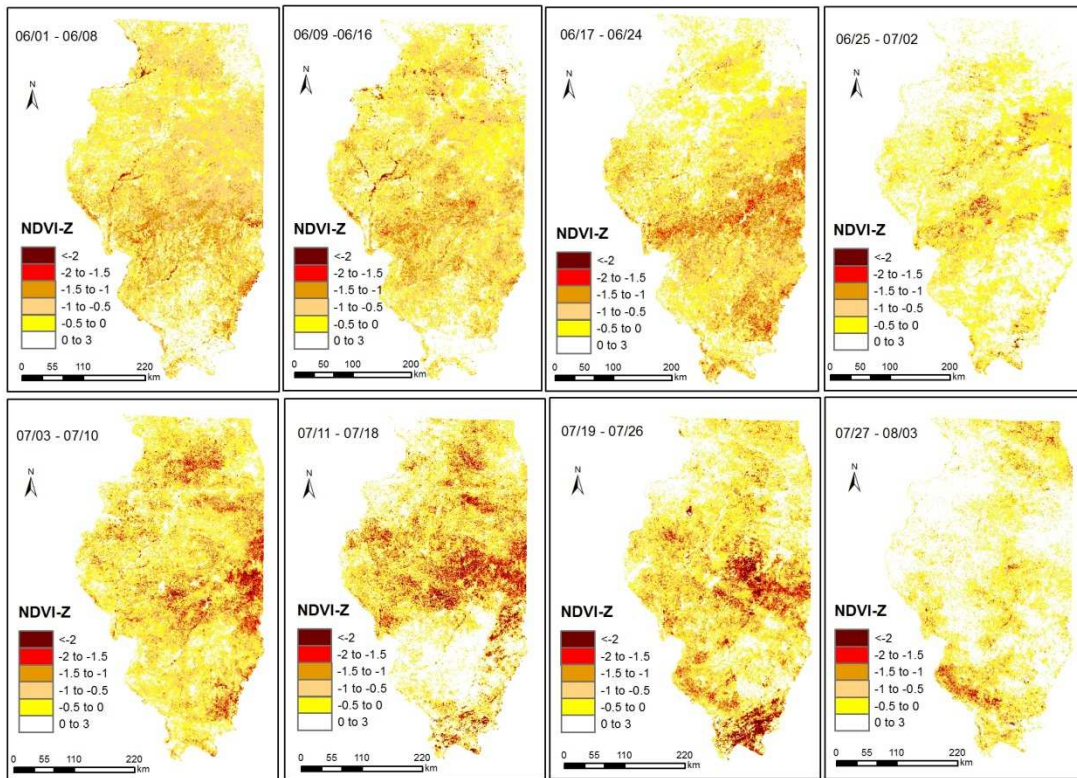
### 2001 Illinois NDVI Anomaly Map I



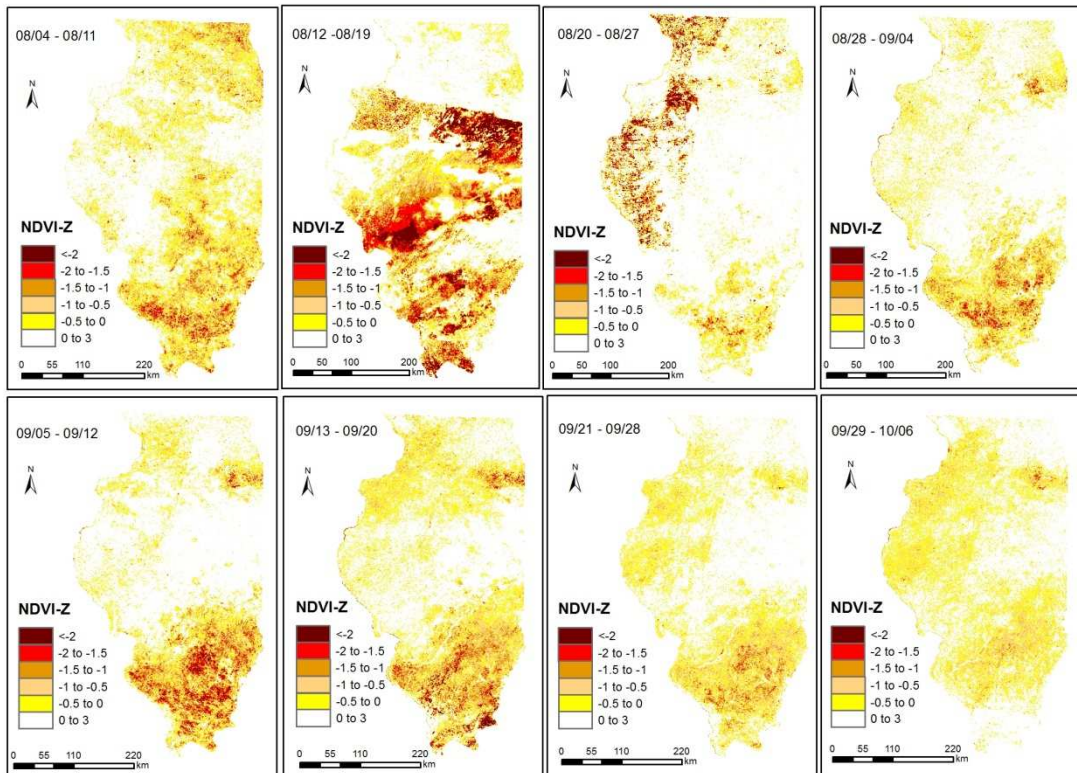
### 2001 Illinois NDVI Anomaly Map II



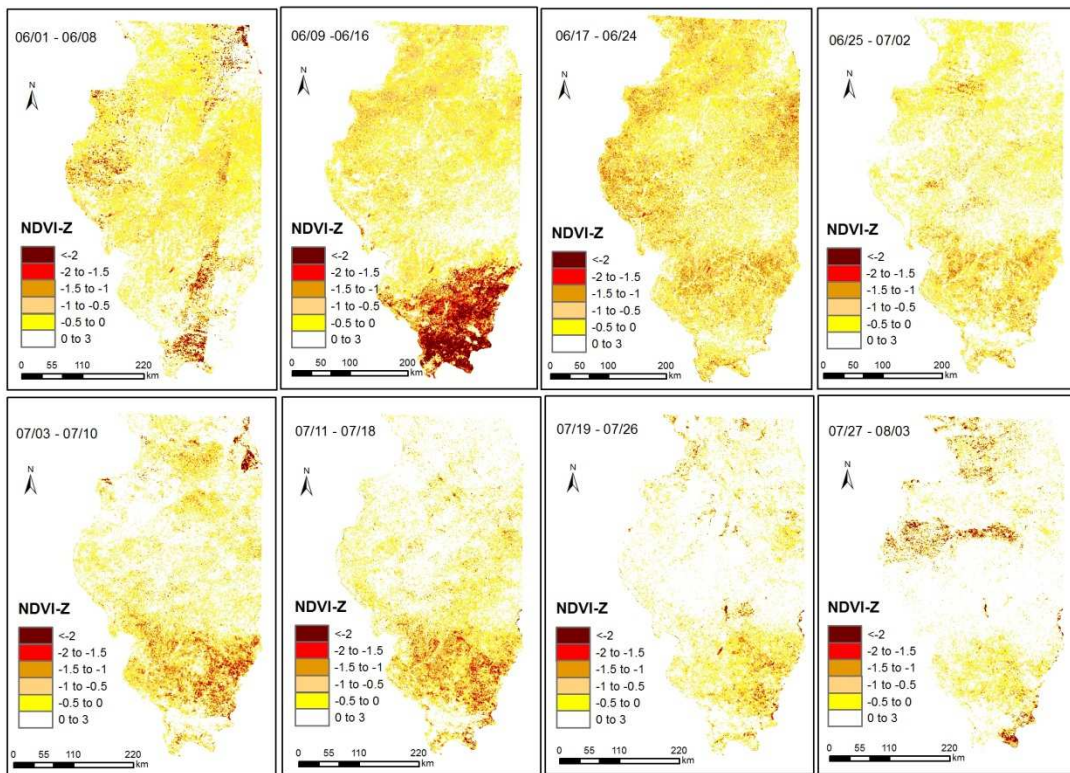
### 2002 Illinois NDVI Anomaly Map I



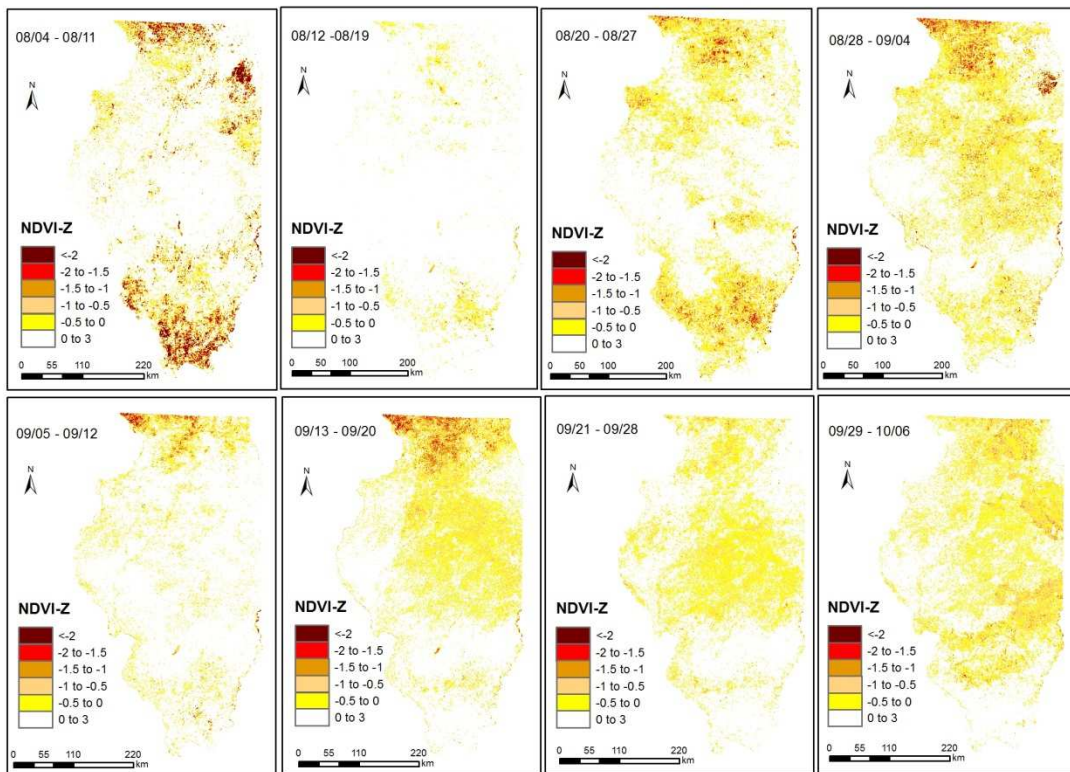
### 2002 Illinois NDVI Anomaly Map II



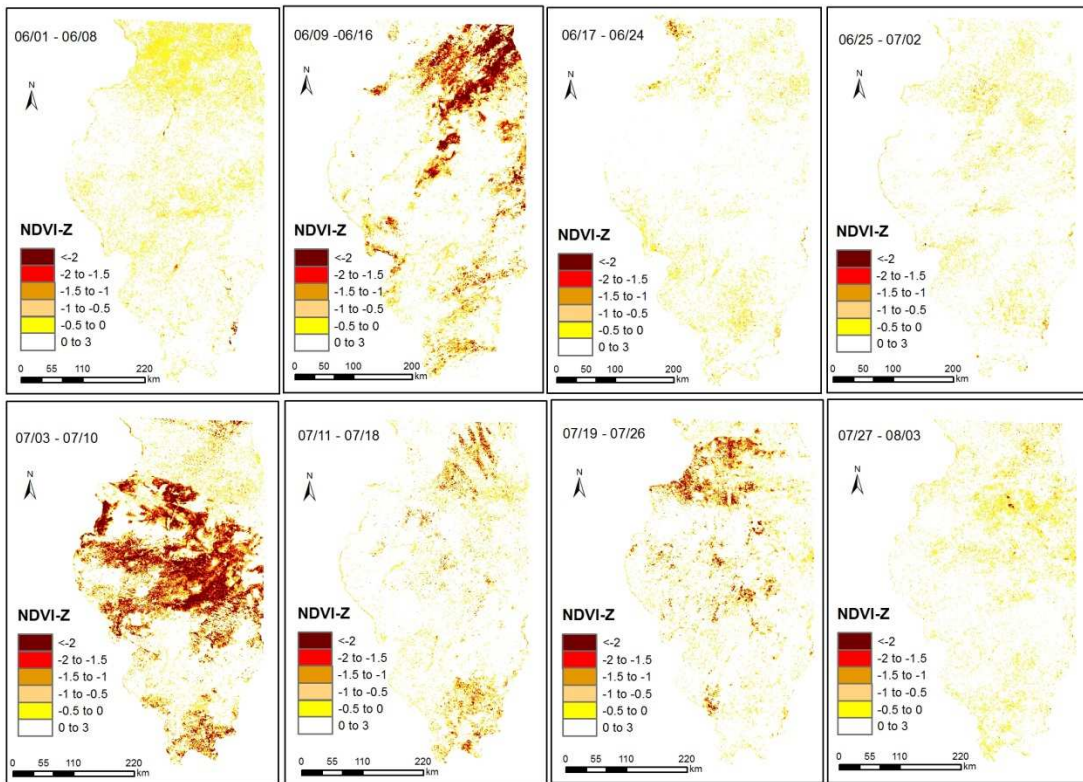
### 2003 Illinois NDVI Anomaly Map I



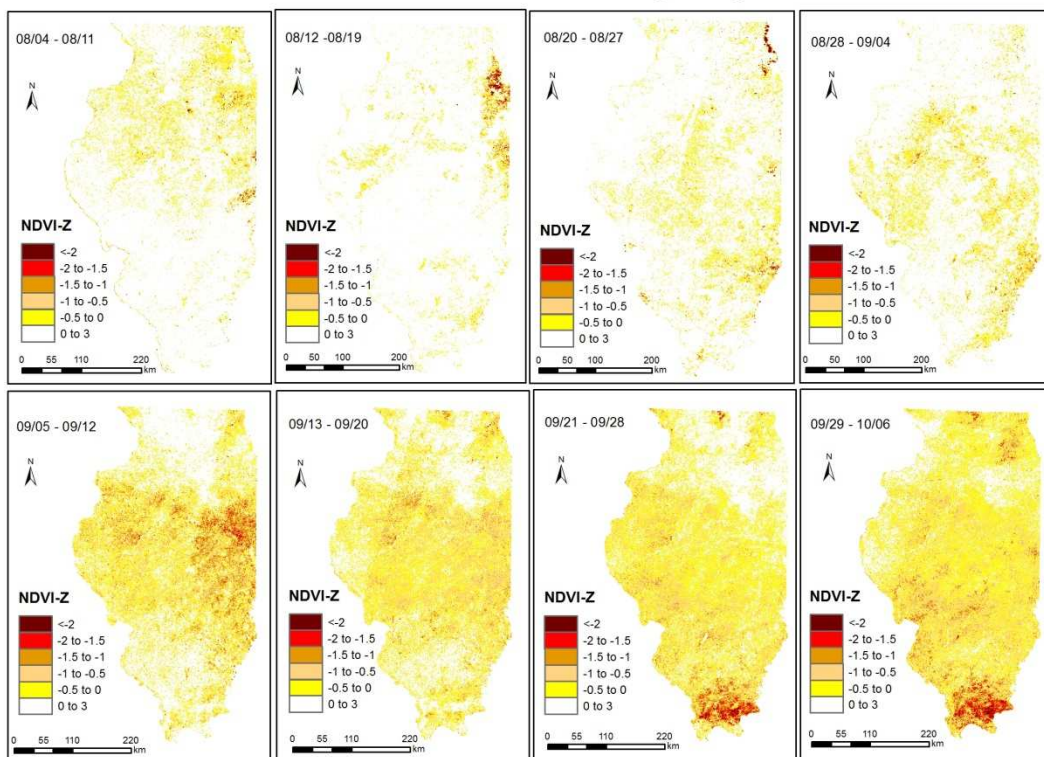
### 2003 Illinois NDVI Anomaly Map II



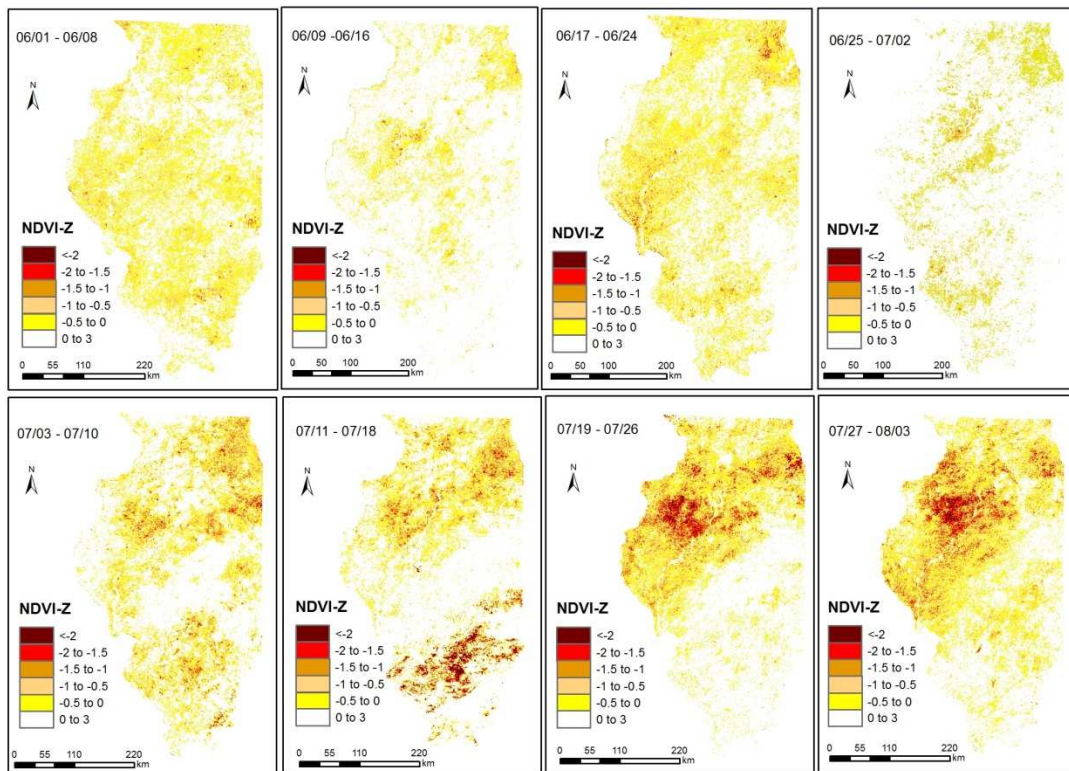
### 2004 Illinois NDVI Anomaly Map I



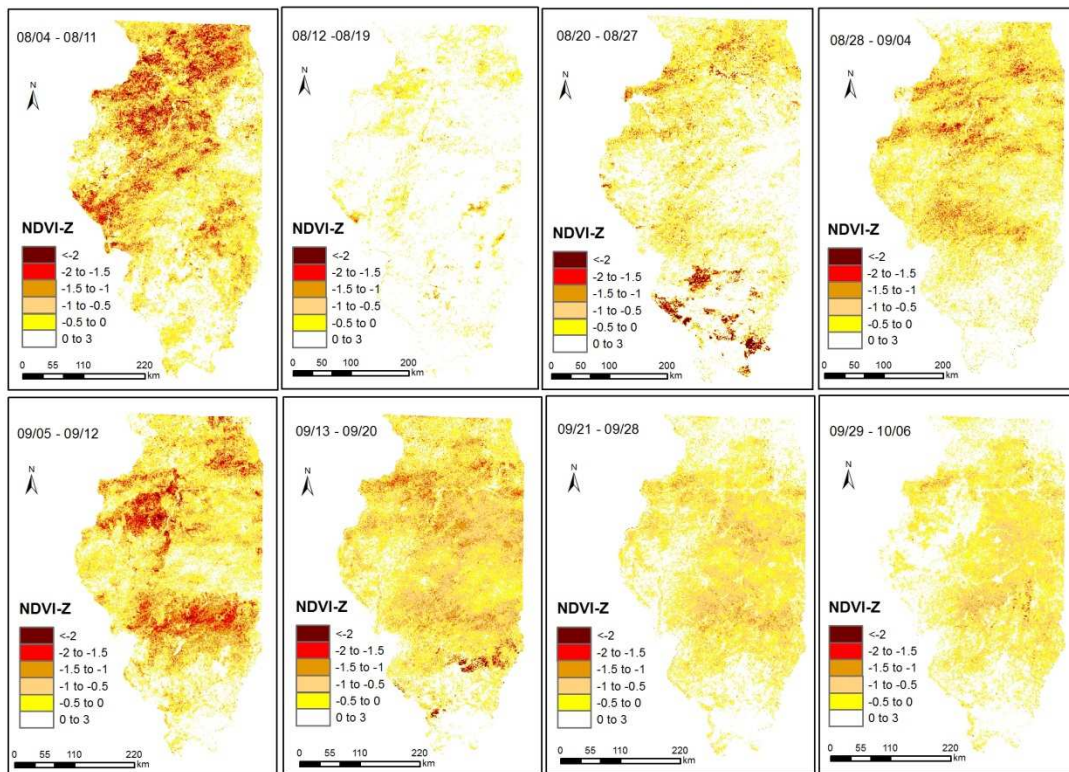
### 2004 Illinois NDVI Anomaly Map II



### 2005 Illinois NDVI Anomaly Map I

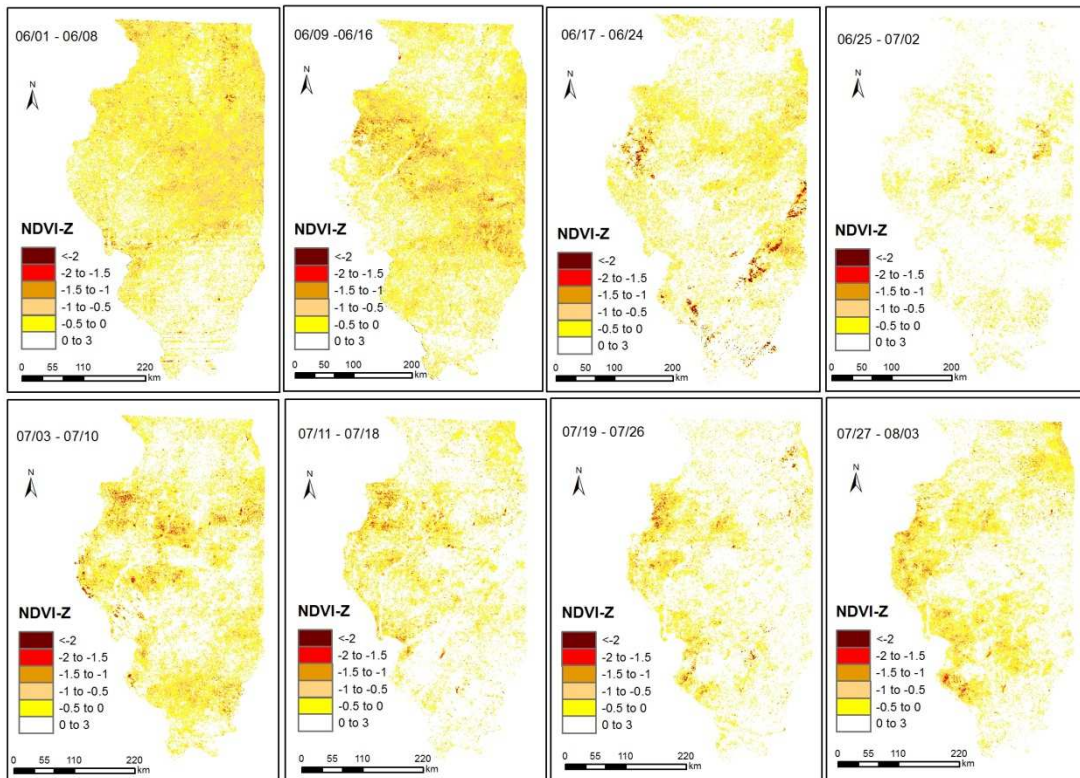


### 2005 Illinois NDVI Anomaly Map II

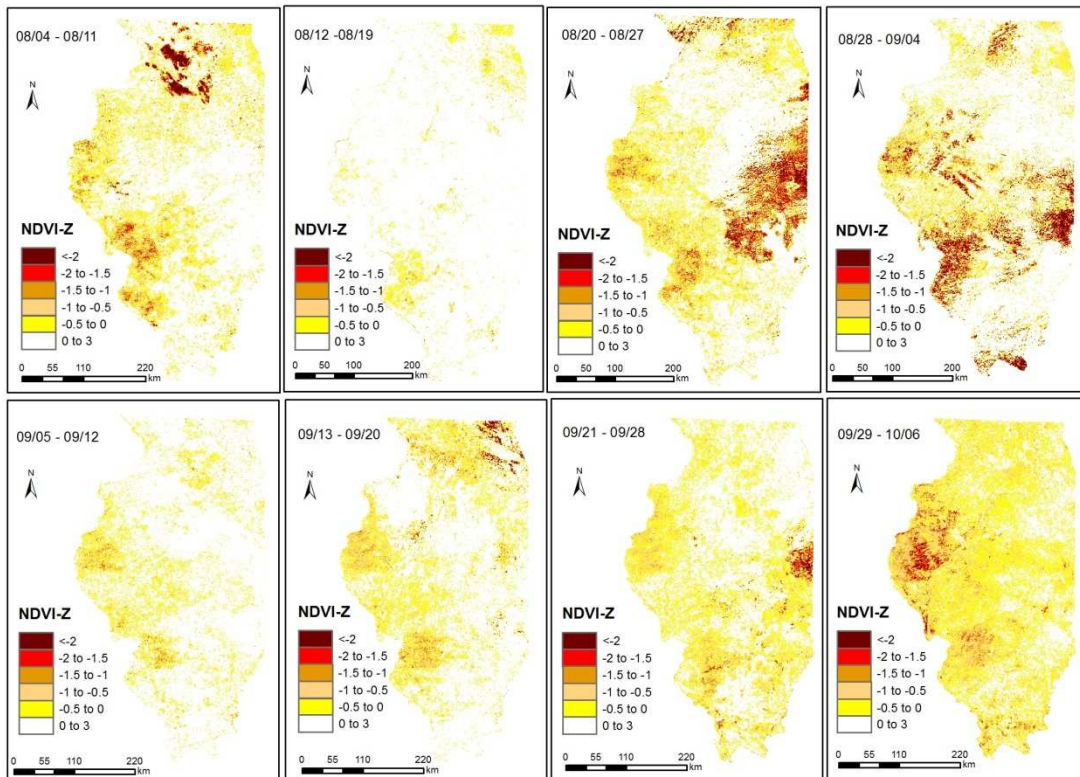




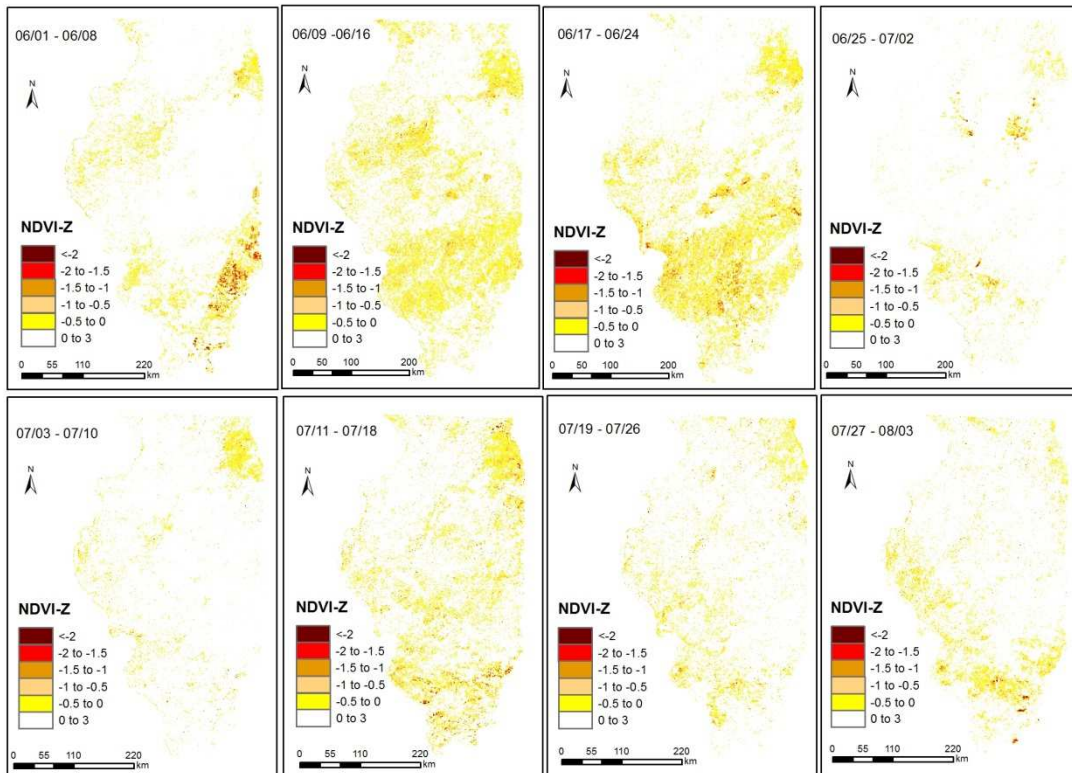
### 2006 Illinois NDVI Anomaly Map I



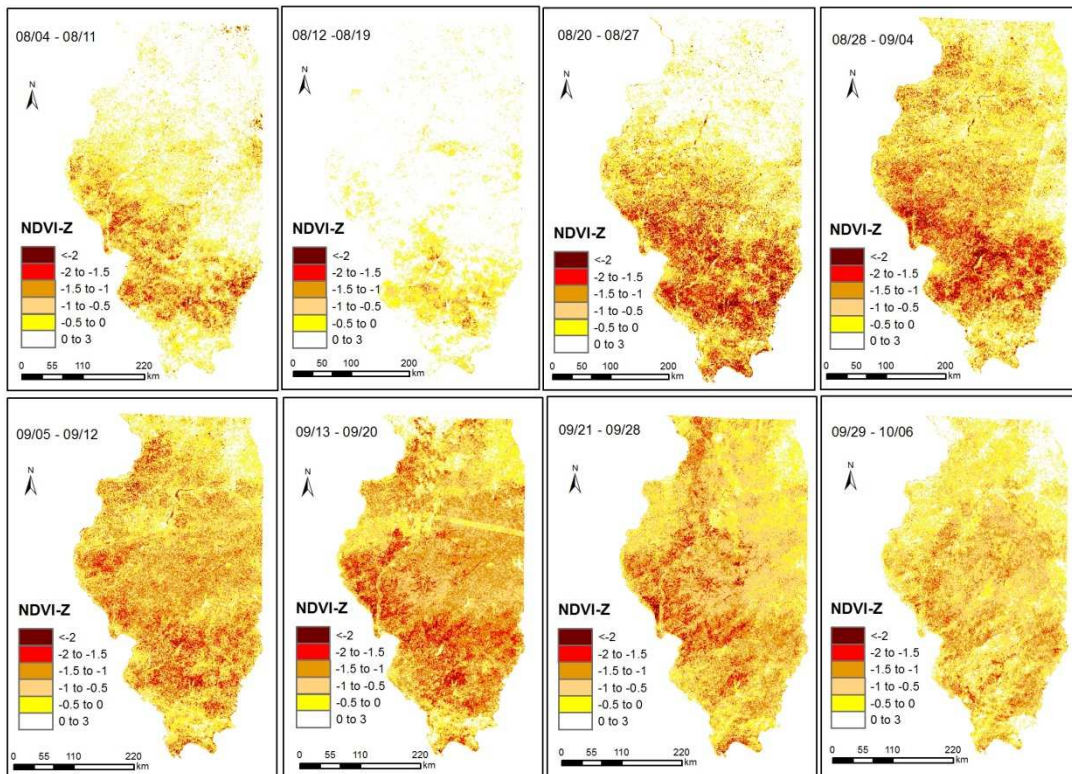
### 2006 Illinois NDVI Anomaly Map II



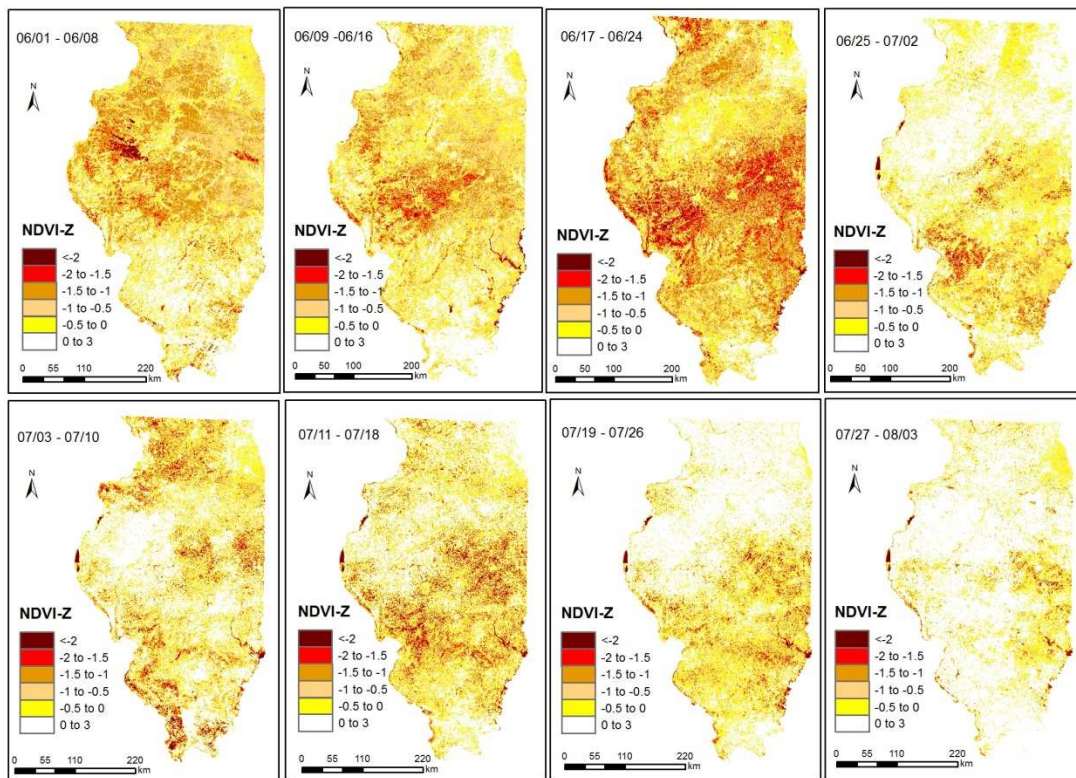
### 2007 Illinois NDVI Anomaly Map I



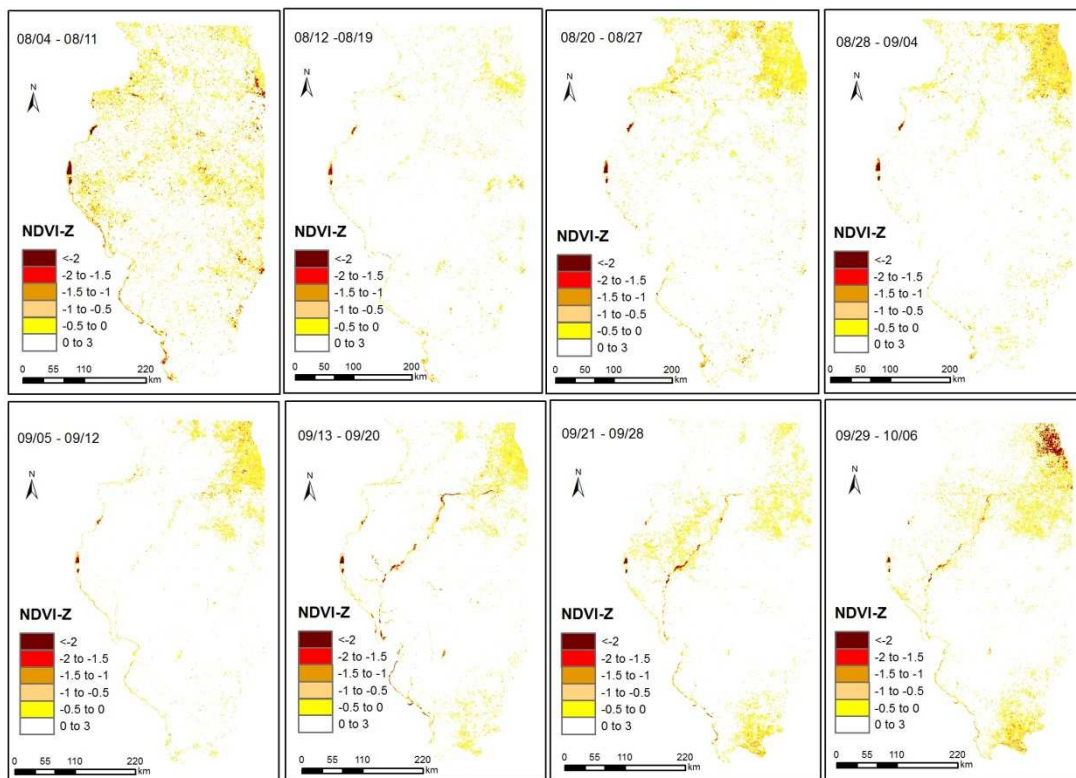
### 2007 Illinois NDVI Anomaly Map II



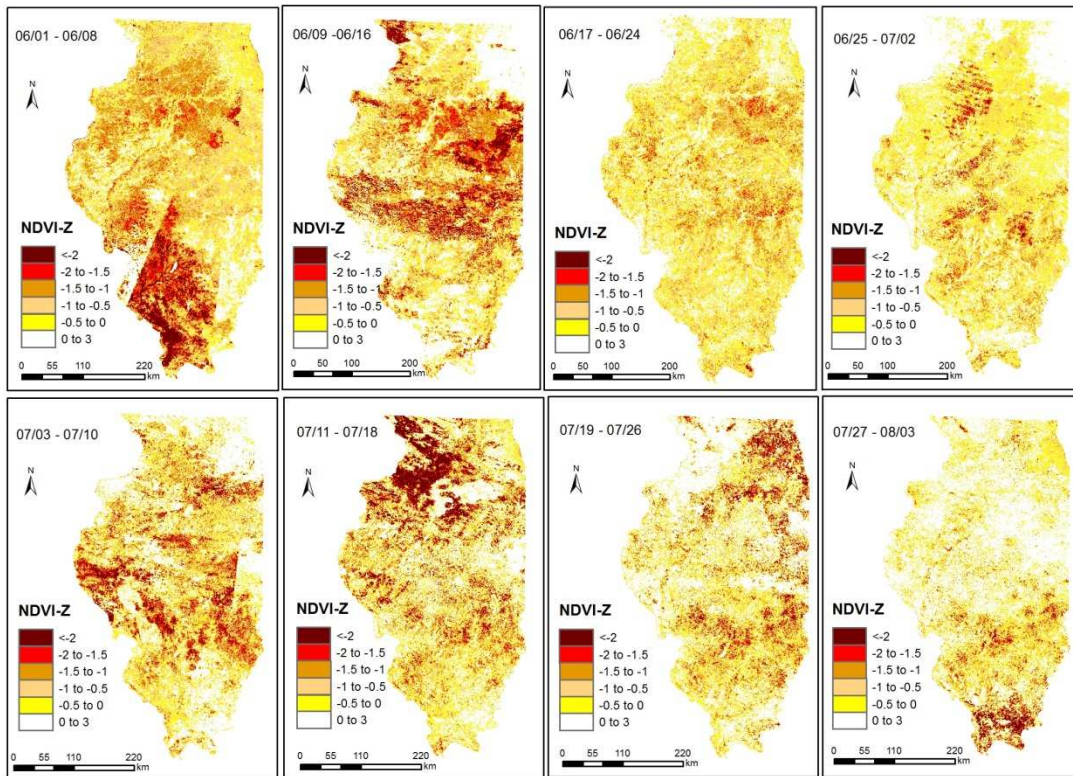
## 2008 Illinois NDVI Anomaly Map I



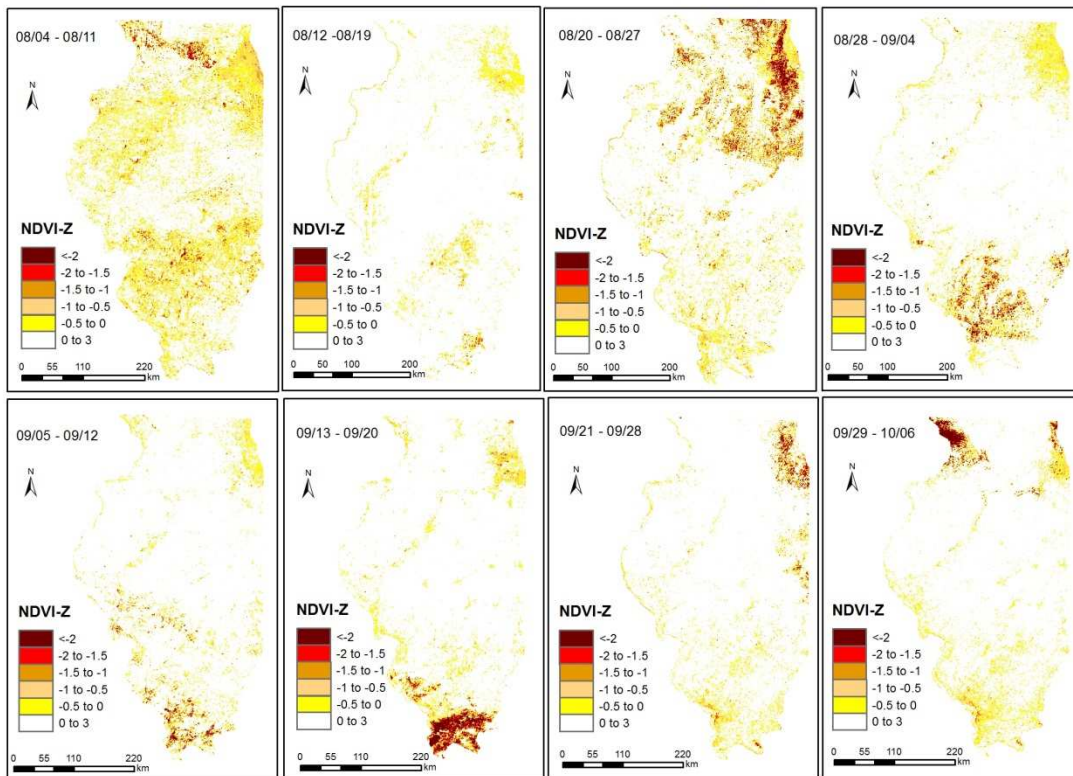
## 2008 Illinois NDVI Anomaly Map II



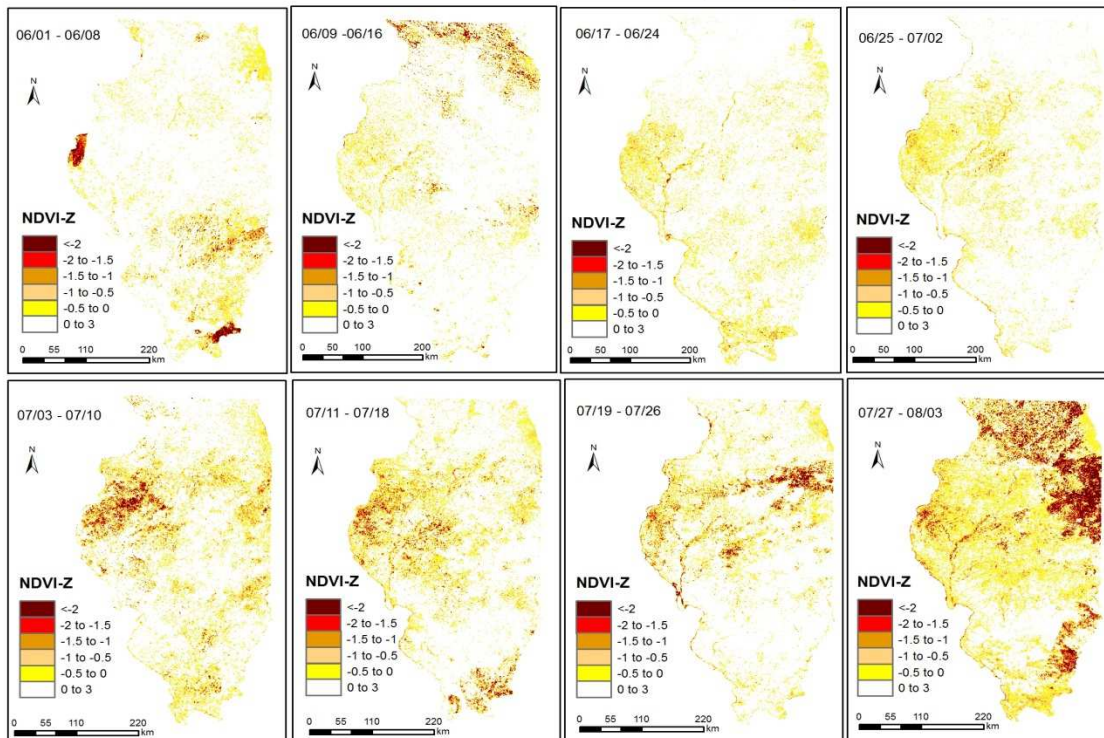
### 2009 Illinois NDVI Anomaly Map I



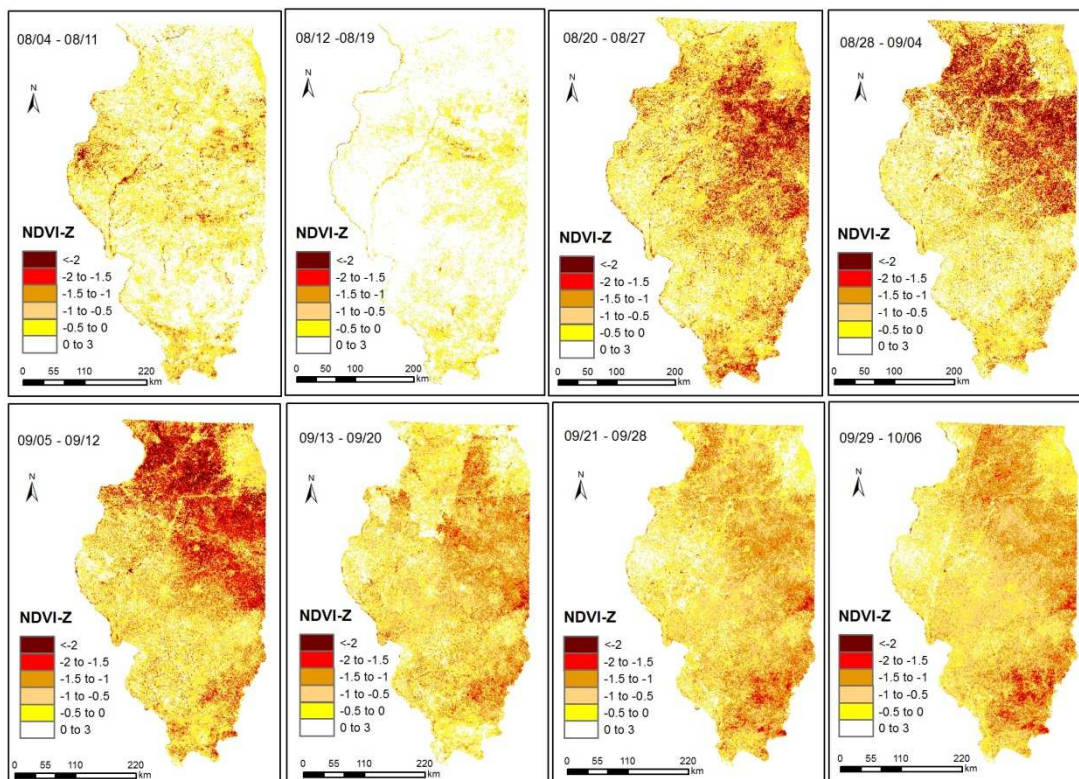
### 2009 Illinois NDVI Anomaly Map II



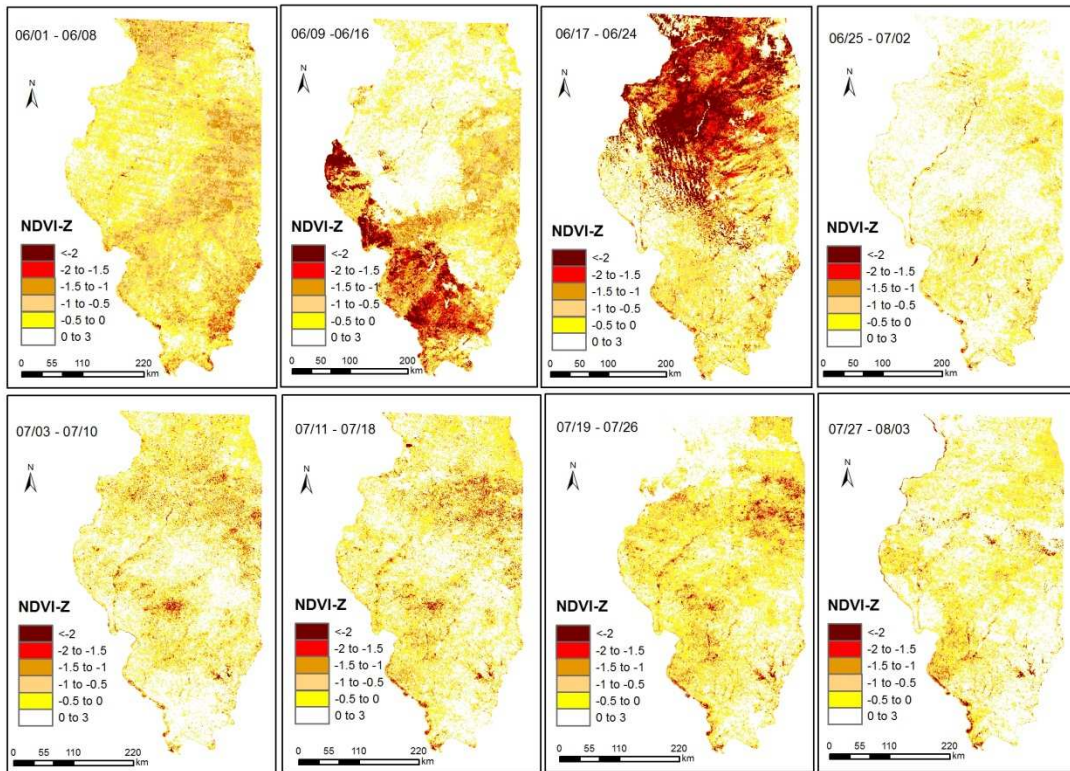
## 2010 Illinois NDVI Anomaly Map I



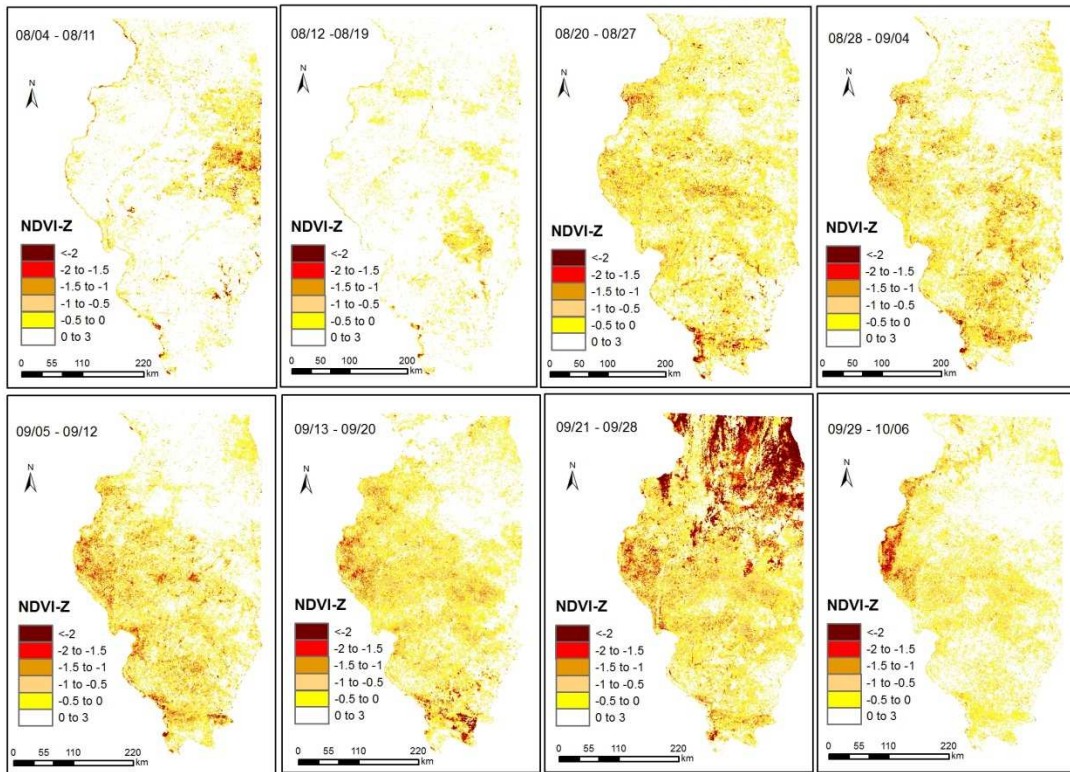
## 2010 Illinois NDVI Anomaly Map II



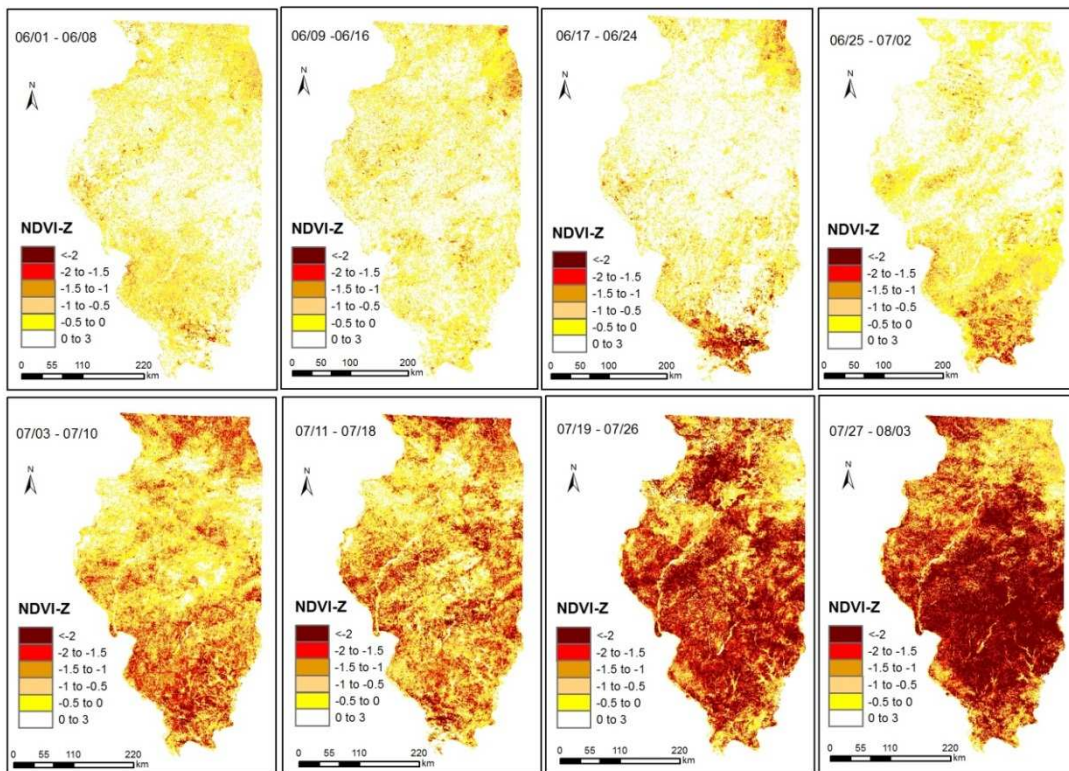
### 2011 Illinois NDVI Anomaly Map I



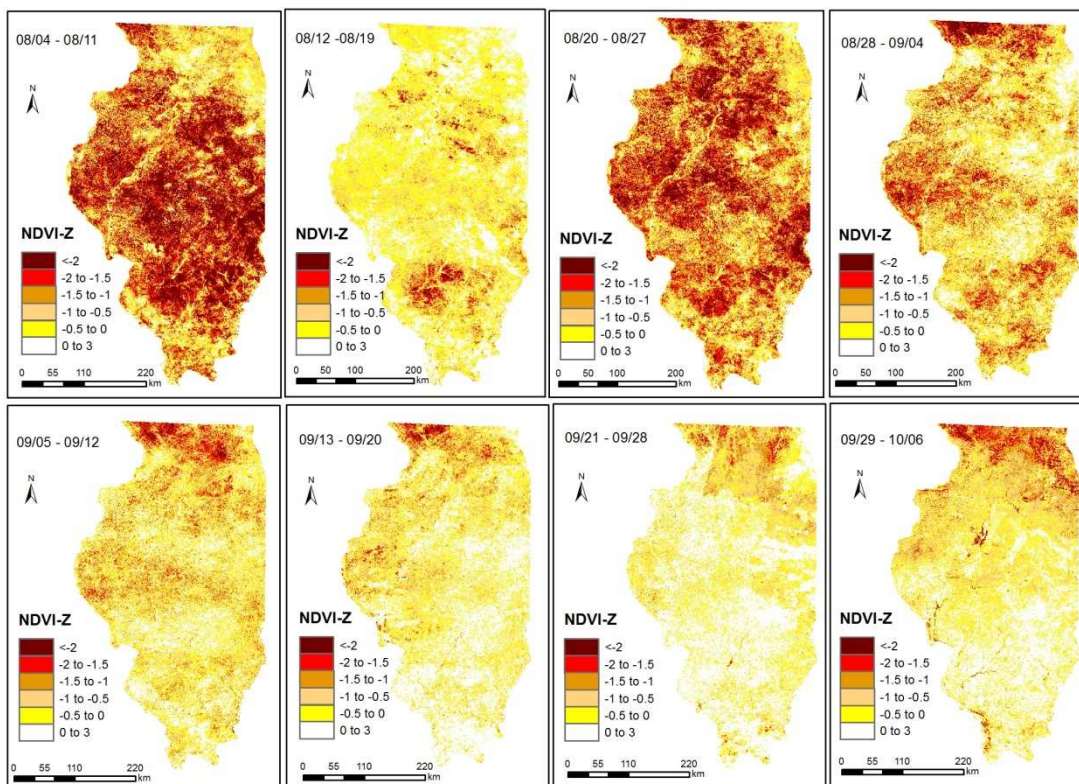
### 2011 Illinois NDVI Anomaly Map II



### 2012 Illinois NDVI Anomaly Map I



### 2012 Illinois NDVI Anomaly Map II



VITA

Graduate School

Southern Illinois University

Guanling Feng

fguanling123@gmail.com

Wuhan University

Bachelor of Geodesy and Geomatics Engineering, May 2011

Thesis Title: Monitoring drought intensity in Illinois with a combined index

Major Professor: Dr. Guangxing Wang